"A STUDY ON ADSORPTION OF HEAVY METAL IONS AND DYES ONTO CHEMICALLY TREATED PTEROCARPUS MARSUPIUM ROXB. BARK"

A thesis Submitted to the Bharathidasan University for the award of the degree of

DOCTOR OF PHILOSOPHY

in

CHEMISTRY

$\mathbf{B}\mathbf{y}$

S.SURYA, M.Sc., M.Phil.,

(Ref. No: 05974/Ph.D.K2/CHEMISTRY/PART-TIME/APRIL 2017)

Under the guidance of

Dr.V.NANDHAKUMAR, M.Sc., M.Phil., B.Ed., Ph.D.

Associate Professor of Chemistry



PG & RESEARCH DEPARTMENT OF CHEMISTRY

A.V.V.M SRI PUSHPAM COLLEGE (AUTONOMOUS)

POONDI – 613 503. THANJAVUR.

TAMILNADU, INDIA

MARCH - 2022

Dr.V.NANDHAKUMAR M.Sc.,M.Phil.,M.Ed., Ph.D

Associate Professor & Research Advisor

P.G. and Research Department of Chemistry

A.V.V.M Sri Pushpam College (Autonomous)

Affiliated to Bharathidasan University

POONDI- 613 503, Thanjavur Dt.

(Email:vnandhakumar12@yahoo.com)



CERTIFICATE

This is to certify that the thesis entitled "A STUDY ON ADSORPTION OF HEAVY METAL IONS AND DYES ONTO CHEMICALLY TREATED *Pterocarpus marsupium* Roxb.bark" is a bonafide record of the original research work done by Mrs. S. SURYA (Ref.No:05974/Ph.D.K2/Chemistry/Part Time/April-2017) under my supervision and guidance. This is also to certify that this thesis has not formed previously the basis for the award of any degree, diploma, associateship, fellowship or other similar titles.

Place: Poondi (Dr. V. NANDHAKUMAR)

Date: -03-2022 Research Supervisor

DECLARATION

I hereby declare that the thesis entitled "A STUDY ON ADSORPTION OF

HEAVY METAL IONS AND DYES ONTO CHEMICALLY TREATED

Pterocarpus marsupium Roxb.bark" is a bonafide record of the original research

work carried out by under the guidance and supervision me

Dr.V.NANDHAKUMAR, Associate Professor, Post Graduate and Research

Department of Chemistry, A.V.V.M Sri Pushpam College (Autonomous), Poondi

Thanjavur Dt.- 613 503

I also declare that this work has not been formed earlier the basis for the award

S.SURYA

of any degree, diploma or fellowship by any other University.

Place: Poondi

Date: -03-2022



Document Information

Analyzed document S. SURYA - CHEMISTRY - INTRO & REVIEW.pdf (D130638954)

Submitted 2022-03-17T10:02:00.0000000

Submitted by Dr.S.Vanitha

Submitter email vanitha@bdu.ac.in

Similarity 1%

Analysis address vanitha.bdu@analysis.urkund.com

Sources included in the report

W	URL: https://en.wikipedia.org/wiki/Pollutant Fetched: 2022-03-17T10:16:00.0000000	88	1
W	URL: https://en.wikipedia.org/wiki/Methylene_blue Fetched: 2022-03-17T10:16:00.0000000		1
W	URL: http://www.lenntech.com/periodic/elements/cr.htm Fetched: 2022-03-17T10:16:00.0000000	00	4



Document Information

Analyzed document S. SURYA - CHEMISTRY - REMAINING CHAPTERS.pdf (D130638957)

Submitted 2022-03-17T10:02:00.0000000

Submitted by Dr.S.Vanitha

Submitter email vanitha@bdu.ac.in

Similarity 3%

Analysis address vanitha.bdu@analysis.urkund.com

Sources included in the report

Sour	ces included in the report		
J	URL: 4d668b52-966f-4feb-bc20-0a009185f1c2 Fetched: 2019-03-13T05:54:27.0530000		9
W	URL: http://winters.com/PDF/winters_catalogue.pdf Fetched: 2021-04-05T13:15:48.2270000	88	1
J	URL: 755e08fd-0cbf-4e07-9930-7a65c88ced48 Fetched: 2019-03-13T05:53:21.9270000		6
W	URL: https://pdfcookie.com/documents/desalination-and-water-treatment-optimization-and-batch-studies-on-adsorption-of-malachite-green-dye-using-rambutan-seed-activated-carbon-68v4mgx5mxvg Fetched: 2022-02-20T04:07:59.1730000		3
W	URL: https://sciforum.net/manuscripts/2370/manuscript.pdf Fetched: 2021-05-24T05:34:25.8800000		2
J	URL: b0543277-ce55-4b68-8260-823ddc2d9e39 Fetched: 2019-03-13T05:54:34.7570000		1
W	URL: http://www.inosr.net/wp-content/uploads/2019/12/INOSR-SR-41-23-41-2018pdf Fetched: 2022-01-16T06:55:41.4430000	88	4
W	URL: https://www.mdpi.com/1996-1944/7/12/8037/htm Fetched: 2022-02-19T11:04:58.9700000		1
W	URL: https://www.researchgate.net/publication/328633506_Removal_of_Congo_Red_Dye_from_A queous_Solution_by_Using_Limonia_acidissima_Shell_as_Adsorbent Fetched: 2019-12-04T08:29:25.9670000	88	2
W	URL: https://sciensage.info/index.php/JASR/article/download/740/13 Fetched: 2022-03-17T10:16:27.3500000		5

ACKNOWLEDGEMENT

First and foremost, praises and thanks to the God, the Almighty, for His showers of blessings throughout my research work to complete the research successfully.

I express my sincere thanks our beloved former secretary and correspondent **SRIMAN AYYA**.

I am sincerely thankful to our president **Shri.T.Krishnasamy vandayar** A.V.V.M. Sri Pushpam College, Poondi.

I would like to express my gratitude to our beloved secretary and correspondent **Shri A.Balasubramania Vandayar**, A.V.V.M. Sri Pushpam College, Poondi.

I would like to express my deep and sincere gratitude to my research supervisor, **Dr. V. NANDHAKUMAR** M.Sc., M.Phil.,M.Ed., Ph.D., Associate Professor and Head of the Department A.V.V.M.Sri Pushpam College, Poondi, Thanjavur for giving me the opportunity to do research and providing invaluable guidance throughout this research. His dynamism, vision, sincerity and motivation have deeply inspired me. He has taught me the methodology to carry out the research and to present the research works as clearly as possible. It was a great privilege and honor to work and study under his guidance.

I would like to express my gratitude to **Dr. R. Sivakumar**, principal, **Dr. S. Kumaravel**, Dean of Sciences, A.V.V.M.Sri Pushpam College, Poondi, Thanjavur District, for providing necessary facilities and their constant encouragement and support.

I am extending my thanks to the **Dr.K.Ramesh** M.Sc.,M.Phil.,B.Ed.,Ph.D., Assistant Professor Of Chemistry, Poompuhar College (Autonomous) Melaiyur.

It is my delight to show gratitude to all my colleagues and friends of Department of Chemistry, A.V.V.M.Sri Pushpam College, Poondi, for their kind cooperation throughout my research work.

I am extremely thanks to **Ms.G.Abinaya**, Assistant professor, Department of chemistry, A.V.V.M. Sri Pushpam College for her valuable help during the period of my study.

I take this precious opportunity to express heartfelt thanks to my **Father-in-Law Capt T.KANNADASAN**, Retd. Army, Pathology Department, Working as my backbone for doing this study and felt happy to convey all this credits happened only Cox of his effective support till the last.

I am very much thankful to my husband **K.ARUNKUMAR** and my lovable Son **A.ADHITHYA** for their love, understanding, prayers and continuing support to complete this research work.

CONTENT

	Title	Page No.
1	INTRODUCTION	1 - 22
2	OBJECTIVE AND SCOPE OF THE PRESENT STUDY	23 - 29
3.	REVIEW OF LITERATURE	30 - 41
4.	EXPERIMENTAL METHODS	42 - 69
5.	RESULTS AND DISCUSSION	70 - 210
6	SUMMARY AND CONCLUSION	211 - 216
REF	ERENCE	217 - 231
RES	EARCH PUBLICATIONS	

Name of the candidate : S.SURYA

Reference number: Ref.No:05974/Ph.D.K2/Chemistry/Part

Time/April-2017

Research supervisor: Dr. V. NANDHAKUMAR,

Associate Professor,

PG & Research Department of Chemistry,

AVVM Sri Pushpam College (Autonomous),

Poondi, Thanjavur Dt. - 613503

Title of the thesis : "A STUDY ON ADSORPTION OF HEAVY

METAL IONS AND DYES ONTO

CHEMICALLY TREATED Pterocarpus

marsupium Roxb.bark"

ABSTRACT

Three different activated carbons were prepared from the barks *Pterocarpus marsupium*. First carbon was prepared using phosphoric acid activation method followed by micro wave physical activation method and designated as *Pterocarpus marsupium* Bark Carbon (PBC). Second activated carbon was prepared by modifying the surface of the PBPAC using hydrochloric acid followed by micro wave activation and designated as Acid modified *Pterocarpus marsupium* Carbon (APBC). Third activated carbon was prepared by modifying the surface of the PBPAC using potassium hydroxide followed by micro wave activation and designated as Base modified *Pterocarpus marsupium* Carbon (BPBC).

All the three carbons were characterized with FTIR spectra SEM images. Physico chemical characteristics such as Zero point charge (pHzpc), bulk density, Surface area, moisture content, fixed carbon content, matter soluble in water, matter soluble in acid, ash content, percentage of yield, methylene blue number and iodine

number were determined and the significances of these properties were well discussed.

Adsorption potentials of these carbons were investigated for the removal adsorbates such as cationic dye Methylene blue, anionic dye Turquoise blue and a carcinogenic metal ion Cr(VI) from aqueous solution by batch method at 305,315,325 and 335K temperatures. The different adsorption parameters such as effect of solution pH, dosage of adsorbent, contact time, initial concentrations of adsorbates were studied to understand the adsorption behaviour of the chosen three adsorbates. Choosing of optimum pH for each adsorbate is discussed with pHzpc of the carbons, electrostatic interaction and species nature of the adsorbates in different solution pH The equilibrium results were fitted to familiar Langmuir, Freundlich, Temkin and Dubinin-Radushkevich isotherms equations to establish the adsorption mechanism. Linearised forms of Lagergren, Ho and Webber - Morris kinetic models were used to understand the kinetics of the systems studied. Suitability of kinetic model was determined with the help of a statistical tool 'Mean of Sum of Squared Errors'. Thermodynamic quantities enthalpy change (ΔH°), entropy change (ΔS°) and Gibbs free energy change (ΔG°) were determined using Van't Hoff's plots. Desorption and Re-adsorption studies were carried out. Efficiency of the prepared carbons to treat effluents of dyeing units, leather tanning were carried out.

FTIR spectra of carbons before and after loading with each adsorbate were compared to understand the adsorption mechanism. Production costs of these carbons were compared with the cost commercial activated carbons.

LIST OF TABLES

Table No	Title	Page No
4.1	Pterocarpus Marsupium barks carbon Preparation parameters	44
4.2	Wavelength (nm) for dye ions/Metal ions	52
4.3	Experimental parameters	53
4.4	Physico-Chemical Characteristics of PBC, APBC AND BPBC	56
4.5	Before FTIR OF PBC ,APBC and BPBC	66
5.1	Effect of dose for Cr(VI) ions adsorption onto PBC, APBC & BPBC	74
5.2	Effect of Contact time for Cr(VI)ions adsorption	76
5.3	Effect of initial concentration on percentage of removal	78
5.4	Effect of initial concentration on amount adsorbed	78
5.5	Effect of temperature of Cr(VI)ions onto Adsorbents	82
5.6	Effect of temperature of Cr(VI)ions onto Adsorbents PBC, APBC & BPBC	83
5.7	Langmuir isotherm results for Cr(VI) ion adsorption onto PBC, APBC & BPBC	87
5.8	R _L values for Cr(VI) ion on adsorbents	88
5.9	Freundlich isotherm results for Cr(VI) ions on adsorbents PBC, APBC & BPBC	91
5.10	Adsorption capacity Kf (mg/g) values	91
5.11	Temkin isotherm results for Cr(VI) ions adsorption onto PBC, APBC & BPBC	94
5.12	Dubinin - Radushkevich isotherm results for Cr(VI) ions	97
5.13	Pseudo first order Kinetics results for the adsorption of Cr(VI) ions onto PBC	101
5.14	Pseudo second order Kinetics results for the adsorption of Cr(VI) ions onto PBC	101
5.15	Pseudo First order Kinetics results for the adsorption of Cr(VI) ions onto APBC	102

5.16	Pseudo second order Kinetics results for the adsorption of Cr(VI) ions onto APBC	102
5.17	Pseudo First order Kinetics results for the adsorption of Cr(VI) ions onto BPBC	103
5.18	Pseudo second order Kinetics results for the adsorption of Cr(VI) ions onto BPBC	103
5.19	MSSE Values for the adsorption of Cr(VI) ions	103
5.20	Intra Particle Diffusion results for adsorption Cr(VI) ions	107
5.21	Thermodynamic study results for the adsorption of Cr(VI) ions	110
5.22	Effect of dose for MB dye onto PBC, APBC& BPBC	119
5.23	Effect of Contact time for MB dye adsorption onto PBC, APBC & BPBC	122
5.24	Effect of Initial concentration on percentage of removal MB dye	124
5.25	Effect of Initial Concentration on amount of adsorption MB dye	124
5.26	Effect of temperature of MB dye onto Adsorbents % Removal	129
5.27	Effect of temperature of MB dye onto Adsorbents Qe	130
5.28	Langmuir isotherm results for MB dye onto adsorbents Q0 & b	136
5.29	Dimensionless separation factor (RL)	136
5.30	Freundlich isotherm results for MB dye onto adsorbents N & KKf	139
5.31	Adsorption capacity Kf (mg/g) values	139
5.32	Temkin isotherm results for MB dye onto adsorbents Q) &B	142
5.33	Dubinin - Radushkevich isotherm results for MB dye onto adsorbents qD, E & B	145
5.34	Pseudo first order Kinetics results for MB dye onto PBC	148
5.35	Pseudo second order Kinetics results for MB dye onto PBC	149
5.36	Pseudo first order Kinetics results for MB dye onto APBC	149
5.37	Pseudo second order Kinetics results for MB dye onto APBC	150
5.38	Pseudo first order Kinetics results for MB dye onto BPBC	150
5.39	Pseudo second order Kinetics results for MB dye onto BPBC	151
5.40	MSSE Values for the adsorption of MB dye	151
5.41	Intra Particle Diffusion results for adsorption MB dye	155

5.42	Thermodynamic Parameter results for MB dye onto adsorbents	158
5.43	Effect of dose for TB dye onto PBC, APBC and BPBC	168
5.44	Effect of Contact time for TB dye adsorption on to PBC , APBC & BPBC	170
5.45	Effect of initial concentration on percentage of removal	172
5.46	Effect of initial concentration on amount of adsorption	173
5.47	Effect of temperature of TB dye onto Adsorbents	178
5.48	Effect of temperature of TB dye onto Adsorbents PBC, APBC & BPBC	179
5.49	Langmuir isotherm results for TB dye onto adsorbents	183
5.50	Dimensionless separation factor(R _L)	184
5.51	Freundlich isotherm results for TB dye onto adsorbents	187
5.52	Adsorption capacity K _f (mg/g) values for various adsorbents	187
5.53	Tempkin isotherm results for TB dye onto adsorbents	190
5.54	Dubinin - Radushkevich isotherm results for TB dye onto adsorbents	193
5.55	Pseudo first order Kinetics results for TB dye on to PBC	196
5.56	Pseudo second order Kinetics results for TB dye on to PBC	197
5.57	Pseudo first order Kinetics results for TB dye on to APBC	197
5.58	Pseudo second order Kinetics results for TB dye onto APBC	197
5.59	Pseudo first order Kinetics results for TB dye onto BPBC	198
5.60	Pseudo second order Kinetics results for TB dye on to BPBC	198
5.61	Intra Particle Diffusion results for adsorption of TB dye onto adsorbents	203
5.62	Thermodynamic Parameter results for adsorption of TB dye onto adsorbents	205

LIST OF FIGURES

Figure No	Title	Page No
4.1	Barks of Pterocarpus Marsupium	42
4.2	Before FTIR Spectrum of PBC	65
4.3	Before FTIR Spectrum of APBC	65
4.4	Before FTIR Spectrum of BPBC	65
4.5	Unloaded PBC	67
4.6	Loaded Cr (VI) PBC	67
4.7	Loaded Cr (VI) APBC	67
4.8	Loaded Cr (VI) BPBC	67
4.9	Unloaded PBC	68
4.10	Loaded MB dye PBC	68
4.11	Loaded MB dye APBC	68
4.12	Loaded MB dye APBC	68
4.13	Unloaded TB dye PBC	69
4.14	Loaded TB dye APBC	69
4.15	Loaded TB dye APBC	69
4.16	Loaded TB dye BPBC	69
5.1	Effect of pH for Cr (VI) onto PBC, APBC & BPBC	72
5.2	Effect of Dose for Cr (VI) onto PBC, APBC & BPBC	73
5.3	Effect of contact time for Cr(VI) onto PBC	75
5.4	Effect of contact time for Cr(VI) onto APBC	75
5.5	Effect of contact time for Cr(VI) onto BPBC	75
5.6	Ci vs % of Removal for Cr (VI) onto PBC	79
5.7	Ci vs qe for Cr (VI) onto PBC	79
5.8	Ci vs % of Removal for Cr(VI) onto APBC	79
5.9	Ci vs % of Removal for Cr (VI) onto BPBC	80
5.10	Ci vs qe for Cr(VI) onto BPBC	80
5.11	Ci vs qe for Cr(VI) onto BPBC	80
5.12	Temperature vs % of Removal for Cr(VI) onto PBC	81

5.13	Temp. vs Qe for Cr(VI) onto PBC	84
5.14	Temperature vs % of Removal for Cr(VI) onto APBC	84
5.15	Temp. vs Qe for Cr(VI) onto APBC	84
5.16	Temperature vs % of Removal for Cr(VI) onto BPBC	85
5.17	Temp. vs Qe for Cr(VI) onto BPBC	85
5.18	Langmuir - Isotherm for Cr(VI) onto PBC	89
5.19	Langmuir - Isotherm for Cr(VI) onto APBC	89
5.20	Langmuir - Isotherm for Cr(VI) onto BPBC	89
5.21	Freundlich Isotherm for Cr(VI) onto PBC	92
5.22	Freundlich Isotherm for Cr(VI) onto APBC	92
5.23	Freundlich Isotherm for Cr(VI) onto BPBC	92
5.24	Tempkin Isotherm for Cr(VI) onto PBC	95
5.25	Tempkin Isotherm for Cr(VI) onto APBC	95
5.26	Tempkin Isotherm for Cr(VI) onto BPBC	95
5.27	D-R Isotherm for Cr(VI) onto PBC	98
5.28	D-R Isotherm for Cr(VI) onto APBC	98
5.29	D-R Isotherm for Cr(VI) onto BPBC	98
5.30	Lagergren plot for Cr(VI) onto PMBC	104
5.31	Lagergren plot for Cr(VI) onto APBC	104
5.32	Lagergren plot for Cr(VI) onto BPBC	105
5.33	Ho plot for Cr(VI) onto PBC	105
5.34	Ho plot for Cr(VI) onto APBC	106
5.35	Ho plot for Cr(VI) onto BPBC	106
5.36	Weber and Morris plot for Cr(VI) onto PBC	108
5.37	Weber and Morris plot for Cr(VI) onto APBC	108
5.38	Weber and Morris plot for Cr(VI) onto BPBC	108
5.39	Van't Hoff plot Cr(VI) onto PBC	111
5.40	Van't Hoff plot Cr(VI) onto APBC	111
5.41	Van't Hoff plot Cr(VI) onto BPBC	111
5.42	Desorption of Cr(VI) ions	112

5.43	FTIR Spectrum of PBC adsorbent before adsorption, PBC at pH2 and Cr(VI) ions loaded PBC	113
5.44	FTIR Spectrum of APBC adsorbent before adsorption, APBC at pH2 and Cr(VI) ions loaded APBC	114
5.45	FTIR Spectrum of BPBC adsorbent before adsorption, BPBC at pH2 and Cr(VI) ions loaded BPBC	115
5.46	EDAX pattern of Cr(VI) adsorbed PBC	116
5.47	Effect of pH for MB dye onto PBC, APBC & BPBC	118
5.48	Effect of Dose for MB dye onto PBC, APBC & BPBC	120
5.49	Effect of contact time MB dye onto PBC	121
5.50	Effect of contact time MB dye onto APBC	121
5.51	Effect of contact time MB dye onto BPBC	121
5.52	Ci vs % of Removal for MB dye onto PBC	125
5.53	Ci vs % of Removal for MB dye onto PBC	125
5.54	Ci vs % of Removal for MB dye onto APBC	126
5.55	Ci vs qe for MB dye onto APBC	126
5.56	Ci vs % of Removal for MB dye onto BPBC	127
5.57	Ci vs qe for MB dye onto BPBC	127
5.58	Temperature vs % of Removal for MB dye onto PBC	131
5.59	Temp. vs Qe for MB dye onto PBC	131
5.60	Temperature vs % of Removal for MB dye onto APBC	132
5.61	Temp. vs Qe for MB dye onto APBC	132
5.62	Temperature vs % of Removal for MB dye onto BPBC	133
5.63	Temp. vs Qe for MB dye onto BPBC	133
5.64	Langmuir - I Isotherm for MB dye onto PBC	137
5.65	Langmuir - I Isotherm for MB dye onto APBC	137
5.66	Langmuir - I Isotherm for MB dye onto BPBC	137
5.67	Freundlich Isotherm for MB dye onto PBC	140
5.68	Freundlich Isotherm for MB dye onto APBC	140
5.69	Freundlich Isotherm for MB dye onto BPBC	140
5.70	Tempkin Isotherm for MB dye onto PBC	143

5.71	Tempkin Isotherm for MB dye onto APBC	143
5.72	Tempkin Isotherm for MB dye onto BPBC	143
5.73	D-R Isotherm for MB dye onto PBC	146
5.74	D-R Isotherm for MB dye onto APBC	146
5.75	D-R Isotherm for MB dye onto BPBC	146
5.76	Lagergren plot for MB dye onto PBC	152
5.77	Ho plot for MB dye onto PBC	152
5.78	Lagergren plot for MB dye onto APBC	153
5.79	Ho plot for MB dye onto APBC	153
5.80	Lagergren plot for MB dye onto BPBC	154
5.81	Ho plot for MB dye onto BPBC	154
5.82	Weber and Morris plot for MB dye onto PBC	156
5.83	Weber and Morris plot for MB dye onto APBC	156
5.84	Weber and Morris plot for MB dye onto BPBC	156
5.85	Van't Hoff plot MB dye onto PBC	159
5.86	Van't Hoff plot MB dye onto APBC	159
5.87	Van't Hoff plot MB dye onto BPBC	159
5.88	Desorption of MB Dye	160
5.89	FTIR Spectrum of PBC adsorbent before adsorption, PBC at pH2 and MB dye loaded PBC	161
5.90	FTIR Spectrum of APBC adsorbent before adsorption, APBC at pH2 and MB dye loaded APBC	162
5.91	FTIR Spectrum of BPBC adsorbent before adsorption, BPBC at pH2 and MB dye loaded BPBC.	163
5.92	Effect of pH	166
5.93	Effect of Dose on PBC,APBC,BPBC	167
5.94	Effect of contact time TB dye onto PBC	169
5.95	Effect of contact time TB dye onto APBC	169
5.96	Effect of contact time TB dye onto BPBC	169
5.97	Ci vs % of Removal for TB dye onto PBC	174
5.98	Ci vs qe for TB dye onto PBC	174

5.99	Ci vs % of Removal for TB dye onto APBC	175
5.100	Ci vs qe for TB dye onto APBC	175
5.101	Ci vs % of Removal for TB dye onto BPBC	176
5.102	Ci vs qe for TB dye onto BPBC	176
5.103	Temperature vs % of Removal for TB dye onto PBC	180
5.104	Temp. vs Qe for TB dye onto PBC	180
5.105	Temperature vs % of Removal for TB dye onto APBC	181
5.106	Temp. vs Qe for TB dye onto APBC	181
5.107	Temperature vs % of Removal for TB dye onto BPBC	181
5.108	Langmuir - I Isotherm for TB dye onto PBC	184
5.109	Langmuir - I Isotherm for TB dye onto APBC	185
5.110	Langmuir - I Isotherm for TB dye onto BPBC	185
5.111	Freundlich Isotherm for TB dye onto PBC	188
5.112	Freundlich Isotherm for TB dye onto APBC	188
5.113	Freundlich Isotherm for TB dye onto BPBC	188
5.114	Tempkin Isotherm for TB dye onto PBC	190
5.115	Tempkin Isotherm for TB dye onto APBC	191
5.116	Tempkin Isotherm for TB dye onto BPBC	191
5.117	D-R Isotherm for TB dye onto PBC	193
5.118	D-R Isotherm for TB dye onto APBC	194
5.119	D-R Isotherm for TB dye onto BPBC	194
5.120	Lagergren plot for TB dye onto PBC	199
5.121	Lagergren plot for TB dye onto APBC	199
5.122	Lagergren plot for TB dye onto BPBC	200
5.123	Ho plot for TB dye onto PBC	200
5.124	Ho plot for TB dye onto APBC	201
5.125	Lagergren plot for TB dye onto BPBC	201
5.126	Weber and Morris plot for TB dye onto PBC	202
5.127	Weber and Morris plot for TB dye onto APBC	203
5.128	Weber and Morris plot for TB dye onto BPBC	203

5.129	Van't Hoff plot TB dye onto PBC	206
5.130	Van't Hoff plot TB dye onto APBC	206
5.131	Van't Hoff plot TB dye onto BPBC	206
5.132	Desorption of TB Dye	207
5.133	FT – IR spectrum of TB dye Loaded with PBC	208
5.134	FT – IR spectrum of TB dye Loaded with APBC	209
5.135	FT – IR spectrum of TB dye Loaded with BPBC	210

Introduction

1.1 Adsorption Method

Adsorption is the accumulation of atoms, molecules, or ions at the surface of a solid phase. It is a mass transfer process (Crawford and Quinn, 2017). The substance adsorbed is called adsorbate, and the solid on which the material is accumulated is called adsorbent. Adsorption occurs due to surface energy of the adsorbent (Arivoli, 2008). The adsorption process can be due to physical forces or chemical forces. Van der Waals and electrostatic forces are the cause of attraction between adsorbent and adsorbate molecules in the case of Physical adsorption. Chemical adsorption is due to chemical bonding between adsorbate molecules and the adsorbent's surface (Hu and Ke, 2020; Abegunde et al., 2020). Physical adsorption is reversible and chemical adsorption is irreversible in nature.

Adsorption, continued to maintain its familiarity among the researchers towards environmental sustainability as it is a simple, non-toxic and economical technique (Olasehinde and Abegunde, 2020b; Zheng et al., 2013). Adsorption technique is used in separation and purification of materials, pollution control, refinery and extraction. It has gained significant attention in water treatment, in spite of various techniques available for water wastewater treatment methods. In present days, the adsorption technique is considered as the most efficient, and selective treatment method for the decontamination of wastewater (Dana, 2017; Gayathri et al., 2019 Kyzas et al., 2019; Sharma et al., 2019; Sun et al., 2019). Simple operational design and complete recovery of dangerous pollutants from wastewater are the advantages of adsorption method (Vijayakumar et al., 2012).

Adsorption of organic and inorganic pollutants from aqueous solution employs a porous material with a large surface area and suitable surface (Rashed, 2013; Wu and Tseng, 2008). Several materials used as adsorbents are clay, alumina, silica gel, activated carbon, synthetic resins, molecular sieve, zeolites, impregnated biomass industrial waste and agricultural waste (Lin and Juang, 2009; Shen et al., 2014; Wu et al., 2014; Krishna et al., 2001; Bilal et al., 2013; Ahmaruzzaman, 2008; Thakur and Semil, 2013). Optimum performance had been carried during by the optimum experimental conditions such as solution pH, initial concentration of adsorbate, temperature, dosage of adsorbents, and contact time (Vadivelan and Kumar, 2005).

Many researchers have reported that the surface modification improved surfaces of several materials significantly.

1.1.1 Adsorbent

An adsorbent is a solid material that permits liquid or gaseous molecules to adhere on its surface. Performance of the adsorbent depends on the physical and chemical properties of the adsorbent's surface, as well as that of the soluble substances (Ip et al., 2009; Babel and Kurniawan, 2003). Required characteristics of an efficient adsorbent are a large surface area and a minimum volume in addition to high mechanical strength, chemical and thermal stability, small pore width and high porosity and hence high adsorption capacity (Adeyemo et al., 2017; Ispas et al., 2009; Askalany et al., 2013). Adsorbents can be in the form of pellets, rods, mouldings, or monoliths to fit the required application (Rezaei and Webley, 2010; Plaza et al., 2010). Adsorbents, find applications in the fields such as treatment of water, separation, catalysis, desiccants and indicators. Commonly used adsorbents in practice are activated carbon, agriculture wastes, industrial wastes, biopolymers, clays and nanomaterials, (Yu and Zhong, 2006; Minobe et al., 1982;Rio et al., 2006; Lu, 1996; Ezeokonkwo et al., 2018; Olasehinde and

Abegunde, 2020a), (da Silva et al., 2009), **Sludge** (Tarletonand Wakeman, 2006; Yadav and Garg, 2011). **Slag.** (Piatak et al., 2015) **Kraft lignin, Fly ash** (Chou, 2012).

1.1.2 Activated carbon

Activated carbon (AC) is a popular adsorbent for the treatment of wastewater because of its large surface area and high affinity towards heavy metal ions and dye molecules (Huang and Wu, 1977; Chen et al., 1996; Kaveeshwar et al., 2018). Activated carbon is an amorphous porous solid consisting micro crystallites with a graphite lattice. They are produced from carbon-rich materials, using either thermal or chemical methods to remove most of the volatile non-carbon.

Activated carbon is characterized by its well-developed pores and large surface area with some functional groups. This surface area is the main key character of an adsorbent which renders a high adsorption capacity to the material to keep adsorbates. It also has several attractive forces to attract the contaminants from the water and get adsorbed. (Baker *et al.*, 1992).

1.1.3 Production of activated carbon

The carbonaceous raw material that is precursor is subjected to dehydration by impregnating it with dehydrating chemicals and then subjected for carbonization followed by activation (Smisek and Cerny *et al.*, 1970; Wigmans *et al.*, 1985). Composition of raw material and the selection of activation method decide the surface area, pore volume, pore size distribution and adsorption capacity. Lignite, Wood, coal, petroleum residues, bone and synthetic high polymers which have rich carbon content are the suitable precursors for the production of activated carbons (Kirk-Othmer *et al.*, 2003).

Carbonization process removes the undesirable by-products such as tar and other hydrocarbons due to drying and heating. In the activation process, the carbonized material is subjected to a high temperature (400–6000° C) in an oxygen-deficient atmosphere. This step removes the low-molecular-weight volatile fraction (Khalili *et al.*, 2000; Teng *et al.*, 1997).

Physical activation and chemical activation are the two main processes in practice to manufacture activated carbon (Bansal and Goyal *et al.*, 2005).

1.1.4 Physical activation

In this process, the carbon rich material is heated under oxygen-deficient atmosphere. Most of the non-carbon elements (hydrogen and oxygen) are removed in gaseous form and the carbons are grouped into an organized crystallographic formation known as elementary graphitic Crystallites. Carbonization of starts above 170°C and gets completed around 500°C-600°C. And the second step is the activation process. In this step, the carbonized product is converted to porous carbon with high surface area when heated at high temperatures (600 -1000°C) in an oxidizing environment. Pores are formed because of the entrance of oxidizing gases into the carbonized product which removes the of reaction products. Steam, CO₂, air, chlorine, sulphur vapours, SO₂, ammonia etc. are used in this physical activation process (Lillo-Rodenas *et al.*, 2001; Lozano-Castello *et al.*, 2001).

1.1.5 Chemical activation

In this method, both carbonization and activation processes take place simultaneously at a lower temperature and even at a shorter duration of time. This method would give better porous carbon with higher yields (Nowicki *et al.*, 2008). The chemical agents used should have dehydrogenation properties which will inhibit the production of

tar and reduce the formation of other volatile products. The precursor materials are treated with oxidizing chemicals such as ZnCl₂, H₃PO₄, KOH, NaOH etc. Aromatization of the carbon skeleton forms a porous structure. Then, the product is heated in an airless atmosphere for pyrolytic disintegration for the development of pore structure which would increase the surface area (Lozano-Castello *et al.*, 2001).

Chemical activation is mainly adopted for the preparation of powdered activated carbons from of lignocellulosic materials (Caturla et al., 1991; Molina-Sabio et al., 1995; Almansa et al., 2004).

Factors affecting Activated Carbon Production

Raw materials, carbonization temperature and activation time determines the nature of the resulting product.

Materials with high carbon content and low ash content like lignite, coal, wood, bone, nutshells, petroleum residues and some agricultural wastes such as tree bark, sawdust, the rice husk coconut shell, etc., are advantageous for the production of activated carbon (Kirk-Othmer *et al.*, 2003). Lignocellulose materials are commonly used as a raw material. Materials with low inorganic content would give activated carbon with low ash content.

The carbonization temperature may be between 200°C and 1100°C (San Miguel *et al.*, 2003). Higher the activation temperature (500°C to 900°) would yield lower amount of the activated carbon. This is because of the removal of a large amount of volatiles (Guo and Lua *et al.*, 2003). The optimum temperature range was between 400°C and 500°C (Srinivasakannan and Mohamad Zailani Abu Bakar *et al.*, 2004).

According to Haimour and Emeish *et al.*, (2006) carbonization temperature of more than 800°C is not advisable to prepare activated carbon. Higher carbonization temperature, higher will be the ash content of the product.

Activation time affects the carbonization process as well as the properties of the resulting activated carbon. An increase of activation time decreases the percentage of yield and increases the surface area. This is due to the volatilization of organic materials. (Kim *et al.*, 2001).

Production of activated carbon from Biomass

The starting material for the manufacture of activated carbon should be available in plenty, inexpensive and can be stored with low degradation. Plant biomass meet the above requirements. There are two types of plant biomass which are 'Virgin biomass' and 'Waste biomass'. Virgin biomass is woody and non-woody biomass which includes agricultural residues such as annual crops like maize and crop residues like bagasse, rice husk, etc. 'Waste biomass' is mainly the municipal solid waste, industrial waste, animal manures, landscaping waste, etc. (Danje *et al.*, 2011).

The constituents and composition of biomass are different for different species (San Miguel *et al.*, 2003).But the major components of biomass are cellulose, hemicelluloses, lignin and oxygen-containing organic polymers. Cellulose is a giant chain of linked sugar molecules and it gives great strength to the wood. It is the main constituent of the cell wall. It is the abundant organic compound of a planet. (Sinha *et al.*, 2004). Hemicellulose is a mixture of polysaccharides, composed of sugars such as glucose, mannose, xylose, arabinose and methyl glucuronic and galacturonic acids (Danje *et al.*, 2011; Pinthong *et al.*, 2009).

Lignin is a complex one of the most abundant organic polymers where the layers of many cell walls are lignin, which gives rigidity to the plants. (Czernik *et al.*, 2002; Solomon Sabiro Shale *et al.*, 2016).

Phosphoric acid activation method

In thermal activation methods, temperature, heating rate, pressure, etc. do not much influence the micropore size distribution (Gonzalez et al., 1997). Hence development of pores could be achieved with chemical activation method.

Plant dry materials mainly contain organic compounds and a small amount of inorganic matter. Transformation these materials into the char requires the removal of hydrogen and oxygen. The yield of the char depends upon the amount of carbon removed as hydrocarbons or CO₂. The chemical activation with a dehydrating compound would increase the yield of char. Earlier researchers (Caturla et al., 1991; Fu et al., 2001) observed that the main degradation took place around 200-350°C, with the evolution of CO₂, CO, H₂O, CH₄, aldehydes, etc. But the heavier hydrocarbons distilled off around 350-500°C. Little weight loss above 500°C indicates the formation of basic structure of the char.

Among the various chemical reagents used for chemical activation, phosphoric acid is the most important one. Phosphoric acid activation generates heterogeneous carbon with large volume of micro porosity with all pore sizes in a common proportion. Highly concentrated phosphoric acid develops meso and macro porosity also. Temperature less than 450°C is enough for phosphoric acid activation is a further advantage (Garrido et al., 1987; Rodriguez - Reinoso and Linares-Solano, 1989b).

Mechanism of phosphoric acid activation:

When the precursor material was impregnated in aqueous phosphoric acid solution, phosphoric acid enters in to the interior channels of the botanical structure of the precursor. This impregnation causes fragmentation of cellulose and other components such as hemicellulose and lignin. Phosphoric acid converts these particles into elastic nature. This acid separates the cellulose fibers and causes a partial depolymerization of the main components of the matrix, decreases the mechanical strength and swells the particles. The de-polymerization, dehydration and condensation produces significant amount of tar on the surface of the particles. This causes more aromatic and reactive products, with some cross-linkings (Solum et al., 1995). Additional cross-linking was induced by the phosphates and re-polymerization of the cellulose was also observed by Molina-Sabio et al., (1995). At higher concentrations of the acid, intensive reorganization modifies the meso- and macroporous structure also.

The degradation of lignin and cellulose is assisted by protons, offered by the acid which dissolves the cellulose. The heat treatment of impregnated material accelerate the dehydrating effect in the interior of the particles a of the cellulose, hemicellulose and lignin components. The temperature also facilitates thermal degradation of bondings in the precursor. Thus the dehydration reduces the dimensions of the particle and the reactant remains inside and act as template for the creation of microporosity.

Chemistry of phosphoric acid activation:

Physical, chemical and morphological changes that occur during activation by phosphoric acid were described Jagtoyen and Derbyshire, (1998)

Generally plant biomasses consist of 42-50% cellulose, 19-25% hemicellulose and 16-25% lignin. Structures of cellulose, hemicellulose and lignin are shown below.

Hemicellulose is a heteropolymer that present along with cellulose in all terrestrial plant cell walls. It is amorphous and can be easily hydrolyzed by dilute acid or base. Lignin is important for the formation of cell walls in wood and bark. Cellulose chains that are held together through hydrogen bonds form the micro-fibrils of the cell walls. Groups of micro-fibrils are connected to form amorphous cellulose and hemicellulose. The spaces between the micro-fibrils are of the order of a few nano meter size as that of mesopores and large micro pores.

Reactions at temperatures lesser than 150°C:

The acid first attacks amorphous polymers that are hemicellulose and lignin at 50°C. The acid cleaves the glycosidic linkages through hydrolysis. These reactions reduce molecular weight and convert the hemicellulose and lignin as extrudable mixtures of wood. Hydrolysis releases CO₂, CO and CH₄. The evolution of CO₂ and CO reduces C = O functionality present as a part in esters and carboxylic acid groups of the parent biomass (hemicellulose and lignin). The releases of CH4 are due to the cleavage of aliphatic side chains which increases the aromaticity. Porter and RoUins, (1972) and

Pandey and Nair (1974) observed that reaction of phosphoric acid with cellulose at low temperatures, produce considerable inter-crystalline and intra-crystalline swellings.

Reactions at temperatures between 150 and 450°C:

Phosphoric acid cross links the cellulose chains, replacing the hydrogen bonds and other linkages. This dilates the structure which develops porosity (Jagtoyen and Derbyshire, 1998). Small poly aromatic units are connected by phosphate and polyphosphate bridges and polyethylene linkages.

When the temperature is increased above 280°C, cyclization and condensation reactions occurs to increase the aromaticity and size of the poly aromatic units. Around 430 °C, extensive growth in the size of the aromatic units occurs due to the continued cleavage of cross-linkings. Thus, phosphoric acid act as catalyst in promoting bond cleavage and also for cyclization and condensation and .It also cross-links the biopolymer fragments through phosphate linkages.

Reactions at high temperatures (Above 450°C):

The structures begins to contract, micropore volumes decrease steadily until 550°C. Above 550°C, a sharp decline in mesopore volume is noticed. 30% of the cell wall thickness also reduces. This is because of decomposition of phosphate linkages formed during dilation. It also causes aromatic condensation. Consequently, it results in a more densely packed manner. Above this temperature range, the elimination aliphatic and oxygen-containing groups with the disappearance of ketones and esters happen.

In summary, Phosphoric acid acts as an acid catalyst to promote bond cleavage and also helps cross-linking for the formation of cyclization and condensation reactions, to combine organic fragments with phosphate and polyphosphate bridges. The insertion of phosphate groups dilates. At temperatures above 450 °C, the phosphate linkages

breakdown causing a secondary contraction and allows alignment of polyaromatic clusters, to produce a more densely packed structure with some reduction in porosity.

1.2 Micro wave heating

Microwave energy has been used in several fields of research and industrial processes Microwave heating is more advantageous than conventional muffle furnace heating as the micro wave heating improves the consistent micropores and pore volumes of the resulting activated carbon (Yagmur *et al.*, 2008).

Microwave heating is based on dielectric change due to either induced or permanent dipoles. Energy transmission occurs by two mechanisms: ion conduction and dipole rotation inside particles (Foo and Hameed *et al.*, 2012; Zhao *et al.*, 2012).

1.2.1 Surface modifications

Surface modification is a common practice in many fields, such as adsorption, corrosion, materials coating, plastic industry and catalysis (Schwarz et al., 1995)

The efficiency of an adsorbent depends on its surface chemistry. Surface, being the boundary with the external environment and it is important for the proper functioning of the material and often dictates the success of the adsorption process. Therefore, it is essential to improve the quality of the surface of an adsorbent

Surface modification is altering the physical, chemical, or biological characteristics of the surface of a material to different forms from the original forms found l to make it fit for the desired purpose.

It involves the removal of the surface impurities (Mwaikambo and Ansell, 1999) of the material and also altering surface energy, surface charge, roughness, surface area, hydrophobicity, reactivity and functional groups (Alekhin et al., 2010; Bertazzo et al.,

2009; Bertazzo and Rezwan, 2010). These changes can be achieved by incorporation, elimination, or freezing some selected elements or functional groups to get the desired changes.

Surface modification can be carried out through many means, including physical and chemical methods (Siperko and Thomas, 1989; Olasehinde and Abegunde, 2020a). Mechanical, thermal and chemical processes can create pores in order to get a large surface area. Acid, alkali or salt are used in chemical technique which improve the surface functional groups and the physical process improves the physical characteristics such as density and solubility. Combination of methods such as mechanochemical and thermochemical process also in practice (Makó et al., 2006; Tole et al., 2019).

1.2.2 Chemical modification

Chemical surface modification directly influences the surface chemistry of the material (Siperko and Thomas, 1989; Manory, 1990). It helps to convert the different inexpensive adsorbents into valuable adsorbents with high adsorptive capacities. Chemical surface causes new surface properties independent of those of the bulk polymer (Sharma et al., 2003; Thakur et al., 2014). It also causes a substantial effect on the due to chemical interactions of a modifying agent on the material (Rostami et al., 2018). A number of modifying chemical agents are exploited in recent times for tailoring the properties of adsorbents which acid, alkali and neutral solutions (Senturk et al., 2009; Vieira et al., 2010).

1.2.3 Acid modification

Acid modification can be done using mineral acids such as hydro chloric nitric, sulphuric, phosphoric, and hypo chlorous acids, (Vlasova et al., 2003; Temuujina et al., 2004; Belchinskaya et al., 2015; Shim et al., 2001; Liu and Xiao, 2018). Organic acids

are generally not used because of their low strength (Terrazas et al., 2005; Kong et al., 2014). Acid treatment of surface enhances the acidic behaviour and hydrophilic nature of the adsorbent's surface (Rehman et al., 2019). Adsorbent's surface treated with acid would have functional groups containing oxygen such as carboxyl, carbonyl, quinone, hydroxyl, lactone and carboxylic anhydride. These functional groups are mostly found on the edges of the basal plane of the activated carbon and influences the chemical nature of the material (Tamon and Okazaki, 1996; Boehm, 2002; Vinke et al., 1994). Researchers have made use of acid-modification of the adsorbents for the removal pollutants from the water.

Huang et al. (2019) used HNO3 acid as a modifying agent for lignite and noticed an increase in the content of polar oxygen-containing functional groups such as hydroxyl, carbonyl, and carboxyl groups and the introduction of nitro groups on the surface of the material with the enhanced the negatively-charged properties and the metal ion adsorption performance. Lesaoana et al. (2019) investigated influence of acid modification by impregnating Macadamia activated carbon with different concentrations of sulphuric, nitric, and phosphoric acids (20 to 60% v/v) and heated in a muffle furnace. They found that these process led to the introduction of functional groups such as CN, NO, sulphur and phosphorus peaks at 1213, 1531, 1204 and 1214 cm-1. Also, they observed an increase of surface area from 545 to 824 m²/g. Park and Jang (2002) made an attempt to modify a activated carbon using HCl acid. They observed increased numbers of various surface oxygen complexes, which enhanced the active sites.

Olasehinde and Abegunde (2020a) observed an aggregated and rough surface morphology upon modification surface of the activated carbon prepared from Raphia taedigera seed using hydrochloric acid as a modifying agent

1.2.4 Alkaline Modification

The surface functional groups of adsorbents can be significantly influenced by modifying agents. Activated carbon on treatment with alkali causes positive charges on the surface that enhances adsorption of negatively charged species (Rehman et al., 2019). This process can improve the non-polar surface, hence, enhances the adsorption capacity of the material for non-polar substances (Liu and Xiao, 2018).

The alkali surface modification can be made by treatment with NaOH, KOH, LiOH, Na₂SiO₃, Na₂CO₃and oxides. Zheng et al. (2013) used NaOH for the alkali modification of activated carbon and discovered a significant reduction in the surface oxygen-containing functional groups with the increase of surface area and the pore volume. The increase of surface area and the pore volume found to increase with the concentration of alkali.

Hayati and Mahmoodi (2012) compared the raw and alkali modified activated carbon for the adsorption of Acid Red 14 and Acid Blue 92 dye molecules from aqueous solution. They found that the NaOH modification improved the surface properties as well the adsorption capacity for the Acid Red 14 and Acid Blue 92 dyes. Ofudje et al. (2015) investigated the raw and alkaline-modified coconut shaft and found the improved surface characteristics of alkali modified adsorbent because of the availability of functional groups such as alcohols, amines, carboxylic acids, ethers, and esters on the cell walls of the alkali treated coconut shaft. Gao et al. (2013) observed a higher surface area and a larger total pore volume for the activated carbon modified with KOH.

1.2.5 Applications of activated carbon:

Activated carbons are mostly used an adsorbent for removing pollutants from air and water such as spill cleanup, gold purification, metal extraction, metal

finishing, purification of electroplating solutions, sewage treatment, groundwater remediation, drinking water filtration, dry cleaning, capturing volatile organic compounds from paint, gasoline dispensing operations, purifying distilled alcoholic beverage, etc.

- Activated carbons are also used for the measurement of Radon concentrations in air.
- Activated carbons are used in the treatment of poisoning.
- Activated carbons are used to store natural gas and hydrogen gas.

1.3 Water pollutants

A pollutant is a substance or energy that adversely affects the usefulness of a resource. Pollutants damage the growth rate of plant or animal species, human amenities, comfort, health, or property values. (https://en.wikipedia.org/wiki/Pollutant) Substances that causes adversely affect the water quality are called water pollutants.

Domestic wastes, chemical wastes such as pesticides, heavy metal ions food processing wastes, textile industry wastes are some of water pollutants. Waterborne diseases such as typhoid, giardiasis, amoebiasis, ascariasis, rashes, pink eye, ear ache, respiratory infections, encephalitis, hepatitis, gastroenteritis, vomiting, diarrhea, stomach aches, etc. are due to water pollution. In addition to that water pollution may lead to cancer, non-Hodgkin lymphoma, hormonal problems which disrupt reproductive processes, damage the liver, nervous system, kidney damage and DNA.

1.3.1 Dye pollution

Dyes are used in paper, pulp, textiles, leather, plastics, cosmetics and food industries (Saadiyah Ahmed Dhahir et al., 2013). The coloured contaminants discharged into environment from these industries poses hazardous problems. Presence of very small

amount of dye in water is undesirable and affects eco-system by inhibiting sunlight penetration. Treatment of effluents of dyeing industry is problematic because of high biological oxygen demand, turbidity, suspended solids, toxic constituents (Sapna Kochher & Sandeep Kumar, 2012). Dyes not only affect the photosynthetic activity in aquatic plants by reducing sun light penetration but also, they are toxic to some aquatic animals due to the presence of aromatics in them (Banat et al., 1996; Fu & Viraraghavan, (2001) and Robinson et al., 2001). Dyes are difficult to be biodegraded as they have complex aromatic molecular structures which make them more static. They also cause direct destruction of some microorganisms and inhibit their catalytic capabilities.

The textile effluent contains dyes and other auxiliary chemicals which have high pollution potential to cause serious environmental problems. According to central pollution control board, approximately a million of known dyes and dye intermediates are available, in India, out of which 5, 000 are manufactured commercially. Seven lakhs tons of dyes are produced every year (Robinson et al., 2001). 2% of the produced dyes are discharged in to effluent by the dye manufacturing industries and 10% is discharged from textile and other related industries. (Esther Forgacs et al., 2004). Environmental protection insists to use eco-friendly technologies (Desphande, 2001).

Classification of Dyes:

Dyes are classified as per their chemical structure and their application type. But classifications vary from country (Sapna Kochher & Sandeep Kumar, 2012). According to the application, dyes are classified as Direct , Acid , Azoic, Basic, Reactive, Disperse, Metal complexes, Mordant , Reactive dyes, Sulphur, Vat, Food, Pigment dyes and Whitening agents.

Dyes are classified anionic (direct, reactive and acid dyes), cationic (basic dyes) and non-ionic (disperse dyes) (Fu & Viraraghavan, 2001) based on the ionic nature of the coloured part when dissolved in water.

The chromophores are generally azo groups or anthroquinone types. The cleavage of azo group is the root cause for the release of toxic amines. Anthroquinone dyes are generally resistant to degradation and remain coloured in the medium. Reactive dyes react with cellulosic textile fibers like cotton and forming covalent bond in an alkaline condition. The reactive groups in the reactive dyes are chlorotriazine, vinyl sulphone, tri chloro pyrimidine etc. Reactive dyes are used in large amount, in recent days in textile industries mainly because of their good fastness properties, bright colour and simple application methods (Ogunlaja et al., 2013).

Dyes in the water bodies ruin the soil quality and hence spoil the ground water also. Conventional water treatment system does not remove reactive dyes, and acid dyes to a large extent. Hence, their removal is very important (Robinson et al., 2001; Juang et al., 1997). Basic dyes are highly visible even in very low concentration as they have bright colours (Banat et al., 1996; Fu & Viraraghavan, 2001; Mittal & Gupta, 1996; Chu & Chen, 2002a,). Dyes having chromium are carcinogenic (Banat et al., 1996 & Gupta et al., 1990). Disperse dyes have tendency to bio-accumulate (Banat et al., 1996). Biological water treatment is not efficient for treating dye waste water due to non-biodegradability of dyes.

1.3.2 Methylene Blue dye

(https://en.wikipedia.org/wiki/Methylene_blue)

Methylene blue is a heterocyclic aromatic chemical substance with a molecular formula of $C_{16}H_{18}N_3SCl$ and a Molar mass of 319.85 g/mol.It belongs to basic dye. Its

IUPAC name is 3, 7-bis (Dimethylamino)- phenothiazin-5-ium chloride. At room temperature, it is an odourless, dark green powder. When dissolved in water it yields a blue coloured solution. It is a potent cationic dye with maximum absorption of light around 680 nm. It is used as a stain and as a pharmaceutical drug. The hydrated form has 3 molecules of water per molecule.

Its harmful effects are hypertension, precordial pain, dizziness, mental confusion, headache, fever, staining of skin, fecal discoloration, vomiting, nausea, abdominal pain, discoloration of urine and bladder irritation

Figure 1.1 Structure of Methylene blue

1.3.3 Turquoise Blue dye

Turquoise Blue dye is an anionic dye used in textile industries. Its molecular formula is $C_{32}H_{14}CuN_8Na_2O_6S_2$. Its deep blue colour aqueous solution absorbs a maximum of light around 605 nm.

Figure 1.2 Structure of TB dye

1.3.4 Dye removal Techniques

Waste water containing dyes is treated using aerobic or anaerobic treatment [7] coagulation flocculation [6], Electrochemical methods [8], Membrane filtration [9] and adsorption methods [10].

1.3.5 Heavy Metal Pollution

The definition for heavy metal is 'metal with density above 7g/cm³ and elements having specific gravities greater than 4.0 and lying in between the copper and bismuth in the periodic table'. (http://en.wikipedia.org/wiki/Heavy metal>Sankaranarayan and Mathyashtha, 1985). Some heavy metals are essential to living organism for their biological activity but when their amount exceeds a certain tolerance limit (threshold limit), they become toxic to them. Heavy metals resist bacterial attack and any other degradation processes .Hence they permanently exist in the environment (El-Nady and Atta *et al.*, 1996).Therefore presence of heavy metals in the environment is a major problem to all living organism. Causes for the heavy metal pollution in water are natural geological weathering, metallurgy of ores, metal coating, use of metals, landfill waste, urban run-off, livestock, re-use of drainage water, fertilizers, pesticides, etc. in agriculture. Heavy metals enter into soil through leaching.

World Health Organization (WHO) insists that the elements antimony, aluminum, arsenic, beryllium, barium, cadmium, chromium, cobalt, copper, lead, iron, manganese, nickel, mercury, palladium, tellurium, selenium, zinc and tin are to be handled with great care. Some of these elements like copper, iron, zinc and trivalent chromium are essential to human physiology at trace levels, but most of them are highly toxic and dangerous specifically arsenic, lead, mercury and cadmium, compounds. These elements have great affinity for sulphur which collapse functions of enzymes.

Carboxylic acid and amino group of protein are bound with heavy metals through dative bonds. Some heavy metals precipitate phosphate and also catalyze the decomposition of bio-compounds. Presence of heavy metals in aquatic medium is tend to bio accumulate (Johnson et al., 2002). Bioaccumulation is an increase of concentration of chemicals in an organism which cause chronic toxicity. (Horsfall and Spiff *et al.*, 2005; Igwe and Abiaet *et al.*, 2003).

The non- biodegradable heavy metals are major reasons for the diseases like cancer, kidney failure, metabolic acidosis, oral ulcer, renal failure, and several health problems to animals, plants, and human beings. Therefore removal of heavy metals from wastewater is the most important one (Bernard *et al.*, 2013).

The important disasters are mercury poisoning to painters in Mina Mata, Japan, mercury poisoning to fishes in Sandoz, Mexico, Sulphur, lead, copper, zinc and cadmium poisoning to bird as well as fisheries in Coto De Donana, Spain. Heavy metals present in aqueous solution as free-ions and as complexes with organic and inorganic ligands.

1.3.6 Chromium

(http://www.lenntech.com/periodic/elements/cr.htm)

Chromium is used in alloys, chrome plating and metal ceramics. Chromium is also used in dyes and paints. Chromium salts are used in the production of coloured glasses. Chromium compounds are used as a catalyst mainly in the tanning of leather. Chromium (IV) oxide (CrO2) is used to manufacture magnetic tape.

Animal kingdom including human beings is exposed to chromium through breathing, eating or drinking and skin contact with chromium or chromium compounds. Contaminated drinking well water may contain the dangerous chromium (IV); chromium (VI) compounds.

Chromium (III) is an essential nutrient for human and its shortage cause disruptions of metabolisms and results in diabetes. But the intake of too much chromium (III) can cause health effects as well. Chromium (VI) is the most dangerous compound to human health. Chromium (VI) causes various health effects. It can cause allergic reactions when contact with skin, stomach upset, ulcers, respiratory problems, weak immune systems, alteration of genetic material, lung cancer, carcinogenicity, kidney damage and liver damage.

1.3.7 Heavy metal removal methods

Heavy metal removal technologies are coagulation, precipitation, ion-exchange, solvent extraction, membrane processing, complexation, ultra-filtration, foam floatation, electrochemical operations, cementation, and membrane operations and adsorption onto activated carbon (Rich and Cherry, 1987, Low *et al.*, 1991). The main drawback of precipitation is sludge production. Though ion exchange is a better technique, it is not economically viable because of the high operational cost. Adsorption method is the best method among all other methods for treating domestic as well as industrial effluents. The sorption process has the advantages of low operating cost, low volume of chemicals and biological sludge to be disposed off and high efficiency for even very dilute effluents. Conventional techniques such as precipitation and ion exchange methods are not efficient in the case very low concentrations (between 1 and 100 mg/ L). In the point of economic view, low-cost sorbents based on agricultural wastes can be a promising alternative.

1.3.8 Pterocarpus marsupium

Pterocarpus marsupium is a large tree with branches reaching a height of up to 33 meters. It is a multi-purpose tree which gives a very valuable timber; it is often planted by the Indian forestry. It is also grown as a shade tree in coffee plantations and in ins home gardens. It is commonly harvested for medicinal purposes as well as providing food and a range of commodities. The wood log is strong, tough, very hard, durable, takes a fine polish and seasons well. Its wood is used for musical instruments, door and window frames, posts, agricultural implements, boat building, carts, railway carriages, railway ties and other various purposes. The tree is found in central and peninsular India, mainly in dry mixed deciduous tropical forests of Gujarat, Madhya Pradesh, and sub-Himalayan tracts, at up to 1000 m altitude.

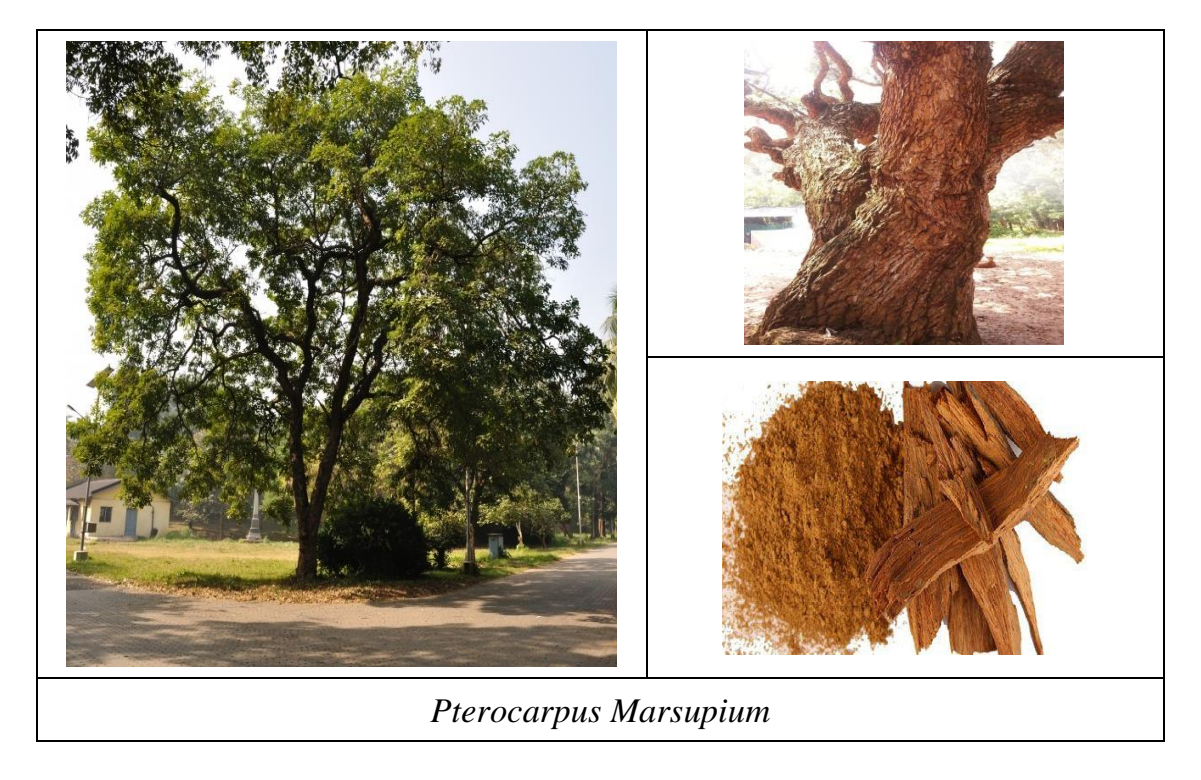


Figure 1.3. Pterocarpus Marsupium

Objective and Scope of the Present Study

Now a day's environmental pollution is becoming a major threat to the living organisms in the earth. The growth of industries in recent decades is tremendous which simultaneously causes environmental issues. Industrial effluents contain various types of organic and inorganic pollutants which affect the aquatic flora and fauna and cause many diseases. Heavy metals and Dyes are significant are water pollutants.

Dye pollutants in the industrial waste water can be removed using aerobic or anaerobic treatment (Hosseini Koupaie *et al.*, 2011), coagulation (García-Montaño *et al.*, 2008) membrane filtration (Alventosa-deLara *et al.*, 2012) and electrochemical treatment (Körbahti *et al.*, 2011). Heavy metal pollutants in the waste water can be removed by electrochemical operations, chemical precipitation, complexation, ion exchange, cementation and membrane operations methods (Rich and Cherry *et al.*, 1987; Low *et al.*, 1991).

Each method has its own advantages and disadvantages. But adsorption technology (Zhang *et al.*, 2014) can be used to remove both dyes and metal ions with less operating cost. Various kinds of adsorbents are in used for the above purposes but activated carbon has attracted special attention as adsorbent because of its good mechanical properties. Well-developed porous structure and huge surface area with active sites.

Generally activated carbons are prepared from coal, peat and lignite in conventional methods which are more expensive. Hence non-conventional materials are tried in recent days to prepare low-cost activated carbon. Earlier researchers produced activated carbons from abundantly available cheap materials like wood, barks and other lingo cellulosic materials. Hence this present work is aimed to prepare activated carbon from waste plant biomass by different chemical activation methods.

2.1 Objective

The objective of this present work is to prepare different adsorbents from waste plant biomass, the barks *Pterocarpus Marsupium* using phosphoric acid and microwave heating method for the removal of dyes and metal water pollutants through adsorption technique.

Specific Objectives:

- ✓ To prepare three different kind of activated carbons from the barks *Pterocarpus Marsupium*. First one is by carbonizing the precursor using phosphoric acid activation method followed by micro wave physical activation and designating it as *Pterocarpus Marsupium* Bark Carbon (PBC). Second one is by modifying the surface of the PBC using hydrochloric acid (Acid modified *Pterocarpus Marsupium* Carbon). Third one is by modifying the surface of the PBC using potassium hydroxide (Base modified *Pterocarpus Marsupium* Carbon).
- ✓ To determine the physicochemical characteristics of the prepared three carbons.

 Intended physicochemical characteristics are surface area, bulk density, moisture content, ash content, water-soluble matter, acid-soluble matter and pH_{zpc} of the prepared activated carbons
- ✓ To analyse the functional groups present on the surface of the prepared three activated carbons using Fourier Transform Infra-Red spectra.

- ✓ To examine the surface morphology of the prepared three activated carbons using Scanning Electron Microscopy.
- To evaluate the adsorption behaviour of the prepared three activated carbons with the cationic dye Methylene blue, anionic dye Turquoise blue (TB) and a carcinogenic metal ion Cr (VI), under batch mode equilibration experiments
- ✓ To determine the optimum pH of the aqueous solution and optimum dosage the adsorbents for each activated carbon and for each chosen adsorbates.
- ✓ To investigate the effect of contact time between adsorbent and adsorbate, initial concentrations of adsorbates and temperature of the solution.
- ✓ To determine the equilibriation time and equilibrium adsorption capacity
- To understand the adsorption kinetics using Lagergren, Ho and Webber-Morris equations respectively for pseudo-first order, pseudo-second order and intraparticle diffusion models and selecting the best kinetic model between pseudo-first order and pseudo-second order adsorption using a statistical tool, Mean of the sum of the squared error (MSSE).
- To fit the equilibrium quantity values in Langmuir, Freundlich Temkin and Dubinin- Radushkevich adsorption isotherms to understand the adsorption process.
- ✓ To determine the thermodynamic quantities of the adsorption process.
- ✓ To understand desorption and re- adsorption process, in order to know recovery of the adsorbates and regeneration ability of the spent adsorbent.

2.2 Scope

Chosen heavy metal ions Cr (VI), is toxic when it exceed the threshold limit in water bodies. This Cr (VI) metal ions is present in the effluents of electroplating, leather, metal processing and dyeing units which pose serious environmental issues because the

accumulation of very low concentration of this metal ions in living organisms will cause several disorders and diseases.

All water soluble dyes when dissolved in water gives ionic species. Depending upon the nature of the charge of coloured part, dyes are categorised as cationic dyes and anionic dyes. If the coloured part of the species is positively charged, it is called cationic dye. If the coloured part of the species is negatively charged, it is called anionic dye. To justify the adsorption potential of the adsorbent it is necessary to select cationic dye and anionic dye. Methylene blue is selected for cationic dyes category and Turquoise blue dye is selected for anionic dyes category. Generally Methylene blue is always preferred as an adsorbate in the adsorption study as it is has good adsorbing power. Turquoise blue is widely used dye in dyeing industries.

Adsorption is one of the oldest and widely used techniques for tertiary water and wastewater treatment. A lot of materials are used as adsorbents. Each adsorbent has its own advantages and disadvantages. But activated carbon is the most popular adsorbent.

Coal is commonly used precursor for the production of activated carbon .But Coal has different surface properties and has different sorption properties Commercial activated carbon is expensive due to high production cost (Abdullah *et al.*, 2009). This high cost has made the researchers to search for alternative adsorbents. Low-cost adsorbents prepared from waste solid and agricultural materials have attracted the researchers in the recent decades.

Waste plant biomass offers an inexpensive and renewable source for the preparation of activated carbon. Therefore, the conversion of this waste plant biomass into activated carbons would be a worthy process.

Many researchers used barks as precursors. Tree barks are common forestry waste, low value products, which are often burned as a fuel or treated as waste material. In these present study barks of the *Pterocarpus Marsupium* is selected as precursor for the preparation of activated carbons. *Pterocarpus Marsupium* tree is found in all over the India and is mainly used for timber purpose. While making timber from the wood logs of *Pterocarpus Marsupium* tree, barks are discarded as waste plant bio mass which causes gaseous pollution while used as fuel. Present study is to convert it as value added product. This value-added application of *Pterocarpus Marsupium* tree bark has important implications for both society and the environment.

The chemical activation methods gives activated carbons with higher porosity, higher yields with less damage to fiber materials. Hence, chemical activation method is preferred than the physical activation method. The most important reagents used for chemical activation are phosphoric acid, zinc chloride and potassium hydroxide.

According to Laine and Lunes, (1992) phosphoric acid activation gives heterogeneous carbon with microporosity. The phosphoric acid increases the volume of micropores with a common proportion. Further, phosphoric acid develops meso and macroporosity. (Garrido et al., 1987).

Recently, microwave energy is used in several fields like research and industrial processes (Yagmu *et al.*, 2008). Microwave heating is based on dielectric changes due to induced or permanent dipoles. Ion conduction and dipole rotation inside particles plays vital role in the energy conversion (Foo and Hameed *et al.*, 2012; Zhao *et al.*, 2012). According to Yagmur *et al.*, (2008), microwave heating would improve the consistent micropore surface area and pore volume of the activated carbon. Hence of microwave heating is adopted instead of conventional muffle furnace heating.

Adsorption being the surface phenomenon, its efficiency relies mainly on the surface chemistry of the material. The method of surface modification and the nature of the material have significant impacts on surface functionalities.

Surface modification by chemical method is a technique that alters the structure and the surface properties of the activated carbon to enhance its adsorption processes. The present work intends to understand the efficiency of the acid as well as base modification on the carbon prepared by phosphoric acid activation method.

The acid modification is an example of a typical wet modification process and can be carried out using mineral acids such as HNO₃, HCl, H₂SO₄, H₃PO₄ and HCl (Vlasova et al., 2003; Belchinskaya et al., 2015;Liu and Xiao, 2018). Organic acids are generally used owing to their low strength (Terrazas et al., 2005; Kong et al., 2014). Acidification of surface of adsorbent improves the acidic behaviour and hydrophilic nature of the surface by reducing the mineral content (Rehman et al., 2019).

An acid treatment enhances the adsorption of positively charged ions. Many researchers have used the acid-modified adsorbents for water decontamination. In this regard HCl acid is used for acid modification in this present study.

Many researchers have used the alkali-modified adsorbents (Hayati and Mahmoodi, 2012; Ofudje et al., 2015 Przepiórski, 2006; Gao et al., 2013). Zheng et al. (2013) found a significant reduction in the surface oxygen-containing functional groups with the increase of specific surface area and the pore volume. According to Rehman et al. (2019) an adsorbent treated with alkali enhances the adsorption of negatively charged species. Alkali modification can be carried out with NaOH, KOH, LiOH, Na₂SiO₃, Na₂CO₃ and oxides. In this regard KOH is used for alkali modification in this present study.

The literature survey infers that no one has prepared the activated carbon from the barks of *Pterocarpus Marsupium* by the above chosen methods. Biomasses are susceptible to pest decomposition. But carbonized material can have a longer shelf life with more surface area and good mechanical strength which are the requirements for a good adsorbent. Hence, the present investigation would be helpful for the abatement of pollutants from the aqueous media through adsorption.

Review of Literature

This chapter deals with a comprehensive literature survey related to the present research work. This chapter includes the review on activated carbon, the precursor *Pterocarpus Marsupium* roxb, barks, phosphoric activation method, chosen dyes, chosen metal ion and few recent adsorption works

3.1 Literature review on activated carbon

Charcoal and sand filters were used for the purification of drinking water by the ancient Hindus in India (450 B.C). Animal and vegetable carbons were used for the treatment of a lot of diseases in 157 AD. Specific adsorptive capacity of charcoal; volumes of gases adsorbed by carbons derived from different sources were determined in1773 AD. The capacities of charcoals to adsorb vapours from different organic chemicals were reviewed in 1785. Granulated bone char as a decolourant was used by most of the sugar refining industries during 1815. Dependency of decolourising property of carbon on the source material, thermal processing and the particle size were demonstrated in 1822. The industrial production of activated carbon from coal began to replace the bone char in the sugar refining process in 1900. In 1909, the first powdered commercial activated carbon (PAC) was produced in Europe. Then onwards it came into wide usage. Two varieties of carbons were produced from sawdust using zinc chloride activation, in Czechoslovakia during 1935- 1940 (Senthilkumar, 2014). Nowadays phosphoric acid activation was popularly used. The adsorbing ability of activated carbons are due to their porous structures and presence of oxygenated functional groups on their surface which depends on the precursor's nature and activation procedures. (Bansal et al., 1988)

3. 2 Literature review on *Pterocarpus Marsupium roxb*.

Abinaya and Sivajiganesan studied the adsorption of N-Blue dye ions from aqueous solution on Micro Wave assisted Pterocarpus Marsupium Bark Carbon (MWPMBC). Analytical techniques have been employed to find characteristics of adsorbent materials. The adsorption study was conducted in batch system. Equilibrium adsorption data were analysed using the adsorption isotherm models: Langmuir, Freundlich, Temkin, Dubinin-Radushkevich .They demonstrated that the prepared adsorbents performed better than widely used commercial adsorbents.

3.3 Literature review on activated carbon prepared from barks

Damilola Momodu et al. (2016) prepared an activated carbon from tree bark (ACB) by a facile and environmentally friendly activation and carbonization process at different temperatures (600, 700 and 800 °C) using potassium hydroxide pellets with different mass loading. The physicochemical and microstructural characteristics of the as obtained material had interconnected microporous/mesoporous architecture. The surface area increased with the increase of carbonization temperatures. The maximum surface area obtained was 1018 m2 g-1 witha high pore volume of 0.67 cm³g-1. The ACB material was used as super capacitor electrode in both a three and two-electrode configuration in different neutral aqueous electrolytes. The electrodes exhibited electric double-layer capacitor (EDLC) behaviour in several electrolytes

Ronak Rahimian and Soroush Zarinabadi (2020) prepared an activated carbon from an almond shell by of chemical activation using phosphoric acid activating agent. It was found that phosphoric acid activating agent increased surface area and adsorption capacity. They proved that the smaller the almond shell particles had higher the contact area for the activating agent which resulted increased absorption.

Apipreeya Kongsuwan et al (2009) used eucalyptus bark as a precursor for the production of activated carbon using phosphoric acid activation process and performed sorption of binary component copper and lead ions and found that optimal pH was 5. The maximum sorption capacities for Cu (II) and Pb (II) were 0.45 and 0.53 mmol g_1. Carboxylic, amine and amide groups were found to involve in the sorptions of Cu (II) and Pb (II). A major mechanism for the uptake of both heavy metals was not ion exchange mechanism but adsorption. Pb (II) ion was adsorbed in a greater amount than Cu (II).

Lu Luo et al (2019) et al were prepared a low-cost activated carbon from forestry fir bark waste using KOH activation method. This activated carbon demonstrated high surface area (1552 m2 g-1) and high pore volume (0.84 cm3 g-1), which caused excellent adsorption methylene blue dye (MB). Equilibrium data were fitted into three nonlinear isotherm models Freundlich, Langmuir and Temkin. Freundlich and Temkin isotherms were best fitted. Kinetics study showed that adsorbent followed pseudo-second-order model.

Feihu Zhang et al (2020) produced activated carbon using the phosphoric acid activation method from barks of Acacia mangium Thermodynamic and kinetic characteristics of phenol adsorption were investigated. The results indicated that the best conditions for the preparation of activated carbon from the bark were phosphoric acid concentration of 50 %, carbonization temperature of 500°C and carbonization time of 90 min. 53.04 % removal of methylene blue adsorption was observed with 6.0 mL/0.1 g. The adsorption behaviour was well expressed by the Freundlich isotherm adsorption equation, and McKay second-order kinetic equation.

3.4 Literature review on phosphoric acid activation

Phosphoric acid was used for activation of variety of cellulosic precursors like coconut shells (Laine et al., 1989), white oak (Jagtoyen & Derbyshire, 1993), nut shells (Toles et al., 1998), peach stones (Monlina et al., 1996), cotton stalks (Girgis & Ishak, 1999), apple pulp (Garcia et al., 2003), Arundo donax cane (Vernerson et al., 2002), Pecan shells (Dastgheib & Rockstraw, 2001), sugarcane bagasse (Girgis et al., 1994; Ahmedna et al., 2000) and peanut hull (Girgis et al., 2002).

Jagtoyen and Derbyshire, (1998) proved that thermal or chemical activation of lignocellulosic materials provoked dehydration, depolymerization and cross linking of biopolymers

Dastgheib & Rockshaw (2001) observed that large surface area (1071 m² g⁻¹) for an activated carbon at temperature 500°C when they prepared activated carbon from pecan shell in the presence of phosphoric acid and air.

Philip & Girgis, (1996) prepared activated carbon from apricot stones using phosphoric acid and found to have high surface area with microporous structure.

Molina et al., (1995, 1996) obtained activated carbon having small proportion of mesoporous network with well-developed microporous structure from peach stones by phosphoric acid activation. They further activated it by CO₂ gas at 825°C.

Girgis et al., (2002) and Guo & Lua, (2000) developed activated carbon from peanut hull and oil palm stones using phosphoric acid, potassium hydroxide and zinc chloride. According to them, phosphoric acid and zinc chloride activation produced mainly microporous network but potassium hydroxide yielded well-developed mesoporous activated carbon.

Activated carbon was prepared from vineyard shoot using phosphoric acid by Corcho et al., (2006). They found that the porosity was better than the activated carbon prepared from the raw material impregnated followed by heating at intermediate temperatures.

Haimour & Emeish, (2006) prepared activated carbon from date pit using phosphoric acid and observed that iodine number increased with the increase of activation temperature, further they reported that the increases of impregnation caused an oscillation in the iodine number.

Senthil kumaar et al., (2006) produced activated carbon from male flowers of coconut tree and jute fibre using 15% phosphoric acid in the ratio 1:3. The result indicated the carbons obtained from coconut flower carbon and jute fibre had 328 and 680 m2/g surface area, 72.36% and 76.14% porosity and 6.23 and 4.56 pHzpc for respectively. This revealed that the fibrous materials gave a large surface area than the other cellulosic materials.

Baccar et al., (2009) prepared phosphoric acid activated carbon from olive-waste cake using. They observed that the surface area increased from 716 to 1020 m²/g with the increase of acid concentration acid from 35 to 65%. Acid concentration more than 85% did not show noticeable increase in the surface area.

Lim et al., (2010) prepared phosphoric acid activated carbon from palm shells. According to them the maximum yield was around 50% in varying impregnation ratio (IR). They observed the improvement of textural characteristics with increase of impregnation ratio up to 2 and beyond that the textural character of the carbon found to decrease. The BET surface area was found to be $1109\text{m}^2/\text{g}$ with an average pore diameter of 3.2 nm and with a pore volume of $0.903\text{cm}^3/\text{g}$ when the IR was 3.

3.5 Literature review on micro wave activation

Mahtab Hejazifara et al. (2011) prepared granular activated carbon from Grapevine rhytidome (the outer layer of bark on trunk) to remove methyl violet dye from aqueous solution. They optimized the preparation conditions from the effects of the different parameters, such as phosphoric acid concentration, acid/precursor weight ratio, impregnation time, microwave power, radiation time and oven heating time. They studied the equilibrium and kinetics of adsorption of methyl violet onto the activated carbon and compared the results with the commercial granular activated carbon. The rate of adsorption onto the prepared activated carbon was found to be faster than commercial activated carbon.

Azrina Aziz et al (2021) optimized the preparative conditions of coconut-shell-based activated carbon (CSAC) and adsorption performance in removing Dichloro Diphenyl Trichloroethane (DDT). The CSAC was prepared by activating the coconut shell via single-stage microwave heating under carbon dioxide flow. The total pore volume, BET surface area and average pore diameter of CSAC were found to be 0.420 cm³/g, 625.61 m²/g, and 4.55 nm, respectively. The surface of the carbon was negatively charged as shown by the zeta potential study. Response surface methodology (RSM) inferred that the optimum preparation conditions were 502 W and 6 min radiation time, which corresponded to 37.91% of CSAC's yield. Isotherm study inferred that DDT-CSAC adsorption system was best described by the Langmuir model with monolayer adsorption capacity of 14.51 mg/g. The kinetic study revealed that the pseudo-second-order model fitted well with this adsorption system. Tonghua Wang et al (2009) applied the microwave heating and ZnCl₂ as activation agent to prepare activated carbon from wood. The process took a few minutes only. The pore structure and surface area of the

prepared carbon materials were tuned by simply changing the ratio of ZnCl₂ to wood and the microwave heating time.

Qing-Song Liu et al (2010) prepared a bamboo based activated carbon with microwave-induced activation process using phosphoric acid as the activating agent. On comparison with the conventional thermal process, the microwave-induced activation process had faster activation rate and higher carbon yield.

3.6 Literature review on surface modification of activated carbons

O. A. Babatunde et al (2016) prepared an activated carbon from *Cocos nucifera*, modified using nitric acid, acetic acid, ascorbic acid and sodium hydroxide. The effect of this chemical modification was evaluated using iodine and carbon tetrachloride adsorption. Characterization of the activated carbons showed a greater development of macro porosity because of the modification. FTIR spectra displayed the presence of carboxyl, hydroxyl, and carbonyl functional groups.

M. Lesaoana et al (2019) prepared activated carbons from *Macadamia* by impregnating with different concentrations of sulphuric, phosphoric and nitric acid ranging from 20 to 60% v/v and heating in a muffle furnace to improve the structural characteristics of the adsorbents for an enhanced removal Cr (VI) ions. The %S content ranging between 2.27 and 3.23% was fond in H2SO4 treated activated carbon the due to incorporation of sulphonate groups during modification. Fourier transform infrared spectroscopy inferred the presence of CN, NO, sulphur and phosphorus peaks proving efficacious attachment of the functional groups because of acid treatments. The surface area of increased from 545 to 824m2/g because of the acid treatment. The removal mechanism was explained by both the Langmuir monolayer and Freundlich multilayer isotherms.

3.7 Literature review on Turquoise blue dye adsorption

Alhayat Getu and Omprakash Sahu (2014) produced an activated carbon from Tapioca peel and used for the adsorption of reactive dye Turquoise Blue H5G from its aqueous solutions. Optimum pH value was determined as 7. Maximum dye was removed within 120 min.

Batch and fixed bed experiments were carried out for the removal of Reactive Turquoise Blue Q-G125% (TB) dye from aqueous solution using cashew apple bagasse (CAB) adsorbent by N. C. G. Silva et al (2015). CAB, a lignocellulosic material and characterized as nonporous material and its surface area cannot be determined by nitrogen adsorption at 77 K. The pseudo-second-order model best described the adsorption kinetic data. The adsorption isotherms of TB onto CAB were well fitted well by the Freundlich model. The maximum adsorption capacity 145.10 mg/g and high levels of dye removal (> 90%) were observed at 60°C. According to thermodynamic results, the adsorption was a spontaneous endothermic process.In the column adsorption study the adsorbed quantity was 32 mg/g with 100 mg/L TB initial concentration at 1 mL/min flow rate and 1.4 cm bed-height.

D. Schimmel1 et al (2010) described the adsorption of reactive Turquoise blue QG dye onto commercial activated carbon in a batch reactor. The kinetic studies were carried out at a pH of 2 and at three different temperatures: 30°C, 45°C and 60°C. Pseudosecond-order models well described the kinetics of dye adsorption.

Pumpkin peel (*Cucurbita pepo L*.) and bracts of Plantain flower (*Musa acuminate*) were modified into activated carbon for the adsorption of turquoise blue dye (TB) by Pamila Ramesh et al (2021). ANN result showed that Levenberg-Marquardt

(LM) algorithm was the best model bearing coefficient of regression (R^2) as 0.9968 and mean square error (MSE) as 0.00013 for the dye removal.

3.8 Literature review on Methylene blue dye adsorption

P. Satheesh Kumar et al (2017) described the feasibility of using Lagerstroemia indica seed (LIS) activated carbon for the cationic dye (methylene blue MB) adsorption from aqueous solution. Maximum colour removal was observed at higher pH. Dye removal was found to decrease from 93% to 85% as the dye concentration was increased from 10 mg/l to 40 mg/l. A maximum removal of 93% is obtained at higher pH. The obtained results showed that the sorption of MB by LIS was best described by the pseudo-second order kinetic model. The results of sorption equilibrium studies indicated that the Langmuir and Freundlich model fitted the data in a better way

Patience Mapule Thabede et al (2020) prepared a carbon from Black cumin seeds (BCC) and then activated with 10 and 20 % sulphuric acid to get a Black cumin activated carbon (BCAC-10) and (BCAC-20) respectively. Adsorption of lead (Pb (II))ions and methylene blue (MB) dye from aqueous solution was studied using the prepared carbon. FTIR results showed the (-COO-), (-NH2), (-HSO-4), (-C=O) functional groups were involved in the adsorption processes of Pb (II) ions and methylene blue (MB) dye. There was an increase in surface area and pore size for both BCAC-10 and BCAC-20 when compared with BCC. The equilibrium data for Pb (II) ions and MB dye were fitted Freundlich isotherm model onto BCC, BCAC-10 and BCAC-20.

Sulphuric acid was utilized by Ali Jawad *et al.*, (2016) for the preparation of activated carbon from a biomass solid waste and coconut leaves as an activator. This sulphuric acid activated carbon was used for the removal of methylene blue dye from aqueous solution. Equilibrium and kinetic studies in batch mode were evaluated by varying

adsorbent dose (0.2–2.5 g/L), solution pH (3–11), initial dye concentration (30–400 mg/L), contact time (0–180 min) and temperature (303–323 K). The Langmuir isotherm model showed fitted well with the equilibrium data than the Freundlich model. The adsorption capacity (q_m) increased with temperature (126.9 mg/g at 303 K, 137.0 mg/g at 313 K and 149.3 mg/g at 323 K). The kinetic results were well described by the pseudo-second order kinetic for each temperature. The activation energy was 29.7 kJ/mol.

Selhan Karago *et al.*, (2008) prepared activated carbons from sunflower oil cake by sulphuric acid activation with different impregnation ratios and used for the removal of methylene blue (MB) from aqueous solutions as adsorbents. Langmuir isotherm showed better fit than Freundlich isotherm for all activated carbon samples. The kinetics of adsorption confirmed the pseudo-second-order kinetics with good correlation. The separation factor (R_L) revealed the favourable adsorption of the MB dye.

Sivakumar *et al.*, (2012) prepared activated carbon from *Balsamodendron* caudatum wood waste by chemical processes and showed excellent improvement in the surface characteristics and with surface functional groups. These activated carbons contained micropores, mesopores and macropores. The volume of these pores varied with the nature of activating agents used. Results of this investigation indicated that the activated carbon prepared using H₂SO₄ impregnation process had the highest surface area and more developed micro, meso and macroporosity.

3.9 Literature review on Cr (VI) ions adsorption

Saroj K. Sharma et al (2008) studied the removal of a chromium in drinking water by applying different treatment methods such as coagulation followed by filtration, ion exchange, adsorption and membrane filtration. They concluded that adsorptive filtration and ion exchange methods are suitable for small-scale applications.

Xin-JiangHu et al (2011) studied the adsorption of chromium (VI) ions from aqueous solution by ethylenediamine-modified cross-linked magnetic chitosan resin (EMCMCR) in a batch adsorption system. Optimum adsorption was observed at pH 2.0. The adsorption rate was found to be extremely fast and the equilibrium was established within 6–10 min. The adsorption data was well interpreted by the Langmuir and Temkin model. The maximum adsorption capacities obtained from the Langmuir model were 51.813 mg g⁻¹, 48.780 mg g⁻¹ and 45.872 mg g⁻¹ at 293, 303 and 313 K, respectively. The adsorption process was delineating by pseudo-second-order kinetic model.

E Mekonnen et al (2015) investigated the adsorption of Cr (VI) onto some selected local adsorbents. Locally available biomasses were obtained from avocado kernel seeds (AKS), *Juniperus procera* sawdust (JPS) and papaya peels (PP) and investigated the removal of Cr (VI) using them as adsorbents. Optimum parameters for the adsorption of 5mg L⁻¹ Cr (VI) was pH: 1, adsorbent dose: 0.5 g, contact time: 160 min and temperature: 313 K. The equilibrium data was best fitted to the Freundlich adsorption isotherm model. The results of kinetic models showed that the pseudo-second-order kinetic model was best correlated the experimental data. The results of thermodynamic parameters showed that the adsorption process was feasible. The positive values of the entropy change suggested the increased randomness at solid-liquid interfaces during the adsorption.

Vinod K.Gupta et al (2010) examined the adsorptive removal of hexavalent chromium from aqueous solution using a low cost fertilizer industry waste. The maximum adsorption was found at 70 min, pH2.0 for the dose of 4.0 g/L at 303 K temperature. Maximum adsorption capacity (15.24 mg/g) of Cr (VI) was observed for 100 mg/L initial Cr (VI) concentration. Langmuir and Freundlich adsorption isotherm models were applied to analyze adsorption data, and found that both were applicable to

this adsorption system in terms of high regression values. Thermodynamic parameters showed that the adsorption of Cr (VI) was feasible, spontaneous and exothermic. Kinetics of adsorption was found to follow the pseudo-second-order rate equation.

Fatemeh Gorzin and MM Bahri Rasht Abadi (2018) were prepared a new low-cost activated carbon from paper mill sludge to remove Cr (VI) ions from aqueous solution. The maximum equilibrium uptake of Cr (VI) was 23.18 mg g_1 at optimum pH 4.0, contact time of 180 min and temperature of 45°C. Analysis of equilibrium adsorption data in terms of many isotherm models revealed that Langmuir isotherm indicated better agreement with the experimental data. The kinetics of Cr (VI) adsorption was well described by the pseudo-second-order model which indicated the dominance of chemisorptions mechanism. Thermodynamic parameters indicated that the Cr (VI) adsorption was feasible and spontaneous.

Jonas Bayuo et al (2019) used ground nutshell as a non-conventional adsorbent for effective removal of chromium (VI) from aqueous solutions. The optimum conditions found to be contact time 120 min, pH 8.0 for the adsorbent dose of 2.0 g/L, initial metal ion concentration 25 mg/L at temperature 41.5 °C. The experimental data were analyzed using three two-parameter isotherm models. The experimental data obtained for the adsorption of chromium (VI) ion fitted well to Temkin isotherm in comparison with the other isotherm models investigated.

Experimental Methods

This chapter describes about the materials used in this work and the procedures adopted for preparation of activated carbons from the barks of Pterocarpus Marsupium by phosphoric acid method. Procedures carried out for the charecterisation of adsorbents, analytical determination of adsorbate concentration, equilibrium, kinetic, thermodynamic and desorption studies are explained.

4.1 Materials

Methylene Blue dye and Turquoise blue dye of Dye star (P) Ltd., India. and K₂Cr₂O₇ of Sigma-Aldrich were employed in this present work. Remaining all chemicals of Analar grade were purchased from MERCK chemicals, India. Double distilled water and Borosil glass wares were used throughout the work..

4.2 Barks of Pterocarpus Marsupium:



Figure 4.1 Barks of Pterocarpus Marsupium

4.3 Production of activated carbons from barks of *Pterocarpus Marsupium*

Three different activated carbons were prepared from the barks *Pterocarpus Marsupium*. First carbon was prepared using phosphoric acid activation method followed by micro wave physical activation method and designated as *Pterocarpus Marsupium* Bark Carbon (PBC). Second activated carbon was prepared by modifying the surface of the PBC using hydrochloric acid followed by micro wave activation and designated as Acid modified *Pterocarpus marsupium* Carbon (APBC). Third activated carbon was prepared by modifying the surface of the PBC using potassium hydroxide followed by micro wave activation and designated as Base modified *Pterocarpus Marsupium* Carbon (BPBC).

The small pieces of dried barks were powdered in a pulveriser. 25 g of the powdered barks was mixed with 100 mL of phosphoric acid solution of desired concentration (25, 50 and 75 %). To ensure the access of the H₃PO₄ to the *Pterocarpus Marsupium* Barks, the slurry was kept at room temperature for 24 hours. Then the slurry was placed to microwave heating (450, 600 and 850 watts and 10, 13 and 15 minutes) for simultaneous carbonization and activation. Then the carbonized samples were successively washed with cold distilled water, 0.5 M HCl, hot distilled water and finally with cold distilled water until the pH of the washings reach 7. Then the carbon was filtered and dried at 425 K. Adsorption of *Pterocarpus Marsupium* Barks carbon with H₃PO₄ generates more interspaces between carbon layers to more surface area and micro porosity. The increase in porosity with H₃PO₄ activation suggests that the porosity created by this reactant is due to spaces left by H₃PO₄ after the corresponding washing. H₃PO₄ activation causes electrolytic action termed as swelling in the molecular structure of cellulose, which leads to the breaking of lateral bonds in the cellulose molecules

resulting in increased inter and intra voids. Totally 27 number of activated carbons were prepared by varying preparation parameters using orthogonal array.

4.4 Optimization of adsorbent preparation parameters

In order to choose the optimum preparation parameters, adsorption capacities of the prepared samples were evaluated by taking Methylene Blue as adsorbate because MB dye is known as good adsorbates on activated carbons.

To the 25 mg of the adsorbent 50 mL of MB dye solution of concentration 100 mg/L was interacted for 1 hour with the stirring of 180 rpm in a rotary shaker.

The results obtained for different samples were given in table. 4.1.

 Table - 4.1 Pterocarpus Marsupium barks carbon Preparation parameters

Sample number	C	RP	RT	Sample Name	% of Removal
1	25	450	10	PBC1	12.25
2	25	600	13	PBC2	16.32
3	25	850	15	PBC3	18.65
4	25	450	10	PBC4	13.45
5	25	600	13	PBC5	17.42
6	25	850	15	PBC6	22.39
7	25	450	10	PBC7	22.14
8	25	600	13	PBC8	25.34
9	25	850	15	PBC9	28.54
10	50	450	10	PBC10	13.64
11	50	600	13	PBC11	17.26
12	50	850	15	PBC12	23.5
13	50	450	10	PBC13	15.01
14	50	600	13	PBC14	19.27
15	50	850	15	PBC15	24.2
16	50	450	10	PBC16	18
17	50	600	13	PBC17	20.12

18	50	850	15	PBC18	26.32
19	75	450	10	PBC19	14.92
20	75	600	13	PBC20	22.88
21	75	850	15	PBC21	31.35
22	75	450	10	PBC22	39.48
23	75	600	13	PBC23	47.695
24	75	850	15	PBC24	55.91
25	75	450	10	PBC25	25.31
26	75	600	13	PBC26	62.68
27	75	850	15	PBC27	70.15

RP= Radiation power in watts; RT = Radiation time in minutes;

C = Concentration of H₃PO₄.

The results inferred that the percentage of removal of MB dye increased with the increase of radiation time, radiation power and concentration of H₃PO₄solution. Hence the adsorbent PBC27 prepared using 75 % ZnCl₂ solution, radiation power 850 watts, radiation time 15 minutes and impregnation time 24 hours was chosen. Here after PBC27 is designated as PBC for simplicity.

The carbon which gave highest methylene blue number was chosen for further adsorption study and designated as PBC (*Pterocarpus Marsupium* barks carbon).

Known mass of the prepared carbons were mixed with 25% solution of HCl and placed in a microwave oven for 10 minutes. Then the carbon was again washed with hot distilled water followed by cold distilled water and designated as Acid modified *Pterocarpus Marsupium* barks carbon (APBC). Similarly Base modified Pterocarpus *Marsupium* barks carbon (BPBC) was prepared by using 25% solution of KOH instead of HCl.

4.5 Characterization of the prepared activated carbon

Prepared activated carbons from barks of *Pterocarpus Marsupium* were characterized by finding out their pH point of zero charge (pHzpc), Bulk density, Surface area, Moisture content, Water soluble matter, Acid soluble matter, Volatile mater, fixed carbon and ash content, yield, Iodine number and Methylene blue number using standard procedures. The surface area was obtained using the BET method with nitrogen gas adsorption at Sastra University, Thanjavur, Tamil Nadu and South India. The surface morphology was studied by SEM to view the pore development. The functional groups present on the surface were determined using FTIR. FTIR spectra and SEM were recorded at St. Joseph College, Tiruchirappalli, Tamil Nadu.

4.5.1 Determination of pH point of Zero Charge: The pH point of zero charge (pHzpc) was determined by drift method. (Lopez-Ramon et al., 1999). 50 mL of 0.01 M NaCl solutions were taken in different, Erlenmeyer flasks. The initial pH of the solution (pH) flask was made as 2, 4, 6, 8 and 10 by adding required drops of 0.1M HCl or 0.1M NaOH solutions. Then 0.5g of the adsorbent was added to each flask, closed and agitated in a shaker for 1 h and kept a side for 48 hours to attain equilibrium with occasional manual shaking. The final pH values (pH_f) of the supernatant liquids were noted. A graph is drawn taking pHi in the 'X' axis and 'pH_f' in the 'Y' axis. A straight line is drawn connecting the points where initial pH and final pH values are same (pHi = pHf). The point of intersection of the straight line and graph is taken as pHpzc

4.5.2 Conductivity: 10 g of carbon was added to 200 mL of distilled water in a beaker and agitated at 200 rpm for 1 hour. The supernatant solution was analyzed for conductivity using conductivity meter (model M-180) (ISI 1977).

- **4.5.3 Bulk Density**: Sufficient amount of carbon was poured in a pre-weighed 50 ml graduated cylinder using trip balance with constant tapping. After filling, the graduated cylinder was weighed. The Bulk density was calculated by dividing the weight of carbon by 50 (ISI 1977).
- **4.5.4 Moisture Content:** The moisture content was determined by oven-drying method. 1gram of carbon was heated to 428K temperature for 3 hrs. Then the sample was cooled in desiccator and then weighed. Weighing and cooling was continued until getting constant weight. The moisture content was determined by following the equation (ISI 1977).

% of Moisture content =
$$\frac{(M - X) \times 100}{M}$$

Where, M = Mass of the carbon (g)

X = Mass of the dried carbon (g)

4.5.5 Acid soluble matter: 10 grams of the carbon was transferred into one litre a beaker 300 mL of 0.25N HCl acid was added and heated to boiling with stirring. Stirring was continued for about 5 min even after the removal of flame. The beaker was kept aside for 10 minutes. The supernatant liquid was filtered through a Gooch crucible. The procedure was repeated thrice with the residue and using 300 mL of acid each time. After the fourth process, the filtrates were combined and concentrated to less than 100 mL and then made up to 100 mL in a SMF. Exactly 50 mL of the concentrate was taken in a china dish and evaporated to dryness. The residue was finally dried at 328 ± 5 K. The dish was then cooled in a desiccator and weighed. The above procedures of drying, cooling and weighing were repeated at 30 min. time intervals till the difference between the two

consecutive weighing's were less than 5 mg. Acid soluble matter was calculated using the following expression (ISI 1977).

% of Acid soluble matter =
$$\frac{M \times 100 \times 2}{M1 (100 \text{ X}) / 100}$$

Where, M = Mass of the residue (g)

M1 = Mass of the carbon (g)

X = % of moisture content

4.5.6 Water soluble matter: It was same procedure followed in determination of acid soluble matter but distilled water was used instead of 0.25 N HCl acid.

% of Water soluble matter =
$$\frac{M \times 100 \times 2}{M1 (100 \text{ X}) / 100}$$

Where, M = Mass of the residue (g)

M1 = Mass of the carbon (g)

X = % of moisture content

4.5 .7 **Volatile matter:** 1 g of the carbon was taken in a crucible and closed with lid in order to protect it from air contact and placed in a furnace and heated to 9273 K within 7 minutes in a furnace. Then the sample was removed, cooled in a desiccator and then weighed. The volatile matter content was determined by following the equation (ISI 1977).

% of Volatile matter =
$$\left(\frac{(M-X) \times 100}{M}\right) - W$$

Where, M = Mass of the carbon (g)

X = % of ash content

W = % of moisture content

4.5.8 Ash content: It was also determined by oven-drying test method. 1g of sample was kept in the furnace at 6773K for 3 hours. Then the hot sample was cooled in a desiccator and then weighed till getting constant weight. The ash content was determined by following equation (ISI 1977).

% of Ash content
$$=\frac{X \times 100}{M}$$

Where, M = Mass of the carbon (g)

X = Mass of the ash (g)

4.5.9 Fixed Carbon Content:

Fixed carbon is calculated using the following equation.

Fixed carbon (%) =
$$100$$
 – (moisture, % + ash, % + volatile matter, %)

4.5.10 Percentage of Yield: Yield is defined as the ratio of weight of the activated carbon obtained to the original weight of the raw material taken. When this fraction is multiplied by 100, it is called percentage of Yield. It is mathematically expressed as

% of Yield =
$$\frac{W2}{W1} \times 100$$

Where, W1 and W2 are weight of the precursor and activated carbon respectively.

4.5.11 Iodine Number: It is determined taking a known weight of the carbon in a clean, dry 250 mL iodine flask equipped with a glass stopper. 10 mL of 5 wt.% hydrochloric acid solution was pipetted into conical flask and heated gently and then boiled to remove sulphur. The flask was then removed from the hot plate and cooled to room temperature. To this 100 mL of 0.1 N iodine solutions was added, shaken and titrated against standardized 0.1N sodium thiosulphate using starch indicator. The amount of iodine

adsorbed per gram of carbon was calculated as follows (ASTM D4607, Yamaguchi et al., 1991).

Iodine number =
$$\frac{[A - ((DF) \times B \times S)]}{M}$$

$$DF = \frac{(I + H)}{F}$$

where, B is the normality of the sodium thio sulphate solution, A is the normality of the Iodine solution, I is the volume of the iodine solution (mL), H is the volume of 5% by weight of HCl (mL), F is the volume of the filtrate (mL), S is the volume of the sodium thiosulphate consumed (mL) and M is the mass of the carbon taken (g).

4.5.12 Methylene Blue Number: Known weight of the carbon was taken in a 250 mL conical flask. A few mL of Methylene Blue solution (1500 mg/L) was added and the conical flask shaken for 5 min. Methylene Blue solution is further added to the decolourised solution. The addition of the Methylene Blue solution was continued by adding 1 mL at a time with shaking the flask till the appearance of colour. One mL was subtracted from the total volume of dye solution consumed for calculation purpose. The decolourizing capacity of the carbon was determined from the following equation (BIS 877-1977, Mental, 1968).

Methylene Blue number =
$$\frac{1.5 \times V}{M}$$

Where, V is the volume of methylene blue (mL),

M is the mass of the carbon (g).

4.6 Preparation of dye solutions

The dye stock solution of 1000 mg/L was prepared by dissolving 1 g of the MB dye and TB dye in 1000 mL of distilled water. From the stock solution, required working concentration of adsorbate solution such as 75, 100, 125 & 150 mg/L and 20, 30, 40 and 50 mg/L were prepared by proper dilution.

4.7 Preparation of metal ion solutions

Cr (VI) metal ion stock solutions of 1000 mg/L were prepared A small amount say 1mL of HCl was added while preparing the Cr (VI) ion solution to avoid the hydrolysis of Cr (VI) ions. The required working concentrations 10, 15, 20 and 25 mg/L were prepared by proper dilution with double distilled water.

4.8 Batch adsorption studies

Equilibrium studies were carried out in a series of Iodine flasks of 250 mL capacity containing the 50 ml adsorbate solution of desired concentration and required amount of adsorbent. Desired pH of the solution was brought by adding drops of Con. HCl or 6N NaOH solutions. These flasks were agitated in a temperature controlled orbital shaker (Orbit, India) at 130 rpm for the desired contact time. Then the flasks were set aside for few minutes and the filtered in Whatmann filter paper (no.40). First 5 mL was discarded because filter paper may adsorb some adsorbates; next 5 mL was collected for the determination of concentration. Concentrations of the solutions were estimated by spectrometrically using standard procedures. Concentrations of the solutions were suitably diluted and measured using Systronics double beam UV-visible spectrophotometer: 2202. The wavelengths used for the chosen dyes are given in the table 4.2.

Table 4.2 Wavelength (nm) for dye ions/Metal ions

Adsorbates	Absorption maxima	
Methylene Blue dye ions	663nm	
Turquoise blue dye ions	604nm	
Cr (VI) ions	680nm	

4.9 Experimental design

Experiments were conducted to find the optimum pH for each adsorbate. Then optimum dose was found by carrying out the experiment having the optimum solution pH. Next experiments were conducted with dose of PDC ranging from 10 to 100 mg/50 mL with the lower initial concentration of adsorbate solutions (say 10 or 20 mg/L). Initial concentrations of adsorbates which give percentage of removal in between 60 and 80 were chosen for further study where the agitation time was 1 h at 305K temperature and at optimum solution pH already fixed. Then experiments were conducted with the optimum dose of adsorbent under optimum solution pH to find out the effect of contact time for chosen initial concentrations. Effect of contact time experiments was carried out till the equilibrium was achieved. Then experiments were conducted to find the effect of temperature with sufficient contact time necessary to attain equilibrium.

Equilibrium data were fitted into Freundlich, Langmuir, Temkin and Dubinin-Radus-Kevich isotherm equations. Data obtained from the effect of contact time experiment was fitted into Lagergren's pseudo first order kinetic equation, Ho's pseudo second order kinetic equation and Webber Morris intraparticle diffusion equation. Best suitable kinetic equation was selected using normalized standard deviation statistical tool.

Thermodynamic parameters were determined from the data obtained from the effect of temperature Van't Hoff's plots. Desorption, re–adsorption study was carried out. Experimental parameters such as initial adsorbate concentration, solution pH, carbon dosage and temperatures adopted in this present wok were listed in the table 4.3.

Table 4.3 Experimental parameters

Time (min)	5 to 180		
	MB dye	7	
pН	TB dye	2	
	Cr (VI) ions	2	
	MB dye	75, 100, 125 &150	
Concentration (mg/L)	TB dye	20, 30, 40 & 50.	
	Cr (VI) ions	10, 15, 20 & 25	
Adsorbent dose (mg/50 mL)	10 to 100		
Temperature (K)	305, 315. 325 & 335		

Range of pH of the dye solutions were decided depending upon the color change of dye with respect to pH of the solution. Initial concentration range for dye solutions was 75 to 150 mg/L for MB dye and 20 to 50 mg/L for TB dye whereas for Cr (VI) ion solutions were 10 to 25 mg/L.

Mass balance equations adopted for the calculation of percentage of removal, the quantity of adsorbate adsorbed (q_t) at time "t", quantity (q_e) of adsorbate adsorbed by adsorbents at equilibrium are given below.

% of Removal =
$$\frac{(C_i - C_t) \times 100}{C_i}$$

$$q_e = (C_i - C_e) \frac{v}{w}$$

$$q_t = (C_i - C_t) \frac{V}{W}$$

Where, V is the volume (L) of the solution, "W" is the mass of the adsorbent (g), Ci, Ct, and Ce are the initial, at time "t," and equilibrium concentrations (mg/L) of the adsorbates, respectively.

4.10 Physico-Chemical Characteristics

4.10.1 Particle size

Smaller particles will have more surface area and hence have more adsorption capacity because of the more adsorption sites per unit mass of the adsorbent. But particles having very low sizes may have lower bulk density and also lower mechanical strength. Hence particles having moderate size were chosen for the present investigation balancing between the surface area and mechanical strength. The selected particle size for the present study was 53 to 90 μ m.

4.10.2 Bulk density

The Bulk density gives an idea about the space present in the material column. Higher bulk density value represents the space occupied by the low material. Further, it is very useful to estimate the packing volume and also the amount of carbon needed for treatment. Higher bulk density will cause faster settling rate and low volume of sludge which is advantageous for the dewatering process (Umoren *et al.*, 2013). The observed apparent density of PBC, APBC and BPBC are 0.52, 0.74 and 0.64 (g/mL) respectively. These low values are due to porous structure caused by micro-crystallites in a random arrangement and with

strong cross-linking between them (Nageswara Raoet *et al.*, 2011). The lower value of PBC, when compared to APBC and BPBC, infers the more porous nature of APBC than BPBC and PBC.

4.10.3 Surface area

Higher Surface area is an essential character of a good adsorbent, which decides the adsorption capacity of the adsorbent because the number of adsorption sites is directly proportional to the surface area. The surface area of an adsorbent depends upon the raw material used for the preparation and the nature of activation method adopted. Usually, the higher surface area of activated carbon prepared from plant biomass was due to the removal of organic content such as esters, humic, lignin substances and waxes. (Jia *et al.*, 2002). The surface area of the PBC, APBC and BPBC are 586, 594 and 574 (m²/g) respectively. The higher value of APBC, when compared to PBC and BPBC, infers the more porous nature of APBC than BPBC and PBC.

4.10.4 Moisture content

Lower moisture content is the expected property for a good adsorbent because the moisture present will dilute the adsorbent when mixed with aqueous adsorbate solution. Hence the additional weight of adsorbent will be required than the expected mass. The moisture content of PBC, APBC and BPBC are 4.36, 4.98 and 5.0 (%) respectively. In general, highly porous activated carbon will have higher moisture content, especially when prepared by acid activation method. Swelling of the adsorbent during washing might be the reason (Malik *et al.*, 2006).

The observed values are comparable with the activated carbon prepared from other plant biomass (Kadirvelu *et al.*, 2001). The lower value of APBC when compared to BPBC and PBC infers the intense heating occurred during the preparation of APBC.

4.10.5 Fixed Carbon content

This property infers the skeleton of carbonin the prepared adsorbent. The higher value is beneficial (Yangand Lua *et al.*, 2003). Fixed Carbon contents of PBC, APBC and BPBC are 89.11–91.54 and 90.05 (%) respectively. In the preparation stage, concentrated sulphuric acid causes dehydration which will not affect the carbon content but activation at high temperature would volatilize some functional groups present in the material. The higher value of APBC compared to other two carbons infers the reduction in functional groups as evidenced from the FTIR spectra.

The Physico-chemical characteristics of PBC, APBC and BPBC are summed up in table 4.4.

Table 4.4 Physico-Chemical Characteristics of PBC, APBC AND BPBC

Properties	PBC	APBC	ВРВС
pH_{zpc}	7.01	6.95	6.85
Particle size, µm	53 – 90	53 - 90	53 – 90
Surface area (BET), m ² /g	586	594	574
Pore volume, cm ³ /g	0.398	0.397	0.381
Pore size (Pore width), nm	2.717	2.050	2.110
Bulk density, g/mL	0.52	0.74	0.64
Fixed Carbon, %	89.11	91.54	90.05
Moisture content, %	4.36	4.98	5.0

4.11 DATA PROCESSING TOOLS:

4.11.1 Isotherms

For solid–liquid adsorption system, adsorption isotherm is important model in the description of adsorption behavior. When the adsorption process reaches equilibrium state, the adsorption isotherm can indicate the distribution of adsorbate molecules between the solid phase and the liquid phase¹⁴⁶. It is significant for understanding the adsorption behavior to identify the most appropriate adsorption isotherm model. In this present study, Langmuir, Freundlich, Temkin and Dubinin Reduskevish isotherm were employed to investigate the adsorption behavior. Adsorption isotherm was studied at four different temperatures viz. 305, 315, 325 and 335 K.

4.11.2 Langmuir isotherm

It is a most widely used model for describing adsorbates sorption on adsorbent.

Langmuir equation relates to the coverage of molecules on a solid surface and the concentration of contacting solution at a fixed temperature.

The Langmuir adsorption isotherm assumes that adsorption takes place at specific homogeneous sites within the adsorbent and has found successful application in many sorption processes of monolayer adsorption (Langmuir.I 1918).⁷¹ The following equation is the Langmuir isotherm:

$$C_e/Q_e = 1 / Q_0 b + C_e/Q_0$$
 4.1

where C_e is the equilibrium concentration (mg/L), Q_e is the amount adsorbed at equilibrium (mg/g) Q_0 and b are Langmuir constants related to adsorption efficiency and energy of adsorption, respectively⁷². The constants Q_0 and b calculated from the slope and intercept of the plot of C_e/Q_e vs C_e are listed in Table 4.4. The essential characteristics of Langmuir isotherm can be expressed by dimensionless separation factor, R_L^{73} .

$$R_L = 1 / (1 + K_L C_0)$$
 4.2

The value of separation factor R_{L} indicates the nature of the adsorption process as given below

R _L value	Nature of the process
$R_L > 1$	Unfavorable
$R_L = 1$	Linear
$0 < R_L < 1$	Favorable
$R_L = 0$	Irreversible

4.11.3 Freundlich isotherm

The Freundlich isotherm is an empirical equation employed to describe heterogeneous adsorption process i.e. adsorption which takes place on a heterogeneous surface through a multilayer adsorption mechanism⁷⁴. The model is based on the distribution of adsorbate between the adsorbent and aqueous phases at equilibrium⁷⁵. Freundlich equation is expressed by the equation:

$$q_e = K_F C_e^{1/n}$$
 4.3

This can be linearized to

$$Log q_e = Log K_F + 1/n Log C_e \qquad \dots 4.4$$

Where q_e is the amount of adsorbates adsorbed (mg/g), C_e is the equilibrium concentration of adsorbates in solution (mg/L), K_f and n are constants incorporating all factors affecting the adsorption capacity and intensity of adsorption, respectively. The linear plot of log q_e versus log C_e gives a linear line with a slope of 1/n and intercept of log K_f .

Adsorption becomes more heterogeneous as the n value gets closer to zero and a value of n below 1 indicates a normal Langmuir isotherm while the value n above 1 is indicative of cooperative adsorption (or) favorable physical adsorption⁷⁶.

4.11.4 Temkin isotherm

Temkin isotherm model consider the effect of indirect adsorbent-adsorbate interactions on adsorption and suggests that the heat of adsorption of all molecules in the layer would decrease linearly with coverage due to these interactions⁷⁷. This model also assumes that adsorption is characterized by a uniform distribution of binding energies. The derivation of the temkin isotherm assumes that the fall in the heat of adsorption is linear rather than logarithmic, as implied in the freundlich equation. The temkin isotherm has commonly been applied in the following form

$$q_e = B_1 ln K_T + B_1 ln C_e$$
 4.5

Where B_1 (J/mg) is the Temkin constant related to the heat of adsorption and K_T is the equilibrium binding constant (Lmg⁻¹). The constant K_T and B_1 can be determined from a plot of q_e versus lnC_e .

4.11.5 Dubinin-Radushkevich isotherm

The Linear form of Dubinin-Radushkevich isotherm is 78

$$\ln q_e = \ln q_D - B\epsilon^2 \qquad \dots \dots 4.6$$

Where, q_D is the theoretical saturation capacity (mg/g) B is a constant related to the mean free energy of adsorption per mole of the adsorbate (mol²/J²) and ϵ is polanyi potential which is related to the equilibrium concentration as follows;

$$\varepsilon = RT \ln (1+1/C_e) \qquad \dots 4.7$$

A plot of ln q_e vs ϵ^2 gives a linear line and the constants q_D and B calculated from the slope and intercept respectively. The mean free energy of adsorption E was calculated from B using the following equation

$$E = 1/(2B)^{1/2}$$
 4.8

Based on this energy of activation we can predict whether an adsorption is physisorption or chemisorption. If these energy is lesser than 8 kJ/mol, the adsorption is physisorption and if the energy is more than 8 kJ/mol, the adsorption is chemisorption in nature.

4.12 Kinetic study

Adsorption equilibrium studies are most important method in determining the efficiency of adsorption. In addition, it is also necessary to identify the adsorption mechanism in a chosen system. With the purpose of investigating the mechanism of adsorption and its potential, kinetic models have been exploited to test the experimental data. The adsorption kinetic show the evolution of the adsorption capacity through time. The information on the kinetics of adsorption is required to select the optimum condition for full-scale adsorbate removal process. Adsorption kinetics is expressed as the solute removal rate that controls the residence time of the adsorbate in the solid–solution interface.

Generally, several steps are involved in the sorption process by porous sorbent particles: (i) Bulk diffusion (ii) Boundary layer or film diffusion (iii) Intra particle transport and (iv) Reaction kinetics at phase boundaries.

In practice, kinetic studies were carried out in batch reactions using various initial adsorbate concentrations. Several adsorption kinetic models have been established to

understand the adsorption kinetics and rate-limiting step. These include pseudo-first, pseudo second-order rate model and intra particle diffusion kinetic models.

4.12.1 Pseudo-first-order model

The pseudo first order adsorption kinetic can be described by the equation as below suggested by Legergren⁷⁹.

$$\log (q_e - q_t) = \log q_e - k_1 / 2.303 \times t$$
 4.9

Where q_e and q_t are the amount of adsorbate adsorbed (mg/g) at equilibrium and at time t (min) respectively and k_1 is the pseudo first order rate constant of adsorption (min⁻¹). The plot is drawn between log (q_e - q_t) versus t to get a straight line. The values k_1 and calculated q_e can be obtained from the slope and intercepts of the straight line respectively.

4.12.2 Pseudo-second-order model

The pseudo second order adsorption kinetic equation is given below as suggested by $\mathrm{Ho^{80}}.$

$$t/q_t = 1/h + 1/q_e t$$
 5.10

Where $h=k_2q_e^2$ (mg g^{-1} min⁻¹) can be regarded as the initial adsorption rate as $t\to 0$ and k_2 is the pseudo first order rate constant of adsorption (g mg⁻¹ min⁻¹). The plot is drawn between t/q_t versus t to get a straight line. The values k_2 and h can be obtained from the slope and intercepts of the straight line respectively.

4.12.3 Intra-particle diffusion

The most commonly used technique for identifying the mechanism involved in the adsorption process is by fitting the experimental data in an intra particle diffusion kinetic model. According to Weber and Morris⁸¹, an intra particle diffusion coefficient k_p is defined by the equation:

$$q_t = k_p t^{0.5} + C$$
 4.11

Where k_p (mg/g/min^{0.5}) is the intra particle diffusion rate constant and C is the thickness of the boundary film. Weber and Morris plot is drawn between q_t and $t^{0.5}$ to understand the intra particle diffusion. The k_p and C values were obtained from the slope and intercept of the linear portions of the curves.

4.12.4 Test for kinetics models

Best fitting kinetic model for a system can be determined by using the statistical tool called Mean of sum of error squares (MSSE)⁸². This can be evaluated by the following formula.

MSSE =
$$\sqrt{\sum} [(q_e)_{exp} - (q_e)_{cal}]^2 / N$$
 4.12

Where N is the number of data points, $(q_e)_{exp}$ is the experimental q_e and $(q_e)_{cal}$ is the calculated q_e .

4.13 Thermodynamic studies

In order to understand the nature and feasibility of adsorption of chosen adsorbent - adsorbate systems, the thermodynamic parameters such as change in free energy (ΔG°), enthalpy change (ΔH°) and entropy change (ΔS°) were determined using the following equations.

$$K_L = C_{solid} / C_{liquid} \qquad 4.13$$

$$\Delta G = -RT lnK_L \qquad (Gibbs Equation) \qquad 4.14$$

$$ln K_L = -\Delta H/RT + \Delta S/R \text{ (Van't Hoff equation)} \qquad 4.15$$

Where, k_L is the equilibrium constant, ΔH° and ΔS° are the standard enthalpy change and entropy changes of adsorption respectively. The values of ΔH° and ΔS° were calculated from the slopes and intercepts of the linear plot of lnK_L vs 1/T. The free energy of specific adsorption ΔG° (kJ/mol) was calculated from the following expression.

$$\Delta G^{\circ} = \Delta H^{\circ} - T\Delta S^{\circ}$$
 4.16

From the sign of ΔH° value we can understand the whether the adsorption is endothermic and exothermic process. From the magnitude of ΔH° value we can know the mechanism of adsorption whether it's physisorption (or) chemisorption. The sign of ΔS° value would infer whether the adsorption proceed increase of randomness (or) decrease of randomness. The spontaneity of adsorption process inferred from sign of ΔG° values.

4.14 Desorption studies

200 mg of adsorbent was added to 200 mL of adsorbate solution of concentration 100 mg/L. The adsorbate solution with the adsorbent was agitated till the attainment of equilibrium. After that, the adsorbent was separated off from the solution using centrifugation. Concentration of the centrifugate was determined from which amount of adsorbate transferred to adsorbent was calculated.

Next the adsorbate loaded adsorbent was collected from the flask, washed with distilled water, then this adsorbent (loaded with adsorbate) was suspended in 100 ml of desorbing solution of required pH and agitated for pre- determined time and then supernatant liquid was separated and its concentration was determined. This desorption process was continued for three times. From the concentration of the collected solutions, quantity of adsorbate desorbed was calculated. Percentage of desorption was calculated

from the quantity already transferred to the adsorbent and the quantity recovered (Sreedhar and Anirudhan, 1999)⁷⁰.

Desorption studies help to elucidate the mechanism of adsorption and recovery of the adsorbates and adsorbents. Desorption of the adsorbent may make the treatment more economical and feasible. Desorption process must be suitable for recovery process without damaging of the capacity of the adsorbent. Hence desorption study was carried out with acid, base and Distilled water.

4.15 Morphological study

Changes in the morphology of adsorbent because of adsorption have been analyzed with FT-IR spectra and SEM analysis.

4.15.1 Fourier Transform Infrared Spectroscopy (FT-IR)

Historically IR has been mostly used for qualitative analysis, to obtain structural information. The instrumental evolution of the day makes non-destructive and quantitative analysis possible, with significant accuracy and precision. The shift of the bands and the changes in signal intensity allow the identification of the functional groups involved in metal ions/dyes adsorption.

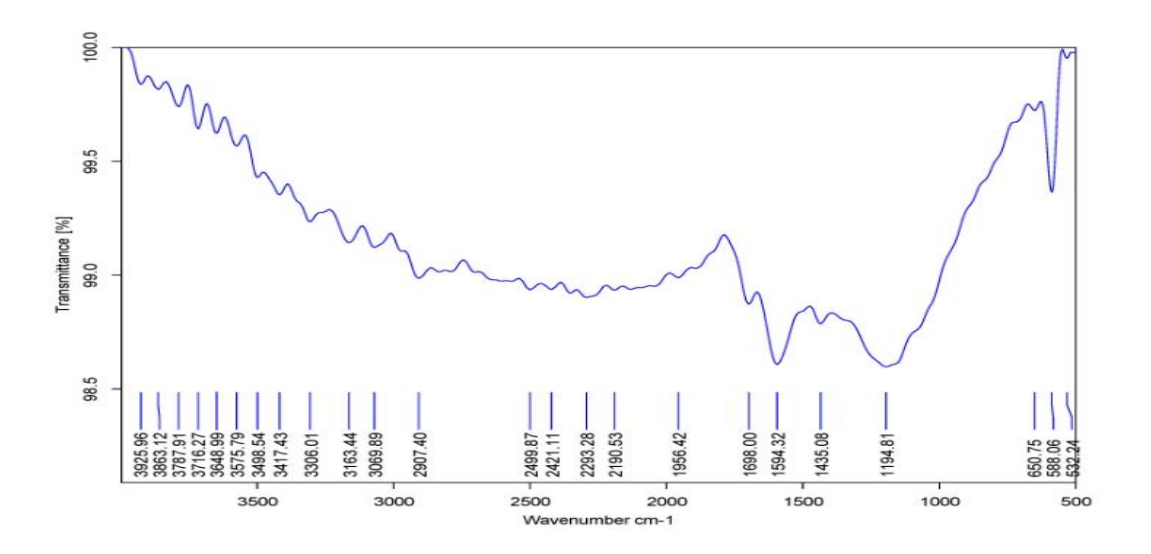


Figure 4.2Before FTIR Spectrum of PBC

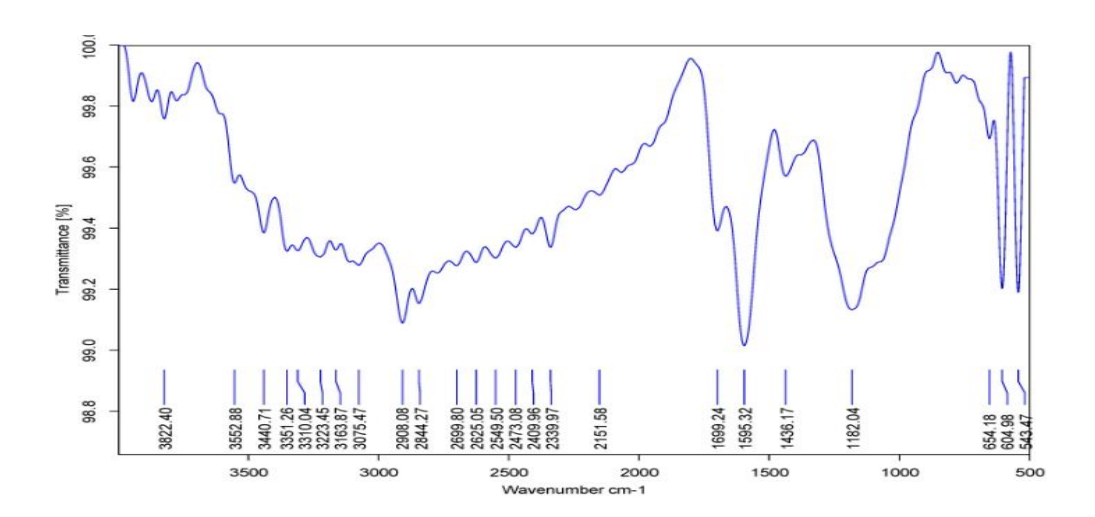


Figure 4.3Before FTIR Spectrum of APBC

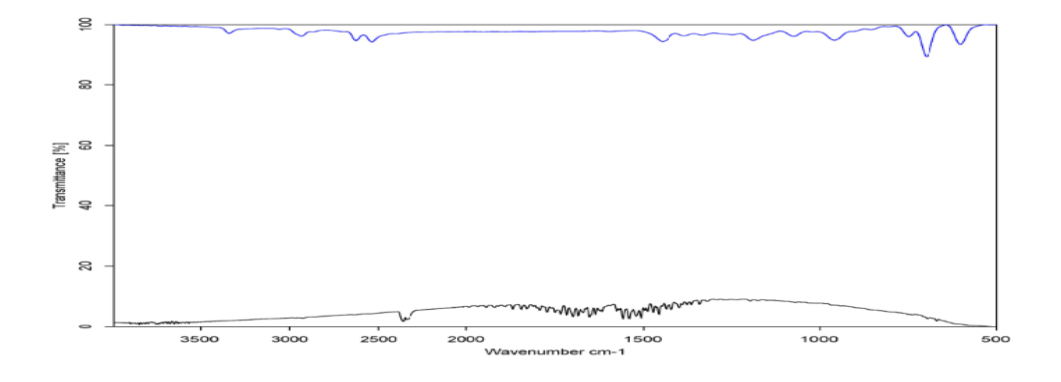


Figure 4.4Before FTIR Spectrum of BPBC

Table 4.4 Before FTIR Spectrum of PBC, APBC AND BPBC

Wave Number (cm ⁻¹)	Range	Functional Groups
588.06	500-730	Halogen Compounds
1594.32	1535-1640	Diketones
1435.08	1405-1445	Alkanes
604.98	500-730	Halogen Compounds
654.18	500-730	Halogen Compounds
1182.04	1150-1270	Ester Carbonyl
1595.32	1535-1640	Diketones
2908.08	2500-3300	Aliphatic saturated hydrocarbon double bond
3440.71	3220-3550	Hydroxyl group
1500	570-1500	Nitro compounds

4.15.2 Scanning Electron Microscope (SEM) Analysis

The SEM has a large depth of field, which allows a large amount of samples to be in focused at one time and produces an image that is a good representation of the three dimensional sample. The combination of higher magnification larger depth of field, greater resolution, compositional and crystallographic information makes the SEM as one of the most heavily used instruments in academic research areas.

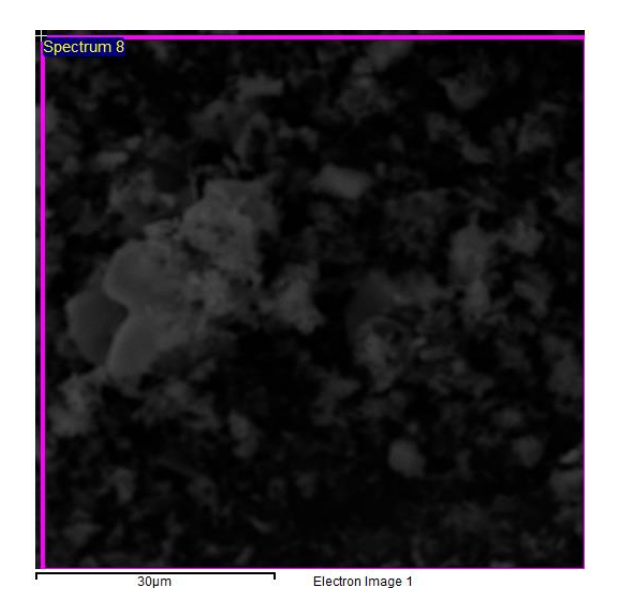


Figure 4.5 Unloaded PBC

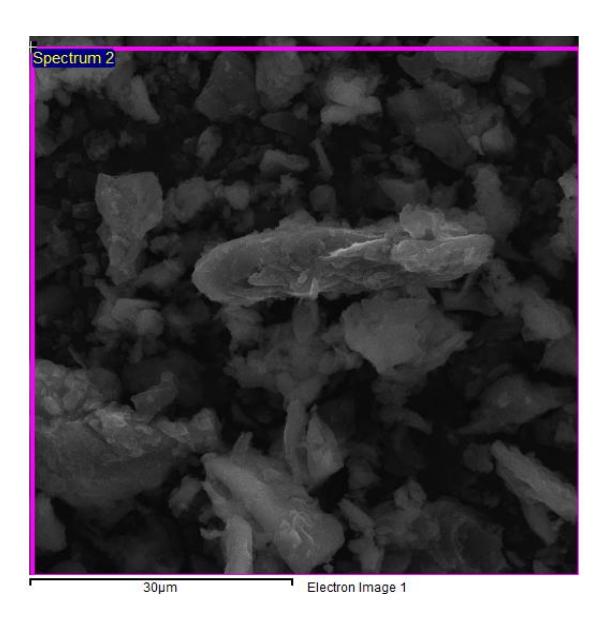


Figure 4.6 loaded Cr (VI) PBC

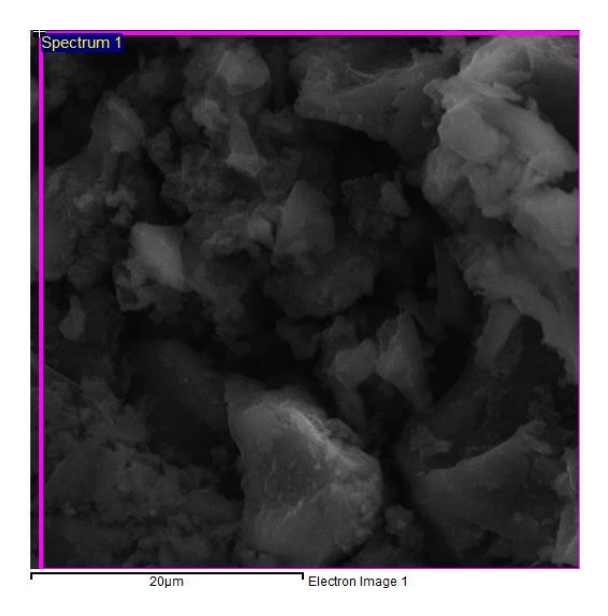


Figure 4.7 loaded Cr (VI) APBC

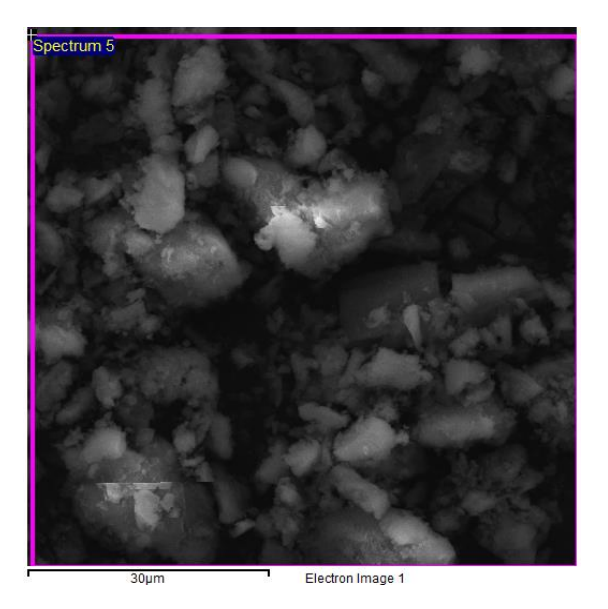


Figure 4.8 loaded Cr (VI) BPBC

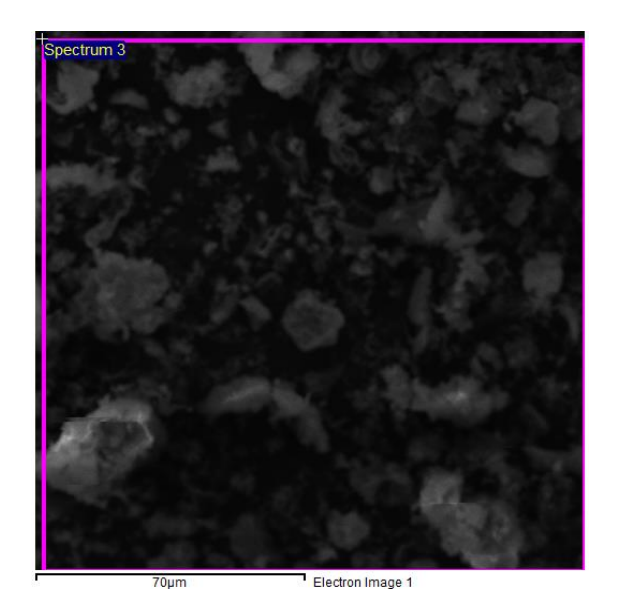


Figure 4.9 Unloaded PBC

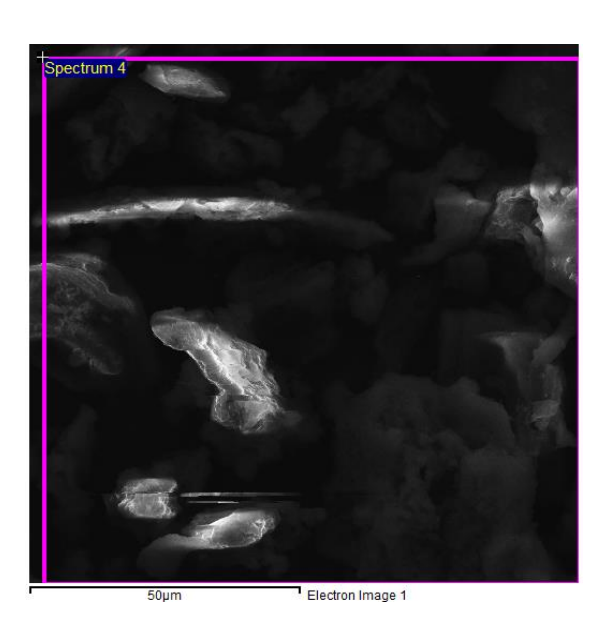


Figure 4.10 loaded MB dye PBC

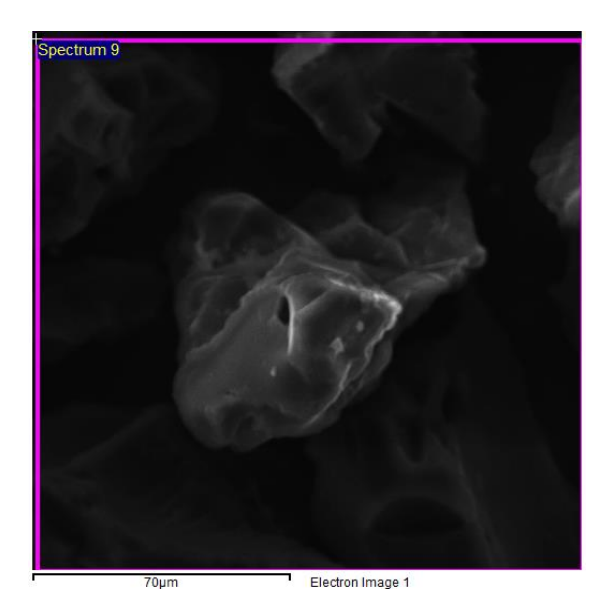


Figure 4.11 loaded MB dye APBC

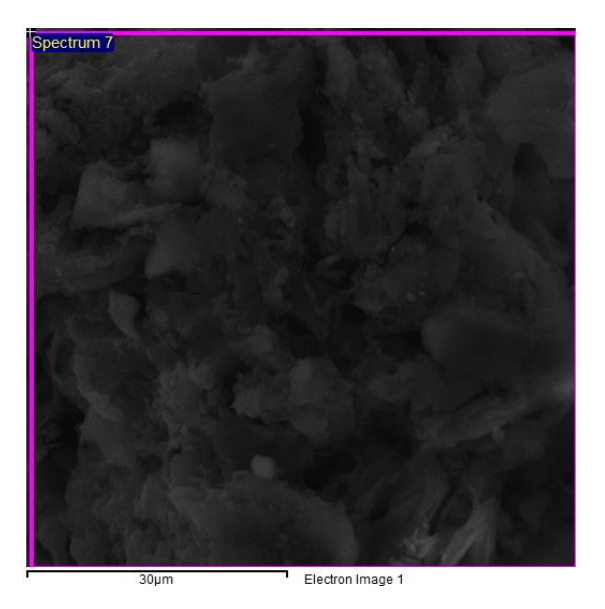


Figure 4.12 loaded MB dye BPBC

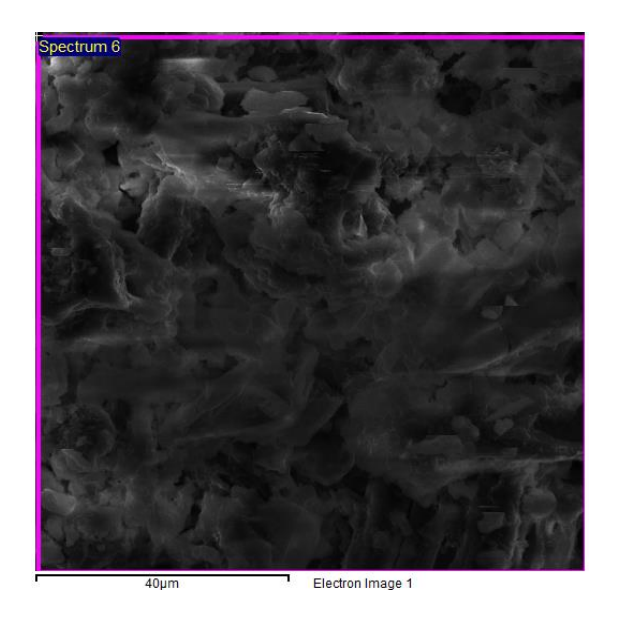


Figure 4.13 Unloaded TB dye PBC

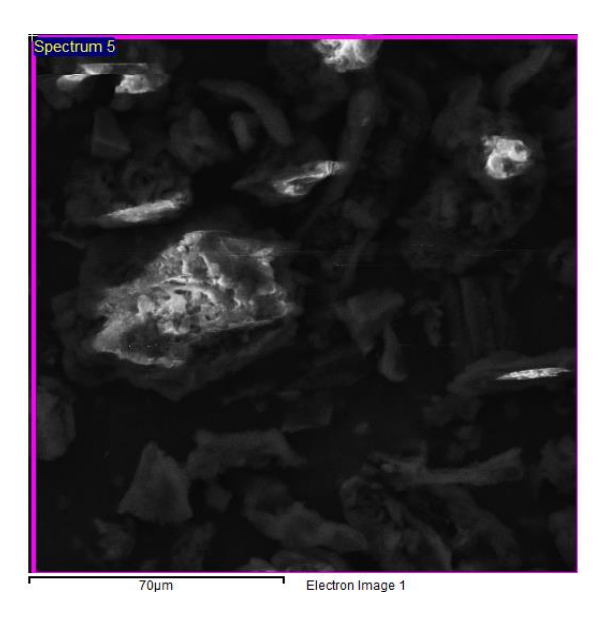


Figure 4.14 loaded TB dye APBC

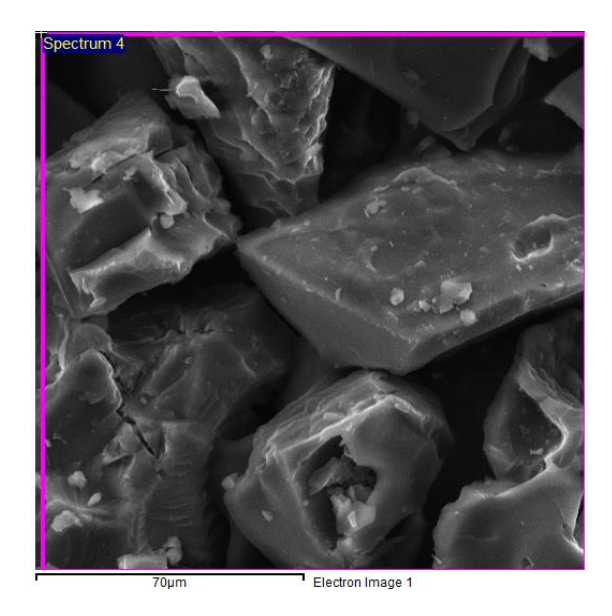


Figure 4.15 loaded TB dye APBC

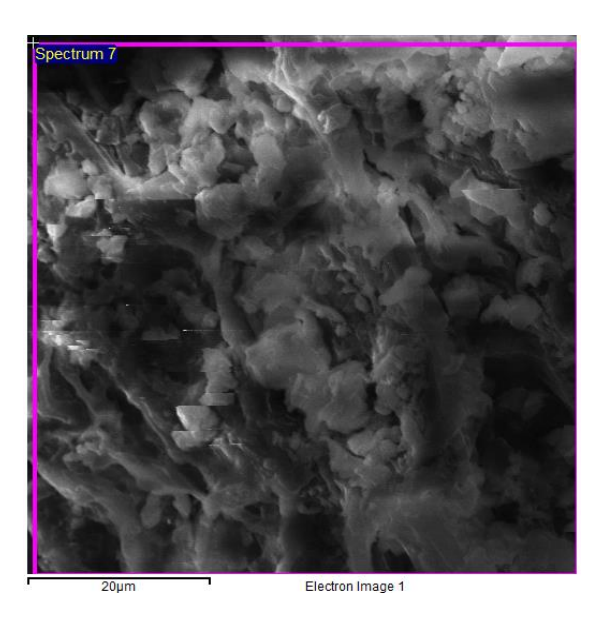


Figure 4.16 loaded TB dye BPBC

Results and Discussion

5.1 STUDIES ON THE ADSORPTION OF Cr (VI) IONS ONTO PBC, APBC AND BPBC

This chapter deals with the study of removal of Hexavalent Chromium (Cr (VI)) ion using activated carbons prepared from then barks of *Pterocarpus Marsupium Roxb*.by Phosphoric acid viz PBC (*Pterocarpus Marsupium* Bark Carbon) APBC (Acid modified *Pterocarpus Marsupium* Bark Carbon) and BPBC (Base modified *Pterocarpus Marsupium* Bark Carbon). The adsorption studies are performed by conducting batch mode experiments by varying the parameters such as solution pH, adsorbent dosage, contact time, initial concentration and Temperature.

Equilibrium data were processed with Freundlich, Langmuir, Temkin and Dubinin-Radushkevich isotherm equations. Values of isotherm constants were determined and their significances were discussed. The adsorption behaviour of the Cr (VI) ions onto PBC, APBC and BPBC were compared.

Data obtained from effect of contact time for different initial concentrations were processed with Lagergren, Ho and Webber Morris kinetic equations. Rate constants and the predicted adsorption capacities were determined. Predicted adsorption capacities were compared with the experimental adsorption capacities. Best fitting model was identified using the statistical tool Mean Summation of Error Squares (MSSE).

Thermodynamic quantities ΔH° , ΔS° and ΔG° were determined using equilibrium data obtained in different temperatures. Inferences obtained from these values were discussed.

Regenerating capability of the adsorbents loaded with Cr (VI) ions were investigated with acidic, alkaline and neutral mediums.

FTIR spectrum, EDAX of adsorbents were studied before and after adsorption of Cr (VI) ions to know the adsorbate – adsorbent interactions.

Findings of the present study are interpreted and discussed in the light of the objectives set forth.

5.1 Effect of pH

The pH of the adsorbate solution is an important parameter governing sorption on different adsorbents. This is partly due to the fact that hydrogen ion itself is a strong competing sorbate and partly to the fact that its ability to influence the chemical speciation of adsorbate. The effect pH of solution was studied by taking pH range from 2 to 10.

Effect of solution pH on the adsorption of Cr (VI) ions on PBC.ABPC and BPBC was shown in the figure 5.1 which shows that removal Cr (VI) ions is maximum at pH 2 and decreased on increasing the pH of the solution for all the adsorbents.

Chromium ions occurred as negatively charged species when dissolved in water. When the pH is lower than pHzpc of the adsorbent, the charge on the surface of the adsorbent is positive (Gottipati Ramakrishna et.al., 2012). At very low pH, the more positive charge accumulated on the surface of the adsorbent and facilitated electrostatic attraction on the negatively charged bichromate ion and hence more adsorption was observed. Moreover at lower pH, the concentration of OH⁻ ions was meager. Hence the competition for the positively charged cite by OH⁻ ions was lesser.

When the pH of the solution was raised, the positive charge on the surface decreased with the increase in OH⁻ ions concentration. The OH⁻ ions being smaller in size tended to adsorb preferentially on adsorbent and rendered repulsive force towards the approaching negative metal anions. Hence the adsorption of Cr (VI) ions was low at higher pH of the solution (Supriya Singh et.al., 2013, Kulkarni Sunil., 2013, Khadka Deba Bahadur et.al., 2014)

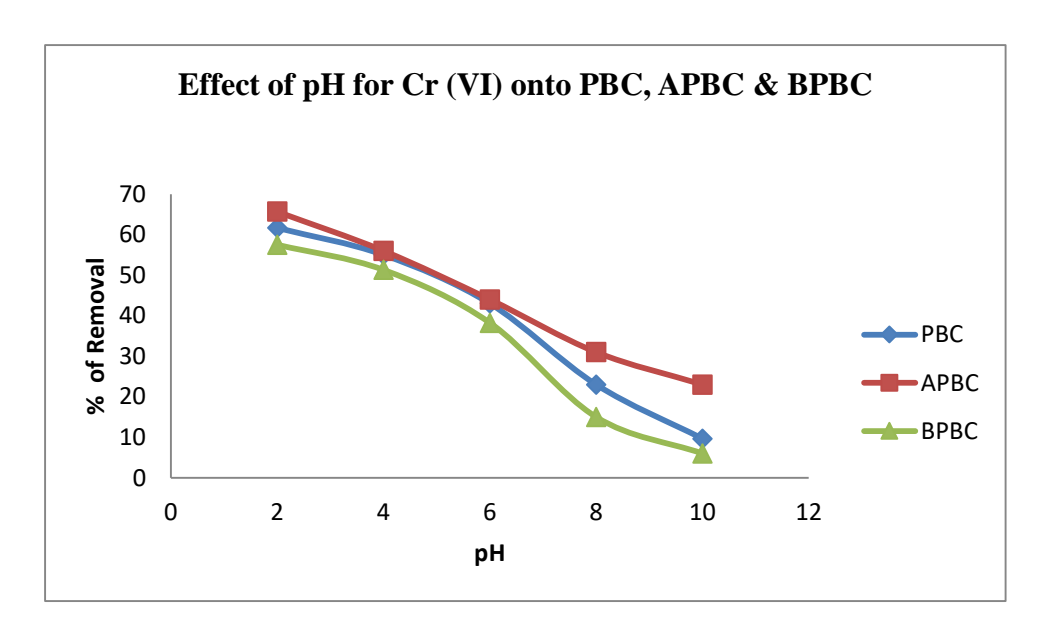


Figure 5.1

On comparing the ability of PBC.APBC and BPBC, the order of increasing percentage of removal was found to be APBC.BPBC and PBC. This kind of order was found in earlier literatures (Selvaraj et.al., 2003).

5.1.1 Effect of adsorbent dosage

Adsorbent dosage is one of the important parameters in adsorption processes because amount of adsorbate adsorbed vary with the dosage of an adsorbent for a given initial concentration of the adsorbate under a given set of operating conditions. figure 5.2 showed the effect of adsorbent dosage for adsorption of Cr (VI)ions onto PBC, APBC and BPBC. As can be seen in this figure, increase of dosage increases the percentage of

removal of adsorbate from the solution. The percentage of removal increased from 12.34 to 95.22 % for Cr (VI) ions onto PBC, 24.33 to 97.66% for Cr (VI) ions onto APBC and 19.00 to 96.55 for Cr (VI) ions onto BPBC for the increase of dosage of 5mg / 50mL to 50mg / 50mL as given in table 5.1.

The increase in the removal efficiency with an increase in the adsorbent dosage, may be attributed to increase of more adsorbent surface is available for the solute to be adsorbed (Hema et.al., 2007).

There is a slight difference in the adsorbing efficiency of Cr (VI) ions was observed among the chosen adsorbents PBC, APBC & BPBC which was shown in the table 5.1. The order of removal of Cr (VI) ions from the aqueous phase is APBC > BPBC > PBC.

Similar trend was observed in earlier literature (Garg et.al., 2003, Selvi et.al., 2003, Demirbas et.al., 2004) Based on these results, the remaining parts of the experiments were carried out with the 30 mg for 50 mL of Cr (VI) ions solution.

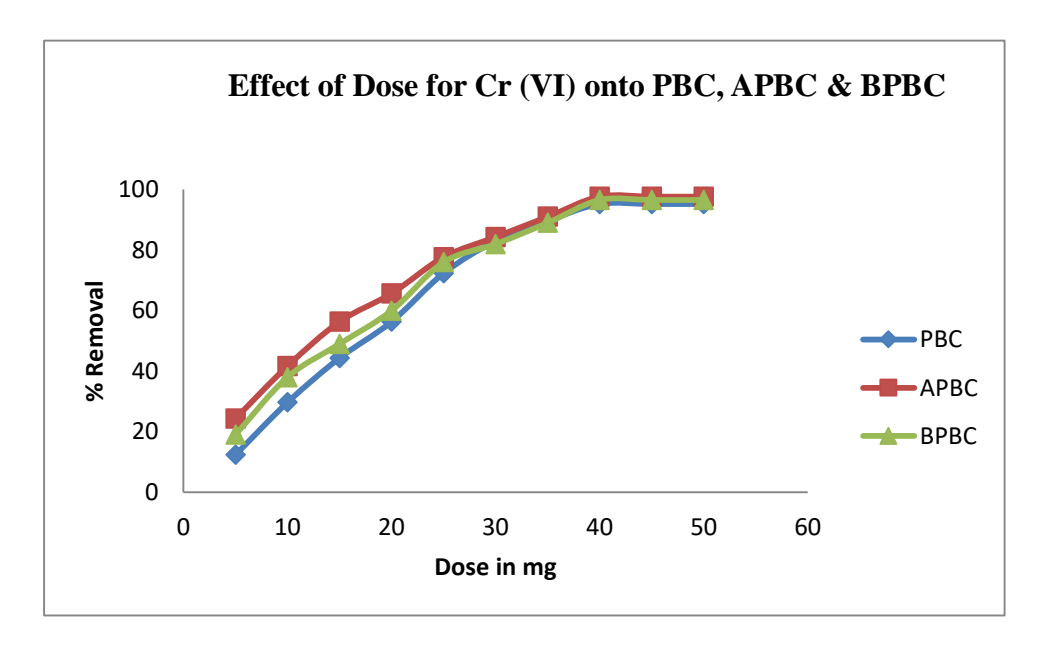


Figure 5.2

Table – 5.1 Effect of dose for Cr (VI) ions adsorption onto PBC, APBC & BPBC

Contact Time: 60min, Ci: 15mg/L, Temp: 305 K

Dose in	Percentage of removal of Cr (VI)ions					
mg/50 mL	PBC	APBC	ВРВС			
05	12.34	24.33	19.00			
10	29.66	41.66	38.00			
15	44.33	56.33	49.00			
20	56.33	65.66	60.00			
25	72.33	77.66	76.00			
30	83.00	84.33	82.00			
35	89.66	91.00	89.00			
40	95.22	97.66	96.55			
45	95.22	97.66	96.55			
50	95.22	97.66	96.55			

5.1.2 Effect of Contact Time

The effect of contact time on the percentage removal from aqueous solution was studied by taking 10, 15, 20 and 25 mg/L of Cr (VI) ions solutions as initial concentrations.

The result of the above study was given in table 5.2 and shown in figures 5.3 to 5.5. The rate of percentage removal was found to be rapid at initial stages and the rate was found to decrease as the time increases and become constant after attaining equilibrium stage. At the initial stage, the ratio of surface area of the adsorbent to the amount of solute in liquid phase is high and hence the concentration of adsorbate in the liquid phase acted as driving force and made the solute to rush towards the adsorbent surface. As the time increases the above ratio began to decrease due to adsorption and hence the rate of adsorption reduced (Renmin Gong et.al., 2005). Equilibrium was found to occur at 80 min in all the cases.

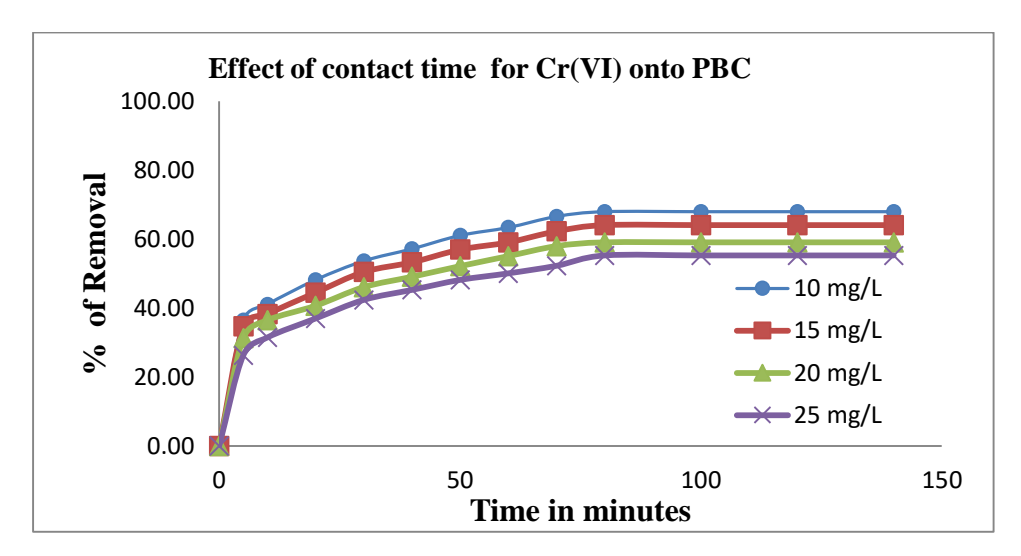


Figure 5.3

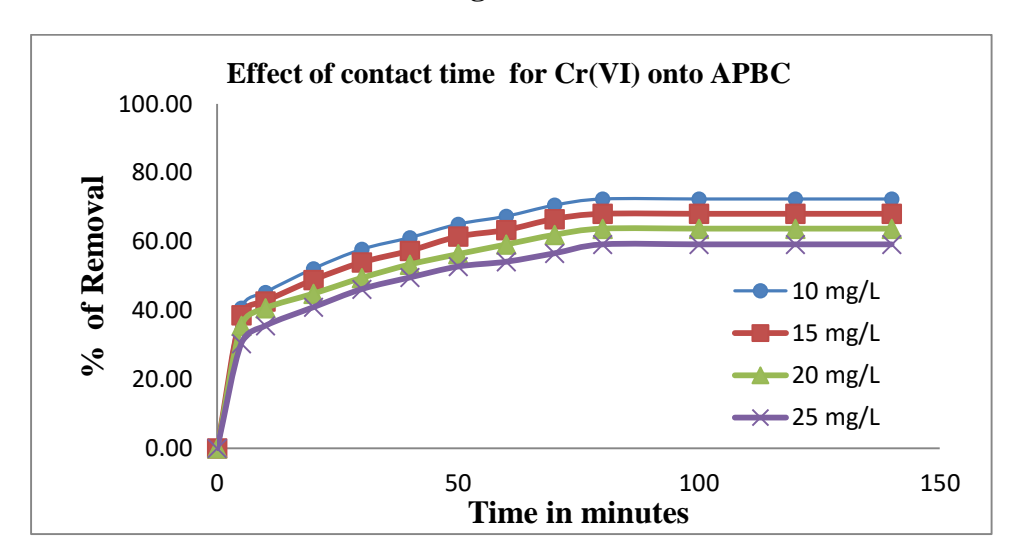


Figure 5.4

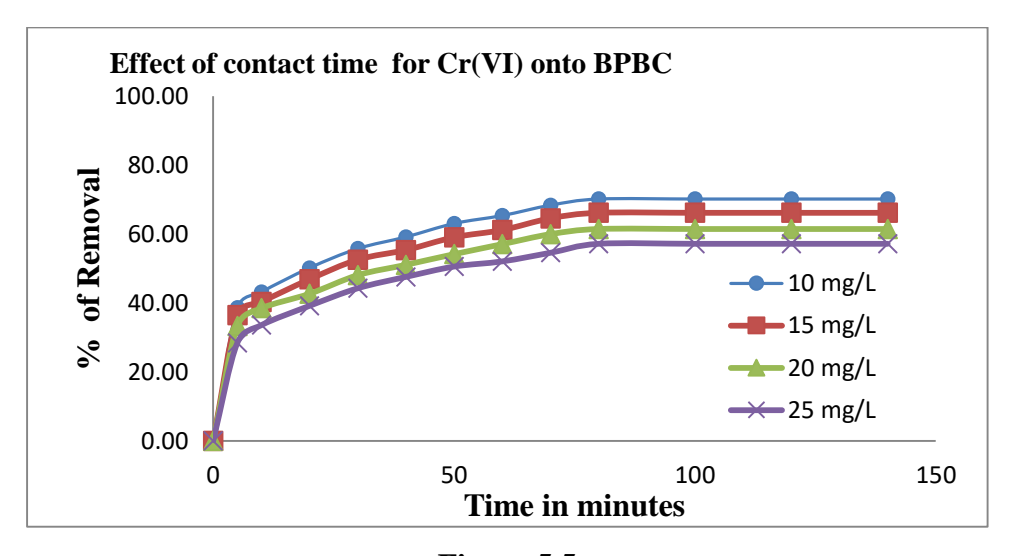


Figure 5.5

Table-5.2 Effect of Contact time for Cr (VI)ions adsorption

[pH: 2, Dose: 30mg/50mL, Temp: 305 K]

Time		PF	BC			APBC				BPBC		
		Initial Concentration in mg/L										
in Minutes	10	15	20	25	10	15	20	25	10	15	20	25
0	0.00	0.00	0.00	0.00	0.00	0.00	0.00	0.00	0.00	0.00	0.00	0.00
5	36.50	34.70	31.30	26.30	40.70	38.70	35.60	30.45	38.60	36.50	33.30	28.40
10	41.10	38.30	36.50	31.50	45.30	42.70	40.70	35.62	43.20	40.30	38.50	33.60
20	48.20	44.50	40.70	37.00	52.20	48.95	44.95	41.02	50.20	46.90	42.70	39.20
30	53.70	50.50	46.10	42.40	57.80	54.00	50.18	46.25	55.80	52.60	48.10	44.30
40	57.20	53.30	49.10	45.30	61.20	57.40	53.40	49.63	59.20	55.40	51.10	47.60
50	61.10	57.50	52.20	48.20	65.10	61.50	56.40	52.80	63.10	59.10	54.20	50.60
60	63.40	59.10	55.10	50.10	67.40	63.40	59.20	54.20	65.40	61.20	57.10	52.10
70	66.60	62.30	58.00	52.30	70.60	66.60	62.00	56.64	68.40	64.60	60.00	54.60
80	68.00	64.10	59.10	55.30	72.40	68.10	63.80	59.23	70.20	66.20	61.50	57.20
100	68.00	64.10	59.10	55.30	72.40	68.10	63.80	59.23	70.20	66.20	61.50	57.20
120	68.00	64.10	59.10	55.30	72.40	68.10	63.80	59.23	70.20	66.20	61.50	57.20
140	68.00	64.10	59.10	55.30	72.40	68.10	63.80	59.23	70.20	66.20	61.50	57.20

5.1.3 Effect of initial concentration

The factor, effect of initial concentration depends on the relation between the adsorbate concentration in the solution phase and the available binding sites on an adsorbent surface. This study showed that the percentage of the removal of adsorbate decreased with the increase of initial concentration of adsorbate solution as given in table 5.3 and shown in figures 5.6, 5.7 & 5.8.

The percentage removal of decreased from 68.00 to 55.30 for PBC, 72.40 to 59.23 for APBC and 70.20 to 57.20 for BPBC at the temperature 305 K as the initial concentration of Cr (VI) ions increased from 10 mg/L to 25 mg/L.

The amount of solute in the liquid phase is higher at a higher of initial concentration. The ratio of available adsorbent surface to the concentration of solute decreases with the increase of initial concentration and hence the percentage of removal decreases with the increase of initial concentration.

However the amount of Cr (VI) ions adsorbed on the adsorbent increased with an increase in the initial concentration of the adsorbate solutions as evidenced from the table 5.4 and figures 5.7, 5.9 & 5.11. The amount of Cr (VI) ions adsorbed increased from 6.80 to 13.83 for PBC, 7.24 to 14.81 for ABPC and 7.02 to 14.30 for PBPC at the temperature 305K as the initial concentration of Cr (VI)ions increased from 10 to 25 mg/L.

This is because the amount of solute adsorbed is proportional to the percentage of adsorbate transferred from liquid phase to solid phase. This fraction increases with an increase in the concentration of solution. For example if 25 percentage is assumed to be transferred, 25 mg of solute will be transferred if the initial concentration of the solution is 100 mg/L. If the initial concentration solution is 200 mg/L, then the amount transferred will be 50 mg.

Table-5.3 Effect of initial concentration on percentage of removal [Cr (VI)ions pH: 2, Dose: 30mg/50mL, Temp: 305 K]

Adsorbates	Initial Concentration	Percentage of Removal
1 usor bates	Ci (mg/L)	Tercentage of Removal
	10	68.00
	15	64.10
DD C	20	59.10
PBC	25	55.30
	10	72.40
	15	68.10
A DD C	20	63.80
APBC	25	59.23
	10	70.20
	15	66.20
DDD C	20	61.50
BPBC	25	57.20

Table-5.4 Effect of initial concentration on amount adsorbed [Cr (VI)ions, pH: 2, Dose: 30mg/50mL, Temp: 305 K]

	Initial Concentration	
Adsorbates		Amount adsorbed
	Ci (mg/L)	(mg/g)
	10	6.80
	15	9.62
DD C	20	11.82
PBC	25	13.83
	10	7.24
	15	10.22
A DD C	20	12.76
APBC	25	14.81
	10	7.02
	15	9.93
DDD C	20	12.30
BPBC	25	14.30

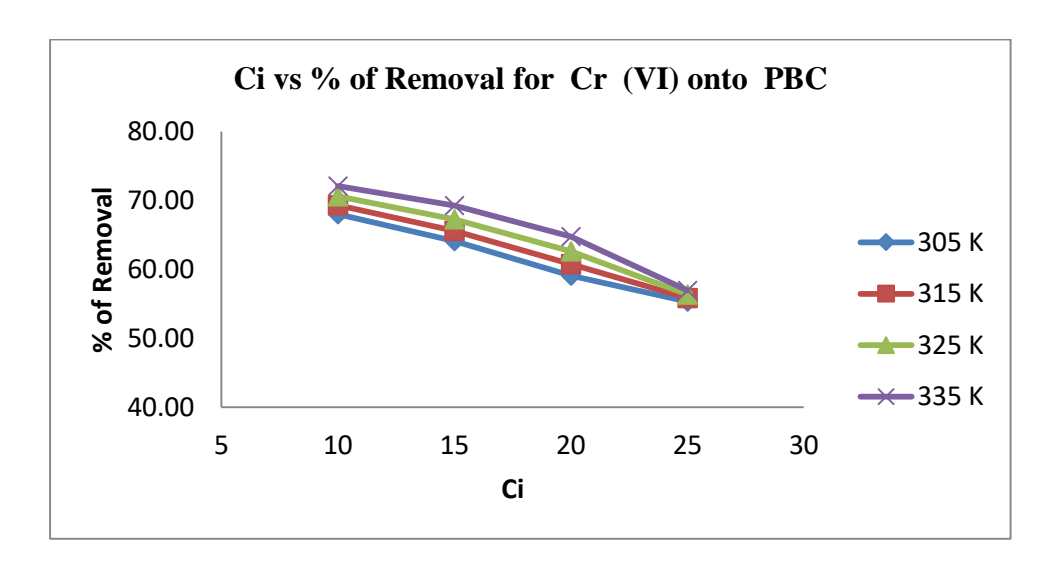


Figure 5.6

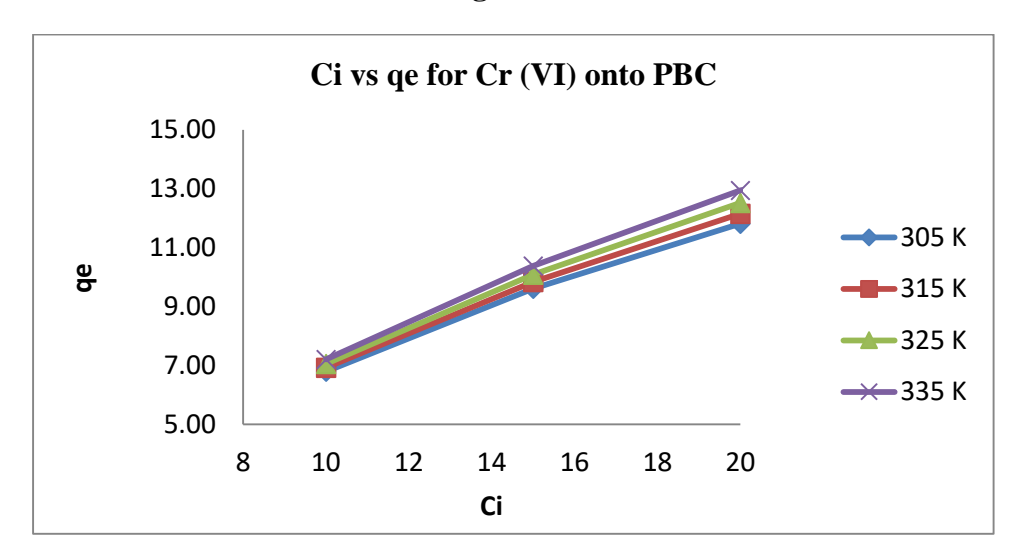


Figure 5.7

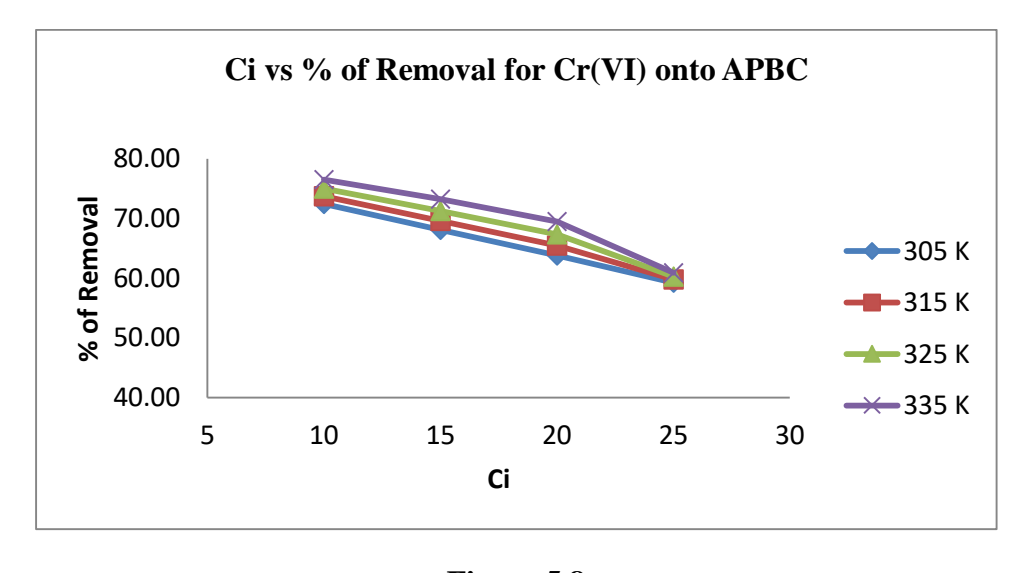


Figure 5.8

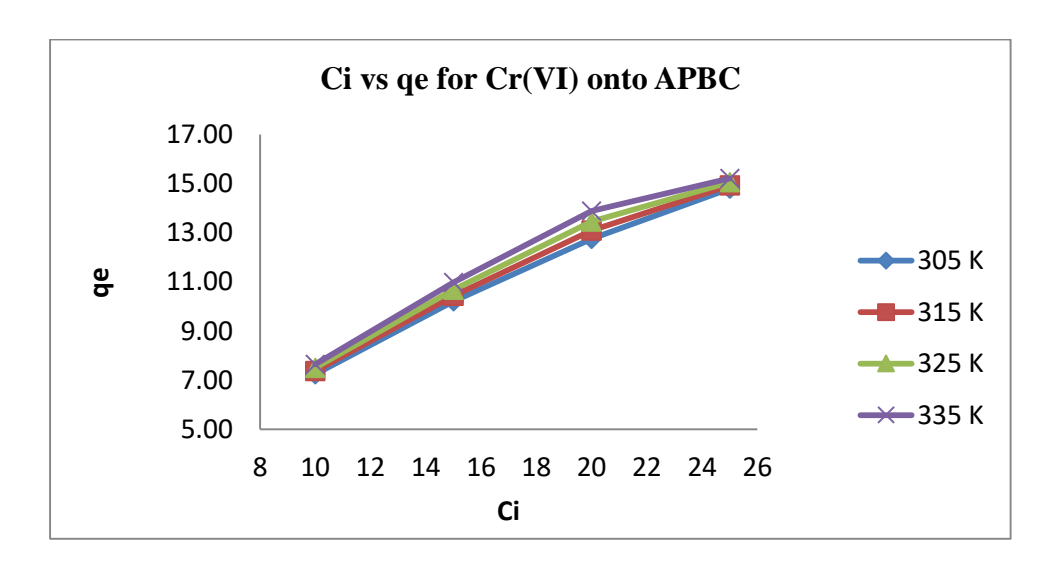


Figure 5.9

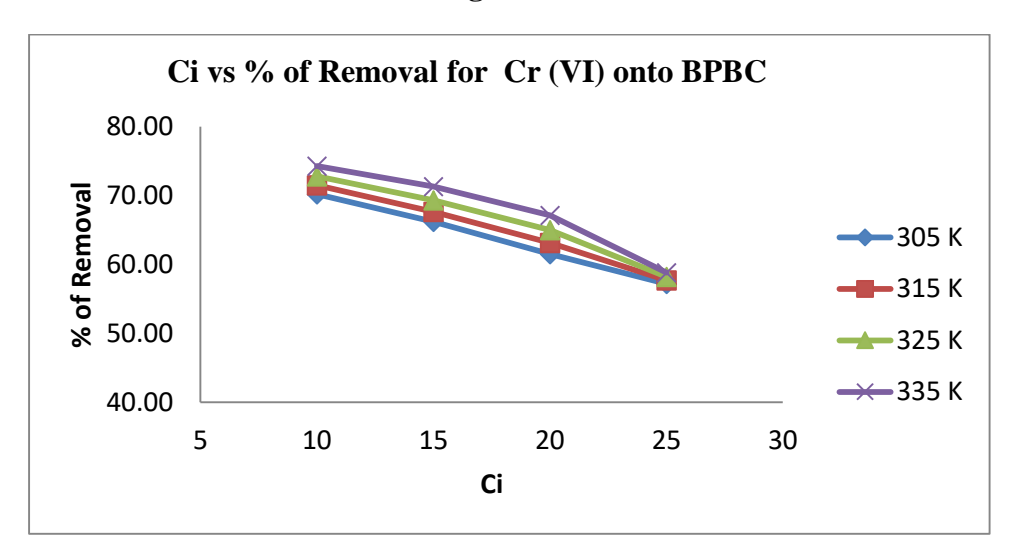


Figure 5.10

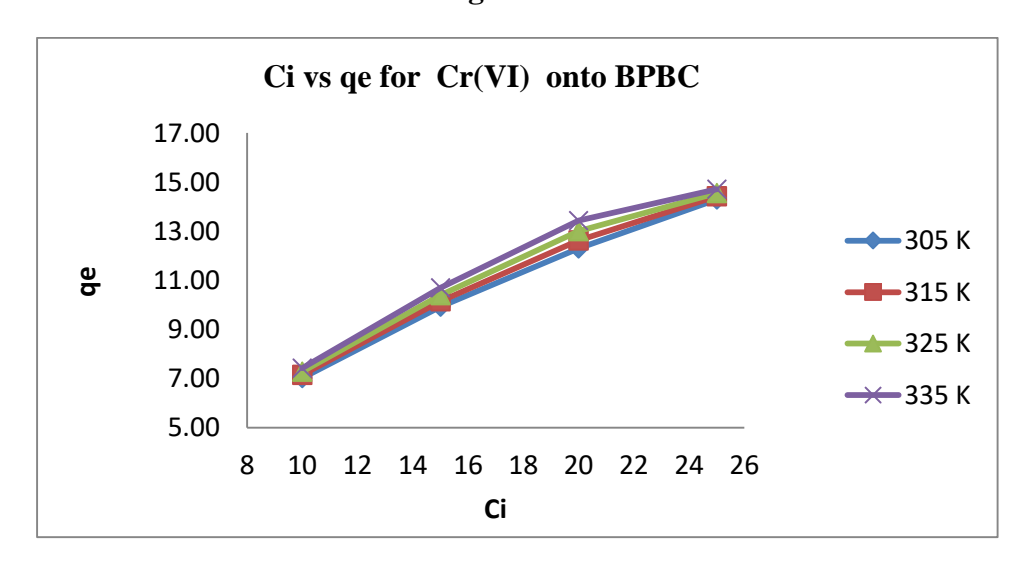


Figure 5.11

5.1.4 Effect of Temperature

Temperature is a well-known factor that influence in the adsorption process. The influence of temperature on adsorption of Cr (VI) ions was investigated at 305, 315, 325 and 335K. The results were presented in table 5.5 to 5.6. Plots drawn between percentage removals versus temperature were given in figures 5.12, 5.14 & 5.16. It could be clearly seen that, the percentage of removal increased with an increase of temperature. When the temperature increased from 305 to 335 K, the % of removal of Cr (VI) ions onto PBC, APBC & BPBC increased from 55.30 to 72.10, 59.23 to 75.00 & 57.20 to 74.30 respectively. It is found that higher temperature eased the sorption of Cr (VI) ions onto all three adsorbents. These results can be explained by the swelling of the adsorbent at higher temperature which enhances the penetration of the additional adsorbate molecules (Rozada et.al., 2003).

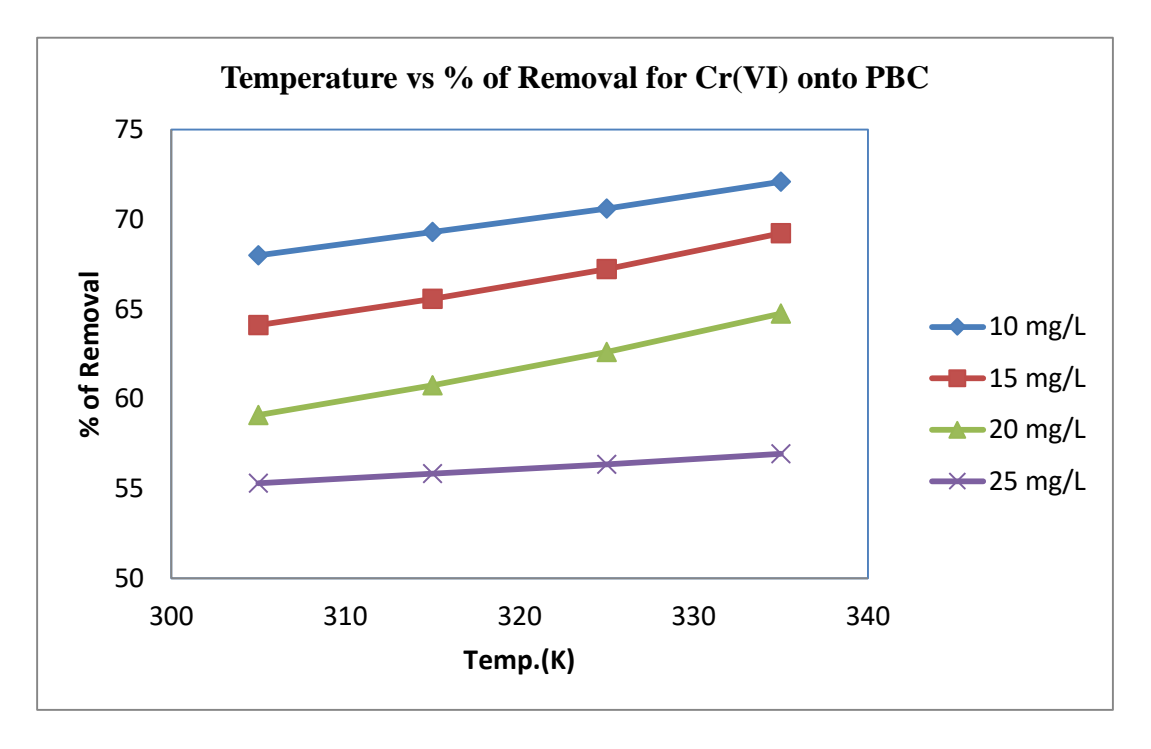


Figure 5.12

Table-5.5 Effect of temperature of Cr (VI)ions onto Adsorbents [pH:2, Dose:30mg/50mL, CT :160min]

Initial	Temperature		% of Removal	
Concentration (mg/L)	(K)	PBC	APBC	ВРВС
	305	68.00	72.40	70.20
	315	69.30	73.70	71.50
10	325	70.60	75.00	72.80
	335	72.10	76.50	74.30
	305	64.10	68.10	66.20
15	315	65.57	69.57	67.67
13	325	67.23	71.23	69.33
	335	69.23	73.23	71.33
	305	59.10	63.80	61.50
20	315	60.75	65.45	63.15
20	325	62.60	67.30	65.00
	335	64.75	69.45	67.15
	305	55.30	59.23	57.20
25	315	55.82	59.75	57.72
43	325	56.34	60.27	58.24
	335	56.94	60.87	58.84

Table–5.6 Effect of temperature of Cr (VI)ions onto Adsorbents PBC, APBC & BPBC

[pH:2, Dose:30mg/50mL, CT:140min]

Initial	Temperature		Qe	
Concentration (mg/L)	(K)	PBC	APBC	ВРВС
	305	6.80	7.24	7.02
	315	6.93	7.37	7.15
10	325	7.06	7.50	7.28
	335	7.21	7.65	7.43
	305	9.62	10.22	9.93
15	315	9.84	10.44	10.15
15	325	10.09	10.69	10.40
	335	10.39	10.99	10.70
	305	11.82	12.76	12.30
20	315	12.15	13.09	12.63
20	325	12.52	13.46	13.00
	335	12.95	13.89	13.43
	305	13.83	14.81	14.30
25	315	13.96	14.94	14.43
	325	14.09	15.07	14.56
	335	14.24	15.22	14.71

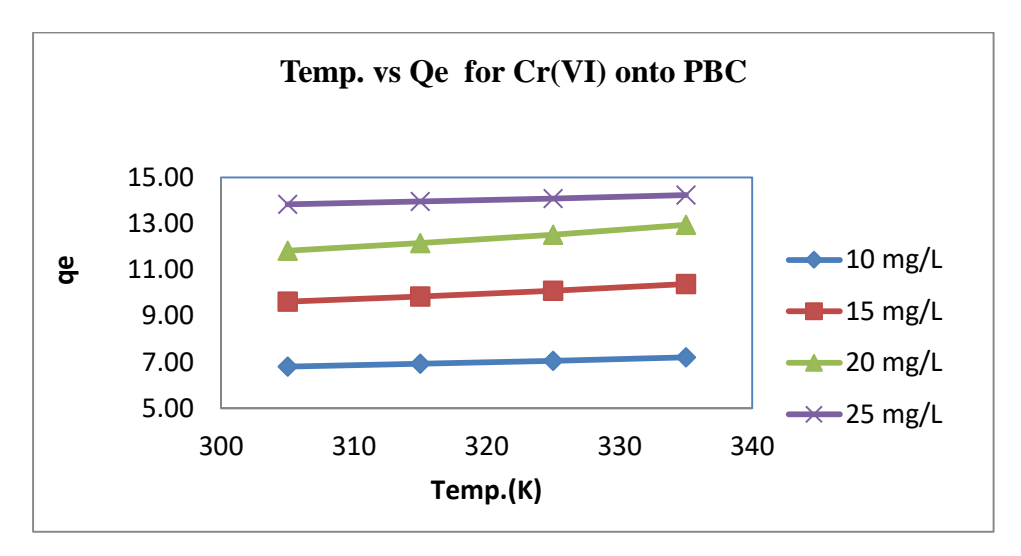


Figure 5.13

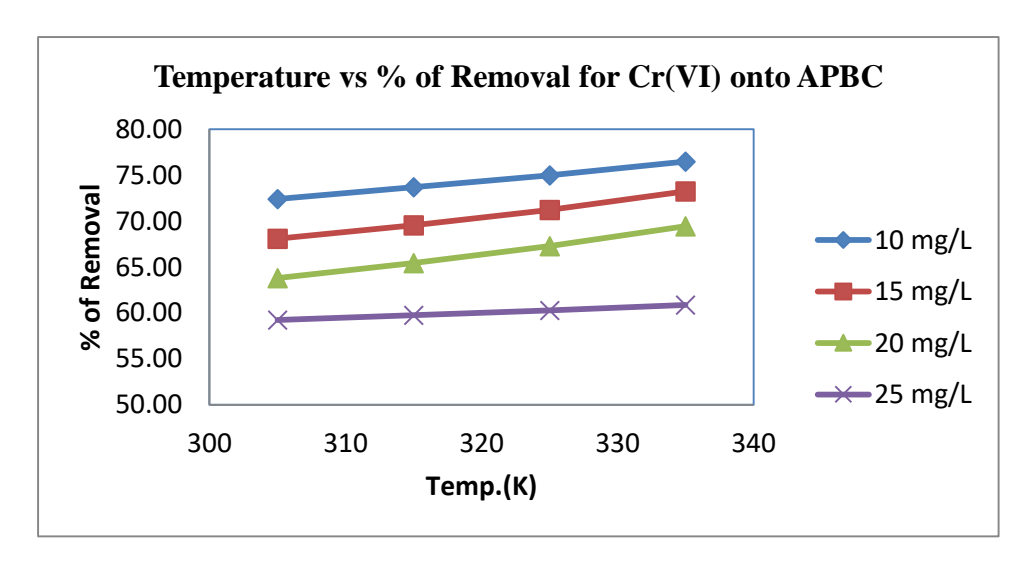


Figure 5.14

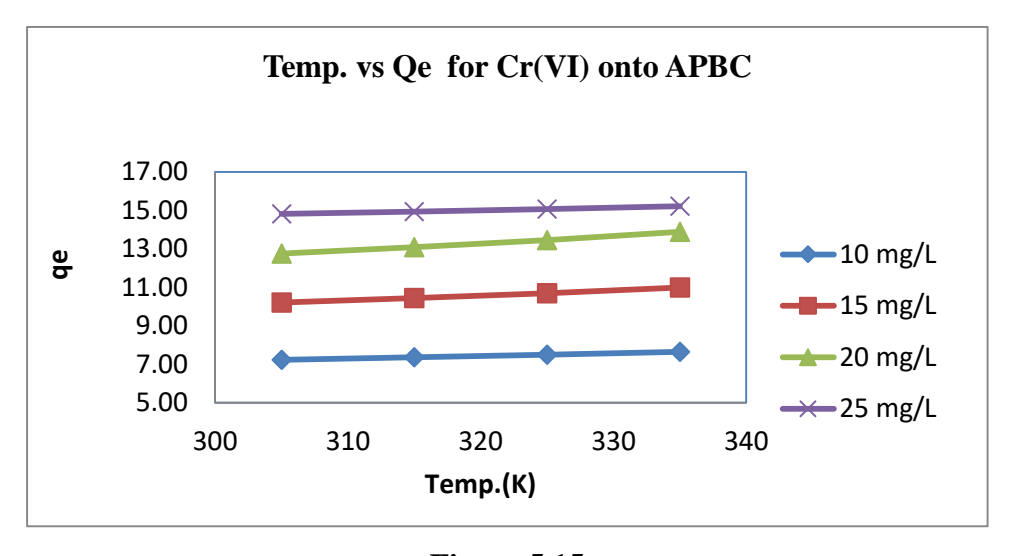


Figure 5.15

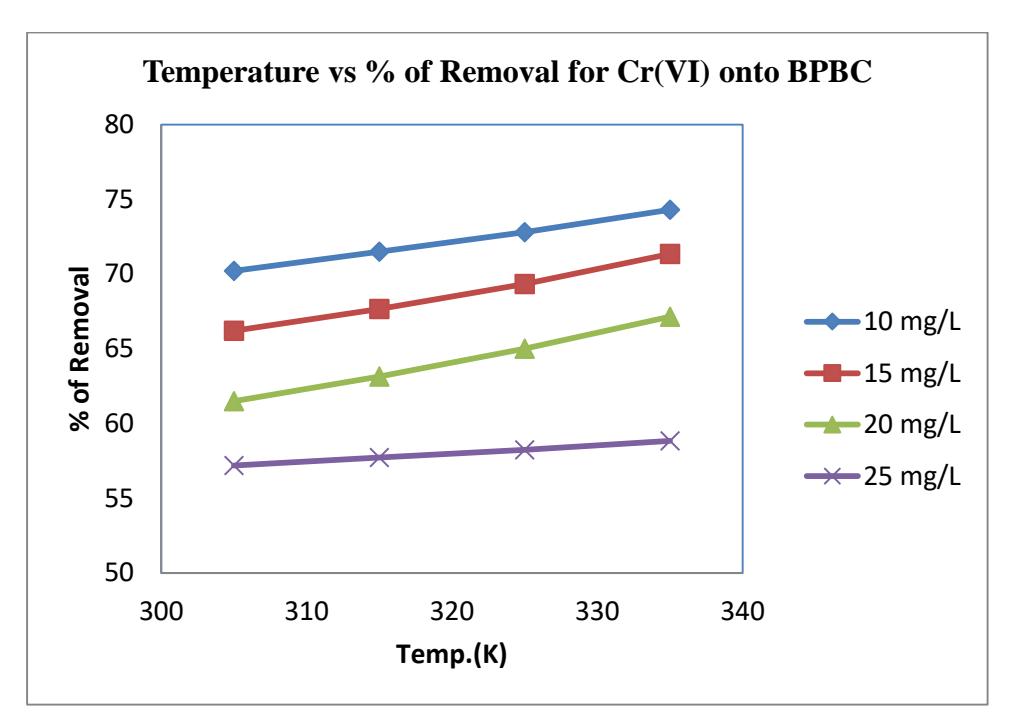


Figure 5.16

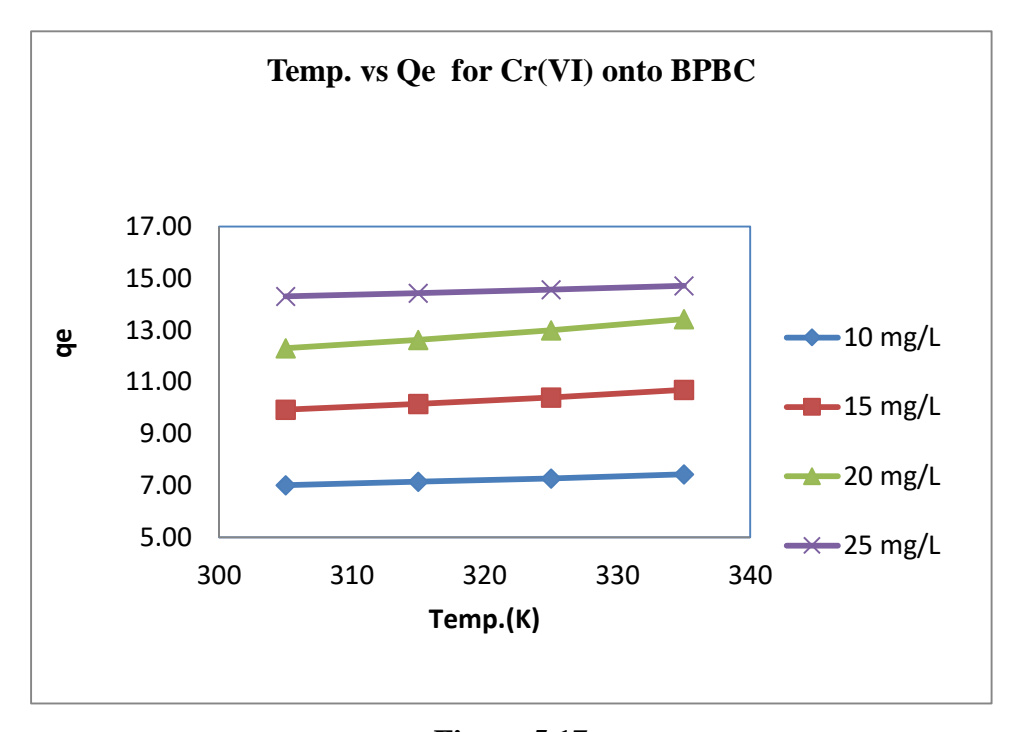


Figure 5.17

5.1.6 Isotherm studies

For solid–liquid adsorption system, adsorption isotherm is important model in the description of adsorption behavior. Adsorption isotherm relates the distribution of adsorbate molecules between the solid phase and the liquid phase at equilibrium state at a particular temperature (Abechi et.al., 2011). Identifying the most appropriate adsorption isotherm model would be helpful to understand the adsorption behavior. In this present study, Langmuir, Freundlich, Temkin and Dubinin Radushkevich isotherm were employed to investigate the adsorption behavior. Adsorption isotherm was studied at four different temperatures viz. 305, 315, 325 and 335K.

5.1.6.1 Langmuir isotherm

Langmuir isotherm plots were drawn between C_e/q_e and C_e which are shown in figures 5.18 to 5.20. The regression coefficient (R^2) values were ranged from 0.9840 to 0.9990 for the four studied temperatures viz.305, 315, 325 and 335Kwhich confirmed the best fitting of the equilibrium data with Temkin isotherms. The value of monolayer adsorption capacity (Q_0) and energy of adsorption (b) determined from this Langmuir isotherm are summarized in table 5.7.

The monolayer adsorption capacity Q0 values (mg/g) for adsorption of Cr (VI) ions onto PBC APBC and BPBC were ranged from 21.739 to 23.810, 22.222 to 23.810 and 21.739 to 23.810 respectively. The adsorption capacity increased with the increase of temperature.

The values of Langmuir constant 'b' (L/mg) the adsorption energy for adsorption of Cr (VI) ions onto PBC, APBC and BPBC were ranged from 0.126 to 0.165, 0.152 to 0.242 and 0.141 to 0.219 respectively. These values indicate that the apparent energy of

sorption is less and ruled out the possibility of strong interaction between the solute and adsorption site.

The order of monolayer adsorption capacity of the three adsorbents namely PBC, APBC and BPBC are in following order for the adsorption of Cr (VI)ions for all the at studied temperatures.

 $Table-5.7\ Langmuir\ isotherm\ results\ for\ Cr\ (VI)\ ion\ adsorption\ onto\ PBC,$ $APBC\ \&\ BPBC$

[Cr (VI)ions, pH:2, Dose:30 mg/50 mL]

	Temperatu	Q0	В	
Adsorbents	re (K)	(mg/g)	(L/mg)	\mathbb{R}^2
	305	21.7390	0.1260	0.9980
	315	22.2220	0.1420	0.9990
PBC	325	23.2560	0.1650	0.9940
120	335	23.8100	0.1930	0.9840
	305	22.2220	0.1520	0.9990
A DD C	315	23.2560	0.1740	0.9980
APBC	325	23.3900	0.1990	0.9930
	335	23.8100	0.2420	0.9850
	305	21.7390	0.1410	0.9990
BPBC	315	22.7270	0.1590	0.9980
	325	23.2560	0.1830	0.9930
	335	23.8100	0.2190	0.9840

The dimensionless separation factor RLvalues calculated for various initial concentrations at different temperatures were lie between 0 and 1 which indicate the favorable adsorption for all the two systems. These RLvalues are presented in table 5.8.

Table-5.8 R_L values for Cr (VI) ion on adsorbents

Temperature (K)	C. ~	$R_{ m L}$				
	Ci mg/L	PBC	APBC	врвс		
	10	0.442	0.396	0.415		
305	15	0.346	0.304	0.321		
303	20	0.284	0.247	0.262		
	25	0.241	0.208	0.221		
	10	0.413	0.365	0.386		
215	15	0.319	0.277	0.295		
315	20	0.260	0.223	0.239		
	25	0.220	0.187	0.201		
	10	0.377	0.334	0.353		
325	15	0.287	0.251	0.267		
323	20	0.232	0.201	0.215		
	25	0.195	0.167	0.179		
	10	0.341	0.292	0.313		
335	15	0.256	0.216	0.233		
333	20	0.206	0.171	0.186		
	25	0.171	0.142	0.154		

The difference may be due to the following factors such pore volume, pore shape and surface characteristics of the adsorbents. In general Langmuir constant values infer a better performance of prepared adsorbents PBC, APBC & BPBC.

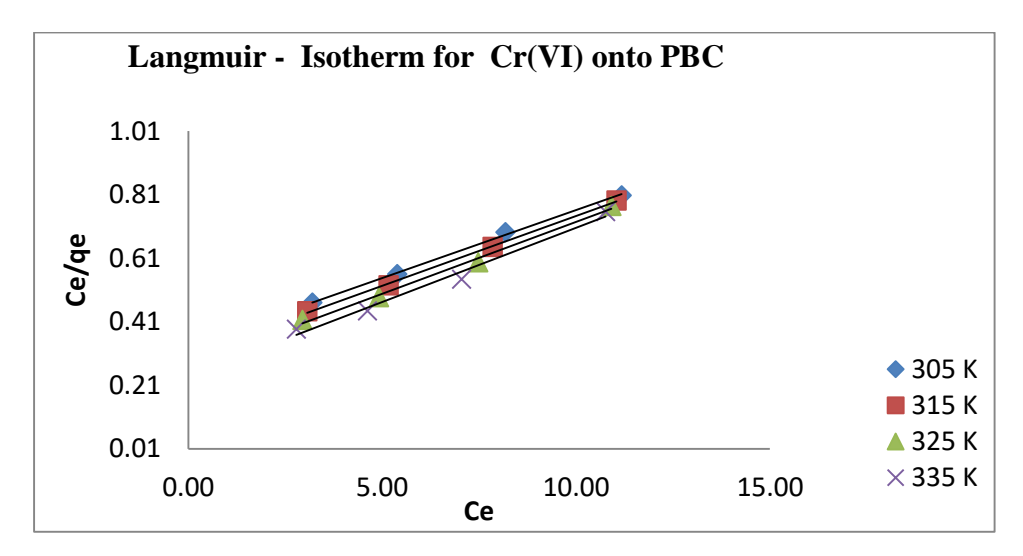


Figure 5.18

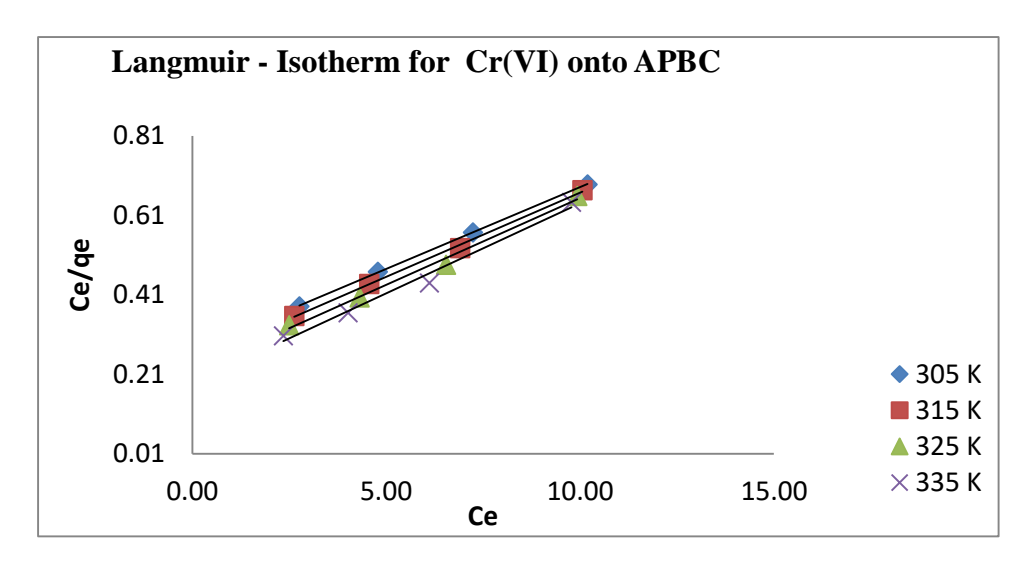


Figure 5.19

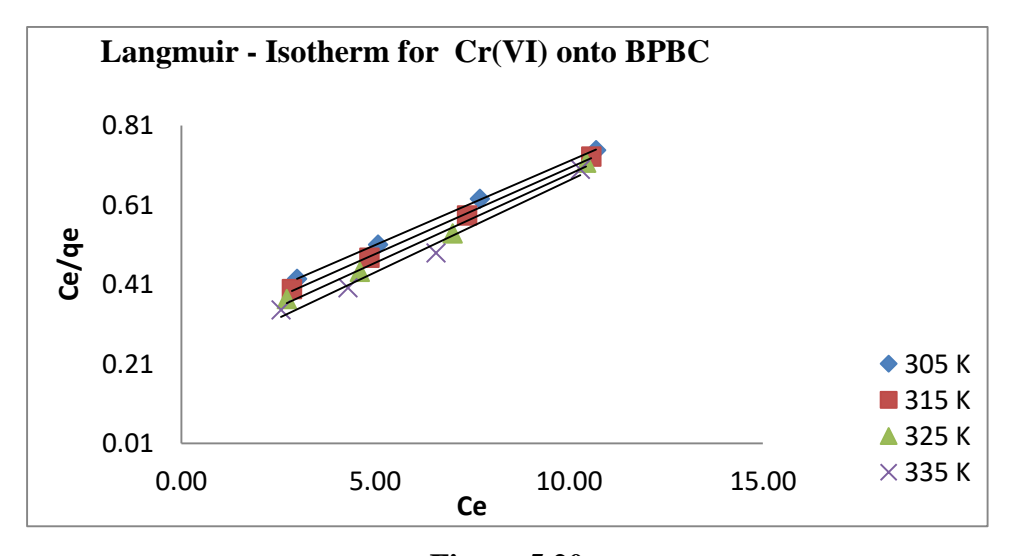


Figure 5.20

5.1.6.2 Freundlich isotherm

Freundlich isotherm plots were drawn between $\log q_e$ and $\log Ce$ which are shown in figures 5.21 to 5.23. The regression coefficient (R²) values were ranged from 0.9470 to 0.9940 for the four studied temperatures viz.305, 315, 325 and 335Kwhich revealed the best fitting of the equilibrium data with Temkin isotherms. The value of adsorption capacity (K_f) and intensity of adsorption (n) determined from this Freundlich isotherm are summarized in table 5.9.

Adsorption capacity Kf (mg/g) for Cr (VI) ions onto PBC, APBC and BPBC were ranged from 3.5975 to 4.4978, 4.2073 to 5.2966 and 3.8994 to 4.8978 respectively. Adsorption capacities of the three adsorbents were in the following order for all the studied temperatures.

It can be understood from the Kf (mg/g) at a particular temperature. These values are given in table $5.10\,$

The adsorption intensity (n) values are ranged from 1.7730 to 2.0367 for all the studied systems. These low values indicate the favorable physical adsorption. Further it is observed that 'n' value increased with the increase of temperature.

Table – 5.9 Freundlich isotherm results for Cr (VI) ions on adsorbents PBC, APBC & BPBC

[Cr (VI) ions, pH:2, Dose:30mg/50mL]

Adsorbents	Temperature (K) n		Kf (mg/g)	\mathbb{R}^2
	305	1.7730	3.5975	0.9930
	315	1.8248	3.8459	0.9870
PBC	325	1.8832	4.1305	0.9740
	335	1.9646	4.4978	0.9510
	305	1.8149	4.2073	0.9940
	315	1.8762	4.5082	0.9860
APBC	325	1.9417	4.8529	0.9720
	335	2.0367	5.2966	0.9470
	305	1.7953	3.8994	0.9930
	315	1.8519	4.1687	0.9860
ВРВС	325	1.9157	4.4875	0.9710
	335	2.0040	4.8978	0.9470

Table-5.10Adsorption capacity Kf (mg/g) values

Temperature (K)	PBC	APBC	BPBC
305	3.5975	4.2073	3.8994
315	3.8459	4.5082	4.1687
325	4.1305	4.8529	4.4875
335	4.4978	5.2966	4.8978

.

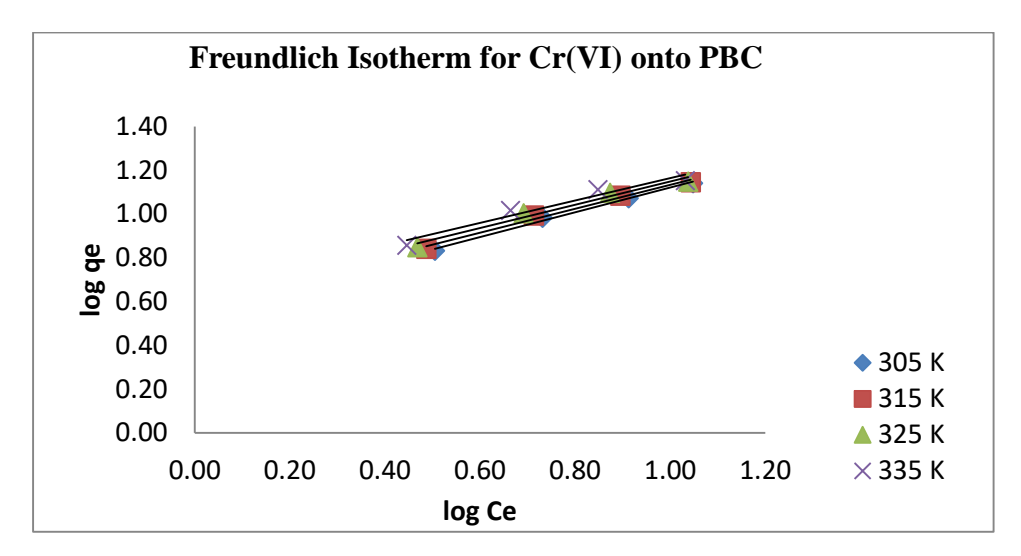


Figure 5.21

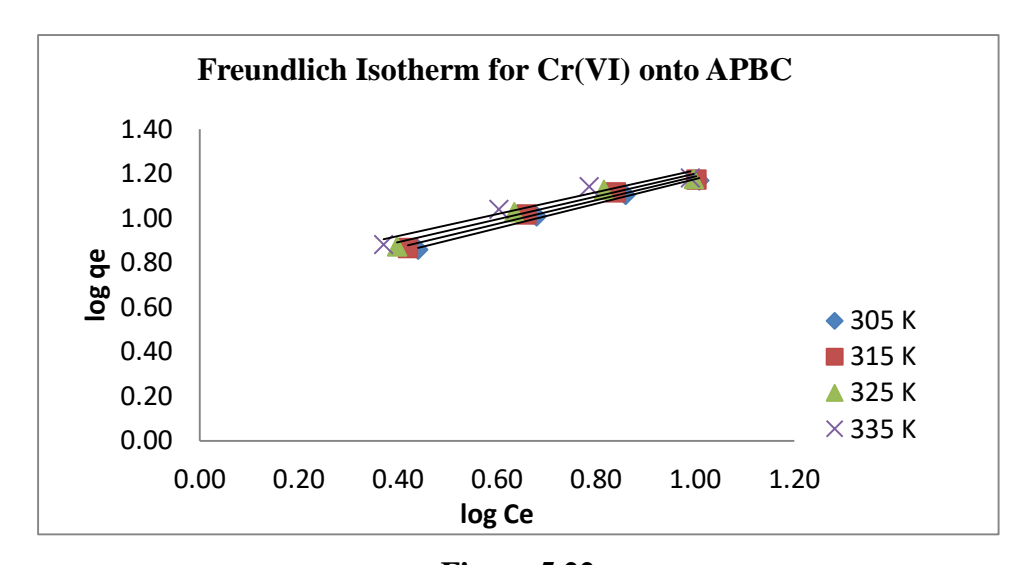


Figure 5.22

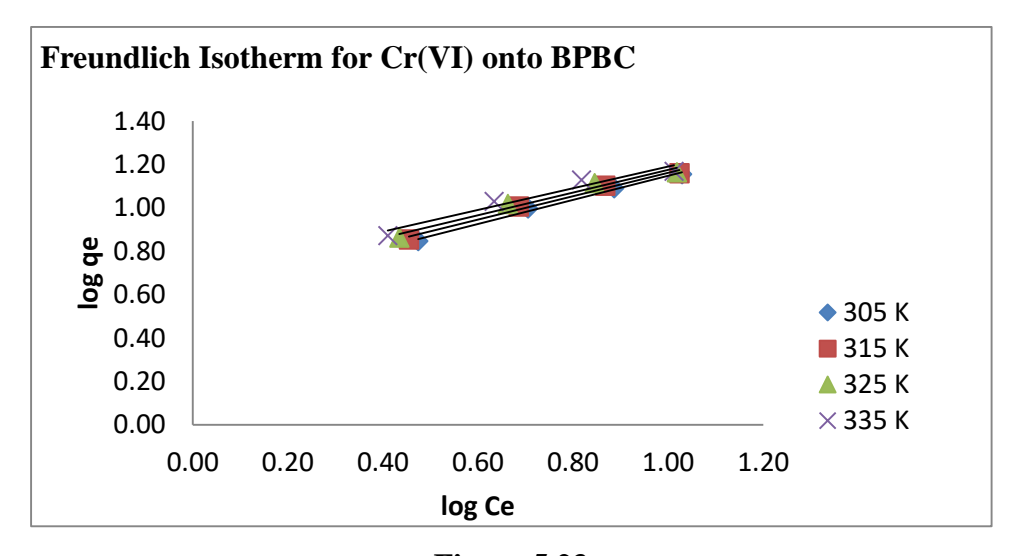


Figure 5.23

5.1.6.3 Temkin isotherm

Temkin plots were drawn between qe and lnCe which were shown in figures 5.24 to 5.26. The regression coefficient (R²) values were ranged from 0.9740 to 0.9990 for the four studied temperatures viz.305, 315, 325 and 335Kwhich revealed the best fitting of the equilibrium data with Temkin isotherms. The Equilibrium binding constant aT values (L/g) and heat of sorption constant bT values determined from Temkin isotherm are summarized in table 5.11.

Equilibrium binding constant aT values (L/g) onto PBC, APBC & BPBC were ranged from 1.051 to 1.474, 1.242 to 1.827 and 1.145 to 1.645 respectively. The heat of sorption constant bT values are ranged from 455.9917 J/mg to 524.8144 J/mg for PBC, 436.5995 to 510.2950 for ABPC and 446.5956 J/mg to 518.2713 J/mg for BPBC for the four studied temperatures viz. 305, 315, 325 and 335 K. These lower values of aT and bT indicate the physisorption nature rather than chemisorption.

 $Table-5.11 Temkin\ is other m\ results\ for\ Cr\ (VI)\ ions\ adsorption\ onto\ PBC,\ APBC\\ \&\ BPBC$

[Cr (VI) ions, pH:2, Dose:30mg/50mL]

Adsorbents	Temperature (K)	bT (J/mg)	aT (L/g)	\mathbb{R}^2
	305	455.9917	1.0510	0.9980
	315	476.5120	1.1540	0.9990
PBC	325	498.4412	1.2820	0.9940
	335	524.8144	1.4740	0.9790
	305	436.5995	1.2420	0.9990
	315	458.3322	1.3810	0.9980
APBC	325	481.6488	1.5580	0.9910
	335	510.2950	1.8270	0.9730
	305	446.5956	1.1450	0.9990
врвс	315	467.8296	1.2650	0.9990
БРВС	325	490.5683	1.4170	0.9920
	335	518.2713	1.6450	0.9740

•

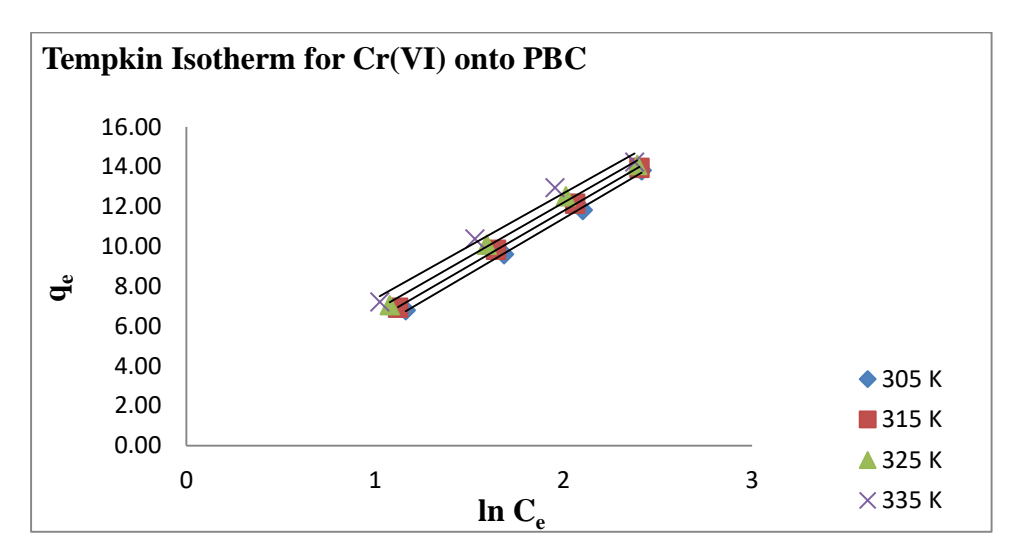


Figure 5.24

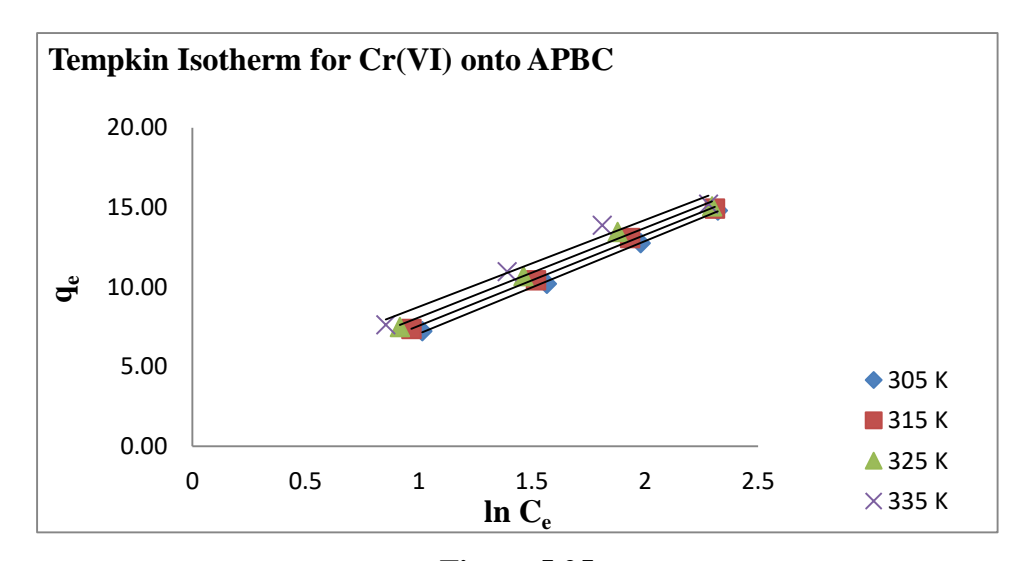


Figure 5.25

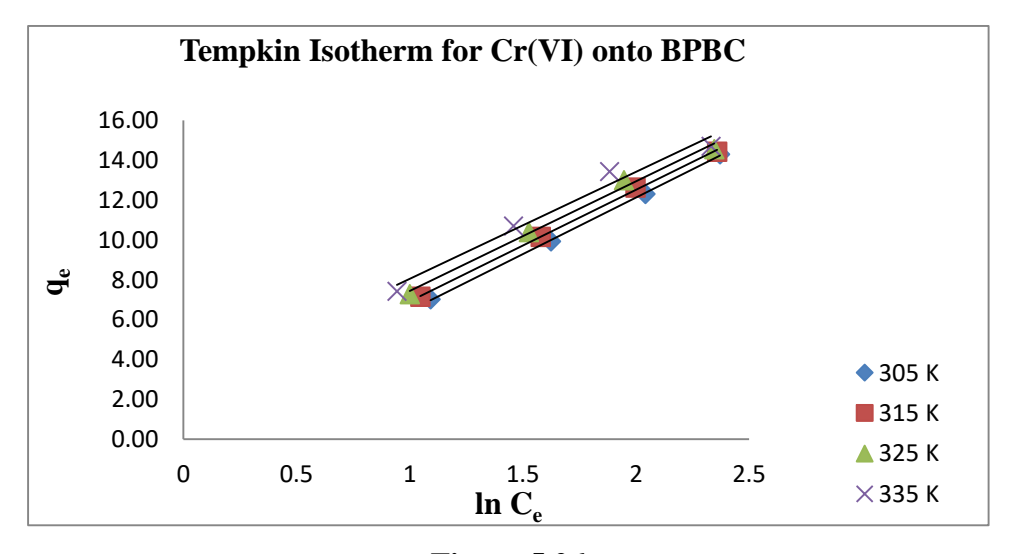


Figure 5.26

5.1.6.4 Dubinin-Radushkevich isotherm

Dubinin–Radushkevich isotherm (DRK plots were drawn between lnqe and $\epsilon 2$ (ϵ : RT ln (1+1/Ce) which were shown in figures 5.27 to 5.29. The regression coefficient (R2) values were ranged from 0.9830 to 0.9870, 0.9720 to 0.9770 and 0.9790 to 0.9830 for the four studied temperatures viz.305, 315, 325 and 335K respectively which revealed the best fitting of the equilibrium data with DRK isotherms. The theoretical saturation capacity q_D values (mg/g) and mean adsorption energy (kJ/mol) values determined are summarized in table 5.12.

The theoretical saturation capacity qD values (mg/g) were ranged from 12.8911 to 14.3467, 13.7600 to 15.2000 and 13.3636 to 14.8280 for PBC, ABPC and BPBC respectively. ABPC found to have a higher saturation adsorption capacity when compared to PBC and BPBC with all the studied temperatures. It is noticed that adsorption capacity increased with an increase in temperature.

The order of theoretical adsorption capacities the adsorbents are in the following order

APBC > BPBC > PBC

The values of mean adsorption energy were ranged from 0.6254 kJ/mol to 0.6127 kJ/mol, 0.6176 to 0.6061 and 0.6210 to 0.6089 for PBC, ABPC and BPBC respectively. These values of E are lesser than 8kJ/mol indicate that the adsorption were physisorption (Sivakumar et.al., 2009).

 $Table-5.12\ Dubinin-Radushkevich\ isotherm\ results\ for\ Cr\ (VI)\ ions$ $[Cr\ (VI)\ ions,\ pH:2,\ Dose:30mg/50mL]$

Adsorbents	Temperature (K)	qD (mg/g)	E (kJ/mol)	R ²
	305	12.8911	0.6254	0.9840
PBC	315	13.2836	0.6217	0.9830
	325	13.7567	0.6176	0.9840
	335	14.3467	0.6127	0.9870
APBC	305	13.7600	0.6176	0.9730
Arbc	315	14.1200	0.6145	0.9720
	325	14.6100	0.6106	0.9740
	335	15.2000	0.6061	0.9770
	305	13.3636	0.6210	0.9800
врвс	315	13.7430	0.6177	0.9790
	325	14.2324	0.6136	0.9810
	335	14.8280	0.6089	0.9830

.

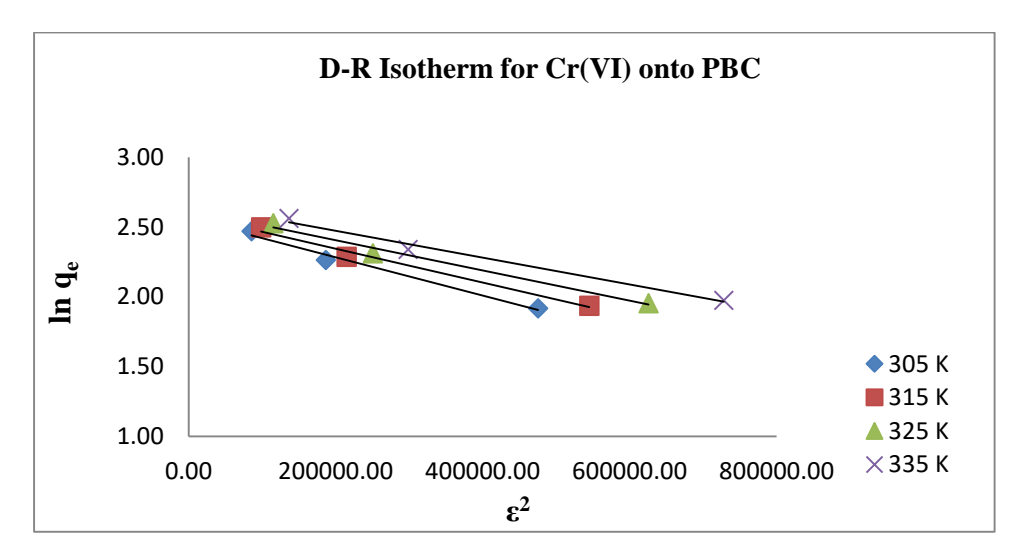


Figure 5.27

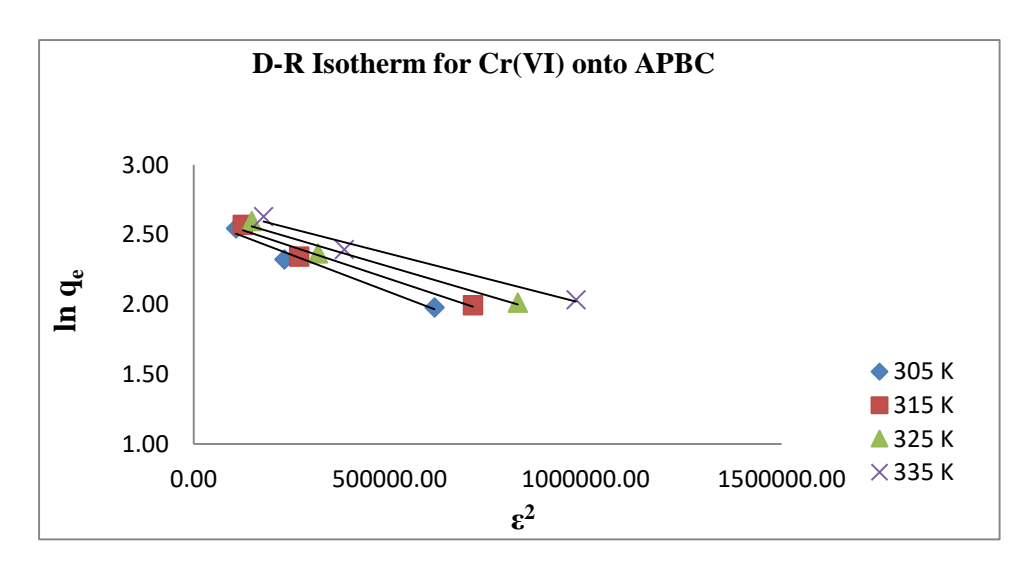


Figure 5.28

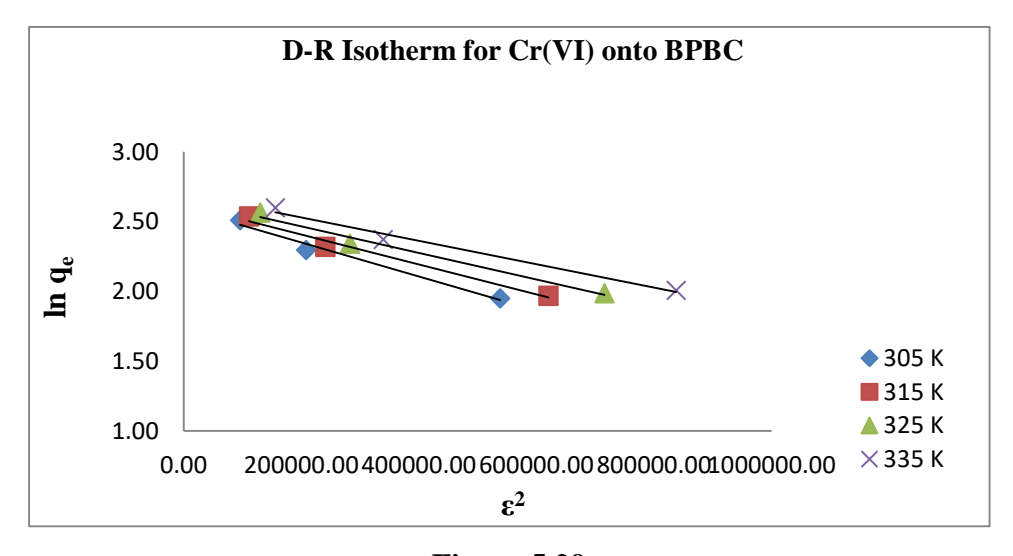


Figure 5.29

5.1.7 Adsorption Kinetics

5.1.7.1 Kinetic study for Cr (VI) ions adsorption onto PBC, APBC and BPBC

The plots drawn for the Lagergren's pseudo first order kinetic models were shown in figure 5.30 to 5.32. The values of regression coefficient (R2) of the plots for pseudo first order kinetic model for ranged from 0.9340 to 0.9430, 0.9200 to 0.9420 and 0.9100 to 0.9420 for PBC, APBC and BPBC. This indicates that the best fitting of data in pseudo first order kinetic model. The pseudo first order rate constant k1 and the calculated adsorption capacity qe (cal) from pseudo first order kinetic model were given in table 5.13, 5.15, &5.17.

The plots drawn for the Ho's pseudo second order kinetic models were shown in figure 5.33 to 5.35. The values of regression coefficient (R2) of the plots for pseudo second order models were ranged from 0.9910 to 0.9940, 0.9910 to 0.9940and 0.9930 to 0.9940. This indicates that the best fitting of data in pseudo second order kinetic model. The regression coefficient values of pseudo second order were greater than the regression coefficient values of pseudo first order models. The pseudo second order rate constant k2 and the calculated adsorption capacity qe (cal) from pseudo second order kinetic model were given in table 5.14, 5.16 & 5.18.

The values of pseudo first order rate constant for PBC, APBC & BPBC k₁ ranged from 0.0345 to 0.0392, 0.0345 to 0.0368 and 0.0345 to 0.0368 respectively and pseudo second order rate constant k2 values for PBC, APBC & BPBC ranged from 0.0085 to 0.0210, 0.0076 to 0.0211 and 0.0089 to 0.0211 respectively. The pseudo second order initial sorption rate, 'h', increased with an increase of initial concentrations of Cr (VI) ions at 305K temperature.

The difference between the calculated adsorption capacity qe (cal) obtained from pseudo first order equation and the experimental adsorption capacity qe (exp) were found to be large. Whereas the difference between the calculated adsorption capacity qe (cal) obtained from pseudo second order equation and the experimental adsorption capacity qe (exp) were found to be small. (table 5.13-5.18).

Best fitting kinetic model is tested with a statistical tool 'Mean of sum of error squares' (MSSE). The MSSE of pseudo first order kinetic model is high when compared to pseudo second order kinetic model (table 5.13, 5.15, 5.17). The lower MSSE values for pseudo second order kinetic model reflect the suitability of second order kinetic model rather than pseudo first order kinetic model for the adsorption of Cr (VI) ions onto PBC, APBC & BPBC adsorption system.

Table - 5.13 Pseudo first order Kinetics results for the adsorption of $Cr\ (VI)$ ions onto PBC

[pH:2, Dose:30mg/50mL, Contact time:120min, Temp:305K]

Pseudo First Order Kinetics						
Concentration (mg/L)	k1×10 ⁻² (min ⁻¹)	qe (cal) (mg/g)	qe (exp) (mg/g)	Δqe	\mathbb{R}^2	MSSE
10	0.0392	4.7098	6.80	2.0902	0.9340	
15	0.0368	6.6222	9.62	2.9928	0.9270	1.61
20	0.0345	8.0724	11.82	3.7476	0.9200	1.61
25	0.0345	10.0462	13.83	3.7788	0.9430	

Table - 5.14 Pseudo second order Kinetics results for the adsorption of Cr (VI) ions onto PBC

[pH:2, Dose:30mg/50mL, Contact time:120min, Temp:305K]

	Pseudo Second Order Kinetics					
Concentration (mg/L)	k2×10 ⁻³ (g/mg.min)	qe (cal) (mg/g)	Δqe	Н	R ²	MSSE
10	0.0210	7.1942	2.0902	1.09	0.9940	
15	0.0141	10.2041	2.9928	1.47	0.9930	0.33
20	0.0116	12.5000	3.7476	1.81	0.9930	0.33
25	0.0085	14.7059	3.7788	1.83	0.9910	

Table - 5.15 Pseudo First order Kinetics results for the adsorption of $Cr\ (VI)$ ions onto APBC

[pH:2, Dose:30mg/50mL, Contact time:120min, Temp:305K]

		Pseudo First Order Kinetics							
Concentration (mg/L)	k1×10 ⁻² (min ⁻¹)	qe (cal) (mg/g)	qe (exp) (mg/g)	Δqe	R ²	MSSE			
10	0.0368	4.8195	7.24	2.4205	0.9200				
15	0.0368	6.8077	10.22	3.4073	0.9190				
20	0.0345	8.3753	12.76	4.3847	0.9020				
25	0.0368	11.0917	14.81	3.7157	0.9420	1.78			

Table - 5.16 Pseudo second order Kinetics results for the adsorption of Cr (VI) ions onto APBC

[pH:2, Dose:30mg/50mL, Contact time:120min, Temp:305K]

	Pseudo Second Order Kinetics						
Concentration (mg/L)	k2×10 ⁻³ (g/mg.min)	qe (cal) (mg/g)	Δqe	h	\mathbb{R}^2	MSSE	
10	0.0211	7.6336	2.4205	1.23	0.9940		
15	0.0150	10.7527	3.4073	1.73	0.9940		
20	0.0112	13.5135	4.3847	2.04	0.9930	0.37	
25	0.0076	15.8730	3.7157	1.92	0.9910		

Table - 5.17 Pseudo First order Kinetics results for the adsorption of Cr (VI) ions onto BPBC

[pH:2, Dose:30mg/50mL, Contact time:120min, Temp:305K]

		Pseudo First Order Kinetics						
Concentration (mg/L)	k1×10 ⁻² (min ⁻¹)	qe (cal) (mg/g)	qe (exp) (mg/g)	Δqe	R ²	MSSE		
10	0.0345	4.7643	7.02	2.2556	0.9270			
15	0.0368	6.7143	9.93	3.2157	0.9220	1 74		
20	0.0368	8.2224	12.30	4.0775	0.9100	1.74		
25	0.0368	10.2329	14.30	4.0670	0.9420			

Table - 5.18 [pH:2, Dose:30mg/50mL, Contact time:120min, Temp:305K]

	Pseudo Second Order Kinetics							
Concentration (mg/L)	k2×10 ⁻³ (g/mg.min)	qe (cal) (mg/g)	Δqe	Н	\mathbb{R}^2	MSSE		
10	0.0211	7.4074	0.3874	1.16	0.9940			
15	0.0144	10.5263	0.5963	1.59	0.9940	0.22		
20	0.0113	12.9870	0.6870	1.91	0.9930	0.33		
25	0.0089	15.1515	0.8515	2.04	0.9930			

Table 5.19 MSSE Values for the adsorption of Cr (VI) ions

Adsorbents	MSSE Values				
Ausorbents	Pseudo first order model	Pseudo second order model			
PBC	1.61	0.33			
APBC	1.78	0.37			
ВРВС	1.74	0.33			

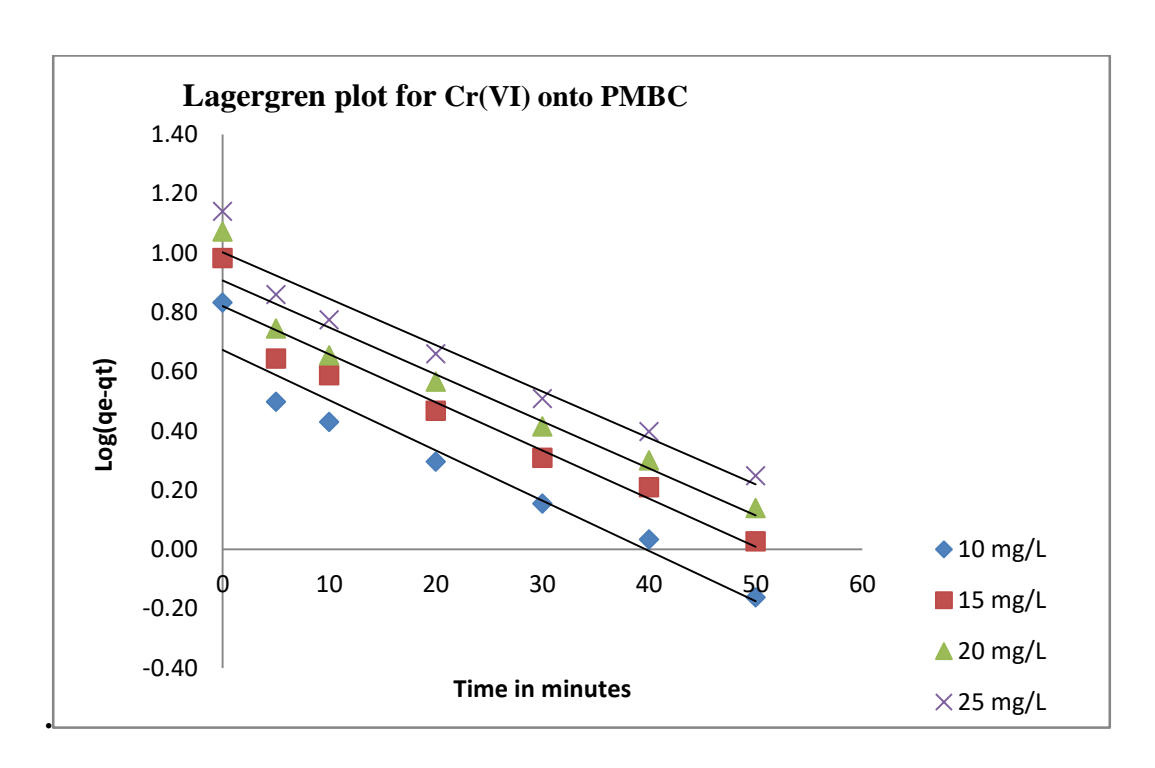


Figure 5.30

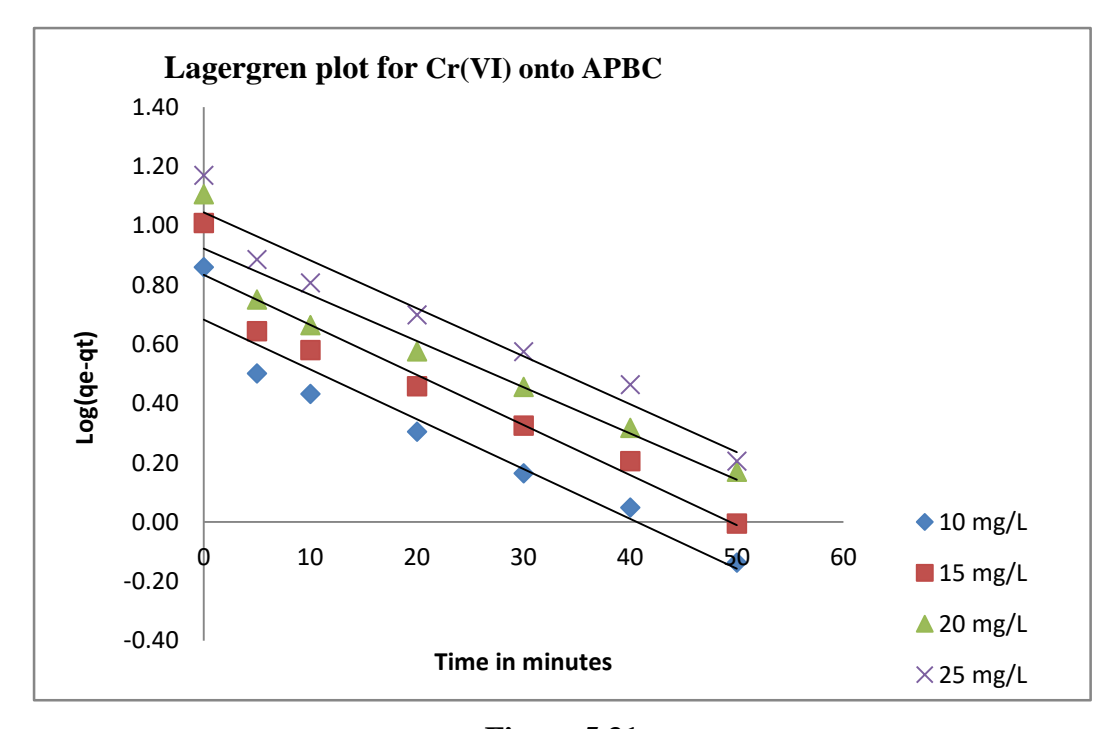


Figure 5.31

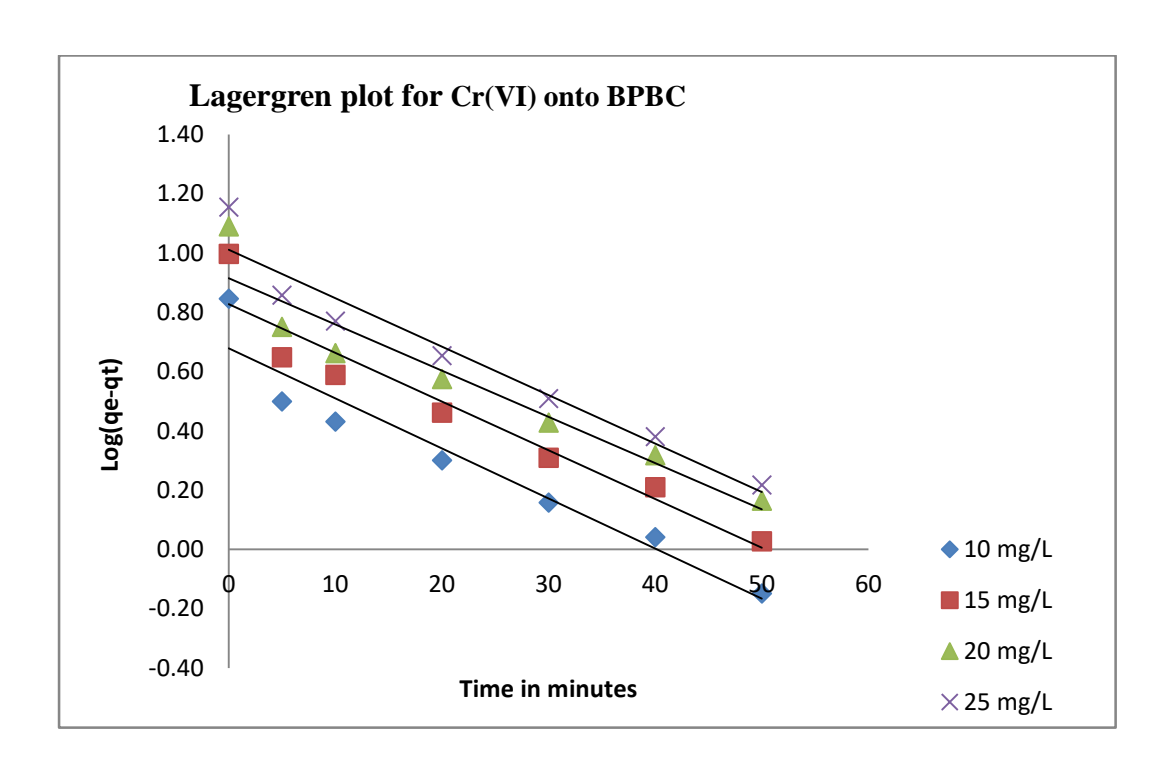


Figure 5.32

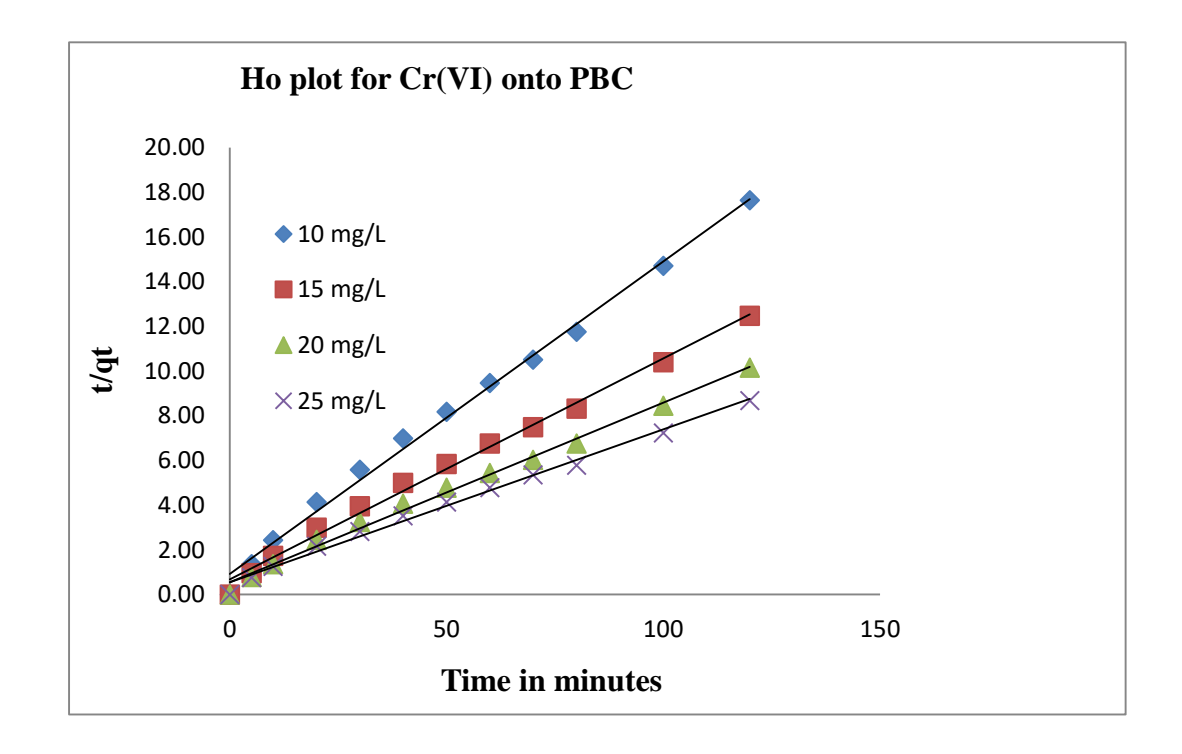


Figure 5.33

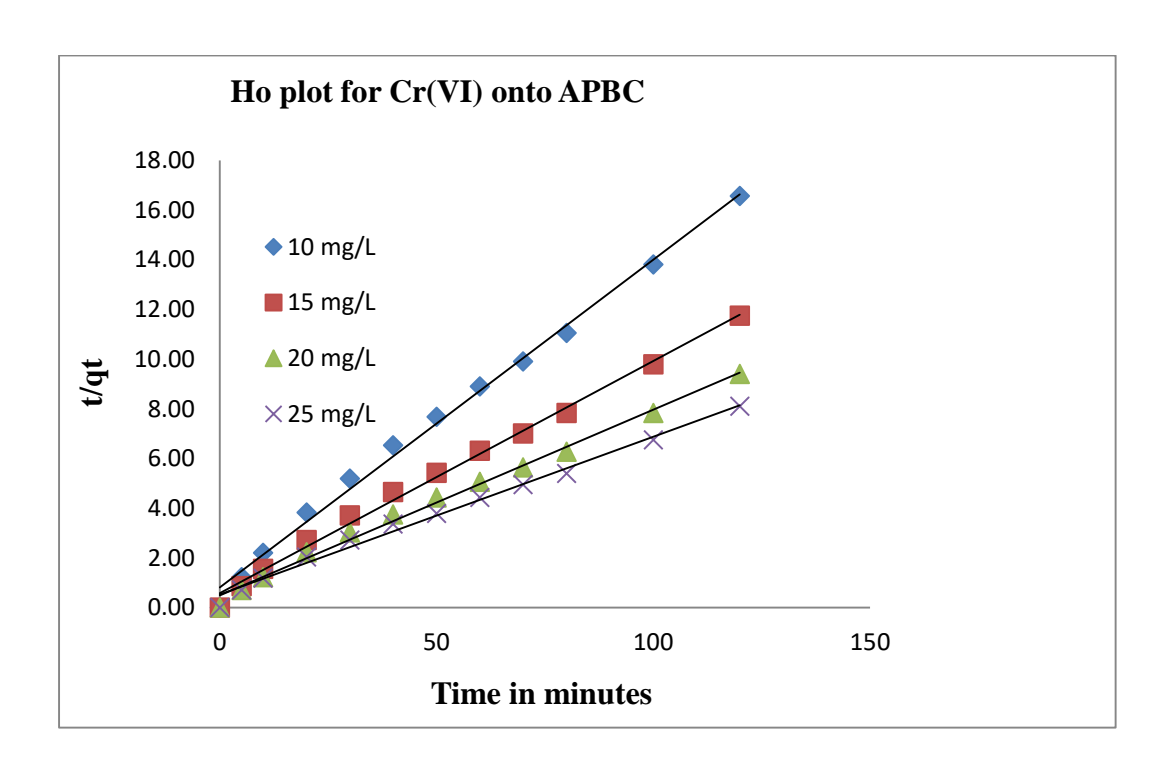


Figure 5.34

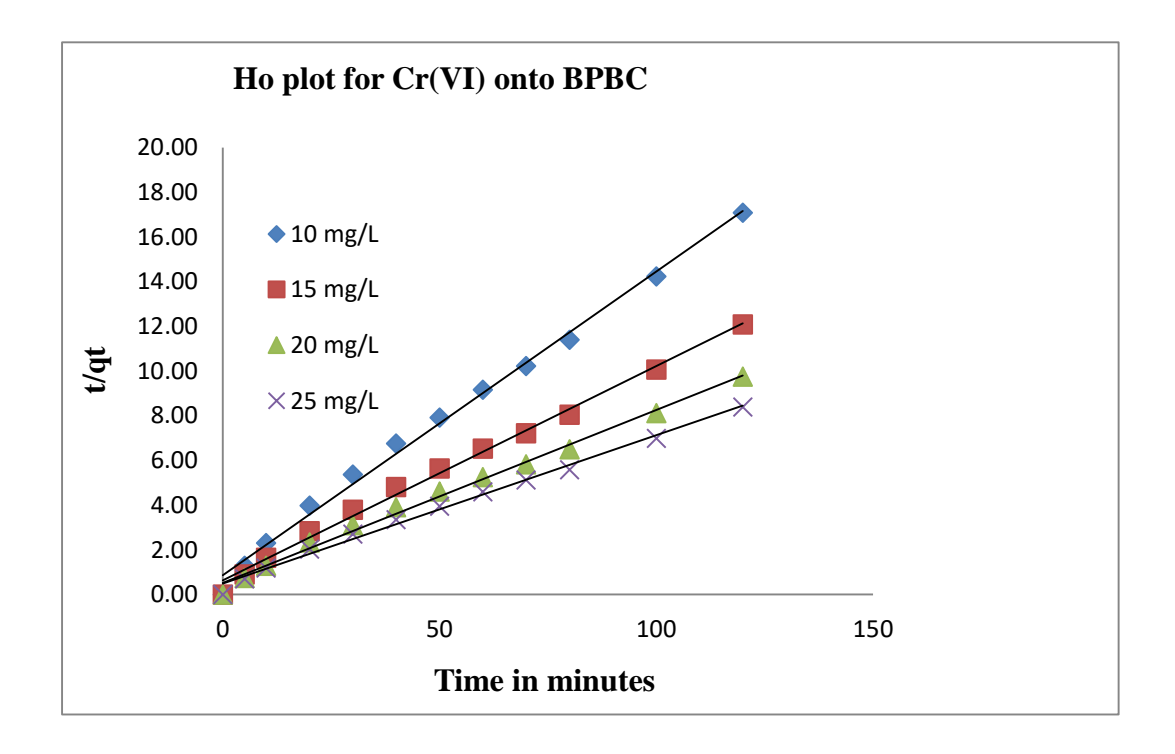


Figure 5.35

5.1.7.2 Intra particle diffusion

The plots for intraparticle diffusion kinetic model was drawn between mass of adsorbate adsorbed per unit mass of adsorbent (qt) versus t^{0.5}. It was noticed that the plot consist more than one phases. The initial portion of the plot indicates a boundary layer effect that is film diffusion while the other phases are due to intraparticle diffusion and instantaneous utilization of the most readily available adsorbing sites on the adsorbent surface. Representative Webber-Morris plot is shown in figure 5.36, 5.37, 5.38.

The slopes of the final linear portions of the plots are shown in figure 5.36 to 5.38. The of intra particle diffusion rate constant Kp was determined from the slope of the final linear portion. The values of K_p and R2 values are given in table 5.20.

The Kp values are found to increase with an increase of Cr (VI)ions concentration that reveals the rate of adsorption governed by the diffusion of adsorbed Cr (VI) ions within the pores of the adsorbent. Present results were showed that pore diffusion limits the overall rate of Cr (VI)ions adsorption (Ahmad et.al., 2016, Rambabu et.al., 2020, Yusuff et.al., 2019).

Table - 5.20 Intra Particle Diffusion results for adsorption Cr (VI) ions [pH:2, Dose:30mg/50mL, Contact time: 120min, Temp:305K]

Ci		kp (mg/g.mi	n)			
(mg/L)	PBC	APBC	BPBC	PBC	APBC	ВРВС
10	0.4880	0.4880	0.4880	0.9970	0.9960	0.9960
15	0.7020	0.7110	0.6860	0.9870	0.9970	0.9900
20	0.8720	0.8860	0.8720	0.9910	0.9990	0.9910
25	1.0620	1.2720	1.089	0.9890	0.9890	0.9950

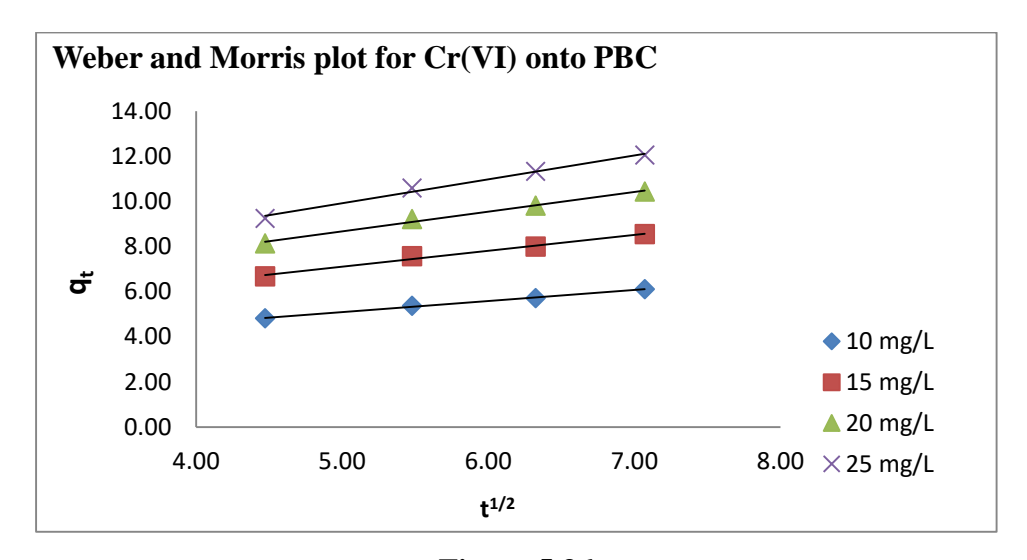


Figure 5.36

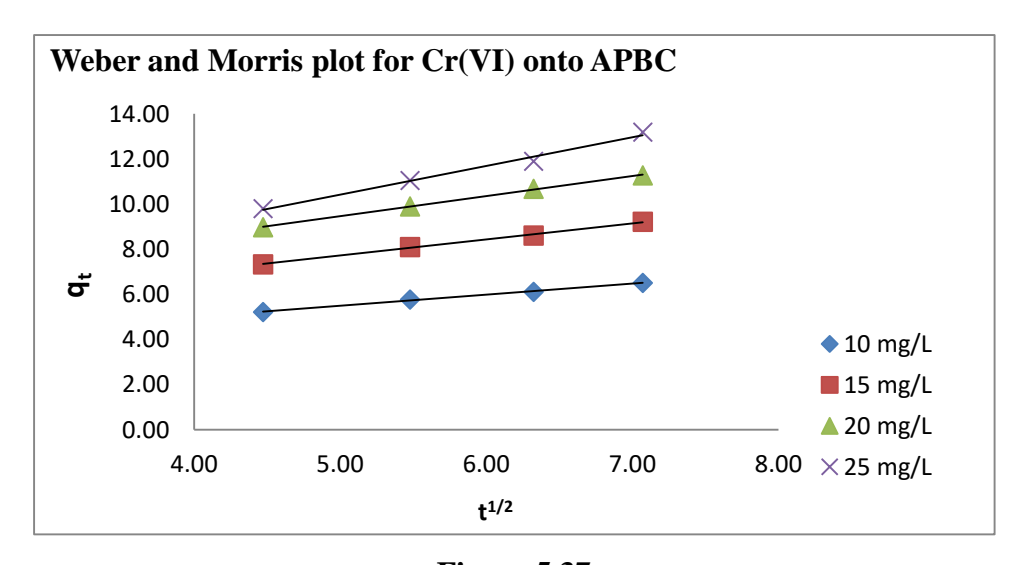


Figure 5.37

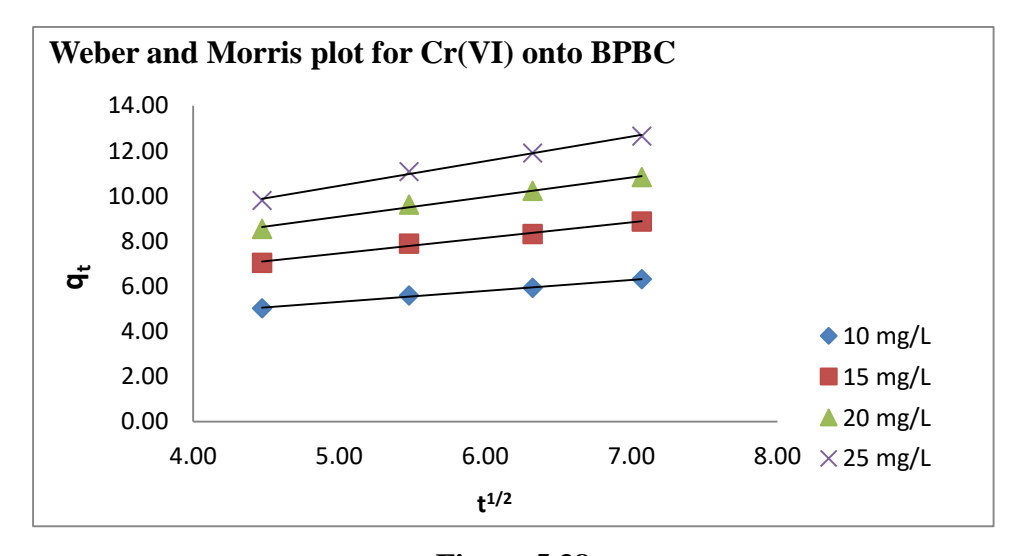


Figure 5.38

5.1.8 Thermodynamic studies

The Van't Hoff plots drawn for the chosen system at four different temperatures are shown in figures 5.39 to 5.41. The thermodynamic parameters calculated are presented in table 5.20.

The negative values of ΔG° (table 5.20) showed that the adsorptions of Cr (VI)ions onto PBC, APBC & BPBC are highly favorable and spontaneous .

The positive values of ΔH° showed the endothermic nature of adsorption which is supported by the fact that the adsorption capacity of the adsorbent increased with an increase in temperature from 305 to 335K. The magnitudes of ΔH° values were within the range of 5.5022 to 7.5275 (kJ/mol). These values are lesser than 90 kJ which indicates the physisorption and ruled out the possibility of chemisorption (Yao et.al., 2010).

The values of ΔS° of the present studied system ranged from 24.2686 to 29.1200. These positive values of ΔS° showed that the randomness at the solid solution interface. During adsorption some structural changes might have occured at the surface of the adsorbent. The adsorbed water molecules which are displaced by the adsorbate species, might have gained more translational entropy than is lost by the adsorbate molecules, thus allowing the prevalence of randomness in the system (Biswajit Das et.al., 2013).

This ΔS° values found to decrease with an increase of initial concentration of the adsorbates solution. While comparing the ΔS° values with respect to the adsorbents, the ΔS° values for the adsorption onto APBC were found to be high when compared to BPBC and PBC.

The enhancement of adsorption capacity of the adsorbents at higher temperatures was attributed to the enlargement of the size of the pore and the activation of the adsorbent surface (Krishna et.al., 2013).

Table 5.21 Thermodynamic study results for the adsorption of Cr (VI) ions [Cr (VI)ions, pH:2, Dose :30mg/50mL]

Adsorbents	Ci (mg/L)		Δ kJ/	ΔH° kJ/mol	ΔS° (kJ/mol)		
		305K	315K	325K	335K		
	10	-1.9117	-2.1327	-2.3675	-2.6448	5.5022	24.2686
	15	-1.4703	-1.6870	-1.9425	-2.2593	6.5124	26.0976
PBC	20	-0.9336	-1.1442	-1.3921	-1.6939	6.7643	25.1665
	25	-0.5397	-0.8122	-1.0058	-1.3593	7.5275	26.4219
	10	-2.4459	-2.6991	-2.9690	-3.2879	6.0700	27.8800
	15	-1.9234	-2.1656	-2.4505	-2.8038	6.9800	29.1200
APBC	20	-1.4373	-1.6735	-1.9507	-2.2877	7.1700	28.1600
	25	-0.9472	-1.0348	-1.1262	-1.2309	7.3400	27.1700
	10	-2.1731	-2.4093	-2.6606	-2.9573	5.7583	25.9646
	15	-1.7049	-1.9344	-2.2046	-2.5395	6.7385	27.6025
ВРВС	20	-1.1879	-1.4109	-1.6730	-1.9917	6.9505	26.6131
	25	-0.6972	-1.0006	-1.2270	-1.4685	7.0553	25.4741

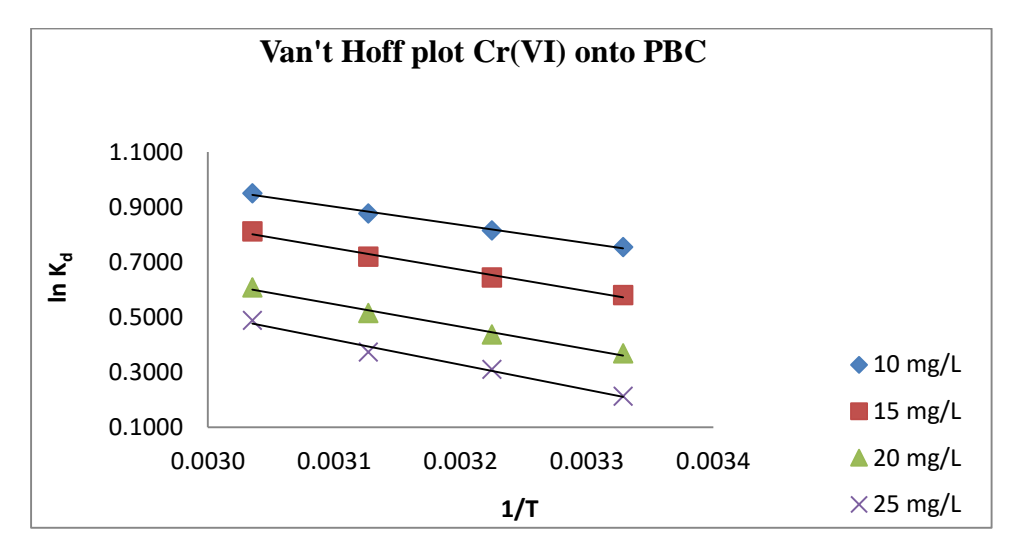


Figure 5.39

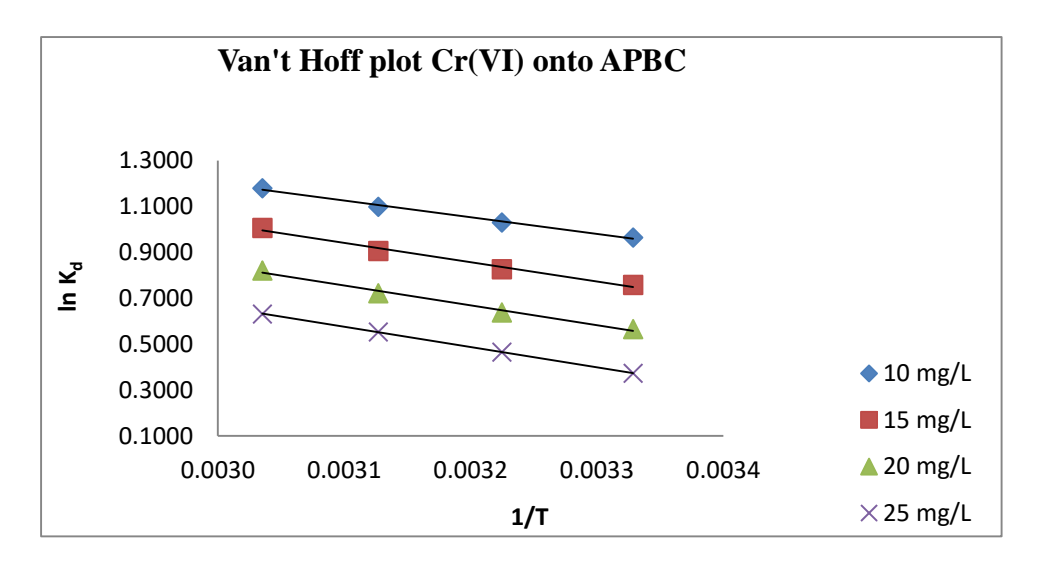


Figure 5.40

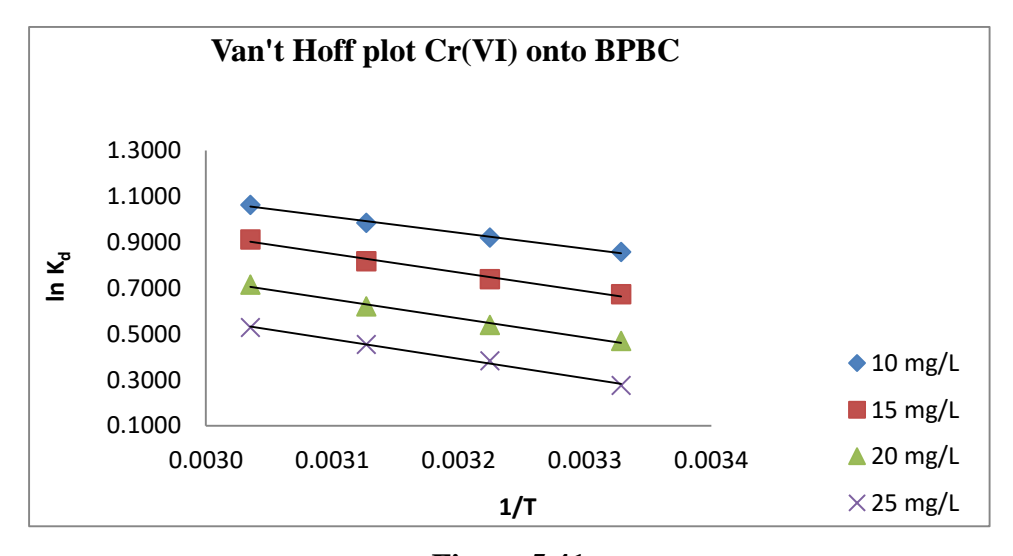


Figure 5.41

5.1.9 Desorption of Cr (VI) ions

Result of desorption of Cr (VI) ions from adsorbents loaded with Cr (VI) ions is presented as column diagram in figure 5.42. The percentage of desorption was more for 0.1N NaOH solution when compared to other desorbing agents water and 0.1N HCl acid. This is due to fact that OH ions replaced the anionic form of Cr (VI) ions (Bicarbonate) more effectively from the adsorbent through ion exchange process. According to Hema et.al., 2007 the reversibility of adsorbed ions , supports the physisorption mechanism.

The maximum percentage of desorption is found to be 68 % which suggests that the some Cr (VI) ions are strongly attached to adsorbent. This strong attachment might be due to chemisorption. Hence it may be concluded that Cr (VI) ions were bound on the surface of the adsorbent both by physical force and chemical forces. The physical force is normally Vander wall's force. The chemical forces probably due to attachment between Cr (VI) ions and the functional group present in the surface of the adsorbent.

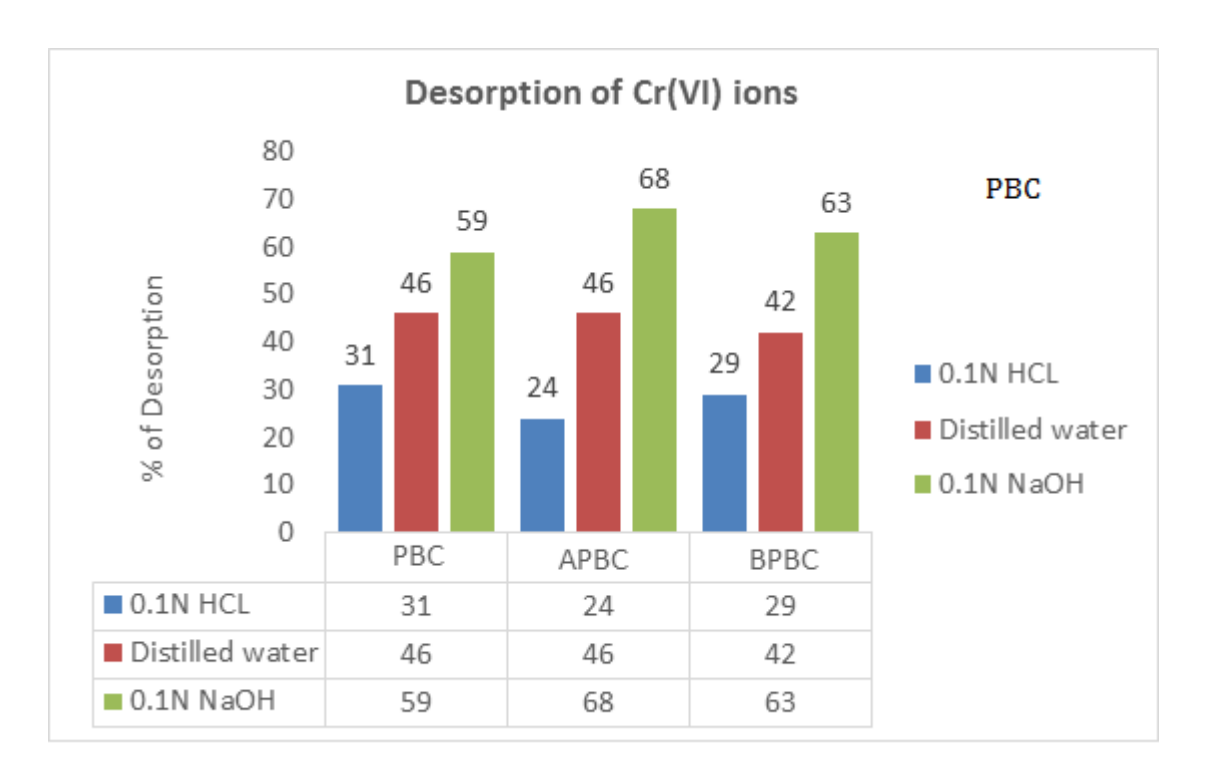


Figure 5.42

5.1.10 Morphological study

Changes in the morphology of adsorbent before and after adsorption were analyzed with FT-IR spectra. EDAX of the adsorbents after adsorption of Cr (VI) ions were also studied.

5.1.10. FT-IR Study for the adsorption of Cr (VI) ions

The FT - IR spectrum of PBC, APBC and BPBC loaded with Cr (VI) ions was shown in figure 5.43 to 5.45.

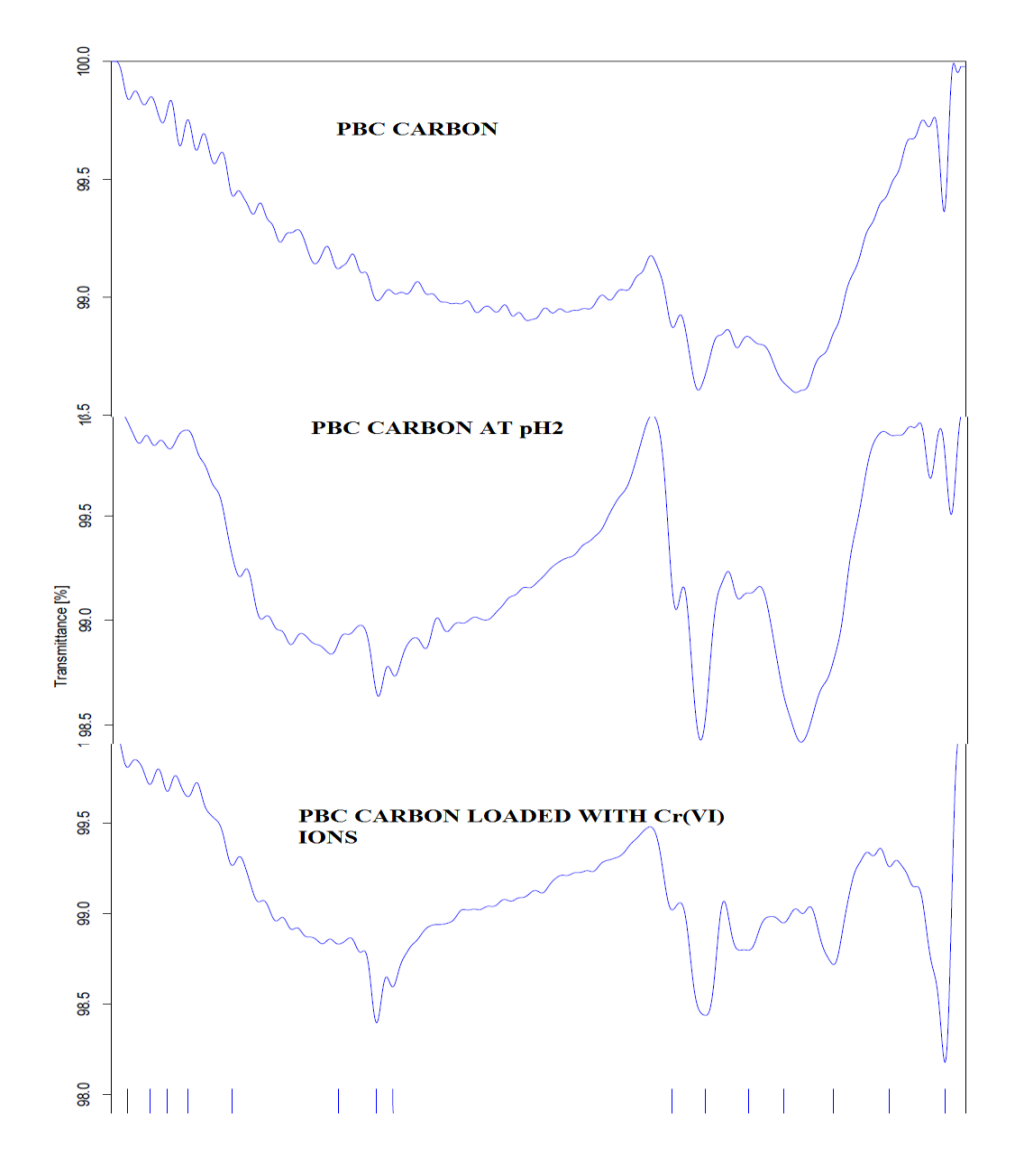


Figure 5.43 FTIR Spectrum of PBC adsorbent before adsorption, PBC at pH2 and Cr (VI) ions loaded PBC

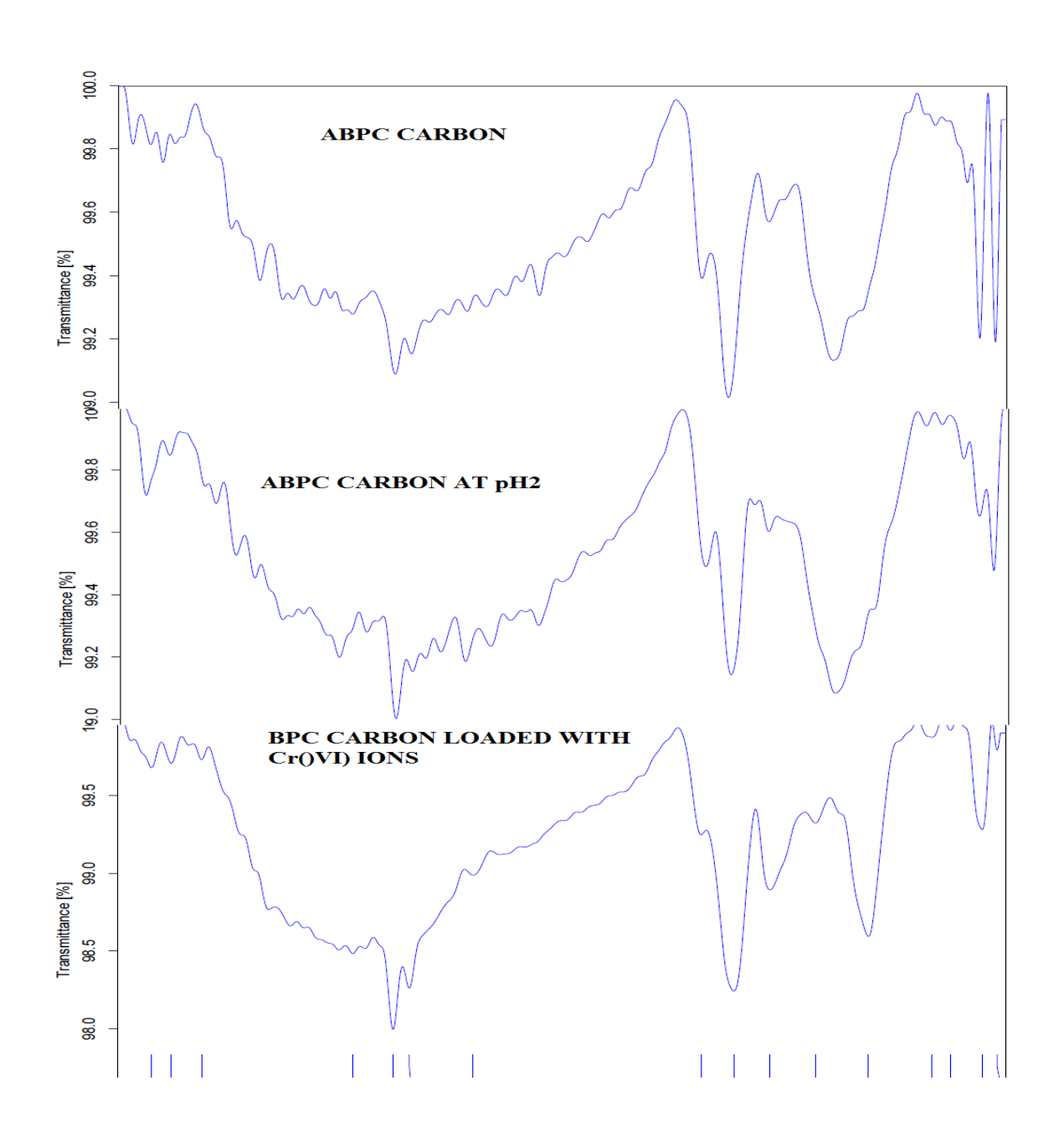
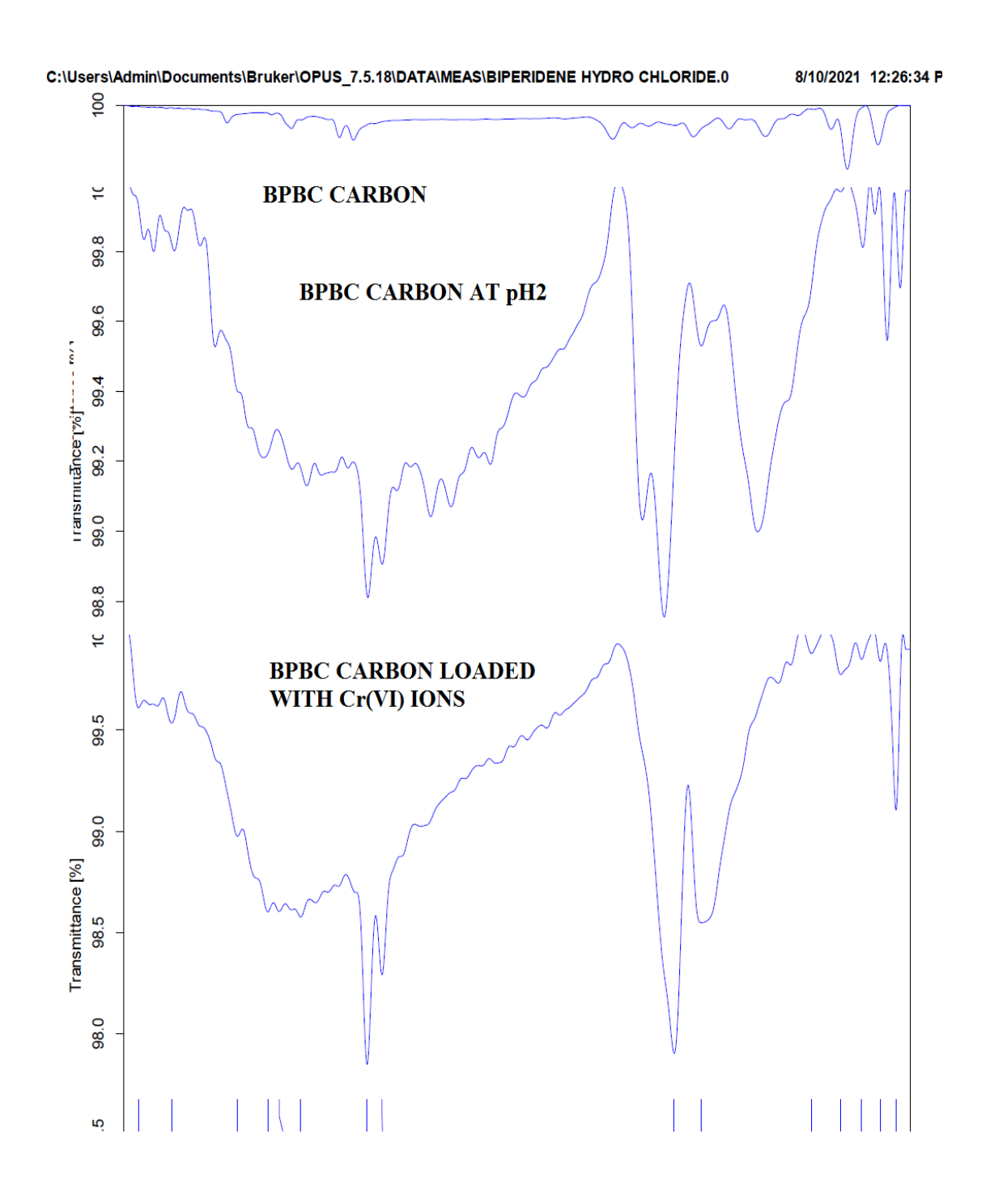


Figure 5.44 FTIR Spectrum of APBC adsorbent before adsorption, APBC at pH2 and Cr (VI) ions loaded APBC



5.45 FTIR Spectrum of BPBC adsorbent before adsorption, BPBC at pH2 and Cr $\,$ (VI) ions loaded BPBC $\,$

Analysis of FTIR peaks of before and after adsorption of Cr (VI) ions onto PBC, APBC and BPBC infer that intensities of the some peaks were changed, some peaks were diminished and few new peaks were formed. This results leads to conclude that possibility of some chemisorption also took place.

5.1.10.3 EDAX pattern adsorbents after adsorption of Cr (VI) ions

Representative EDAX pattern of Cr (VI) ions loaded PBC was shown in figure 5.46. The well-defined peak of Cr (VI) ions shows that well fitted Cr (VI) ions into the crystalline structure of the adsorbent. Less intense peaks infers the surface adsorption through Vander Walls force.

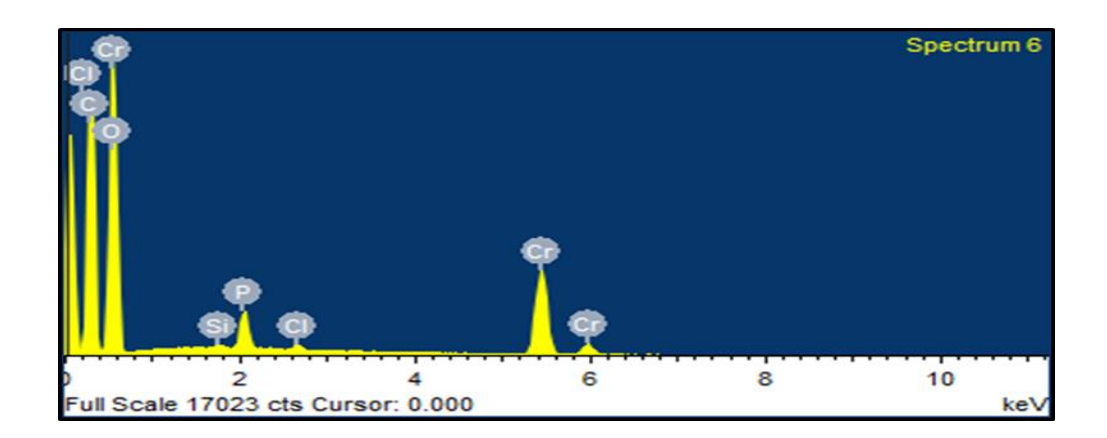


Figure. 5.46EDAX pattern of Cr (VI) adsorbed PBC

5.2 STUDIES ON THE ADSORPTION OF MB DYE ONTO PBC, APBC AND BPBC

5.2.1 Effect of pH

Dye adsorption is largely affected by the solution pH. When dyes are present in water, they ionize into charged species. The speciation is controlled by the pH of the solution. Therefore, in an adsorption system, the extent to which a certain dye will be attracted and adhere to the adsorbent will vary with the pH.

Figure 5.47 shows the percentage removal of MB by the adsorbents {PBC, APBC and BPBC} at different pH values. The pH values examined for the adsorption of MB onto adsorbents were 2, 4, 6, 8 and 10.

The percent removal was increased when the solution pH is raised from 2 to 10. Steep increase is observed from pH 2 to 7 after that it increased slightly till pH 10. This can be explained on the basis of pH and ZPC of the adsorbents and speciation of the dye molecule. At lower pH, the COOH group of the dye was protonated with the positive charge. This positive charge density of reduced molecular ion decreases with the increase of solution pH. At alkaline pH the carboxylic group becomes carboxylate anion.

On the other hand positive charge accumulated on the surface of the adsorbent increases with the lowering of the solution pH. Hence at low pH, high positive charge density on the adsorbent surface does not favour the adsorption of dye cations due to the electrostatic repulsion. As the pH increased, the dye removal from the solution increased as the electrostatic repulsion decreased with the decrease of hydrogen ion concentration. Several researchers have reported that Methylene blue adsorption usually increases as the pH is increased. (Suk Soon Choi et al, H.J choi et al, Yuh-shan et al)

pH_{ZPC} of the adsorbents is 6.8. At pH higher than 6.8, surface of the adsorbent acquires negative charge which facilitates the adsorption of cationic dye molecules. But it was observed that the difference between the percentage of removal at pH 7 and at pH 10 was small. Therefore further adsorption studies of MB dye was carried out keeping the pH 7, (though higher percentage of removal observed at pH 10) in order to avoid neutralization of solution after adsorption is over. The electrostatic interaction and hydrogen bonding were proposed as dominant adsorption mechanisms at basic and acidic pH respectively. But the hydrophobic-hydrophobic interaction was a dominant mechanism at neutral pH (L.wu, w. et al, H.Zhuang et al).

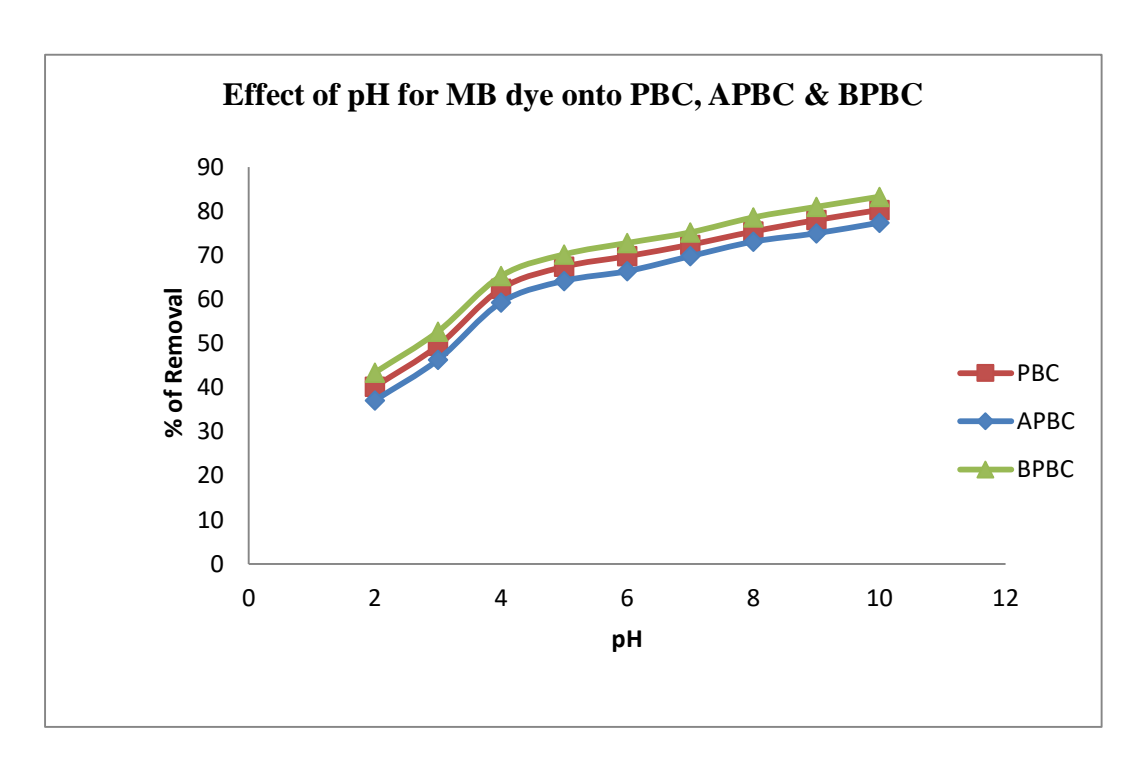


Figure 5.47

5.2.2 Effect of Adsorbent Dosage on MB Dye Removal

Adsorbent dosage is the parameter that strongly influences the adsorption process by affecting the adsorption capacity of the adsorbents PBC, APBC and BPBC. The effect of adsorbent dosage is investigated for the removal of Methylene blue dye from aqueous

solution by varying the dosage of the adsorbent from 5 mg to 50 mg. Batch mode experiments are carried out by using 30 mg/L of dye solution containing 50 mL at 305K and at pH 7 by varying the adsorbent dosage. It is observed that the percentage removal of dye increased when the adsorbent dosage is varied from 5 to 50mg (For PBC from 33.22 % to 98.1 %, for APBC from 30.00 % to 95.71 %, and BPBC from 35.45 % to 99.70%). This results obtained are shown in table 5.21 and graphically represented in figure 5.48.

The increase in the percentage removal of MB dye with adsorbent dosage could be attributed to an increase in the surface area of the adsorbent with the more number of adsorption sites available for adsorption.

Table – 5. 22 Effect of dose for MB dye onto PBC, APBC& BPBC (Contact Time=80min)

	MB Dye					
Dose in mg	% Removal of PBC	% Removal of APBC	% Removal of BPBC			
05	33.22	30.0	35.45			
10	44.20	41.1	47.16			
15	54.20	51.8	57.13			
20	70.30	67.43	73.23			
25	80.3	77.27	83.20			
30	89.1	86.66	92.00			
35	94.2	91.81	97.24			
40	98.1	95.71	99.70			
45	98.1	95.71	99.70			
50	98.1	95.71	99.70			

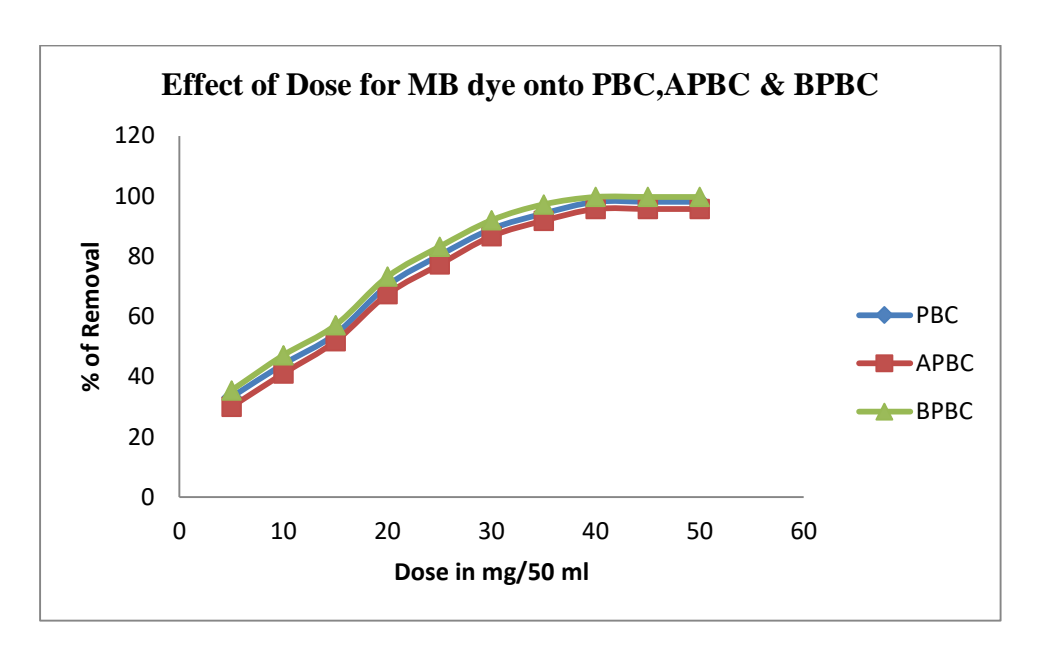


Figure 5.48

5.2.3 Effect of Contact time

The adsorption of the MB dye by activated carbon was studied at various time intervals (0-120 min) and at a concentration from 75 to 150 mg/L. figure 5.49 to 5.51 shows that MB dye uptake is rapid up to 80 min, and after that proceed at a slower rate and finally attain saturation. The initial fast reaction may be due to the increased number of vacant sites available at the initial stage, as a result there exists increased concentration gradient between adsorbate in solution and adsorbate in the adsorbent (PBC, APBC& BPBC).

Generally adsorption involves a surface reaction process, the initial adsorption is fast. Then, a slower adsorption would follow as the available adsorption site which is gradually decreased. This is due to the fact that a large number of active sites on the surface are easy to be occupied on the solid and from the bulk phases at initial stages. Entering of dye molecules into pores is interior surface relatively slow process. Maximum percentage of BPBC adsorption (68.51% in 75mg/L of solution) occurs at 70 mins that after the percentage adsorption remains unaltered

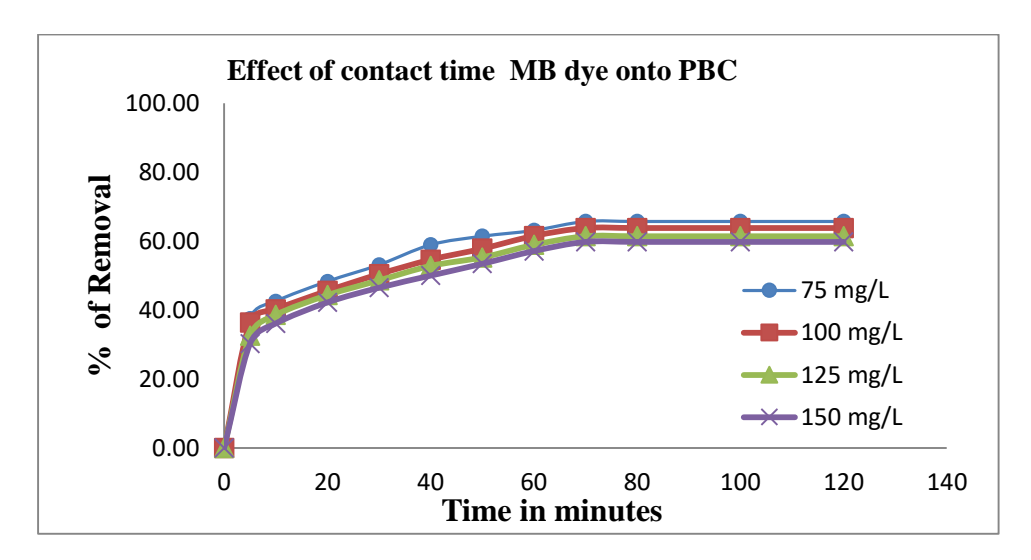


Figure 5.49

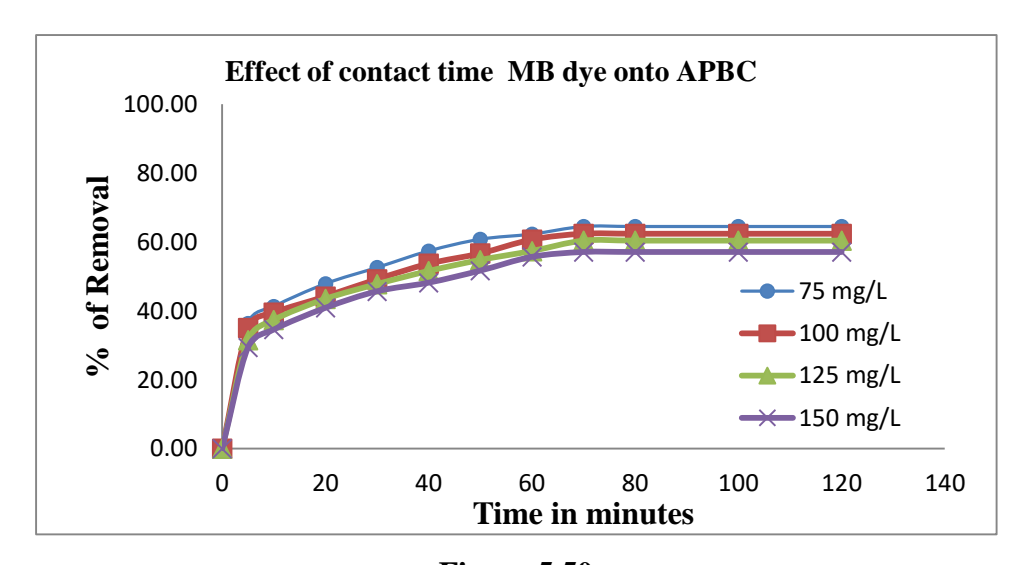


Figure 5.50

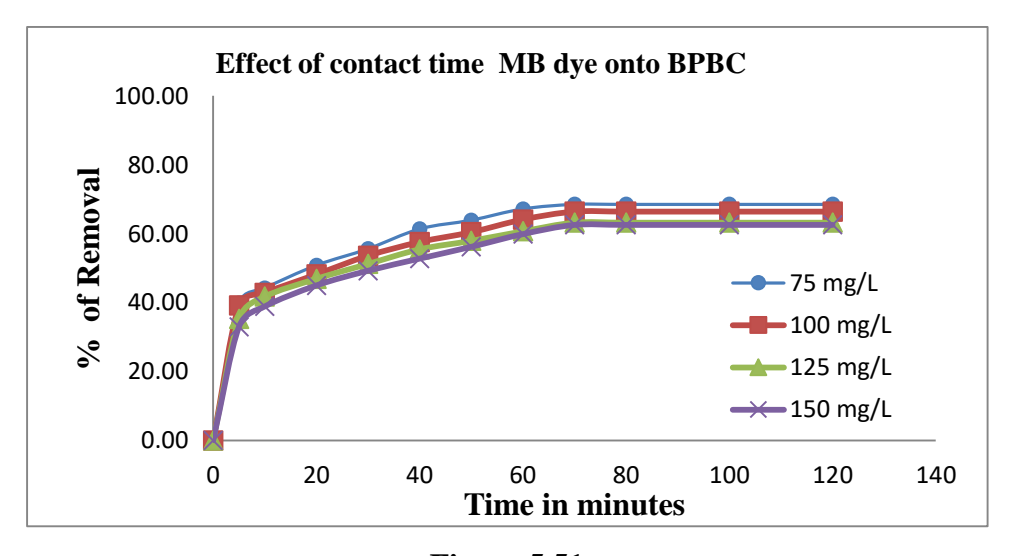


Figure 5.51

Table–5.23 Effect of Contact time for MB dye adsorption onto PBC, APBC & BPBC

[pH= 7;Dose= 30mg/50mL]

Time	% Removal of PBC			% Removal of APBC			% Removal of BPBC					
In	Initial Concentration in mg/L											
Minutes	75	100	125	150	75	100	125	150	75	100	125	150
0	0.00	0.00	0.00	0.00	0.00	0.00	0.00	0.00	0.00	0.00	0.00	0.00
5	37.54	36.41	32.57	30.25	36.40	35.10	31.50	29.40	39.87	39.20	35.27	33.00
10	42.58	40.25	38.61	36.15	41.30	39.50	37.40	34.60	44.20	42.85	41.76	38.90
20	48.35	45.62	44.36	42.25	47.90	44.20	43.50	40.90	50.84	48.21	46.92	45.00
30	53.15	50.45	48.64	46.51	52.60	49.20	47.80	45.70	55.62	53.62	51.23	49.26
40	58.98	54.65	52.84	50.03	57.40	53.70	51.60	48.20	61.40	57.60	55.48	52.78
50	61.45	57.84	55.31	53.46	60.80	56.70	54.80	51.70	63.94	60.45	57.93	56.21
60	63.14	61.54	58.95	57.15	62.30	60.70	57.40	55.70	67.20	64.13	60.71	59.90
70	65.74	63.84	61.45	59.81	64.50	62.40	60.40	57.10	68.51	66.42	63.21	62.56
80	65.74	63.84	61.45	59.81	64.50	62.40	60.40	57.10	68.51	66.42	63.21	62.56
100	65.74	63.84	61.45	59.81	64.50	62.40	60.40	57.10	68.51	66.42	63.21	62.56
120	65.74	63.84	61.45	59.81	64.50	62.40	60.40	57.10	68.51	66.42	63.21	62.56

5.2.4 Effect of Initial Concentration

The study of the distribution of the dye between the adsorbent and the dye solution at equilibrium is important to assess the adsorption capacity of the adsorbent for the dyestuffs. The initial concentration of the dye solutions are varied from 75 to 150 mg/L and batch mode experiments are performed at 305K- 335K and at pH 7.0.

The study reveals that the percentage removal of MB dye from aqueous solution used in this study decreases from 65.74 % to 59.81 % for PBC, from 64.50 % to 57.10% for APBC and from 68.51 % to 62.56 % for BPBC. But the amount of dye accumulated on the solid phase increases with the increase of the initial concentration of the dye solution. The amount of MB dye onto adsorbent increased from 49.31 to 89.72, 48.38 to 85.65 and 51.38 to 93.84 at the temperature 305K respectively for the PBC, APBC and BPBC. This is due to an increase in the driving force of the concentration gradient. As the initial dye concentration increases, mass transfer driving force became larger and the interaction between the dye and adsorbent was enhanced, hence resulting in higher adsorption capacity. The results are depicted in table 5.23- 5.24 and in figures 5.52 to 5.57.

Table-5.24 Effect of Initial concentration on percentage of removal

[MB dye pH= 7, Dose= 30mg/50mL]

Adsorbents	Initial Concentration Ci (mg/L)	Percentage of Removal
	75	65.74
	100	63.84
	125	61.45
PBC	150	59.81
	75	64.50
	100	62.40
	125	60.40
APBC	150	57.10
	75	68.51
	100	66.42
	125	63.21
BPBC	150	62.56

Table-5.25 Effect of Initial Concentration on amount of adsorption

[MB dye, pH = 7;Dose = 30mg/50mL]

Adsorbents	Initial Concentration Ci (mg/L)	Amount adsorbed (mg/g)			
	75	49.31			
	100	63.84			
	125	76.81			
PBC	150	89.72			
	75	48.38			
	100	62.40			
	125	75.50			
APBC	150	85.65			
	75	51.38			
	100	66.42			
	125	79.01			
BPBC	150	93.84			

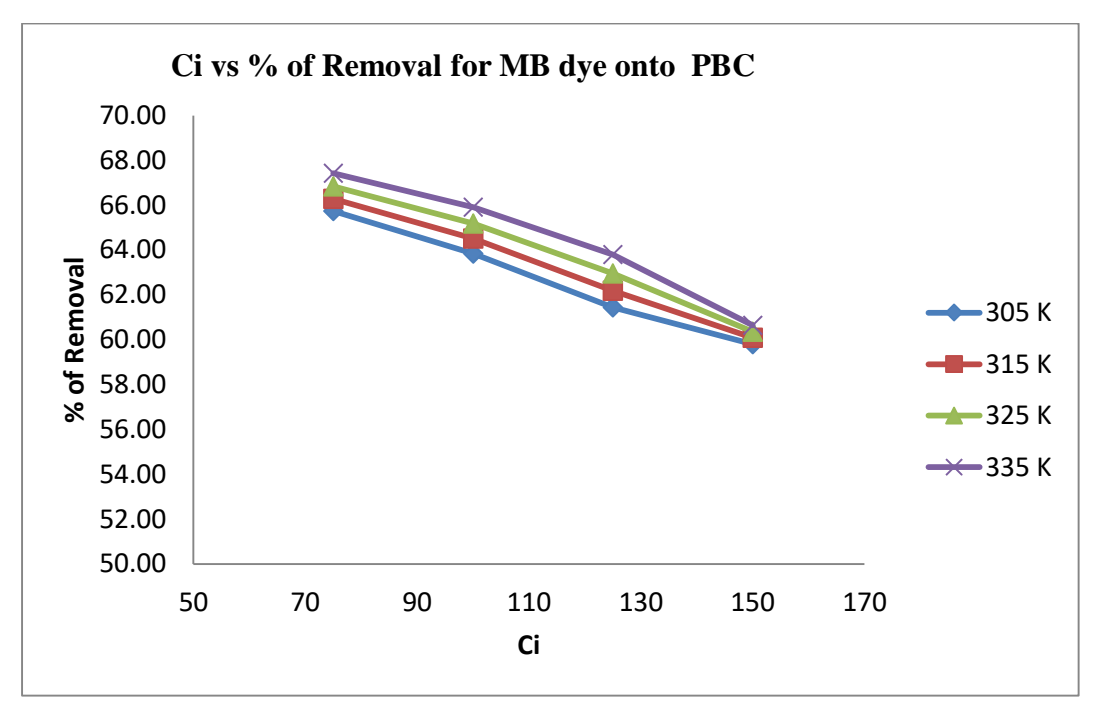


Figure 5.52

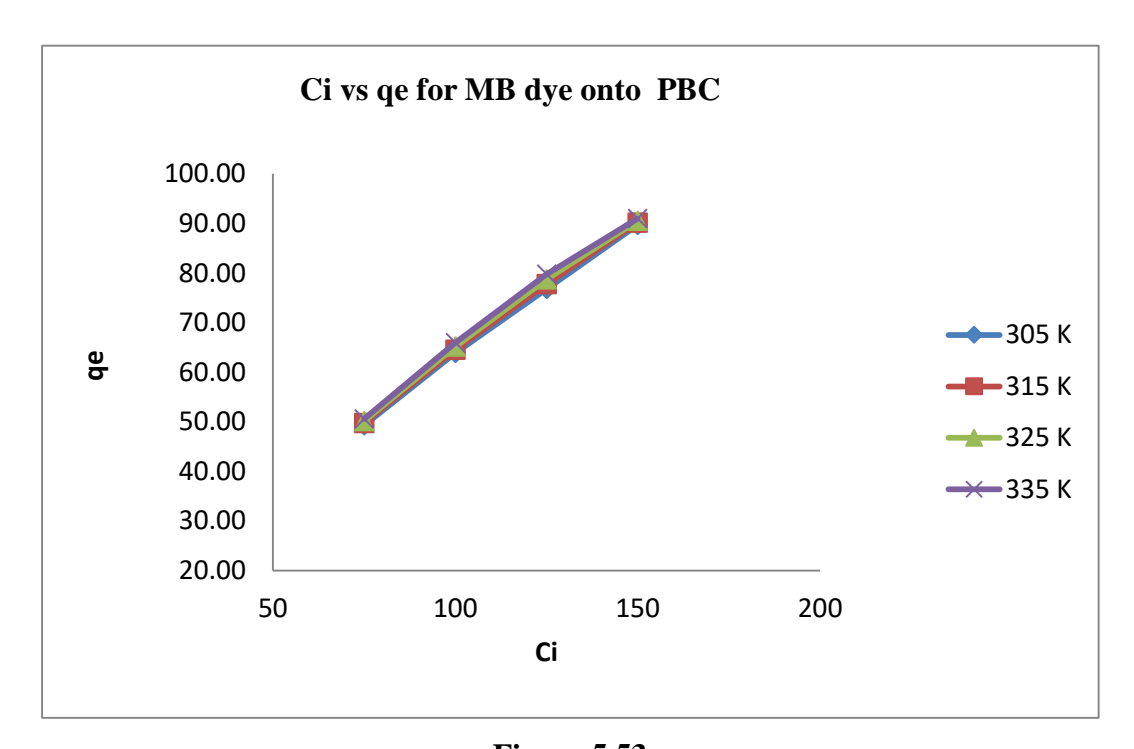


Figure 5.53

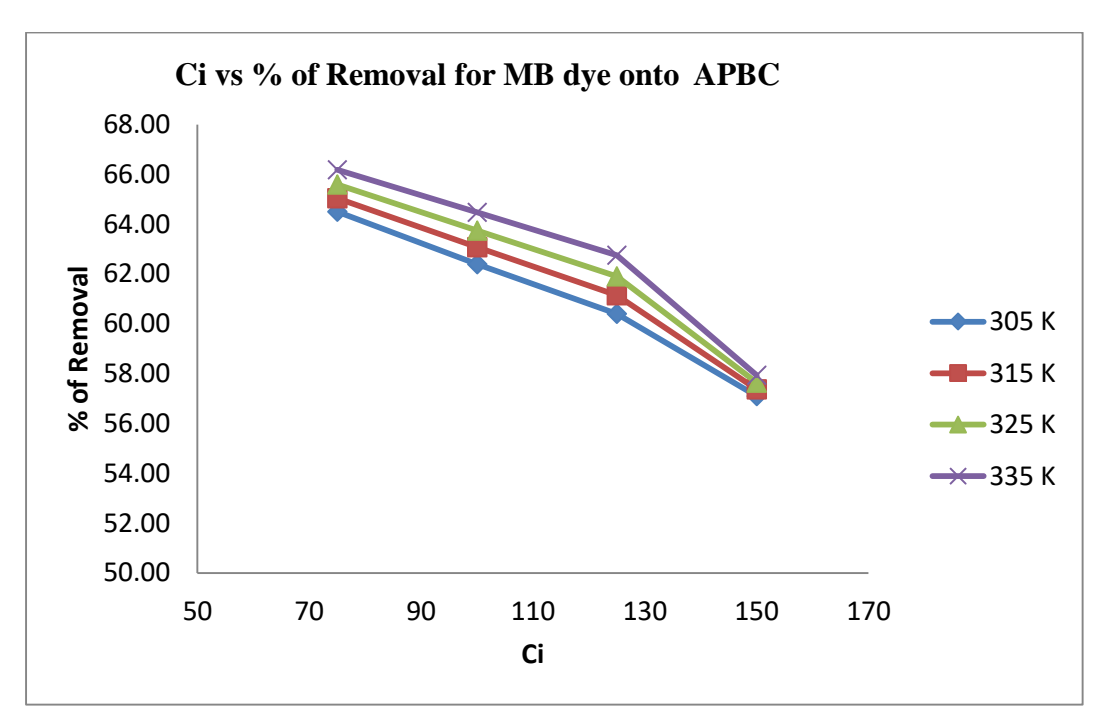


Figure 5.54

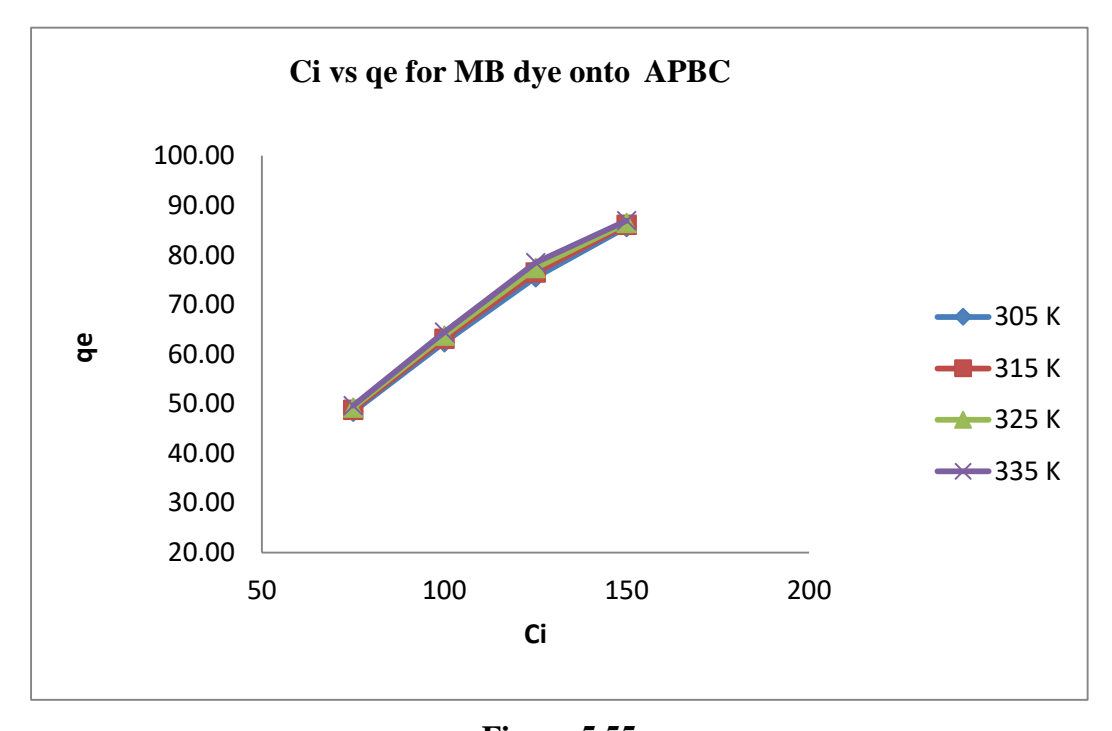


Figure 5.55

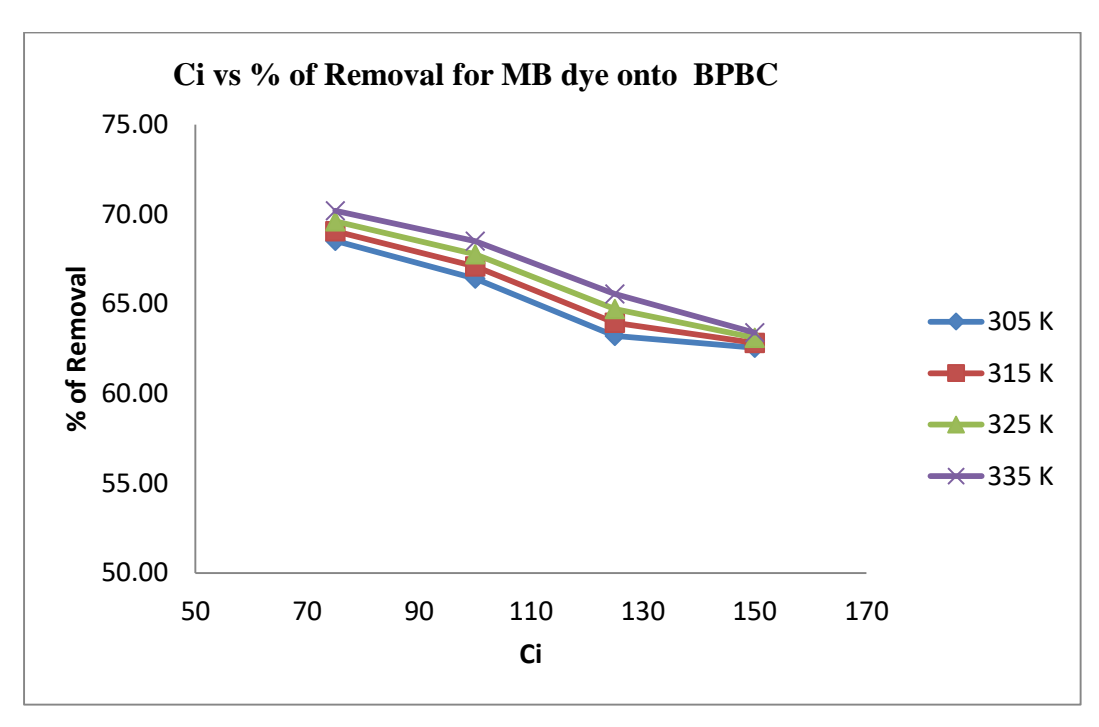


Figure 5.56

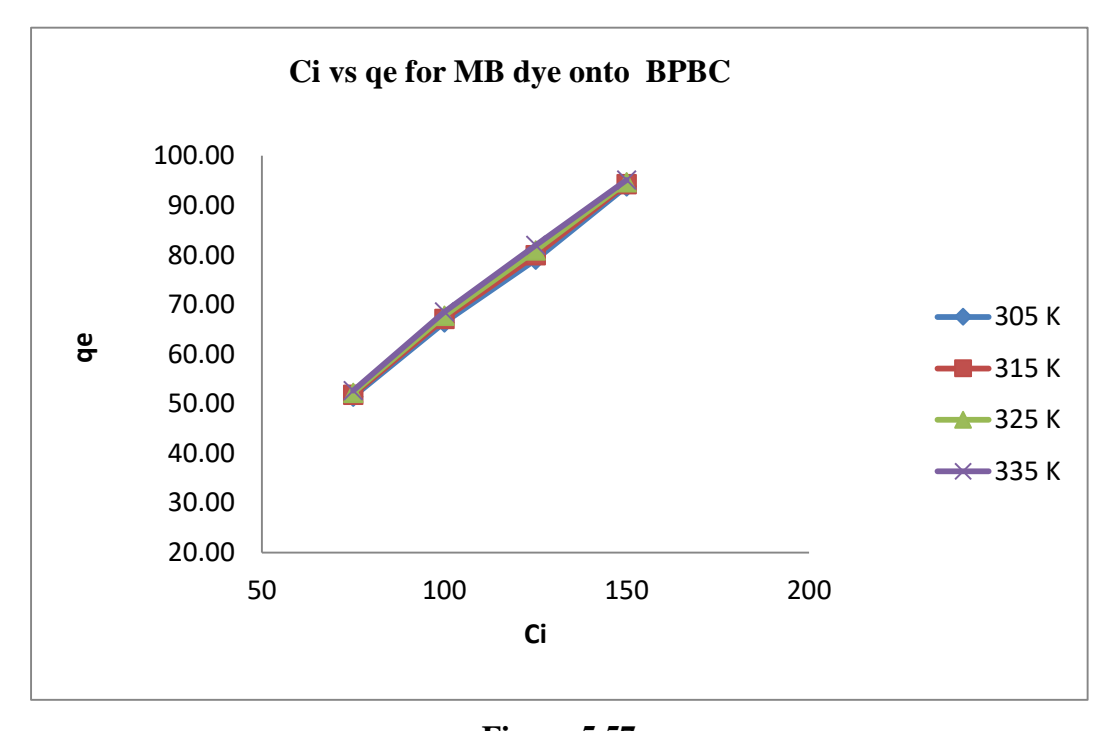


Figure 5.57

5.2.5 Effect of Temperature

Temperature plays an important role in controlling the strength of the adsorptive forces between the adsorbent and adsorbate molecules. The effect of temperature on the removal of MB onto PBC, APBC and BPBC was studied under 305K, 315K, 325K and 335K. The percentage removal of MB dye is presented in table 5.26 & 5.27 and shown in figures 5.58 to 5.63.

As the temperature increased from 305K to 335K, the removal of dye percentage in aqueous solution well as adsorption capacity increases with the increase of temperature. This isdue to the increase of the rate of diffusion of the adsorbate molecules across the external boundary layer and in the internal pores of the adsorbent particle as the viscosity of the solution decreases.

Table–5.26 Effect of temperature of MB dye onto Adsorbents

[pH=7;Dose=30mg/50mL;CT =120min]

Initial Concentration	Town and true (V)	% of Removal			
(mg/L)	Temperature (K)	PBC	APBC	ВРВС	
	305	65.74	64.50	68.51	
	315	66.29	65.05	69.06	
75	325	66.83	65.59	69.60	
	335	67.42	66.18	70.19	
	305	63.84	62.40	66.42	
100	315	64.51	63.07	67.09	
100	325	65.18	63.74	67.76	
	335	65.91	64.47	68.49	
	305	61.45	60.40	63.21	
125	315	62.19	61.14	63.95	
123	325	62.95	61.90	64.71	
	335	63.80	62.75	65.56	
	305	59.81	57.10	62.56	
150	315	60.08	57.37	62.83	
130	325	60.36	57.65	63.11	
	335	60.65	57.94	63.40	

Table–5.27 Effect of temperature of MB dye onto Adsorbents

[pH=7;Dose=30mg/50mL;CT =120min]

Initial Concentration	Temperature (K)	Qe			
(mg/L)	Temperature (K)	PBC	APBC	ВРВС	
	305	49.31	48.38	51.38	
75	315	49.72	48.79	51.79	
75	325	50.13	49.20	52.20	
	335	50.57	49.64	52.64	
	305	63.84	62.40	66.42	
100	315	64.51	63.07	67.09	
100	325	65.18	63.74	67.76	
	335	65.91	64.47	68.49	
	305	76.81	75.50	79.01	
125	315	77.74	76.43	79.94	
123	325	78.69	77.38	80.89	
	335	79.75	78.44	81.95	
	305	89.72	85.65	93.84	
150	315	90.13	86.06	94.25	
130	325	90.54	86.47	94.66	
	335	90.98	86.91	95.10	

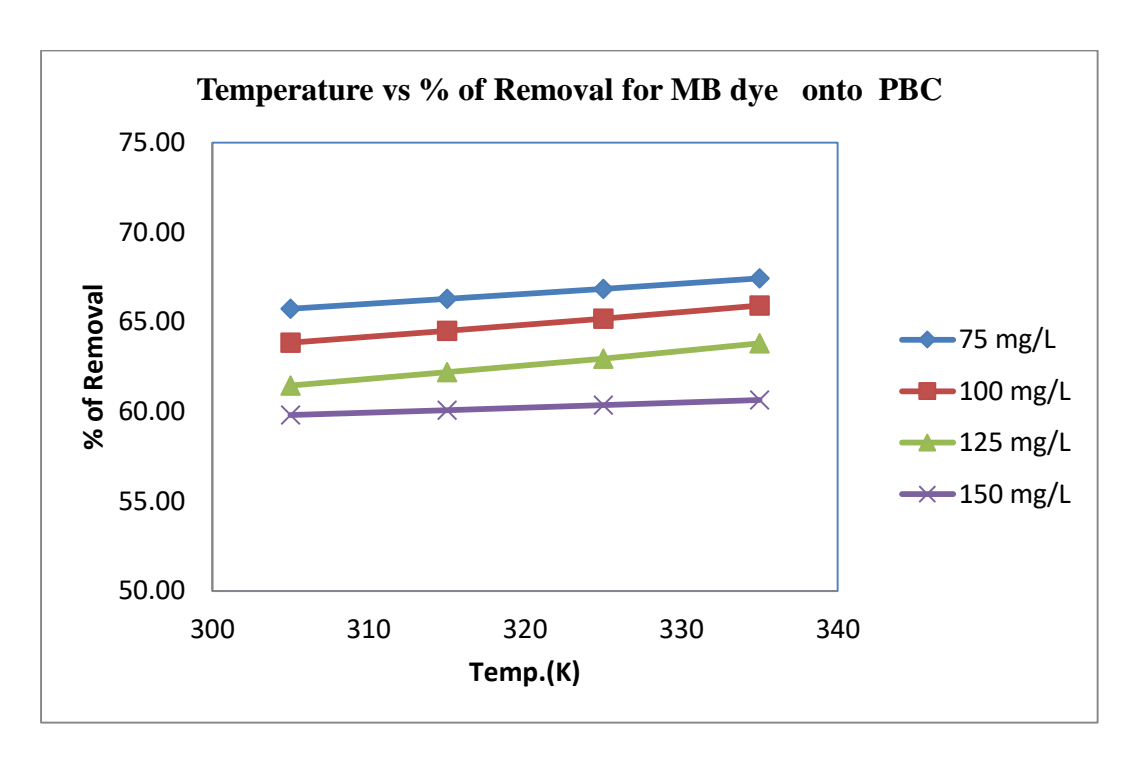


Figure 5.58

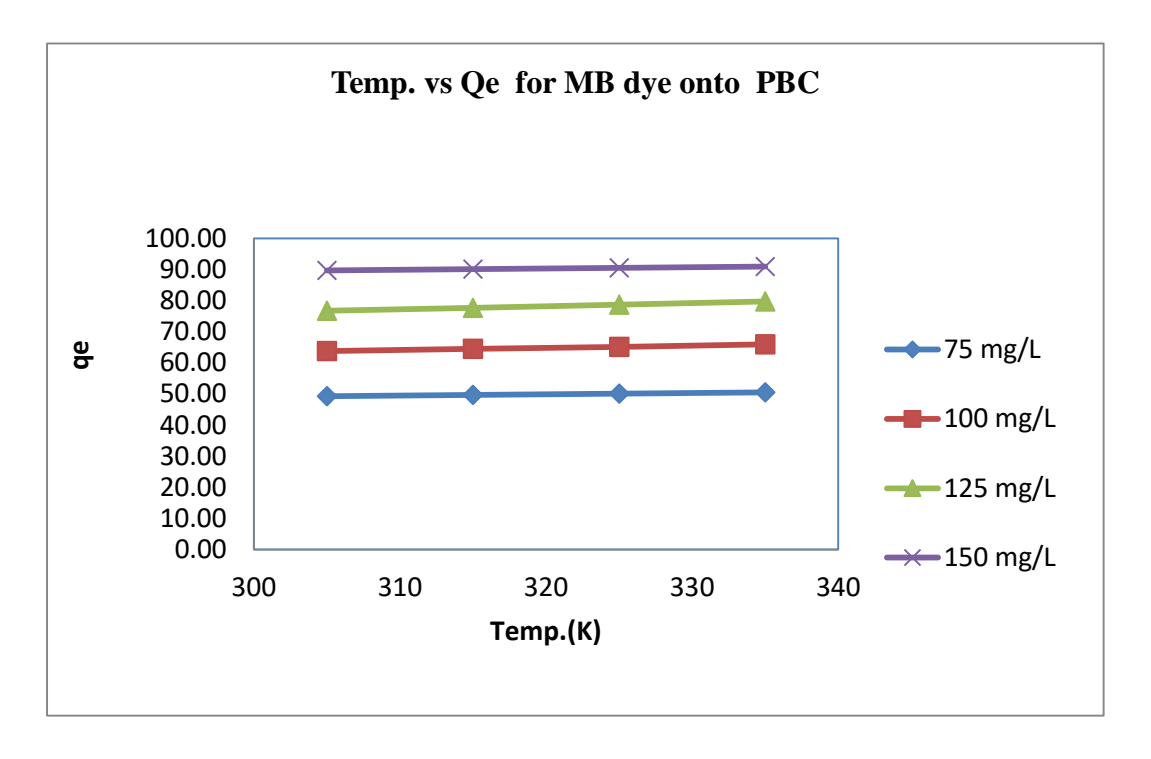


Figure 5.59

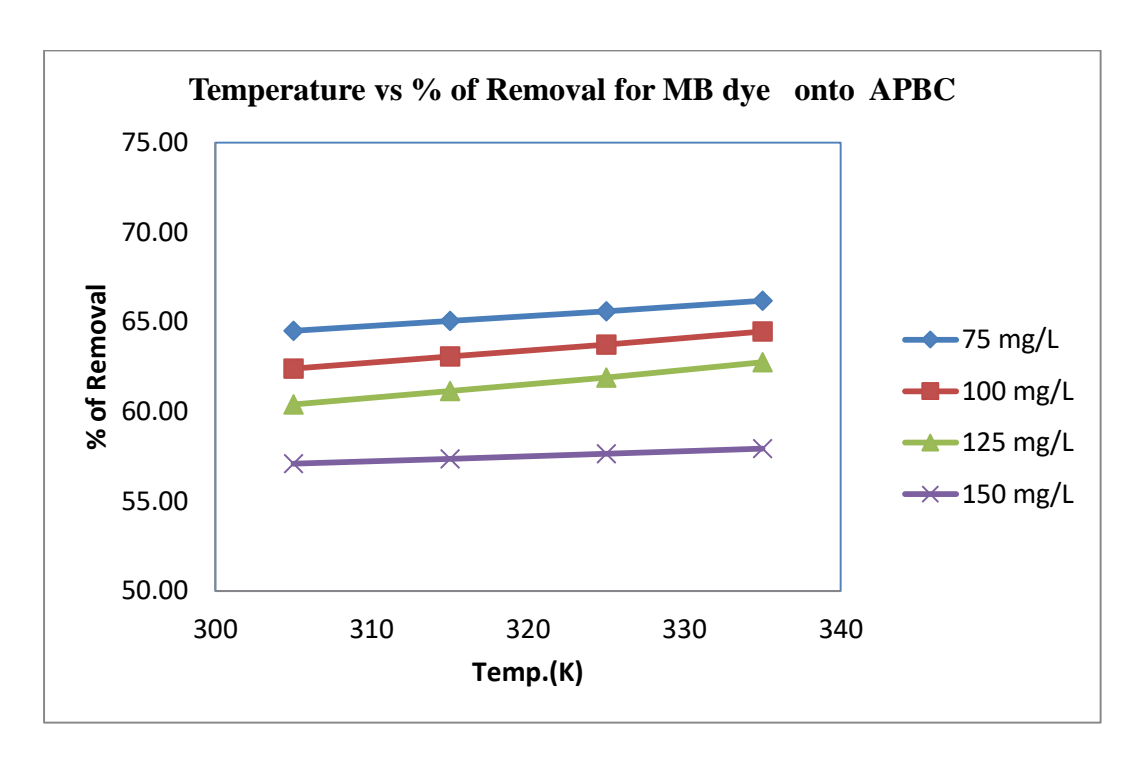


Figure 5.60

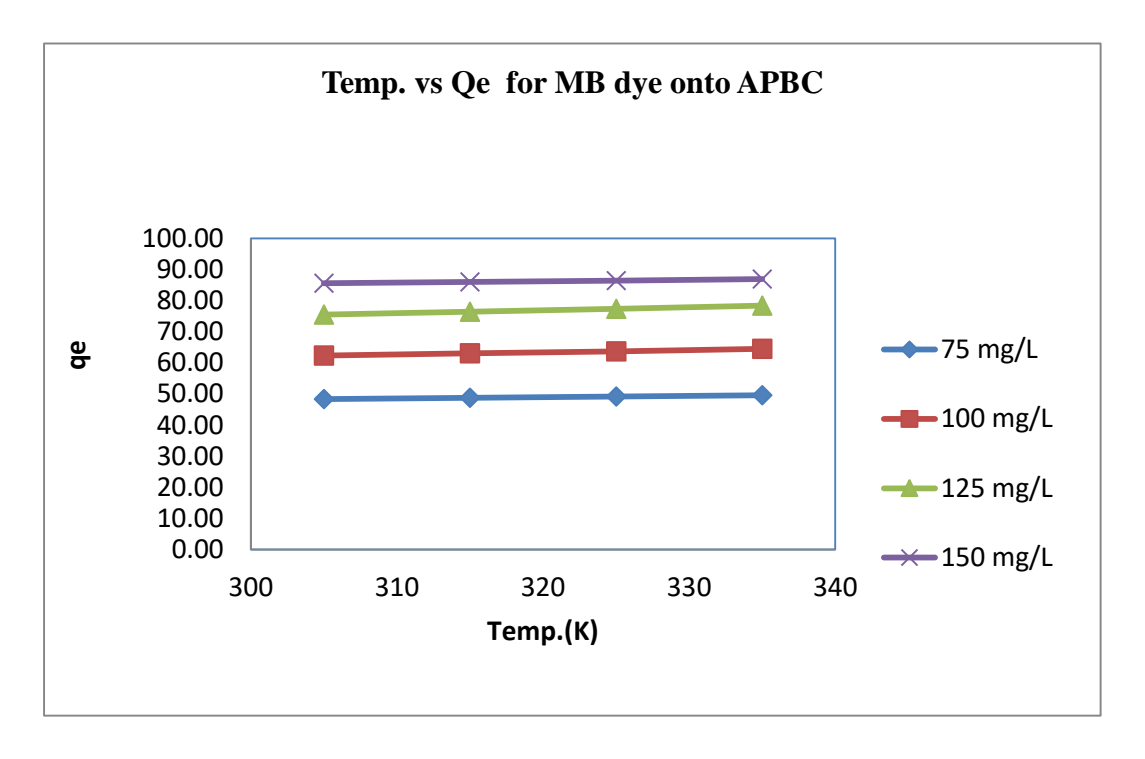


Figure 5.61

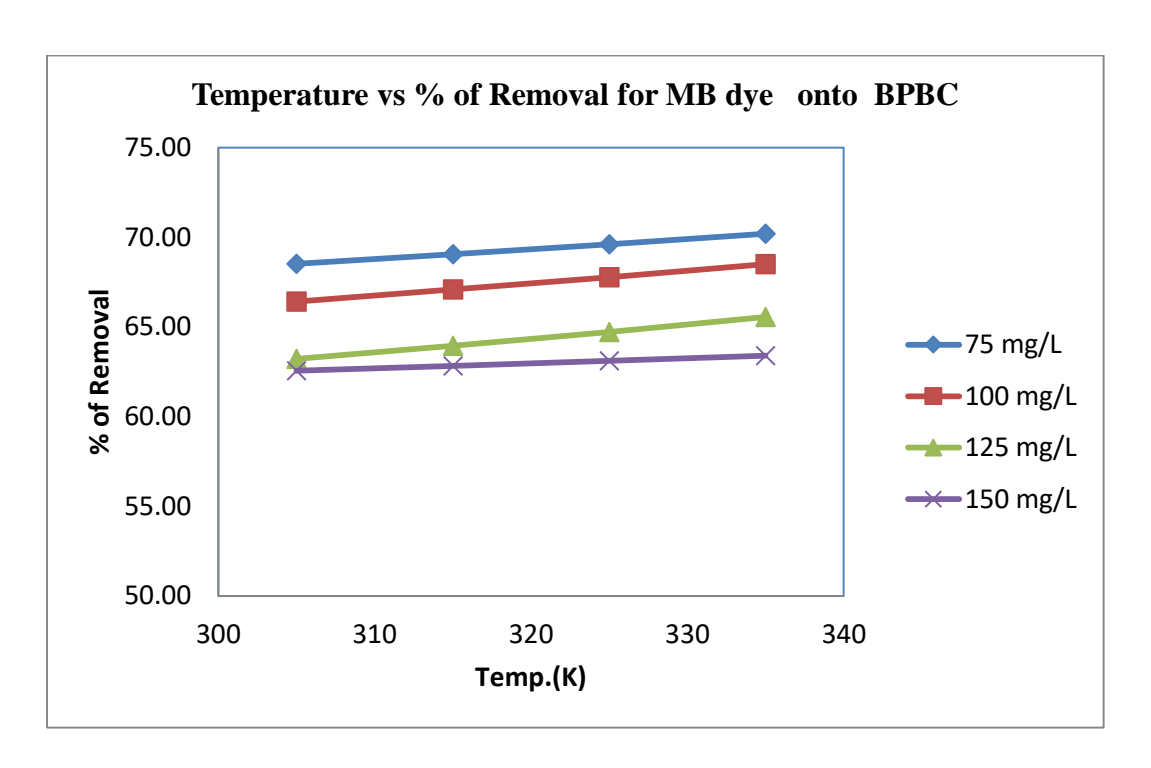


Figure 5.62

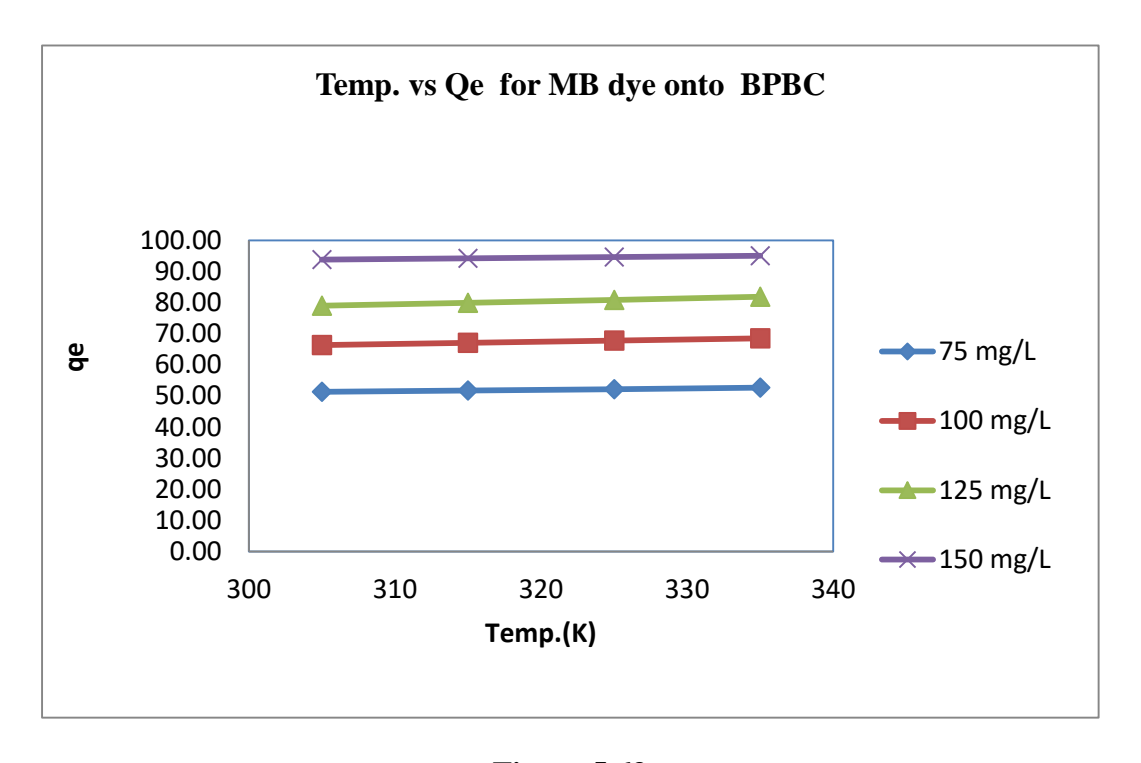


Figure 5.63

5.2.6 ADSORPTION ISOTHERMS

Adsorption equilibrium studies offer the basic physicochemical data for investigating the applicability of the adsorption process. Adsorption isotherms are mathematical models which were framed on the basis of set of assumptions. These models clearly explain the distribution of the adsorbate species among solid and liquid phases. Based on adsorption isotherms the heterogeneity or homogeneity of the adsorbate surface, the type of coverage, and the possibility of interaction between the adsorbate and adsorbent can be known.

The equilibrium data for the adsorption of MB dyes onto the adsorbents PBC, APBC and BPBC are applied to the Langmuir, Freundlich, Tempkin and Dubinin-Radushkevich adsorption isotherms. Analysis of the equilibrium data by fitting them into chosen isotherm model is an important step to find a suitable isotherm model that can be used for the design of an adsorption system.

Investigation of adsorption isotherm models are much significant for the description of how a adsorbate distributes itself between the solid and liquid phase and are helpful to optimize the experimental conditions for obtaining high percentage removal of dye.

5.2.6.1 Langmuir Isotherm

Langmuir isotherm plots were drawn between C_e/q_e and C_e which are shown in figures 5.64 to 5.66. The regression coefficient (R^2) values were ranged from 0.9621 to 0.9990 for the four studied temperatures viz. 305, 315, 325 and 335K which confirmed the best fitting of the equilibrium data with langmuir isotherms. The value of monolayer adsorption capacity (Q_0) and energy of adsorption (b) determined from this Langmuir isotherm are summarized in table 5.28.

The monolayer adsorption capacity Q0 values (mg/g) for adsorption of MB dye onto PBC APBC and BPBC were ranged from 208.333 to 227.273, 175.439 to 188.679 and 208.333 to 222.222 respectively. The adsorption capacity increased with the increase of temperature.

The values of Langmuir constant 'b' (L/mg) the adsorption energy for adsorption of MB dye onto PBC, APBC and BPBC were ranged from 0.013 to 0.011, 0.016 to 0.013 and 0.015 to 0.013 respectively. These values indicate that the apparent energy of sorption is less and ruled out the possibility of strong interaction between the solute and adsorption site.

The order of monolayer adsorption capacity of the three adsorbents namely PBC, APBC and BPBC are in following order for the adsorption of MB dye for all the studied temperatures.

BPBC	>	PBC	>	APBC	

Table – 5.28 Langmuir isotherm results for MB dye onto adsorbents

[MB dye, pH=7;Dose=30mg/50mL]

Adsorbents	Temperature (K)	-		R ²
	305	208.333	0.013	0.9873
	315	212.766	0.013	0.9959
	325	222.222	0.011	0.9990
PBC	335	222.222	0.011	0.9964
	305	175.439	0.016	0.9621
	315	181.818	0.015	0.9741
APBC	325	185.185	0.014	0.9838
TH BC	335	188.679	0.013	0.9918
	305	208.333	0.015	0.9958
BPBC	315	212.766	0.014	0.9908
DI BC	325	217.391	0.013	0.9801
	335	227.273	0.013	0.9630

The dimensionless separation factor RLvalues calculated for various initial concentrations at different temperatures were lie between 0 and 1 which indicate the favorable adsorption for all the systems. These RLvalues are presented in table 5.29.

Table 5.29 Dimensionless separation factor (RL)

Adsorbents	Temperature (K)						
Ausorbents	305	315	325	335			
PBC	0.4990	0.5159	0.5372	0.5528			
APBC	0.4528	0.4735	0.4894	0.5047			
BPBC	0.4663	0.4830	0.4986	0.5140			

The difference may be due to the following factors such pore volume, pore shape and surface characteristics of the adsorbents. In general Langmuir constant values infer a better performance of prepared adsorbents PBC, APBC & BPBC.

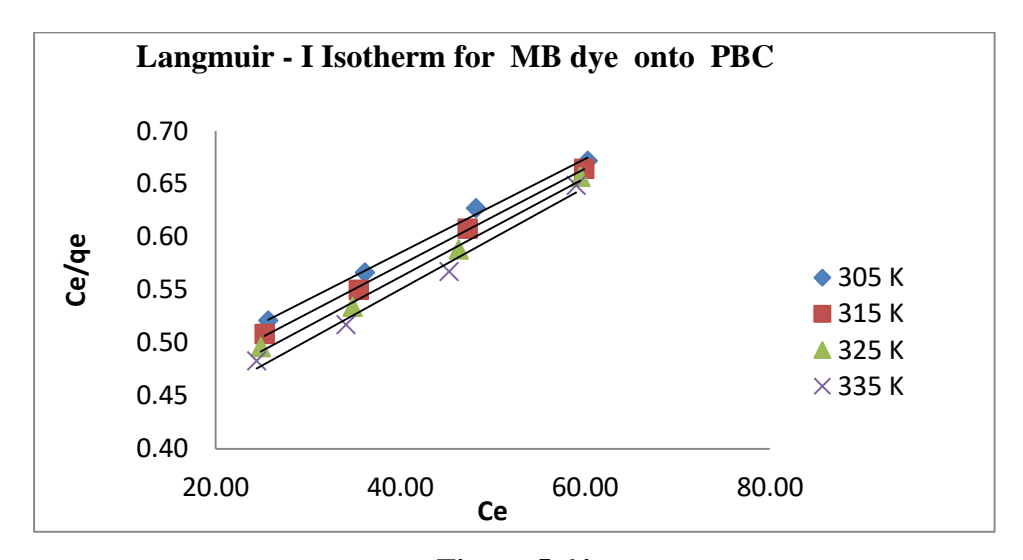


Figure 5.64

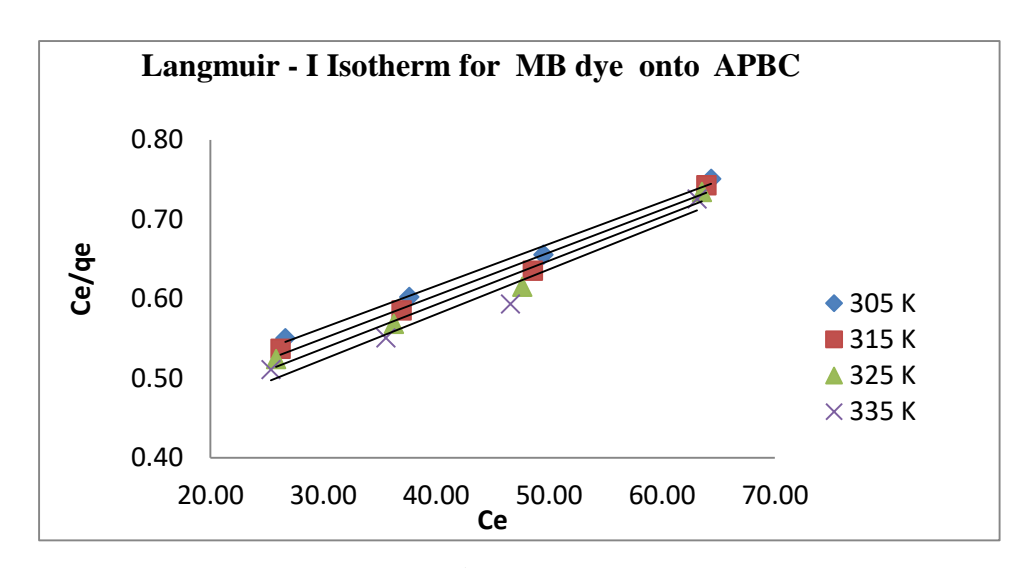


Figure 5.65

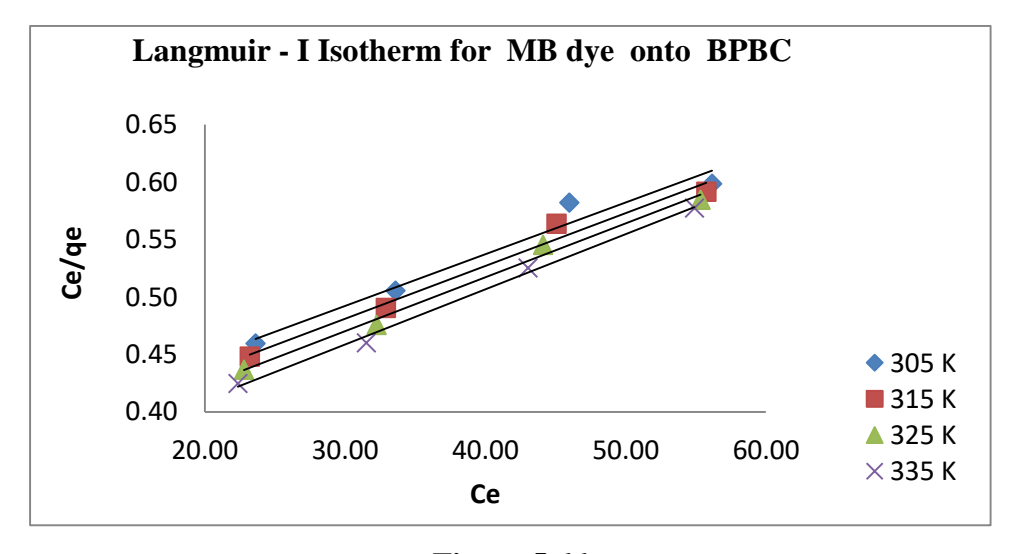


Figure 5.66

5.2.6.2 Freundlich Isotherm

Freundlich isotherm plots were drawn between $\log q_e$ and $\log Ce$ which are shown in figures 5.67 to 5.69. The regression coefficient (R²) values were ranged from 0.9716 to 0.9980 for the four studied temperatures viz.305, 315, 325 and 335K which revealed the best fitting of the equilibrium data with freundlich isotherms. The value of adsorption capacity (K_f) and intensity of adsorption (n) determined from this Freundlich isotherm are summarized in table 5.29.

Adsorption capacity K_f (mg/g) for MB dye onto PBC, APBC and BPBC were ranged from 6.0618 to 5.1582, 6.7468 to 5.7240 and 7.0453 to 6.0618 respectively. Adsorption capacities of the three adsorbents were in the following order for all the studied temperatures.

It can be understood from the Kf (mg/g) at a particular temperature. These values are given in table 5.31

The adsorption intensity (n) values are ranged from 1.7730 to 2.0367 for all the studied systems. These low values indicate the favorable physical adsorption. Further it is observed that 'n' value increased with the increase of temperature .

 $Table-5.30\ Freundlich\ isotherm\ results\ for\ MB\ dye\ onto\ adsorbents$ $[MB\ dye,\ pH=7,\ Dose=30mg/50mL]$

Adsorbents	Temperature (K)	N	Kf (mg/g)	\mathbb{R}^2
	305	1.4923	6.0618	0.9900
PBC	315	1.4708	5.7227	0.9940
PDC	325	1.4516	5.4313	0.9970
	335	1.4335	5.1582	0.9980
	305	1.5967	6.7468	0.9716
APBC	315	1.5711	6.3636	0.9806
AFDC	325	1.5482	6.0325	0.9871
	335	1.5267	5.7240	0.9922
	305	1.5335	7.0453	0.9953
BPBC	315	1.5129	6.6788	0.9967
DrDC	325	1.4945	6.3606	0.9965
	335	1.4771	6.0618	0.9951

Table-5.31 Adsorption capacity Kf (mg/g) values

Temperature (K)	PBC	APBC	ВРВС
305	6.0618	6.7468	7.0453
315	5.7227	6.3636	6.6788
325	5.4313	6.0325	6.3606
335	5.1582	5.7240	6.0618

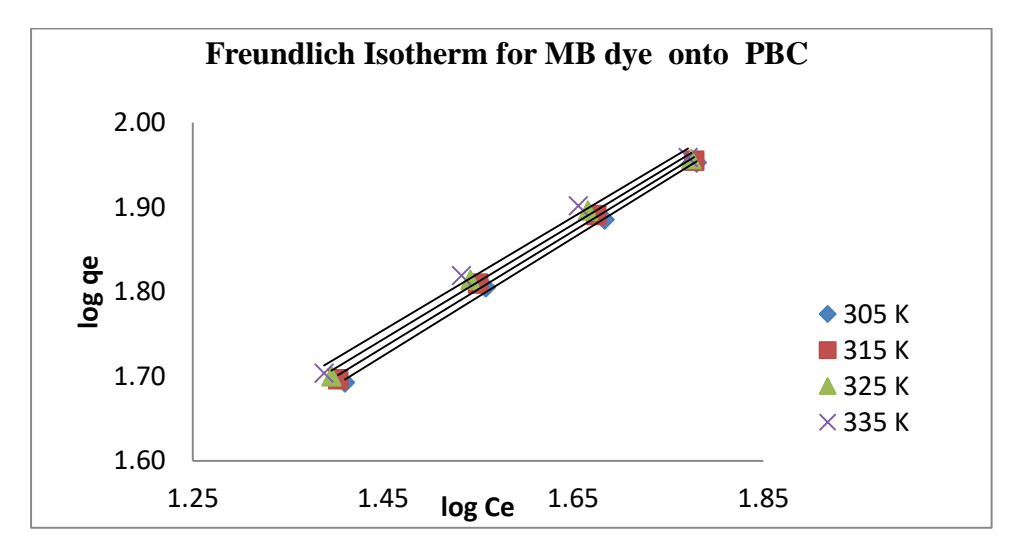


Figure 5.67

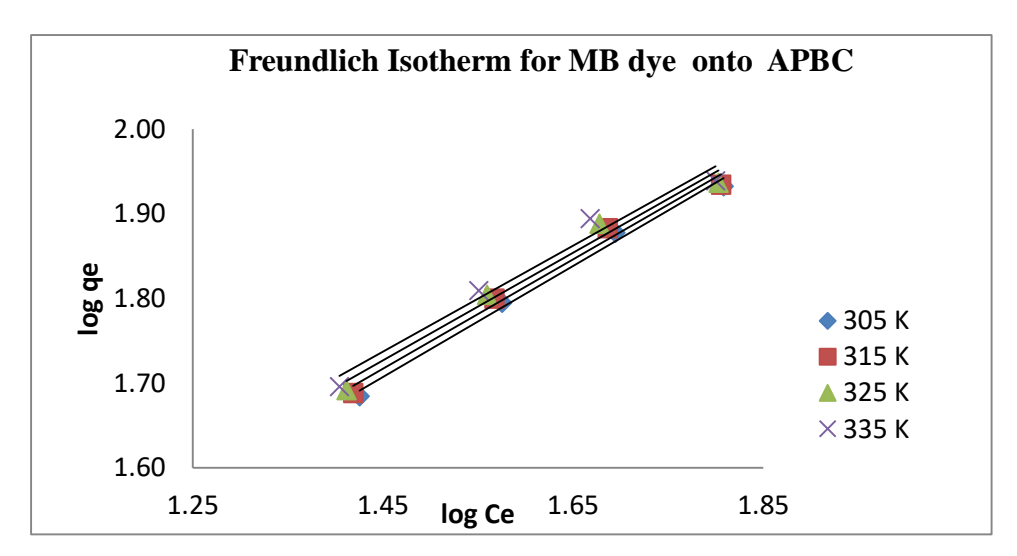


Figure 5.68

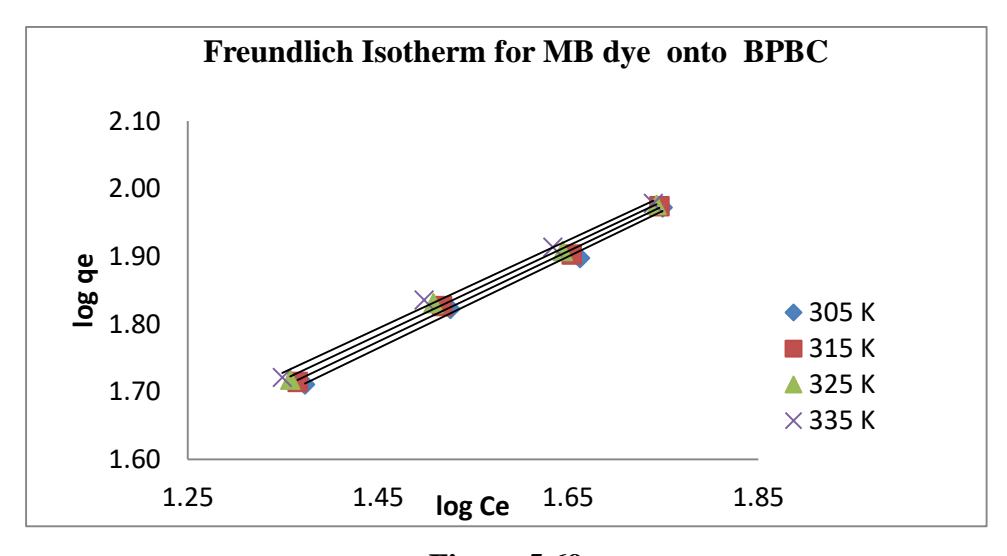


Figure 5.69

5.2.6.3 Temkin isotherm

Temkin plots were drawn between qe and lnCe which were shown in figures 5.70 to 5.72. The regression coefficient (R²) values were ranged from 0.9833 to 0.9990 for the four studied temperatures viz.305, 315, 325 and 335K which revealed the best fitting of the equilibrium data with Temkin isotherms. The Equilibrium binding constant aT values (L/g) and heat of sorption constant bT values determined from Temkin isotherm are summarized in table 5.32.

Equilibrium binding constant aT values (L/g) onto PBC, APBC & BPBC were ranged from 0.1096 to 0.1222, 0.1162 to 0.1315 and 1.1281 to 0.1373 respectively. The heat of sorption constant bT values are ranged from 54.1022 J/mg to 60.3665 J/mg for PBC, 59.3163 to 66.5311 for APBC and 52.4613 J/mg to 59.6375 J/mg for BPBC for the four studied temperatures viz. 305, 315, 325 and 335 K. These lower values of aT and bT indicate the physisorption nature rather than chemisorption.

 $Table-5.32\ Temkin\ isotherm\ results\ for\ MB\ dye\ onto\ adsorbents$ $[MB\ dye,\ pH=7;Dose=30mg/50mL]$

Adsorbents	Temperature (K)	Q0 (mg/g)	B (L/mg)	R ²
	305	208.333	0.013	0.9873
PBC	315	212.766	0.013	0.9959
PBC	325	222.222	0.011	0.9990
	335	227.273	0.011	0.9964
	305	175.439	0.016	0.9621
APBC	315	181.818	0.015	0.9741
AFBC	325	185.185	0.014	0.9838
	335	188.679	0.013	0.9918
	305	208.333	0.015	0.9958
BPBC	315	212.766	0.014	0.9908
	325	217.391	0.013	0.9801
	335	222.222	0.013	0.9630

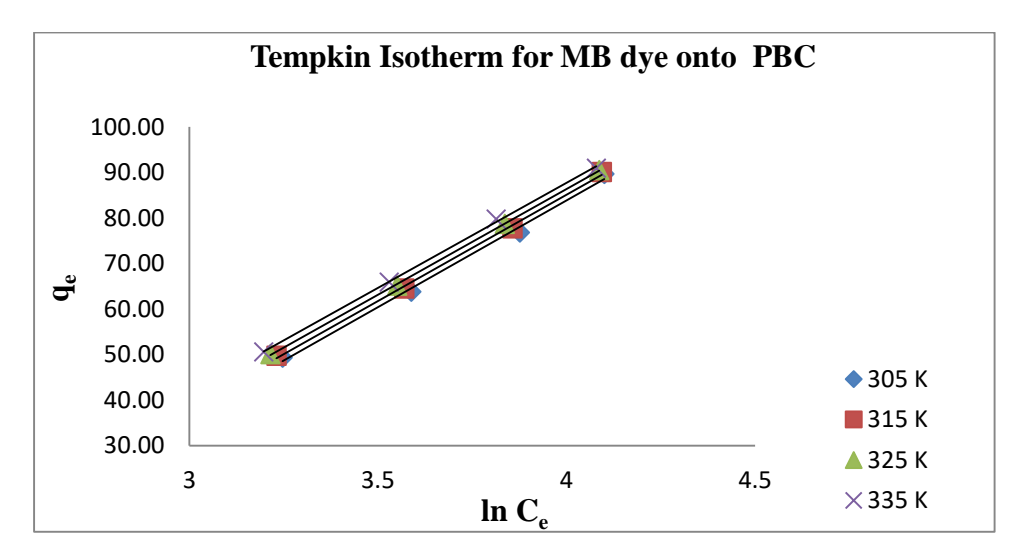


Figure 5.70

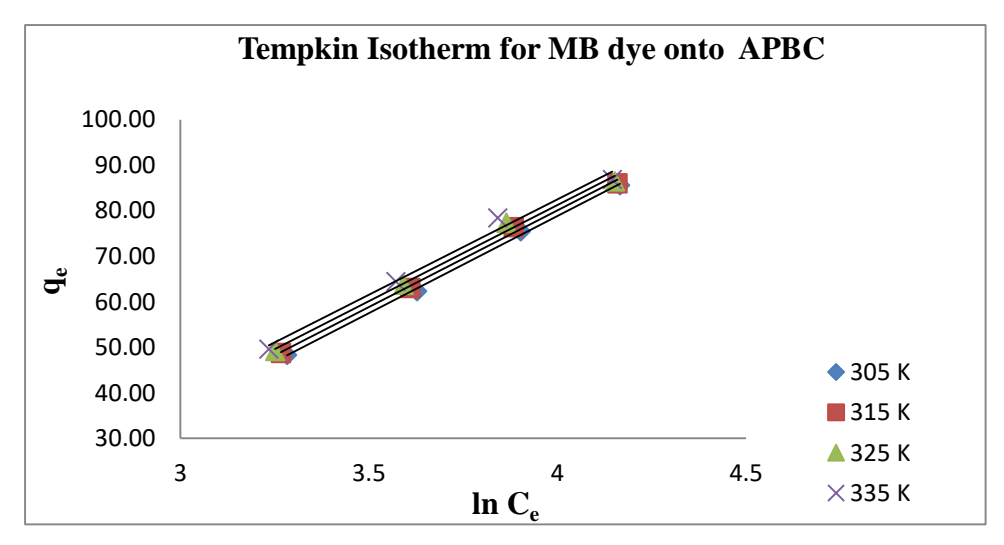


Figure 5.71

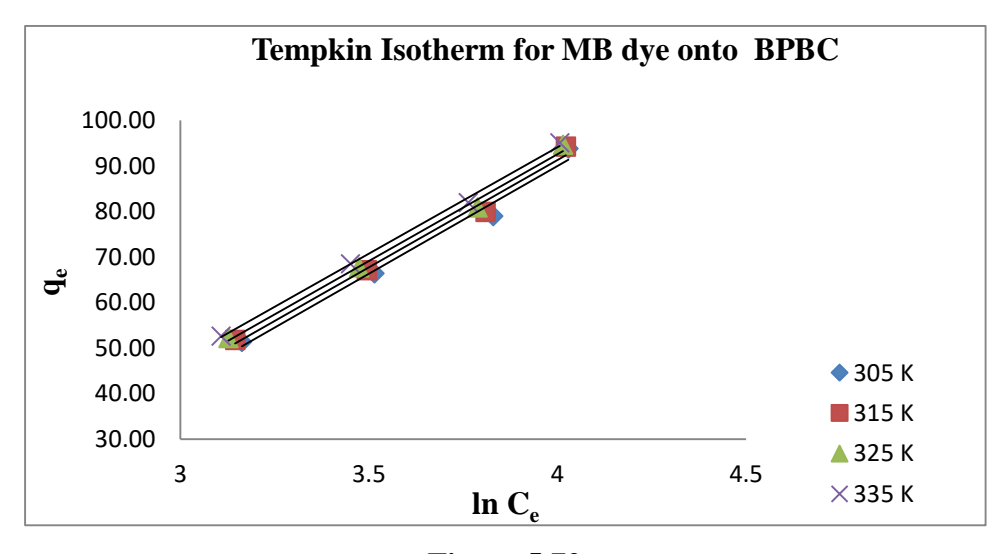


Figure 5.72

5.1.6.4 Dubinin–Radushkevich isotherm

Dubinin–Radushkevich isotherm (DRK plots were drawn between lnqe and $\epsilon 2$ (ϵ : RT ln (1+1/Ce) which were shown in figures 5.73 to 5.75. The regression coefficient (R2) values were ranged from 0.9600 to 0.9780, 0.9720 to 0.9810 and 0.9846 to 0.9690 for the four studied temperatures viz.305, 315, 325 and 335K respectively which revealed the best fitting of the equilibrium data with DRK isotherms. The theoretical saturation capacity q_D values (mg/g) and mean adsorption energy (kJ/mol) values determined are summarized in table 5.33.

The theoretical saturation capacity qD values (mg/g) were ranged from 96.3683 to 98.9062, 92.5903 to 95.1238 and 98.7086 to 101.3082 for PBC, APBC and BPBC respectively. BPBC found to have a higher saturation adsorption capacity when compared to PBC and APBC with all the studied temperatures. It is noticed that adsorption capacity increased with an increase in temperature.

The order of theoretical adsorption capacities the adsorbents are in the following order

BPBC > PBC > APBC

The values of mean adsorption energy were ranged from 0.4674 kJ/mol to 0.4665 kJ/mol, 0.4699 to 0.4685 and 0.4666 to 0.4653 for PBC, APBC and BPBC respectively. These values of E are lesser than 8kJ/mol indicate that the adsorption were physisorption (Sivakumar et.al., 2009).

 $Table-5.33\ Dubinin-Radushkevich\ isotherm\ results\ for\ MB\ dye\ onto\ adsorbents$ $[MB\ dye,\ pH=7;Dose=30mg/50mL]$

Adsorbents	Temperature (K)	qD (mg/g)	E (J/mol)	В	\mathbb{R}^2
	305	96.3683	0.4678	2.2851	0.9600
РВС	315	97.1422	0.4674	2.2893	0.9670
PBC	325	98.0202	0.4670	2.2935	0.9730
	335	98.9062	0.4665	2.2977	0.9780
	305	92.5903	0.4699	2.2644	0.9720
APBC	315	93.3338	0.4694	2.2696	0.9770
APBC	325	94.1775	0.4690	2.2737	0.9810
	335	95.1238	0.4685	2.2789	0.9840
	305	98.7086	0.4666	2.2967	0.9460
DDDC	315	99.6009	0.4662	2.3009	0.9540
ВРВС	325	100.4007	0.4657	2.3062	0.9610
	335	101.3082	0.4653	2.3094	0.9690

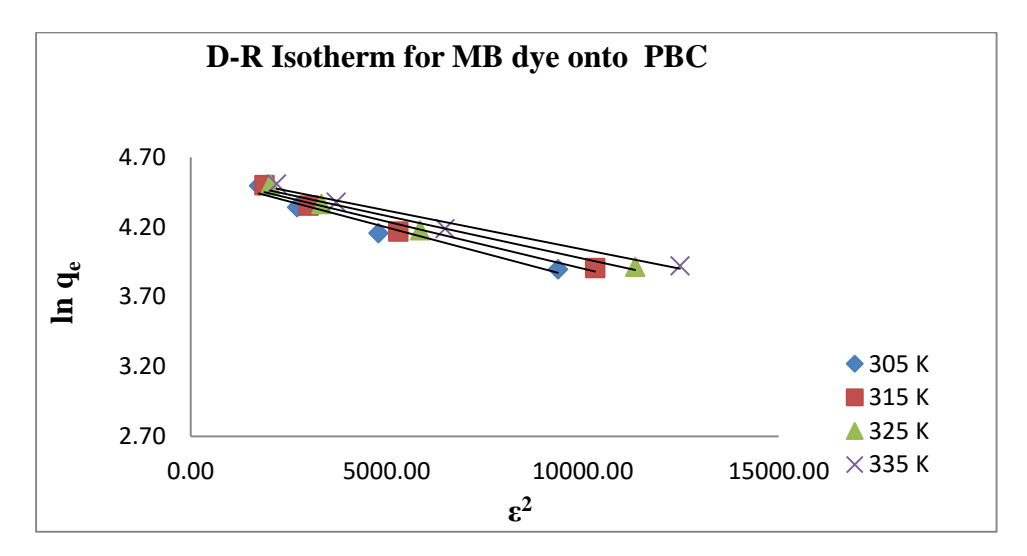


Figure 5.73

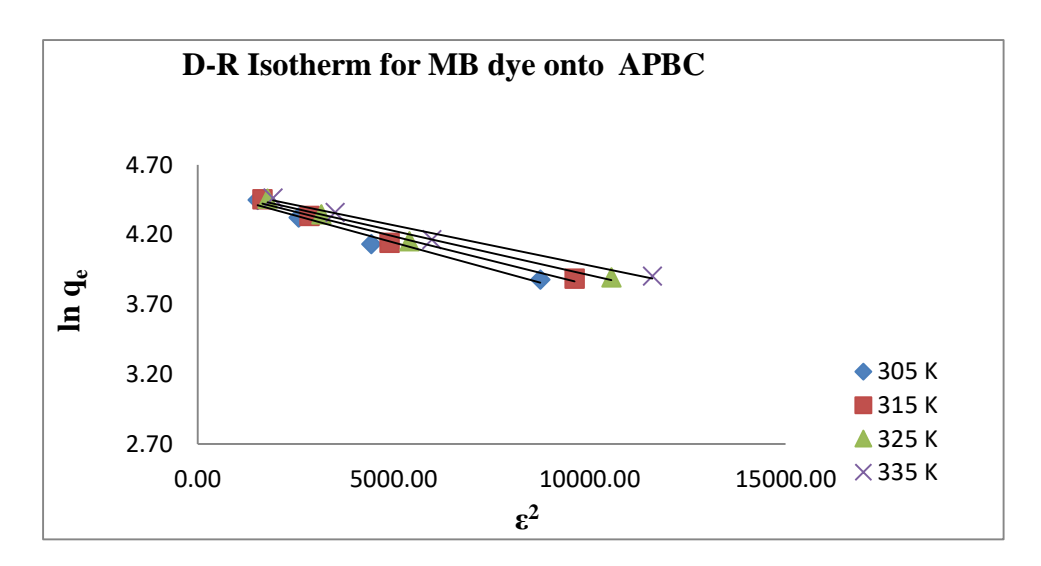


Figure 5.74

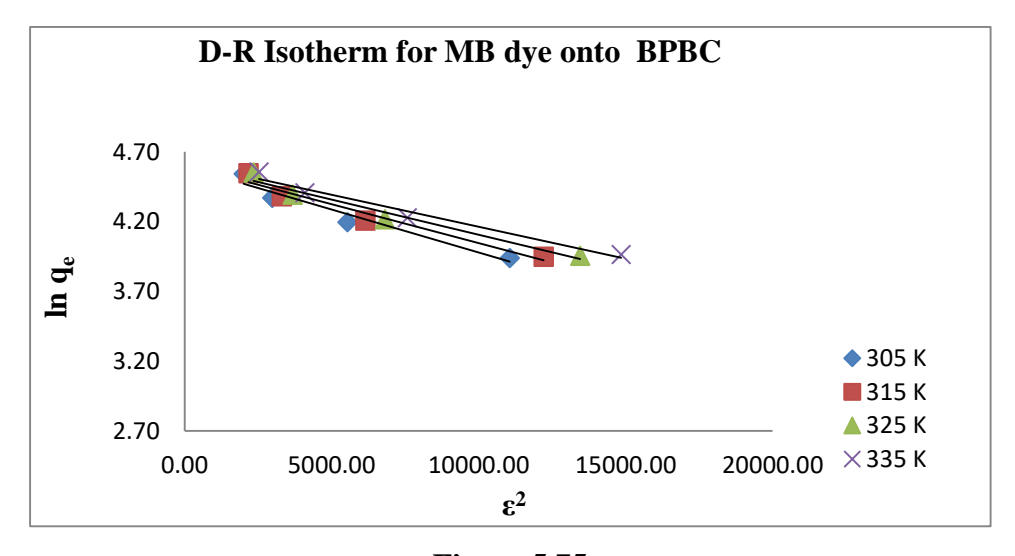


Figure 5.75

5.2.7 Adsorption Kinetics

5.2.7.1 Kinetic study for MB dye adsorption onto PBC, APBC and BPBC

The plots drawn for the Lagergren's pseudo first order kinetic models were shown in figures 5.76, 5.78 & 5.80. The values of regression coefficient (R²) of the plots for pseudo first order kinetic model for ranged from 0.9810 to 0.9970, 0.9790 to 0.9940 and 0.9850 to 0.9940 for PBC, APBC and BPBC. This indicates that the best fitting of data in pseudo first order kinetic model. The pseudo first order rate constant k1 and the calculated adsorption capacity qe (cal) from pseudo first order kinetic model were given in table 5.34, 5.36, & 5.38.

The plots drawn for the Ho's pseudo second order kinetic models were shown in figures 5.77, 5.79 & 5.81. The values of regression coefficient (R²) of the plots for pseudo second order models were ranged from 0.9960 to 0.9930, 0.9940 to 0.9960 and 0.9940 to 0.9970. This indicates that the best fitting of data in pseudo second order kinetic model. The regression coefficient values of pseudo second order were greater than the regression coefficient values of pseudo first order models. The pseudo second order rate constant k2 and the calculated adsorption capacity qe (cal) from pseudo second order kinetic model were given in table 5.35, 5.37 & 5.39.

The values of pseudo first order rate constant for PBC, APBC & BPBC k_1 ranged from 0.0327 to 0.0415, 0.0341 to 0.0415 and 0.0327 to 0.0408 respectively and pseudo second order rate constant k_2 values for PBC, APBC & BPBC ranged from 0.0015 to 0.0037, 0.0018 to 0.0038 and 0.0016 to 0.0037 respectively. The pseudo second order initial sorption rate, 'h', increased with an increase of initial concentrations of MB dye at 305K temperature.

The difference between the calculated adsorption capacity qe (cal) obtained from pseudo first order equation and the experimental adsorption capacity qe (exp) were found to be large. Whereas the difference between the calculated adsorption capacity qe (cal) obtained from pseudo second order equation and the experimental adsorption capacity qe (exp) were found to be small. ((Table 5.34-5.39).

Best fitting kinetic model is tested with a statistical tool 'Mean of sum of error squares' (MSSE). The MSSE of pseudo first order kinetic model is high when compared to pseudo second order kinetic model (table.5.40). The lower MSSE values for pseudo second order kinetic model reflect the suitability of second order kinetic model rather than pseudo first order kinetic model for the adsorption of MB dye onto PBC, APBC & BPBC adsorption system.

Table - 5.34 Pseudo first order Kinetics results for MB dye onto PBC [pH=7;Dose=30mg/50mL;Contacttime=120min;Temp=305K]

Comment	Pseudo First Order Kinetics						
Concentration (mg/L)	k1×10 ⁻² (min ⁻¹)	qe (cal) (mg/g)	qe (exp) (mg/g)	Δqe	R ²	MSSE	
75	0.0415	27.80	49.31	21.5078	0.981		
100	0.0336	41.84	63.84	21.9992	0.997	17.10	
125	0.0327	51.25	76.81	25.5617	0.994	17.19	
150	0.0332	33.78	89.72	55.9318	0.991		

Table - 5.35 Pseudo second order Kinetics results for MB dye onto PBC [pH=7;Dose=30mg/50mL;Contact time=120min;Temp=305K]

	Pseudo Second Order Kinetics					
Concentration (mg/L)	k2×10 ⁻³ (g/mg.min)	qe (cal) (mg/g)	Δqe	h	R ²	MSSE
75	0.0037	51.55	2.2413	9.86	0.996	
100	0.0025	67.11	3.2740	11.21	0.994	1.05
125	0.0020	80.64	3.8326	13.21	0.994	1.95
150	0.0015	95.23	5.5231	13.97	0.993	

Table - 5.36 Pseudo first order Kinetics results for MB dye onto APBC [pH=7;Dose=30mg/50mL;Contact time=120min;Temp=305K]

	Pseudo First Order Kinetics						
Concentration (mg/L)	k1×10 ⁻²	qe (cal) (mg/g)	qe (exp) (mg/g)	Δqe	R ²	MSSE	
75	0.0415	28.18	48.38	20.1976	0.979		
100	0.0350	42.67	62.40	19.7322	0.994	16 10	
125	0.0348	48.98	75.50	26.5221	0.993	16.19	
150	0.0341	33.77	85.65	51.8824	0.988		

Table - 5.37 Pseudo second order Kinetics results for MB dye onto APBC [pH=7;Dose=30mg/50mL;Contact time=120min;Temp=305K]

	Pseudo Second Order Kinetics							
Concentration (mg/L)	K2×10 ⁻² (g/mg.min)	qe (cal) (mg/g)	Δqe	h	\mathbb{R}^2	MSSE		
75	0.0038	50.76	2.3864	9.77	0.996			
100	0.0025	65.78	3.3894	10.95	0.994	1.80		
125	0.0020	79.36	3.8650	12.72	0.994	1.00		
150	0.0018	90.09	4.4400	14.31	0.994			

Table - 5.38 Pseudo first order Kinetics results for MB dye onto BPBC

[pH=7;Dose=30mg/50mL;Contact time=120min;Temp=305K]

	Pseudo First Order Kinetics							
Concentration (mg/L)	k1×10 ⁻²	qe (cal) (mg/g)	qe (exp) (mg/g)	Δqe	R^2	MSSE		
75	0.0408	28.26	51.38	23.1206	0.985			
100	0.0359	41.05	66.42	25.3712	0.994	10 67		
125	0.0327	51.25	79.01	27.7617	0.994	18.67		
150	0.0336	33.63	93.84	60.2120	0.994			

Table - 5.39 Pseudo second order Kinetics results for MB dye onto BPBC [pH=7;Dose=30mg/50mL;Contact time=120min;Temp=305K]

	Pseudo Second Order Kinetics						
Concentration (mg/L)	K2×10 ⁻² (g/mg.min)	qe (cal)	Δqe	h	R ²	MSSE	
75	0.0037	53.76	2.3809	10.57	0.996		
100	0.0026	69.44	3.0244	12.56	0.997	1.85	
125	0.0023	82.64	3.6321	15.43	0.996	1.03	
150	0.0016	99.00	5.1699	15.60	0.994		

Table 5.40 MSSE Values for the adsorption of MB dye $\,$

Adsorbents	MSSE Values				
	Pseudo first order model	Pseudo second order model			
PBC	17.19	1.95			
APBC	16.19	1.80			
ВРВС	18.67	1.85			

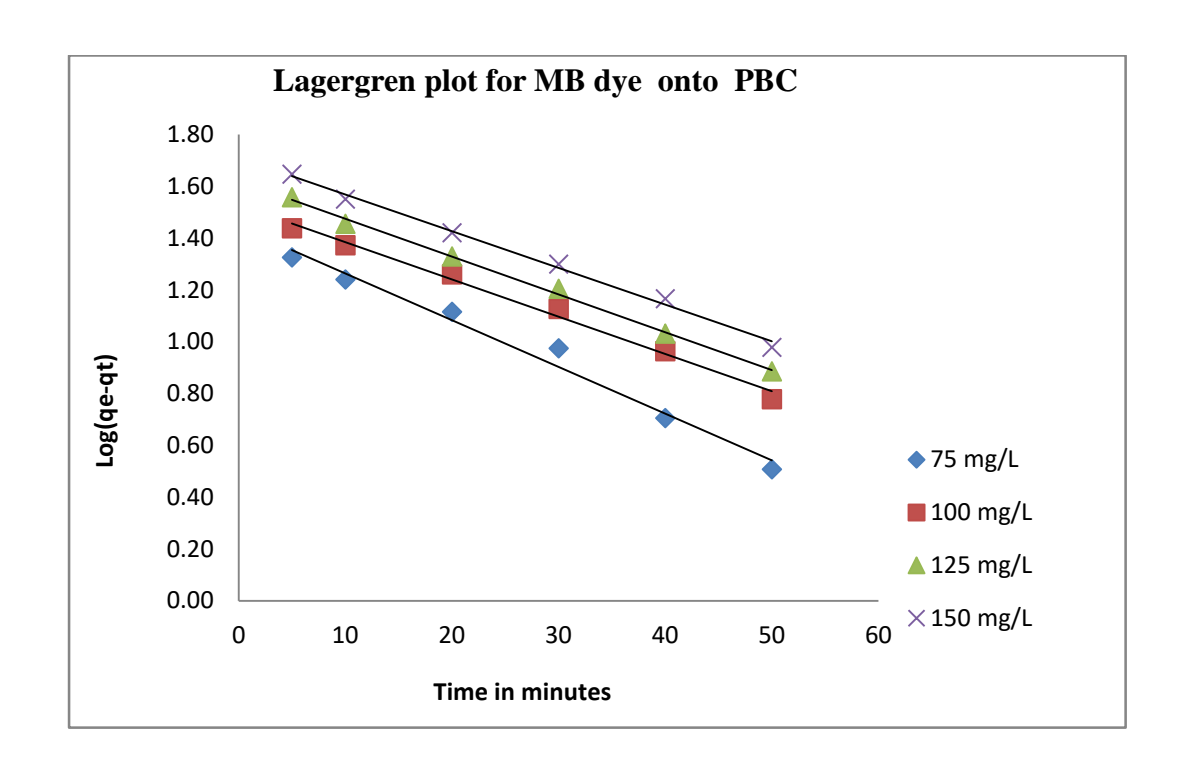


Figure 5.76

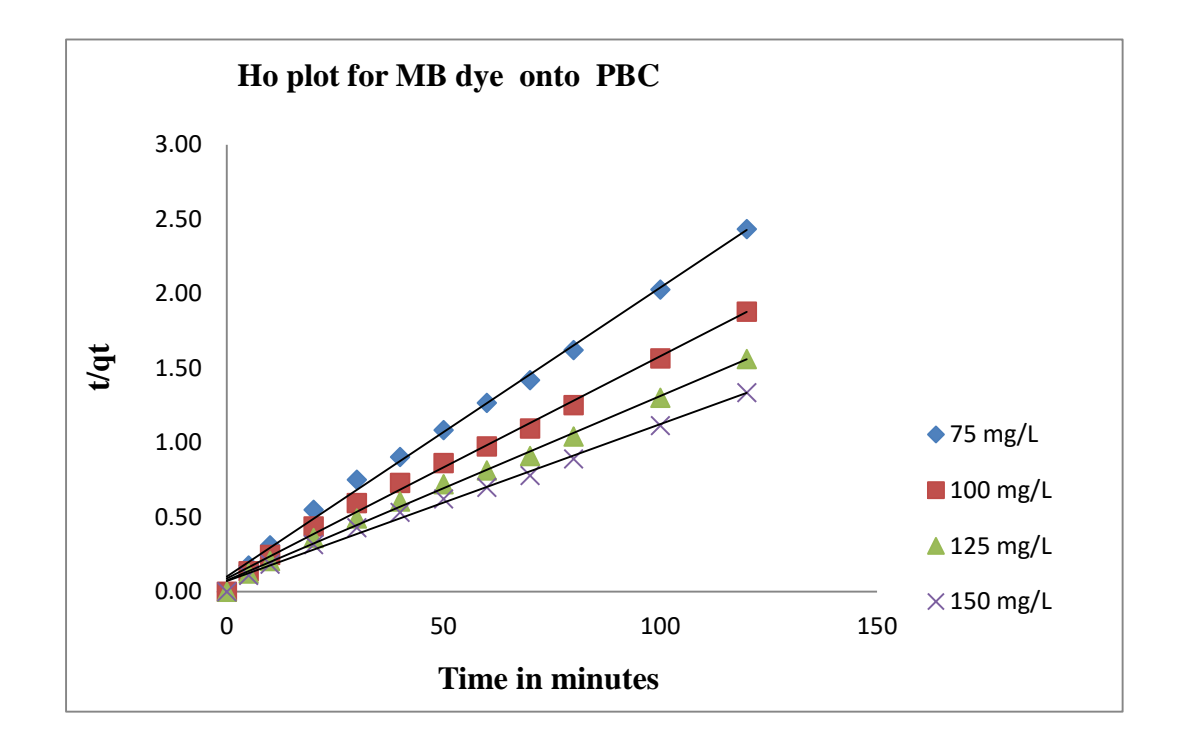


Figure 5.77

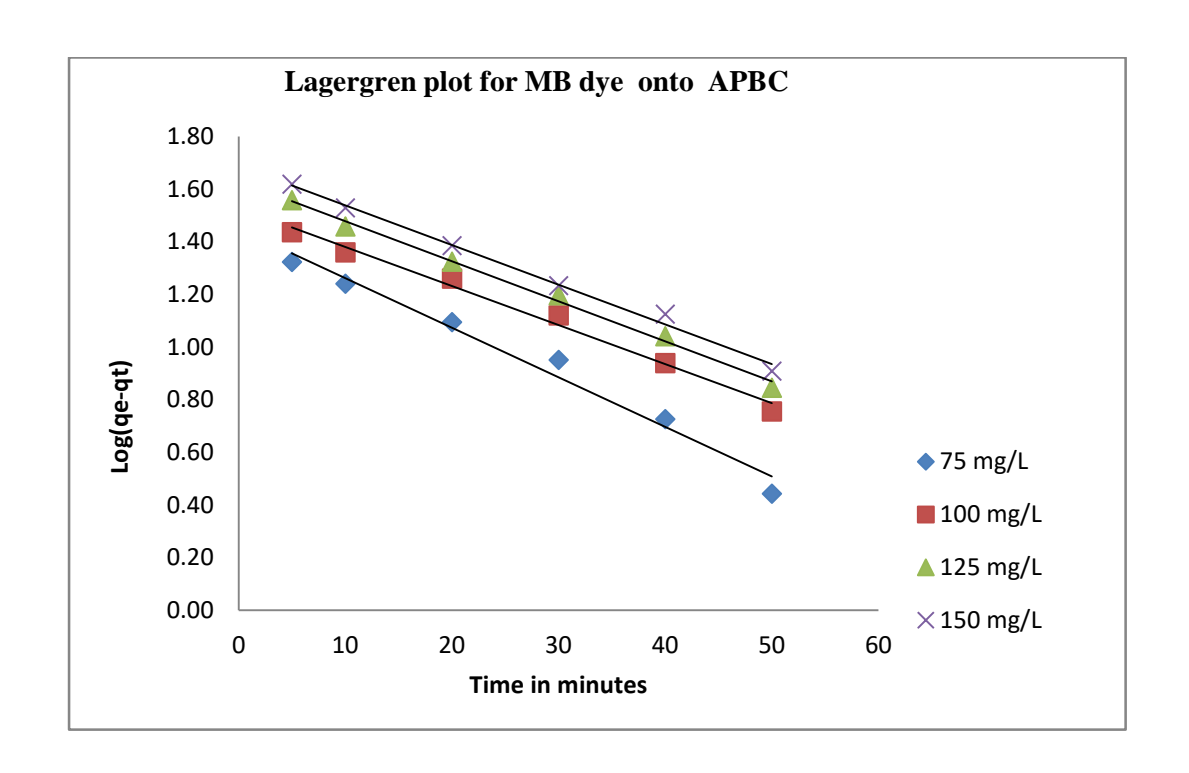


Figure 5.78

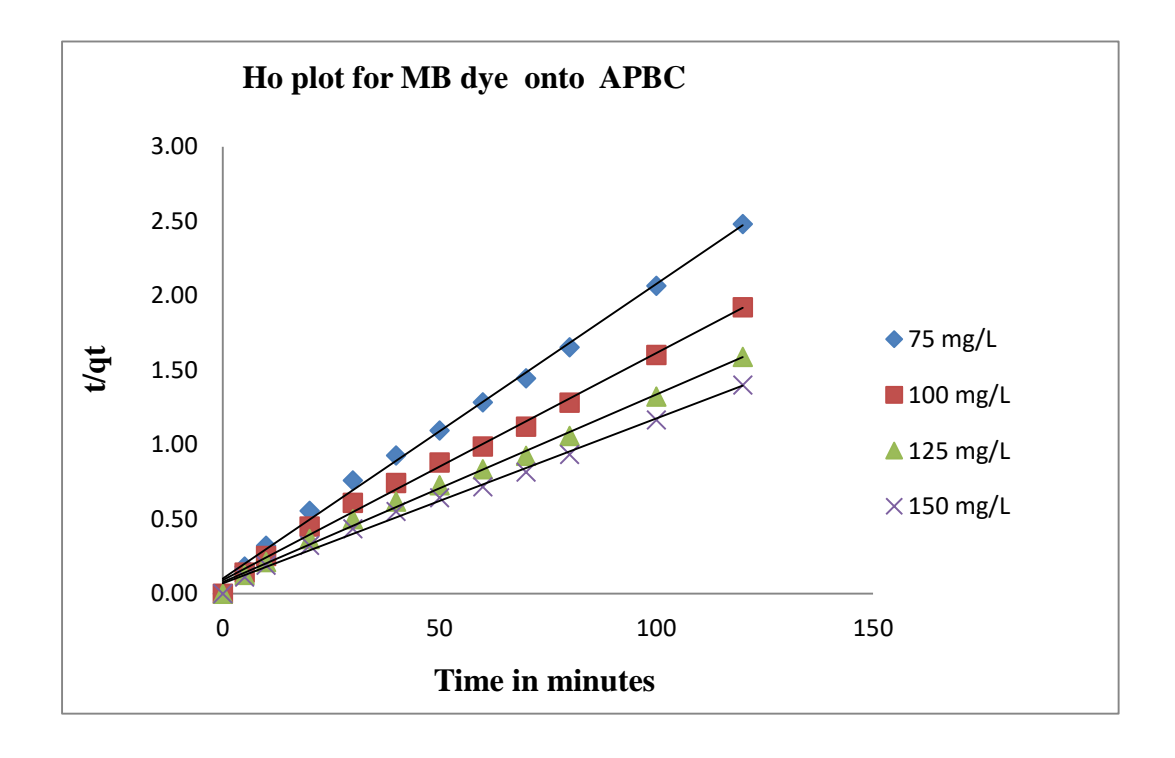


Figure 5.79

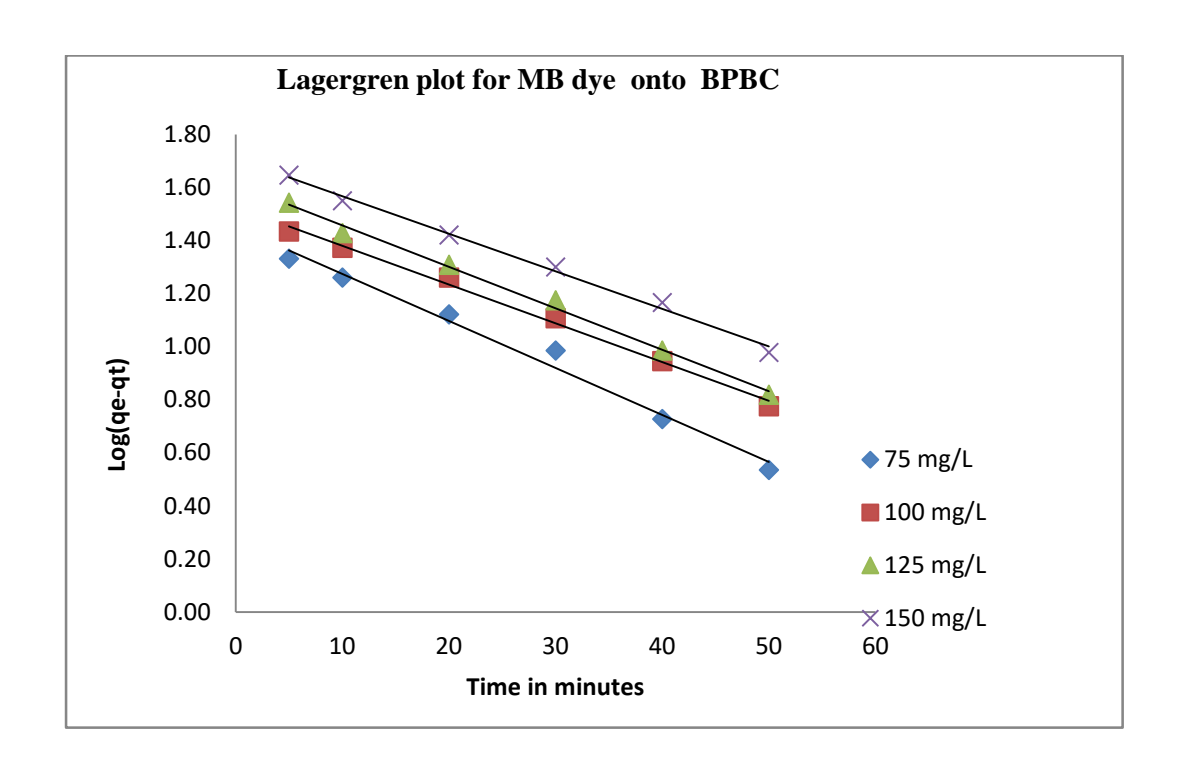


Figure 5.80

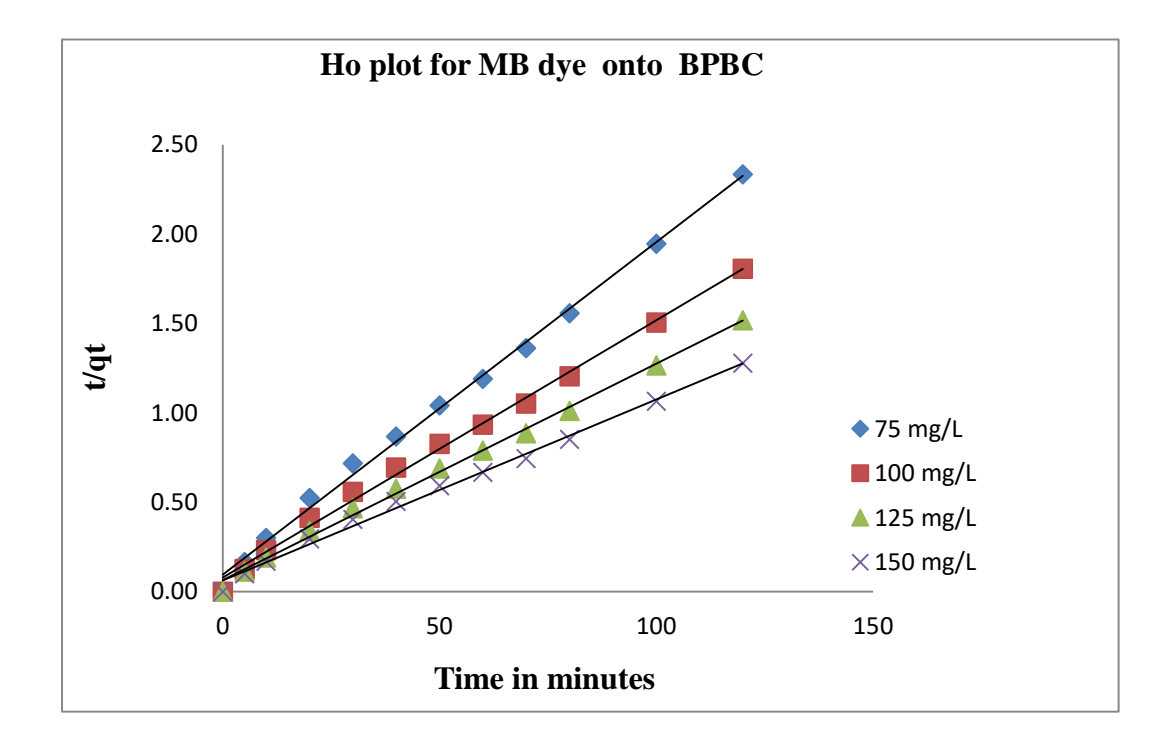


Figure 5.81

5.1.7.2 Intra particle diffusion

The plots for intraparticle diffusion kinetic model was drawn between mass of adsorbate adsorbed per unit mass of adsorbent (qt) versus t^{0.5}. It was noticed that the plot consist more than one phases. The initial portion of the plot indicates a boundary layer effect that is film diffusion while the other phases are due to intraparticle diffusion and instantaneous utilization of the most readily available adsorbing sites on the adsorbent surface. Representative Webber-Morris plot is shown in figure 5.82.

The slopes of the final linear portions of the plots are shown in figure 5.82 to 5.84. The of intra particle diffusion rate constant Kp was determined from the slope of the final linear portion. The values of K_p and R^2 values are given in table 5.41.

The Kp values are found to increase with an increase of MB dye concentration that reveals the rate of adsorption governed by the diffusion of adsorbed MB dye within the pores of the adsorbent. Present results were showed that pore diffusion limits the overall rate of MB dye adsorption (Ahmad et.al., 2016, Rambabuet.al., 2020, Yusuff et.al., 2019).

Table - 5.41 Intra Particle Diffusion results for adsorption MB dye [pH=7;Dose=30mg/50mL;Contacttime= 120min;Temp=305K]

Ci		kp (mg/g.mi	n)	\mathbb{R}^2			
(mg/L)	PBC	APBC	BPBC	PBC	APBC	ВРВС	
75	3.93	3.77	3.92	0.987	0.9980	0.9880	
100	4.73	4.87	4.73	0.999	0.9970	0.9940	
125	5.73	5.45	5.41	0.995	0.9990	0.9950	
150	6.44	6.07	6.44	0.999	0.9920	0.9990	

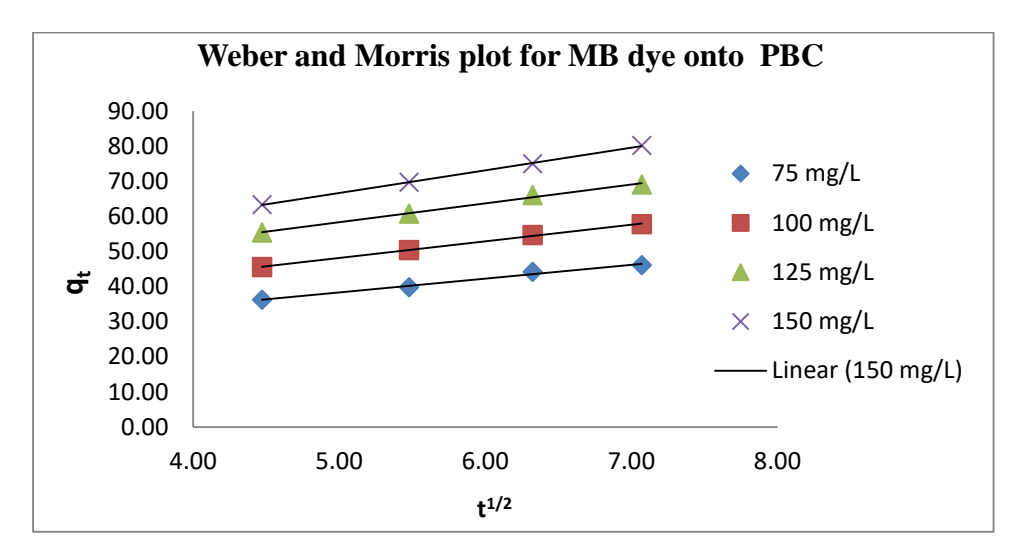


Figure 5.82

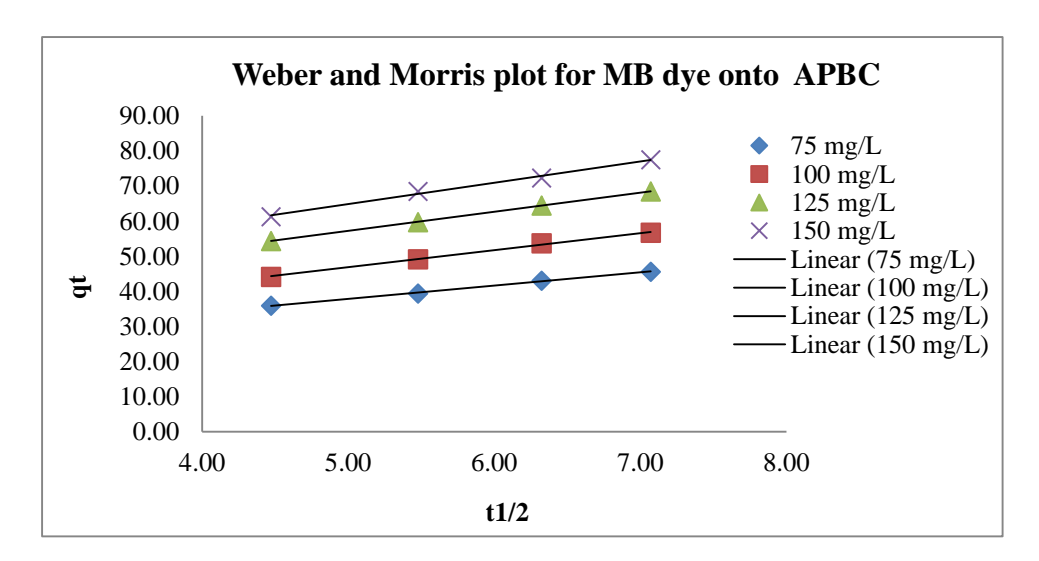


Figure 5.83

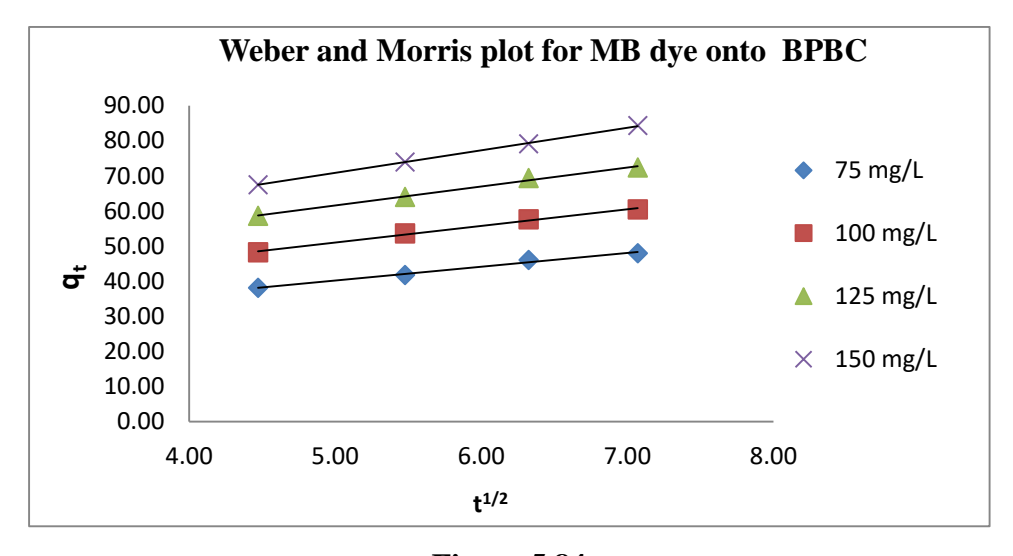


Figure 5.84

5.2.8 Thermodynamic studies

The Van't Hoff plots drawn for the chosen system at four different temperatures are shown in figures 5.85 to 5.87. The thermodynamic parameters calculated are presented in table 5.42.

The negative values of ΔG° (table 5.42) showed that the adsorptions of MB dye onto PBC, APBC & BPBC are highly favorable and spontaneous .

The positive values of ΔH° showed the endothermic nature of adsorption which is supported by the fact that the adsorption capacity of the adsorbent increased with an increase in temperature from 305 to 335K. The magnitudes of ΔH° values were within the range of 1.9141 to 3.2358 (kJ/mol). These values are lesser than 90 kJ which indicates the physisorption and ruled out the possibility of chemisorption (Yao et.al., 2010).

The values of ΔS° of the present studied system ranged from 11.2256 to 14.5794. These positive values of ΔS° showed that the randomness at the solid solution interface. During adsorption some structural changes might have occured at the surface of the adsorbent. The adsorbed water molecules which are displaced by the adsorbate species, might have gained more translational entropy than is lost by the adsorbate molecules, thus allowing the prevalence of randomness in the system (Biswajit Das et.al., 2013).

This ΔS° values found to decrease with an increase of initial concentration of the adsorbates solution. While comparing the ΔS° values with respect to the adsorbents, the ΔS° values for the adsorption onto BPBC were found to be high when compared to APBC and PBC.

The enhancement of adsorption capacity of the adsorbents at higher temperatures was attributed to the enlargement of the size of the pore and the activation of the adsorbent surface (Krishna et.al., 2013).

Table 5.42 Thermodynamic Parameter results for MB dye onto adsorbents

[pH=7;Dose =30mg/50mL]

Adsorbents	Ci (mg/L)	ΔG° kJ/mol				ΔH°	ΔS°
		305K	315K	325K	335K	kJ/mol	(kJ/mol)
	75	-1.65	-1.76	-1.88	-2.01	3.2358	13.7846
PBC	100	-1.44	-1.56	-1.69	-1.84	3.0236	13.7647
rbc	125	-1.18	-1.31	-1.44	-1.60	2.6278	13.319
	150	-1.01	-1.07	-1.14	-1.21	1.9547	11.8125
APBC	75	-1.51	-1.62	-1.73	-1.85	2.9964	13.3082
	100	-1.28	-1.40	-1.52	-1.67	2.8858	12.6622
	125	-1.07	-1.19	-1.32	-1.47	2.5842	12.3546
	150	-0.73	-0.78	-0.83	-0.89	1.9141	11.2256
врвс	75	-1.97	-2.09	-2.22	-2.37	2.5466	14.5794
	100	-1.73	-1.86	-2.00	-2.17	2.7227	13.2442
	125	-1.37	-1.50	-1.64	-1.81	2.0615	13.2060
	150	-1.30	-1.38	-1.45	-1.53	2.2564	11.4983

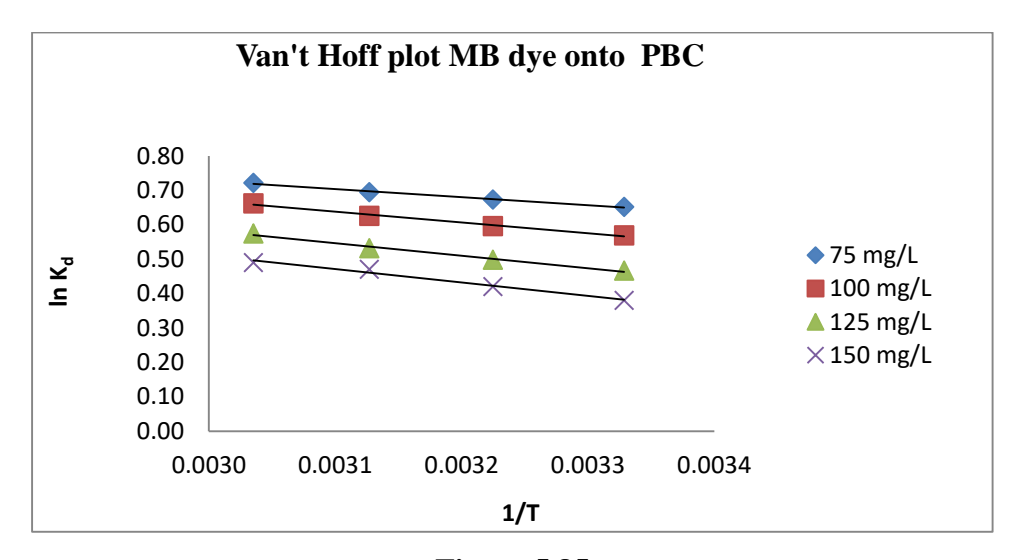


Figure 5.85

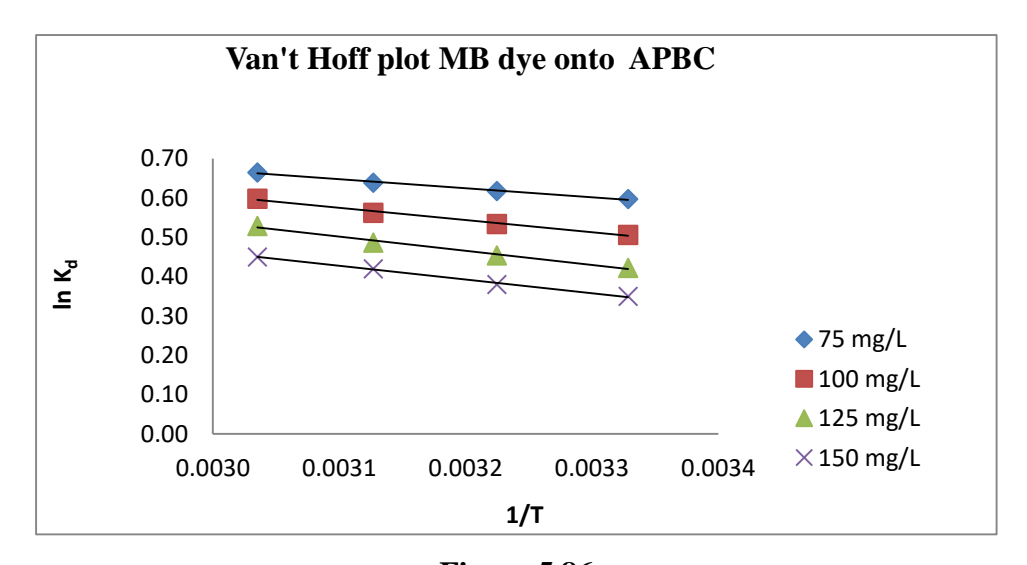


Figure 5.86

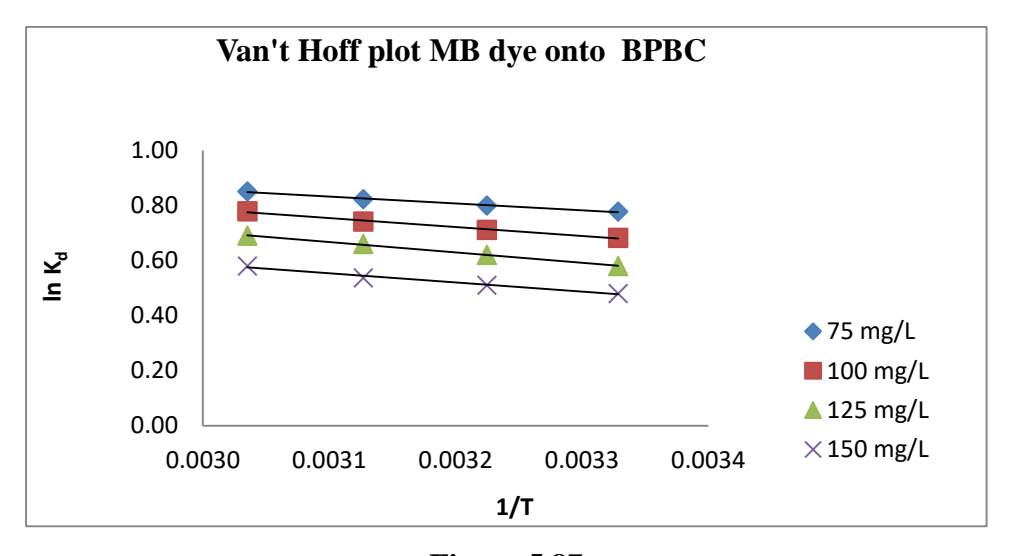


Figure 5.87

5.2.9 Desorption of MB dye

Result of desorption of MB dye from adsorbents loaded with MB dye is presented as column diagram in figure 5.88. The percentage of desorption was more for 0.1N HCl solution when compared to other desorbing agents Distilled water and 0.1N NaOH. The adsorbent surface is completely covered by H⁺ ions while the coordination sphere of chelated metal ions/dyes is disrupted. Thereafter, the dyes cannot compete with H⁺ ions for adsorption sites and subsequently dyes are released from the adsorbent surface into the solution. (Li et al 2009)

The maximum percentage of desorption is found to be 50 % which suggests that the MB dyes are strongly attached to adsorbent. This strong attachment might be due to chemisorption. Hence it may be concluded that MB dye were bound on the surface of the adsorbent both by physical force and chemical forces. The physical force is normally Vander wall's force. The chemical forces probably due to attachment between MB dye and the functional group present in the surface of the adsorbent.

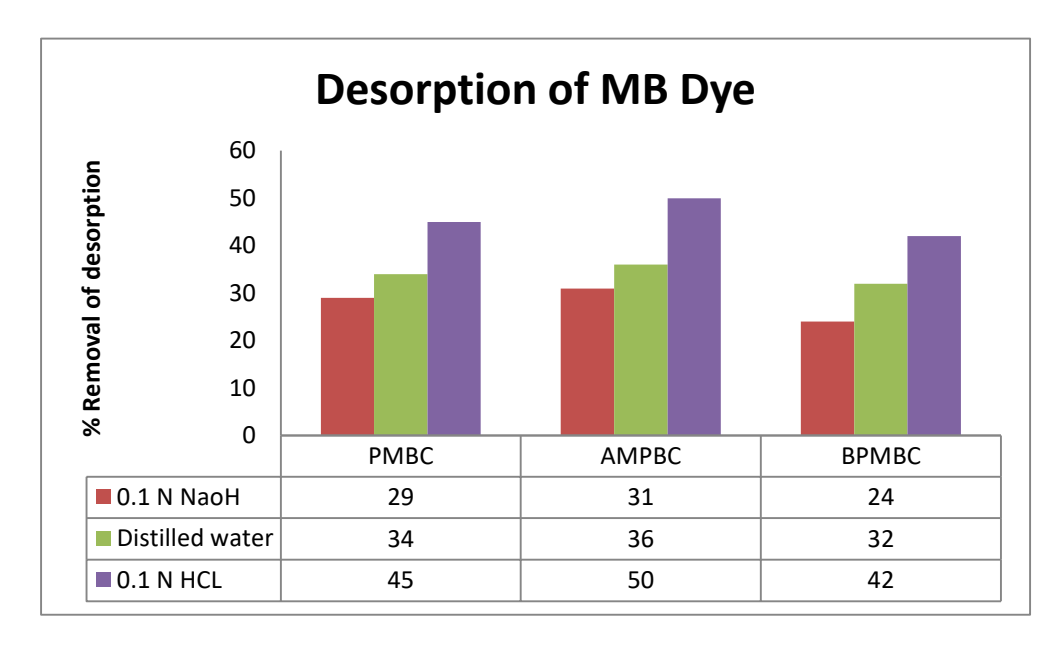


Figure 5.88

5.2.10 Morphological study

Changes in the morphology of adsorbent because of adsorption have been analyzed with FT-IR spectra.

5.2.10.1 Fourier Transform Infrared Spectroscopy (FT-IR)

Historically IR has been mostly used for qualitative analysis, to obtain structural information. The instrumental evolution of the day makes non-destructive and quantitative analysis possible, with significant accuracy and precision. The shift of the bands and the changes in signal intensity allow the identification of the functional groups involved in metal ions/dyes adsorption.

5.2.10.1 FT-IR Study for MB dye

The FT – IR spectrum of PBC, APBC and BPBC loaded with MB dye was shown in figure 5.89-5.91.

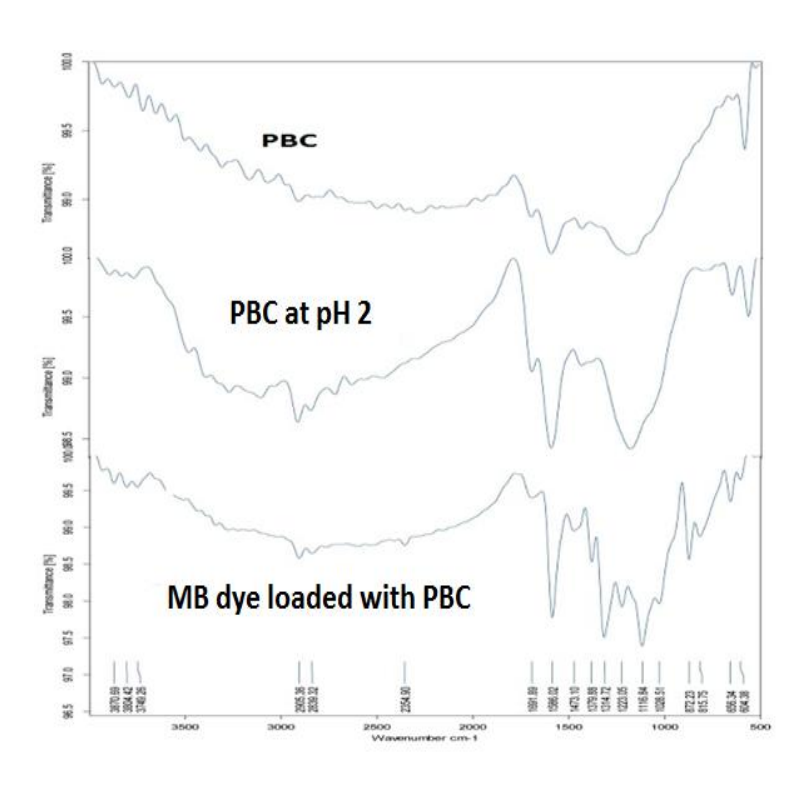


Figure 5.89 FTIR Spectrum of PBC adsorbent before adsorption, PBC at pH2 and MB dye loaded PBC

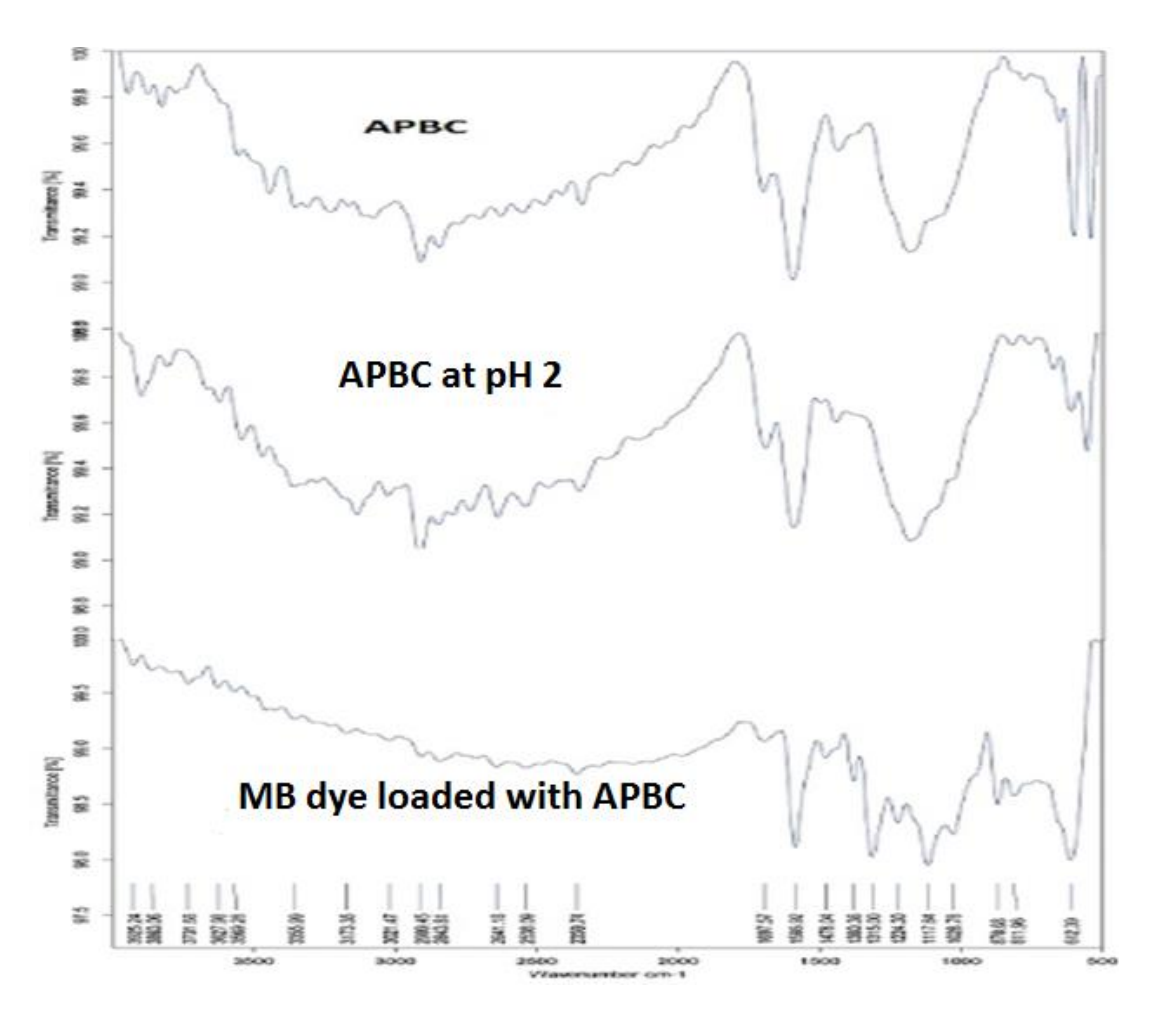


Figure 5.90 FTIR Spectrum of APBC adsorbent before adsorption, APBC at pH2 and MB dye loaded APBC

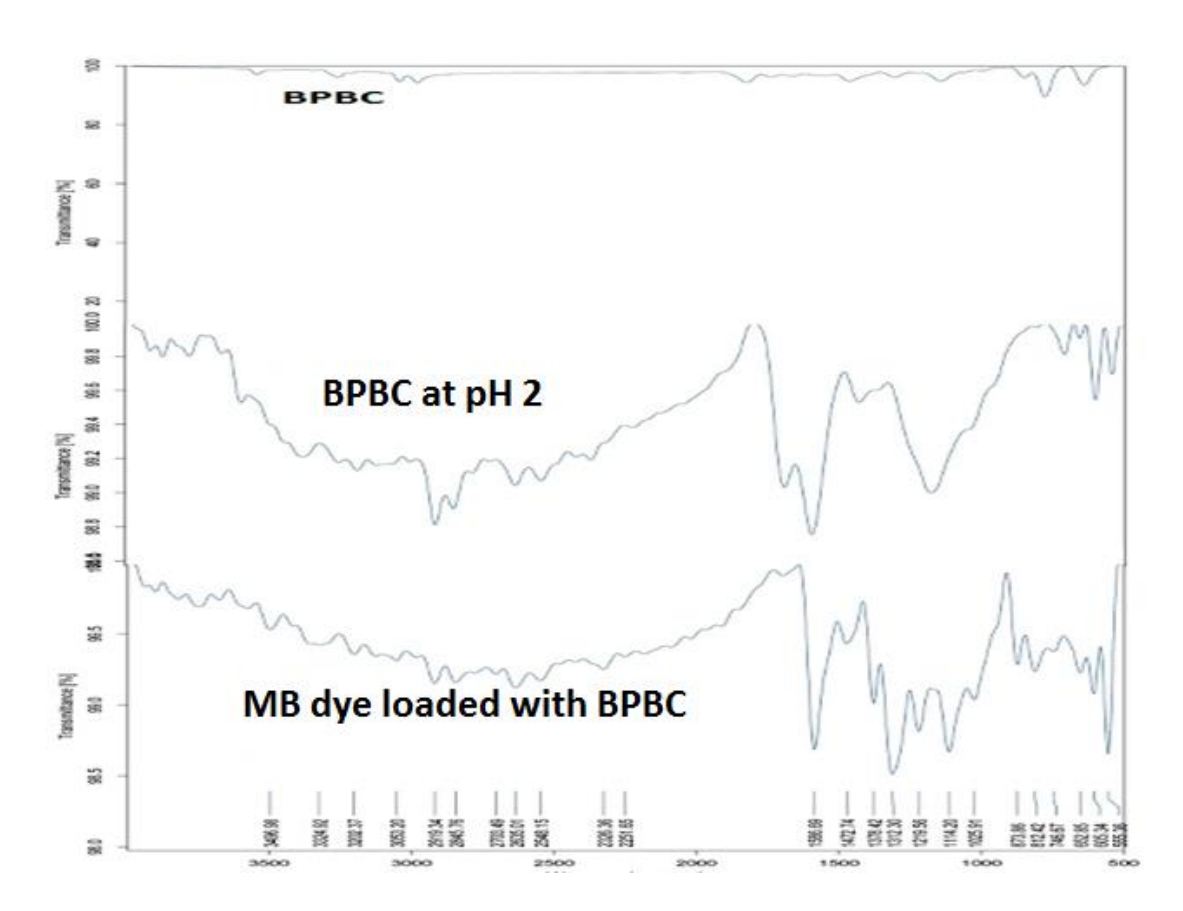


Figure 5.91 FTIR Spectrum of BPBC adsorbent before adsorption, BPBC at pH2 and MB dye loaded BPBC.

The FTIR pattern for after adsorption of MB dye onto PBC, APBC and BPBC. The appreciable new peaks were formed found after adsorption of BPBC between the ranges 500-3500 cm⁻¹, when compared to PBC and APBC. Which may be due to formation of more active sites or new chemical bonds. This results leads to conclude that physisorption with partial chemisorption also took place.

5.3 STUDIES ON THE ADSORPTION OF TB DYE ONTO PBC, APBC AND BPBC

This chapter deals with the study of removal of Turquoise blue (TB) dye using activated carbons prepared from then barks of *Pterocarpus Marsupium Roxb*.by Phosphoric acid viz PBC (*Pterocarpus Marsupium* Bark Carbon) APBC (Acid modified *Pterocarpus Marsupium* Bark Carbon) and BPBC (Base modified *Pterocarpus Marsupium* Bark Carbon). The adsorption studies are performed by conducting batch mode experiments by varying the parameters such as solution pH, adsorbent dosage, contact time, initial concentration and Temperature.

Equilibrium data were processed with Freundlich, Langmuir, Temkin and Dubinin-Radushkevich isotherm equations. Values of isotherm constants were determined and their significances were discussed. The adsorption behaviour of the TB Dye onto PBC, APBC and BPBC were compared.

Data obtained from effect of contact time for different initial concentrations were processed with Lagergren, Ho and Webber Morris kinetic equations. Rate constants and the predicted adsorption capacities were determined. Predicted adsorption capacities were compared with the experimental adsorption capacities. Best fitting model was identified using the statistical tool Mean Summation of Error Squares (MSSE).

Thermodynamic quantities ΔH° , ΔS° and ΔG° were determined using equilibrium data obtained in different temperatures. Inferences obtained from these values were discussed.

Regenerating capability of the adsorbents loaded with TB dye were investigated with acidic, alkaline and neutral mediums.

FTIR spectrumof adsorbents were studied before and after adsorption of TB dye to know the adsorbate – adsorbent interactions.

Findings of the present study are interpreted and discussed in the light of the objectives set forth.

5.3.1 Effect of pH

The pH of the adsorbate solution is an important parameter governing sorption on different adsorbents. This is partly due to the fact that hydrogen ion itself is a strong competing sorbate and partly to the fact that its ability to influence the chemical speciation of adsorbate. The effect pH of solution was studied by taking pH range from 2 to 10.

Effect of solution pH on the adsorption of TB dye on PBC.ABPC and BPBC was shown in the figure 5.92 which shows that removal of TB dye is maximum at pH 2 and decreased on increasing the pH of the solution for all the adsorbents.

Turquoise blue dye occurred as negatively charged species when dissolved in water. When the pH is lower than pHzpc of the adsorbent, the charge on the surface of the adsorbent is positive (Gottipati Ramakrishna et.al., 2012). At very low pH, the more positive charge accumulated on the surface of the adsorbent and facilitated electrostatic attraction on the negatively charged bichromate ion and hence more adsorption was observed. Moreover at lower pH, the concentration of OH⁻ ions was meager. Hence the competition for the positively charged cite by OH⁻ ions was lesser.

When the pH of the solution was raised, the positive charge on the surface decreased with the increase in OH⁻ ions concentration. The OH⁻ ions being smaller in size tended to adsorb preferentially on adsorbent and rendered repulsive force towards

the approaching negative metal anions. Hence the adsorption of TB dye was low at higher pH of the solution (Supriya Singh et.al., 2013, Kulkarni Sunil., 2013, KhadkaDebaBahadur et.al., 2014)

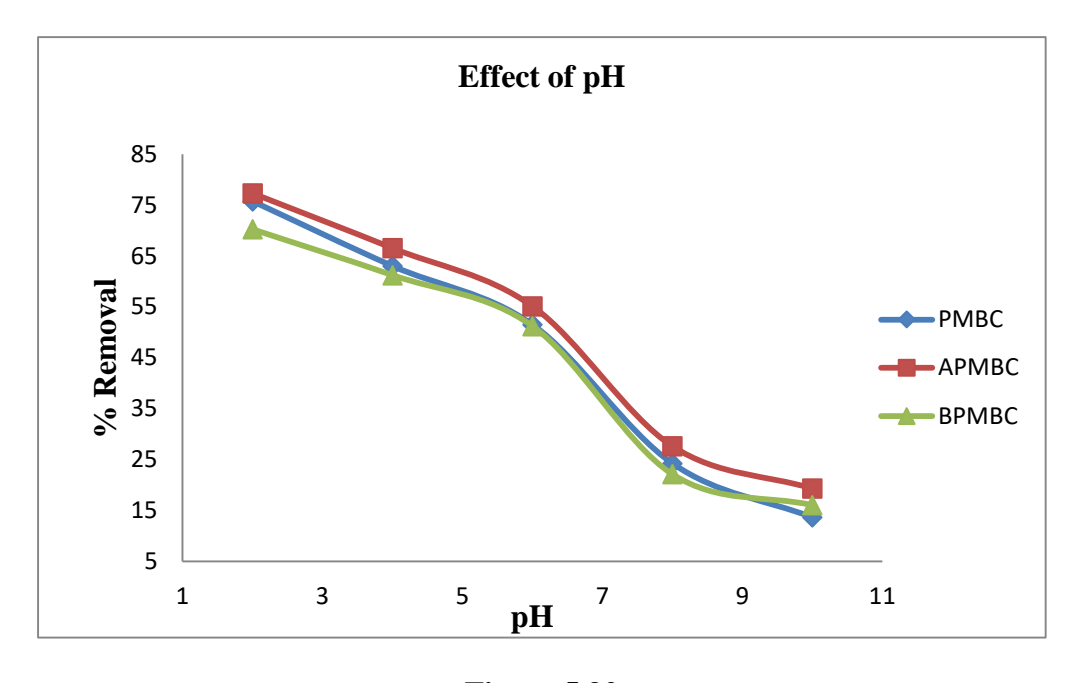


Figure 5.92

On comparing the ability of PBC.APBC and BPBC, the order of increasing percentage of removal was found to be APBC.BPBC and PBC. This kind of order was found in earlier literatures (Selvarajet.al., 2003).

5.3.2 Effect of adsorbent dosage

Adsorbent dosage is one of the important parameters in adsorption processes because amount of adsorbate adsorbed vary with the dosage of an adsorbent for a given initial concentration of the adsorbate under a given set of operating conditions. figure 5.93 showed the effect of adsorbent dosage for adsorption of TB dye onto PBC, APBC and BPBC. As can be seen in this figure, increase of dosage increases the percentage of removal of adsorbate from the solution. The percentage of removal increased from 12.34 to 95.22 % for TB dye onto PBC, 24.33 to 97.66% for TB dye onto APBC and 19.00 to

96.55 for TB dye onto BPBC for the increase of dosage of 5mg / 50mL to 50mg / 50mL as given in table 5.43.

The increase in the removal efficiency with an increase in the adsorbent dosage, may be attributed to increase of more adsorbent surface is available for the solute to be adsorbed (Hemaet.al., 2007).

There is a slight difference in the adsorbing efficiency of TB dye was observed among the chosen adsorbents PBC, APBC & BPBC which was shown in the table 5.1. The order of removal of TB dye from the aqueous phase is APBC >BPBC> PBC.

Similar trend was observed in earlier literature (Garget.al., 2003, Selvi et.al., 2003, Demirbas et.al., 2004)Based on these results, the remaining parts of the experiments were carried out with the 30 mg for 50 mL of TB dye solution.

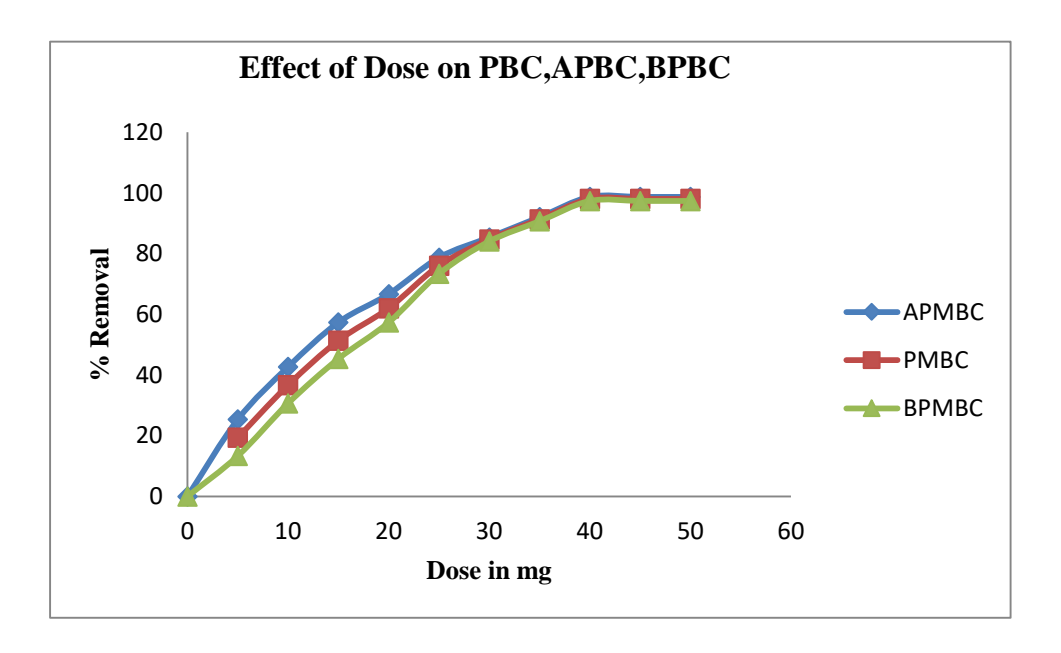


Figure 5.93

Table – 5.43 Effect of dose for TB dye onto PBC, APBC and BPBC (Contact Time=70min)

		TB dye					
Dose inmg	% Removal of PBC	% Removal of APBC	% Removal of BPBC				
05	25	13	19				
10	43	31	37				
15	57	45	51				
20	67	57	62				
25	79	73	76				
30	85	84	85				
35	92	91	91				
40	99	97	98				
45	99	97	98				
50	99	97	98				

5.3.3 Effect of Contact Time

The effect of contact time on the percentage removal from aqueous solution was studied by taking 10, 15, 20 and 25 mg/L of TB dye solutions as initial concentrations.

The result of the above study was given in table 5.42 and shown in figures 5.94 to 5.96. The rate of percentage removal was found to be rapid at initial stages and the rate was found to decrease as the time increases and become constant after attaining equilibrium stage. At the initial stage, the ratio of surface area of the adsorbent to the amount of solute in liquid phase is high and hence the concentration of adsorbate in the liquid phase acted as driving force and made the solute to rush towards the adsorbent surface. As the time increases the above ratio began to decrease due to adsorption and hence the rate of adsorption reduced (Renmin Gong et.al., 2005). Equilibrium was found to occur at 80 min in all the cases.

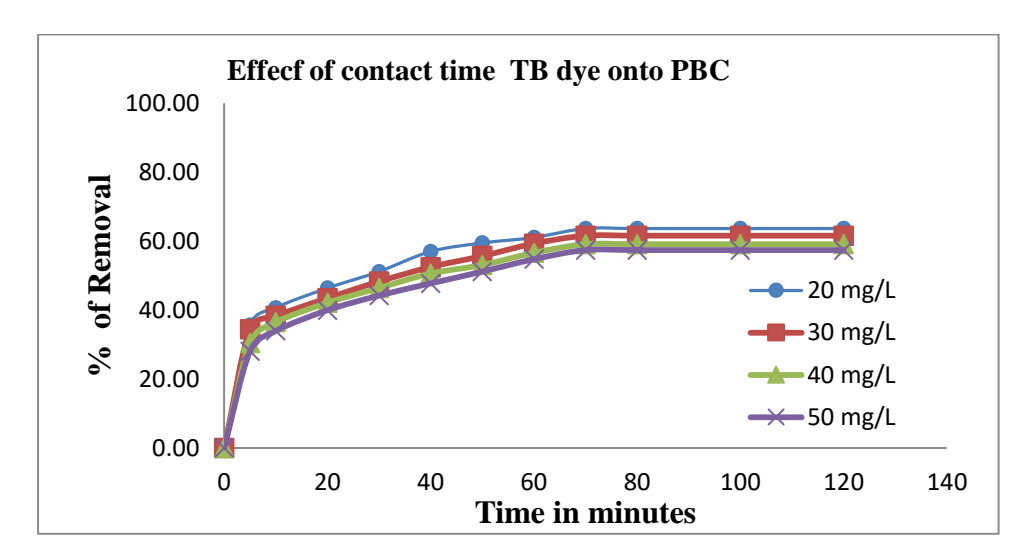


Figure 5.94

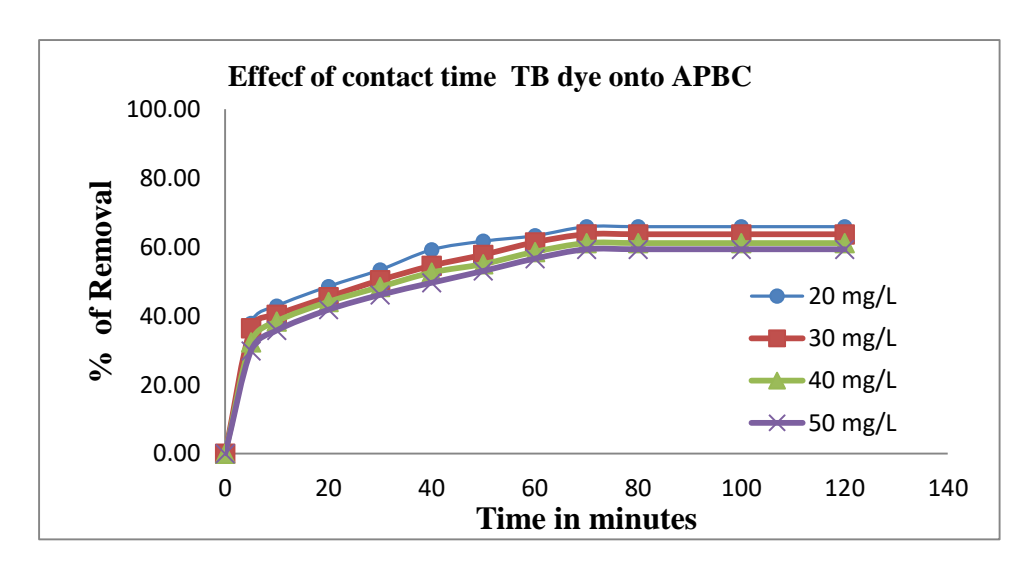


Figure 5.95

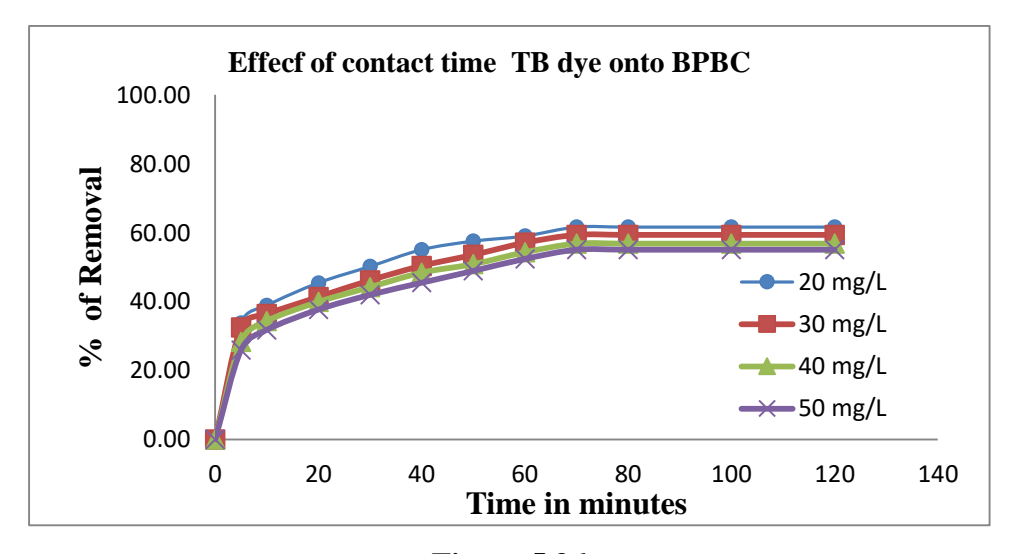


Figure 5.96

 $Table-5.44\ Effect\ of\ Contact\ time\ for TB\ dye\ adsorption\ onto PBC\ \&\ BPBC$

		% Removal of PBC % Removal of APBC			% Removal of BPBC		C					
Time		Initial Concentration in mg/L										
In Minutes	20	30	40	50	20	30	40	50	20	30	40	50
0	0.00	0.00	0.00	0.00	0.00	0.00	0.00	0.00	0.00	0.00	0.00	0.00
5	35.69	34.48	30.46	28.08	37.84	36.50	32.40	29.90	33.84	32.55	28.35	25.91
10	40.73	38.32	36.50	33.98	42.88	40.34	38.44	35.80	38.88	36.39	34.39	31.81
20	46.40	43.49	42.15	39.98	48.55	45.51	44.09	41.80	45.45	41.36	39.94	37.71
30	51.20	48.32	46.43	44.24	53.38	50.37	48.40	46.10	50.21	46.19	44.22	41.97
40	57.03	52.52	50.63	47.76	59.21	54.57	52.60	49.62	55.08	50.39	48.42	45.49
50	59.50	55.71	53.10	51.19	61.68	57.76	55.07	53.05	57.55	53.58	50.89	48.92
60	61.09	59.31	56.64	54.78	63.27	61.36	58.61	56.64	59.04	57.08	54.33	52.41
70	63.69	61.61	59.14	57.44	65.90	63.70	61.14	59.34	61.64	59.38	56.83	55.07
80	63.69	61.61	59.14	57.44	65.90	63.70	61.14	59.34	61.64	59.38	56.83	55.07
100	63.69	61.61	59.14	57.44	65.90	63.70	61.14	59.34	61.64	59.38	56.83	55.07
120	63.69	61.61	59.14	57.44	65.90	63.70	61.14	59.34	61.64	59.38	56.83	55.07

5.3.4 Effect of initial concentration

The factor, effect of initial concentration depends on the relation between the adsorbate concentration in the solution phase and the available binding sites on an adsorbent surface. This study showed that the percentage of the removal of adsorbate decreased with the increase of initial concentration of adsorbate solution as given in table 5.45 and shown in figures 5.97, 5.99& 5.101.

The percentage removal of decreased from 68.00 to 55.30 for PBC, 72.40 to 59.23 for APBC and 70.20 to 57.20 for BPBC at the temperature 305 K as the initial concentration of TB dye increased from 10 mg/L to 25 mg/L.

The amount of solute in the liquid phase is higher at a higher of initial concentration. The ratio of available adsorbent surface to the concentration of solute decreases with the increase of initial concentration and hence the percentage of removal decreases with the increase of initial concentration.

However the amount of TB dye adsorbed on the adsorbent increased with an increase in the initial concentration of the adsorbate solutions as evidenced from the table 5.46 and figures 5.98, 5.100 & 5.102. The amount of TB dye adsorbed increased from 6.80 to 13.83 for PBC, 7.24 to 14.81 for ABPC and 7.02 to 14.30 for PBPC at the temperature 305K as the initial concentration of TB dye increased from 10 to 25 mg/L.

This is because the amount of solute adsorbed is proportional to the percentage of adsorbate transferred from liquid phase to solid phase. This fraction increases with an increase in the concentration of solution. For example if 25 percentage is assumed to be transferred, 25 mg of solute will be transferred if the initial concentration of the solution

is $100 \ mg/L$. If the initial concentration solution is $200 \ mg/L$, then the amount transferred will be $50 \ mg$.

Table–5.45 Effect of initial concentration on percentage of removal $[TB\ dye\ pH=2Dose=40mg/50mL]$

Adsorbents	Initial Concentration Ci (mg/L)	Percentage of Removal
	20	59.50
PBC	30	55.71
FBC	40	53.10
	50	51.19
	20	61.68
APBC	30	57.76
AIBC	40	55.07
	50	53.05
	20	57.55
врвс	30	53.58
DrbC	40	50.89
	50	48.92

Table–5.46 Effect of initial concentration on amount of adsorption $[TB\ dye,\ pH=2; Dose=40mg/50mL]$

Adsorbents	Initial Concentration Ci (mg/L)	Amount adsorbed (mg/g)
	20	12.74
PBC	30	18.48
FBC	40	23.66
	50	28.72
	20	13.18
APBC	30	19.11
AIDC	40	24.46
	50	29.67
	20	12.33
врвс	30	17.81
DIDC	40	22.73
	50	27.54

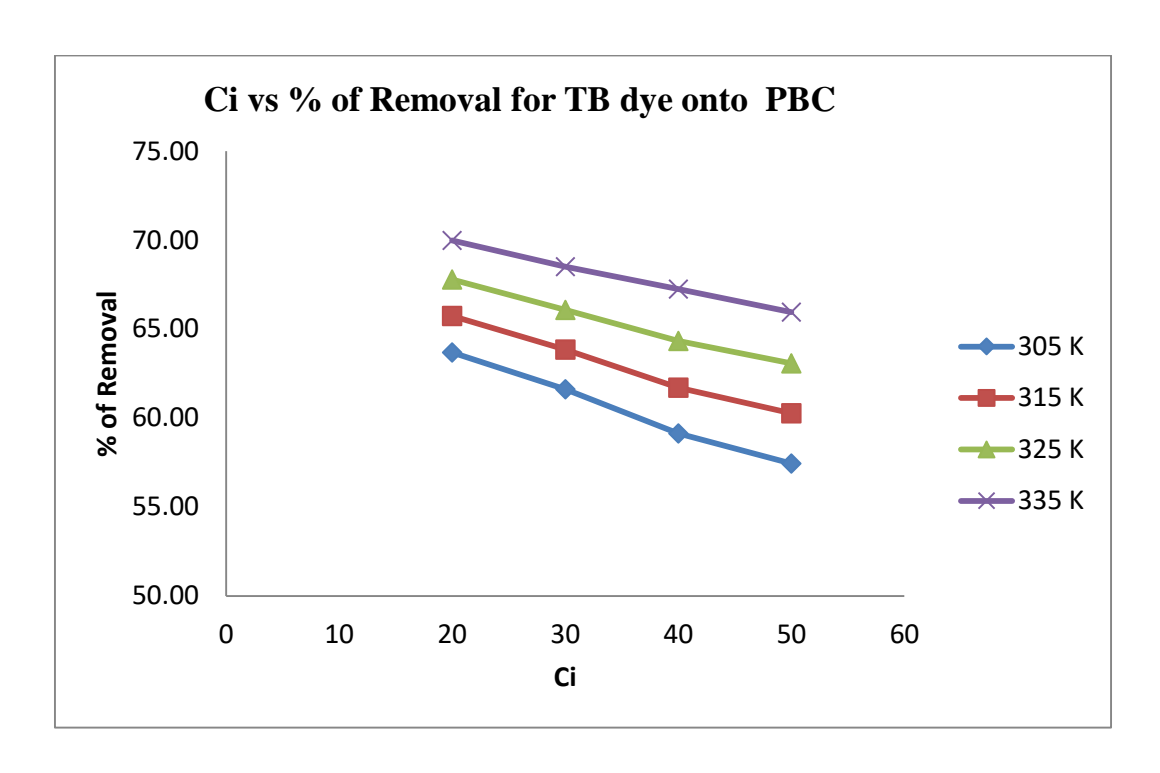


Figure 5.97

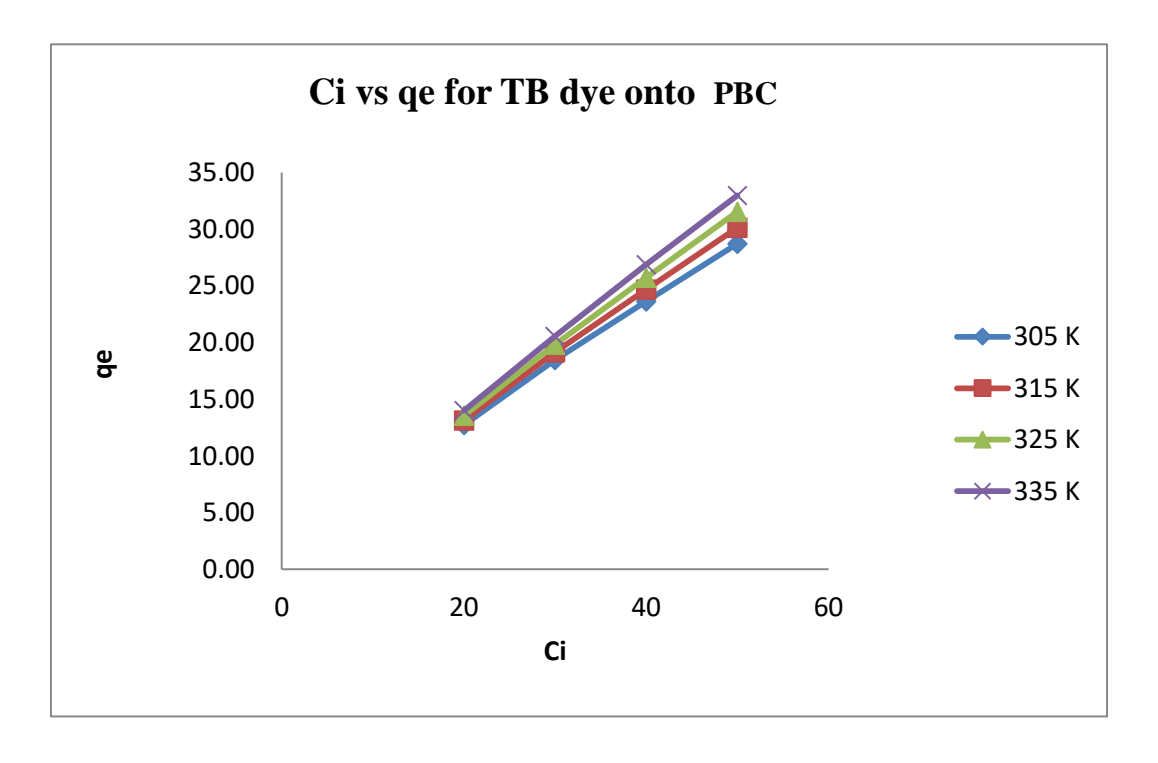


Figure 5.98

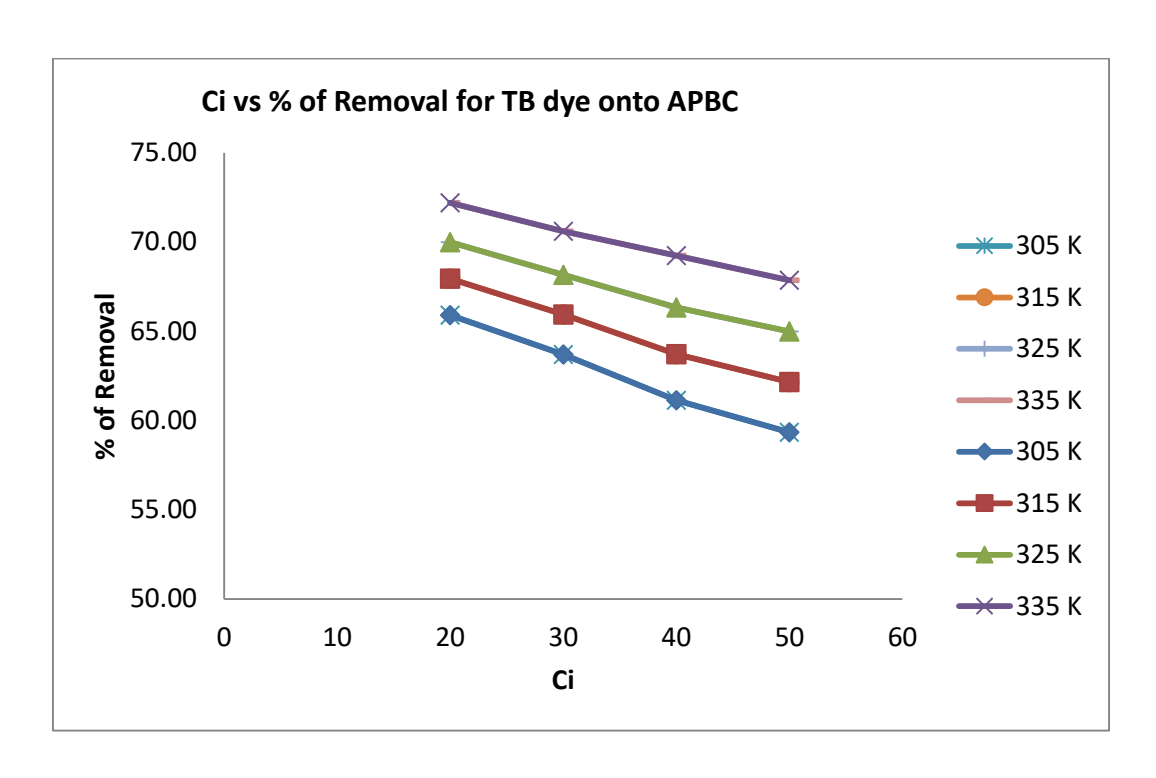


Figure 5.99

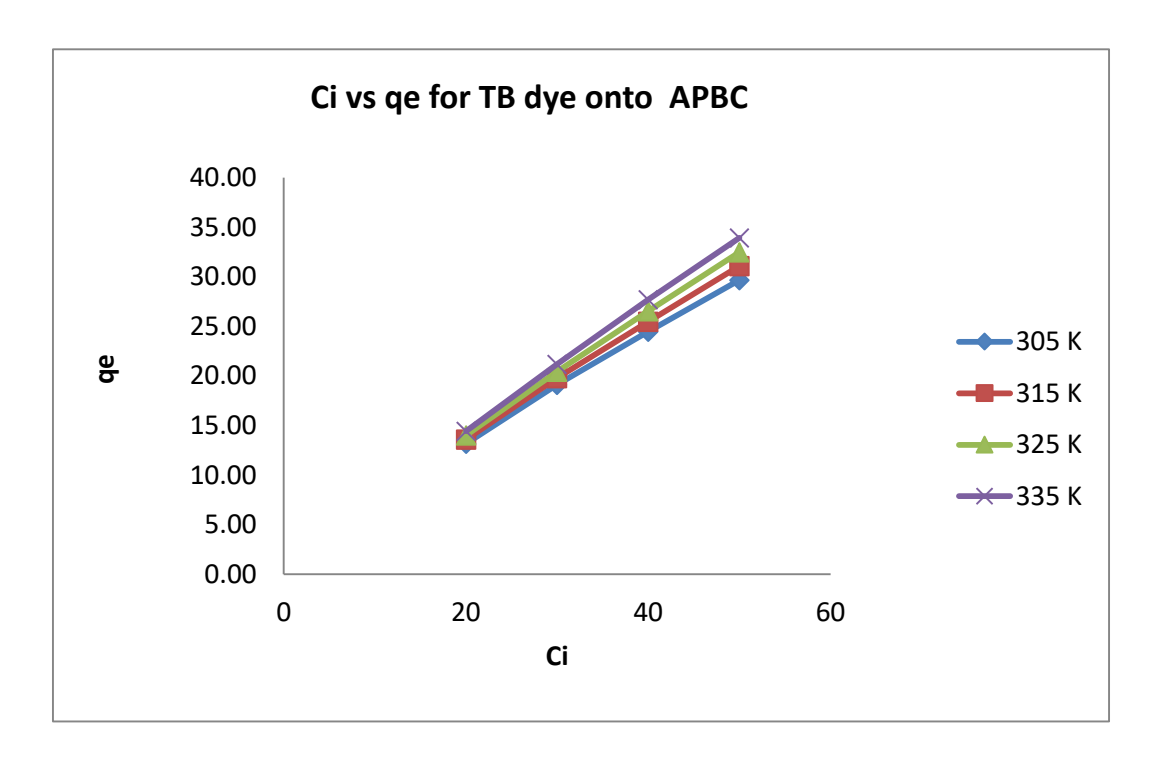


Figure 5.100

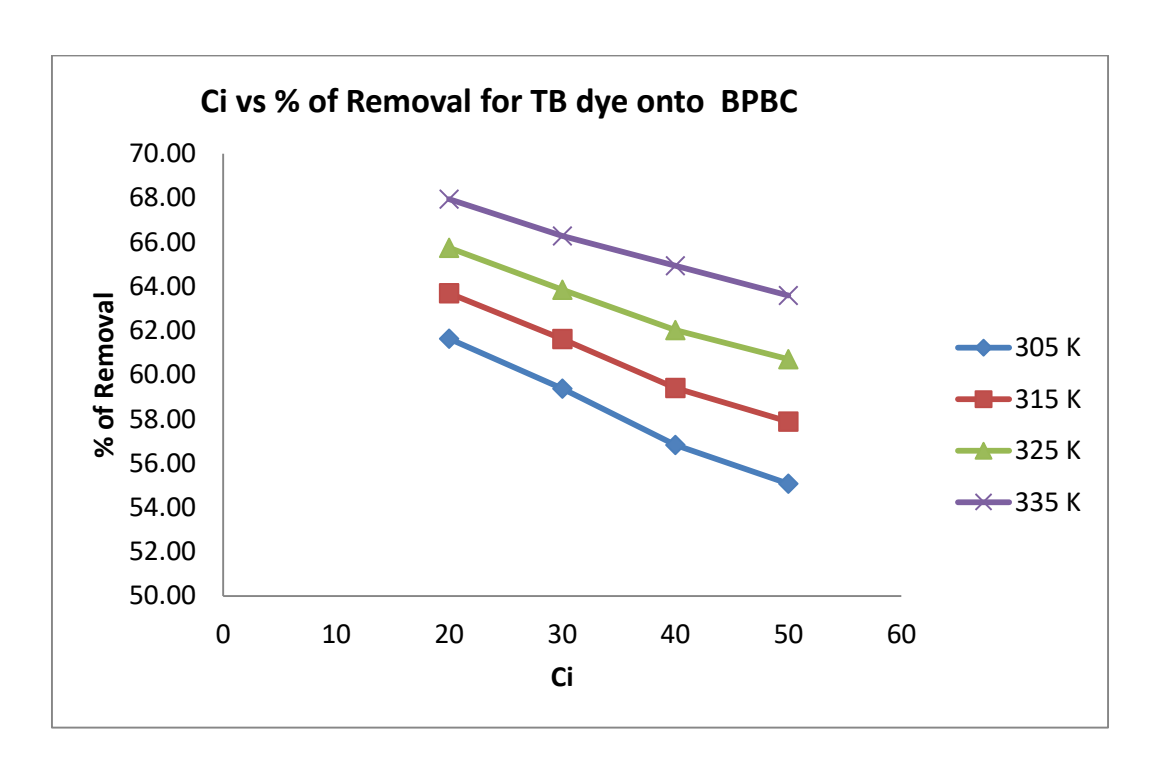


Figure 5.101

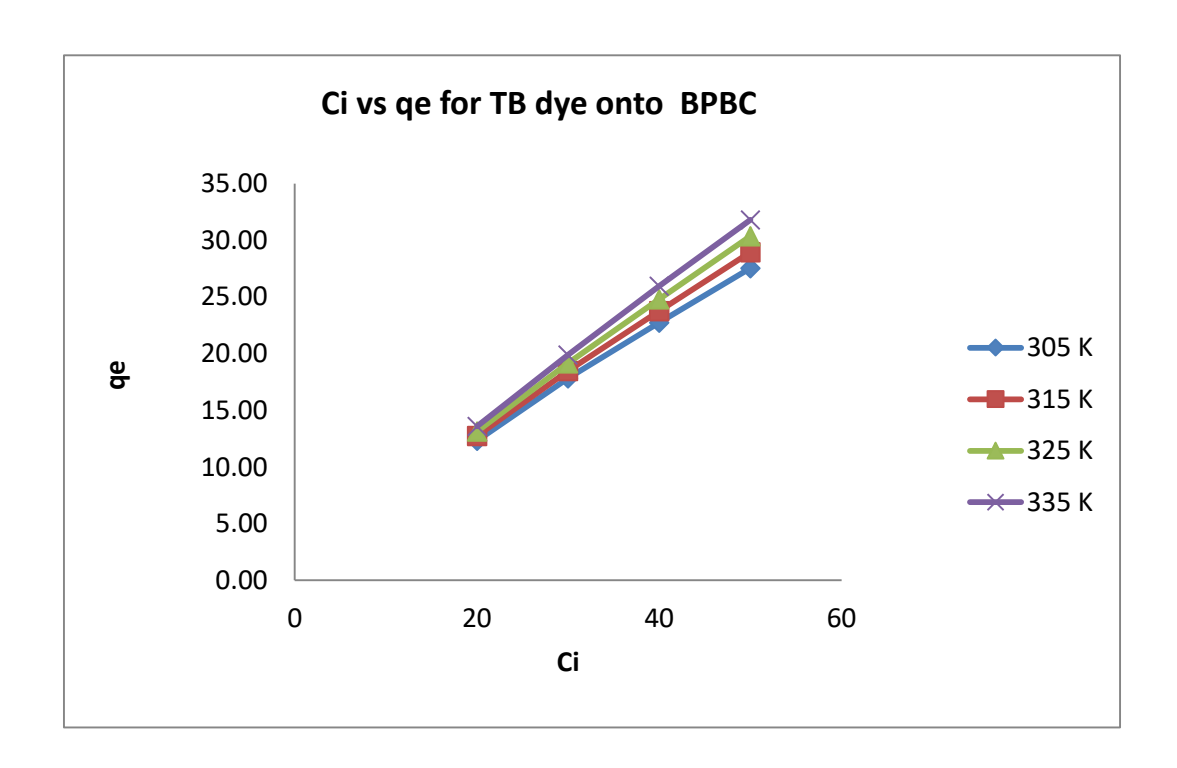


Figure 5.102

5.3.5 Effect of Temperature

Temperature is a well-known factor that influence in the adsorption process. The influence of temperature on adsorption of TB dye was investigated at 305, 315, 325 and 335K. The results were presented in table 5.47 to 5.48. Plots drawn between percentage removals versus temperature were given in figures 5.103, 5.105 & 5.107. It could be clearly seen that, the percentage of removal increased with an increase of temperature. When the temperature increased from 305 to 335 K, the % of removal of TB dye onto PBC, APBC & BPBC increased from 55.30 to 72.10, 59.23 to 75.00 & 57.20 to 74.30 respectively. It is found that higher temperature eased the sorption of TB dye onto all three adsorbents. These results can be explained by the swelling of the adsorbent at higher temperature which enhances the penetration of the additional adsorbate molecules (Rozada et.al., 2003).

Table-5.47 Effect of temperature of TB dye onto Adsorbents

[pH=4;Dose=30mg/50mL;CT =160min]

Initial		Qe			
Concentration (mg/L)	Temperature (K)	PBC	APBC	ВРВС	
	305	12.74	13.18	12.33	
20	315	13.15	13.59	12.74	
20	325	13.56	14.00	13.15	
	335	14.00	14.44	13.59	
	305	18.48	19.11	17.81	
30	315	19.15	19.78	18.48	
30	325	19.82	20.45	19.15	
	335	20.55	21.18	19.88	
	305	23.66	24.46	22.73	
40	315	24.69	25.49	23.76	
40	325	25.74	26.54	24.81	
	335	26.90	27.70	25.97	
	305	28.72	29.67	27.54	
50	315	30.13	31.08	28.95	
50	325	31.54	32.49	30.36	
	335	32.98	33.93	31.80	

Table–5.48 Effect of temperature of TB dye onto Adsorbents PBC, APBC & BPBC

[pH:2, Dose:30mg/50mL, CT:140min]

Initial Concentration	Temperature (K)	Qe			
(mg/L)	Temperature (K)	PBC	APBC	ВРВС	
	305	6.80	7.24	7.02	
10	315	6.93	7.37	7.15	
10	325	7.06	7.50	7.28	
	335	7.21	7.65	7.43	
	305	9.62	10.22	9.93	
15	315	9.84	10.44	10.15	
13	325	10.09	10.69	10.40	
	335	10.39	10.99	10.70	
	305	11.82	12.76	12.30	
20	315	12.15	13.09	12.63	
20	325	12.52	13.46	13.00	
	335	12.95	13.89	13.43	
	305	13.83	14.81	14.30	
25	315	13.96	14.94	14.43	
23	325	14.09	15.07	14.56	
	335	14.24	15.22	14.71	

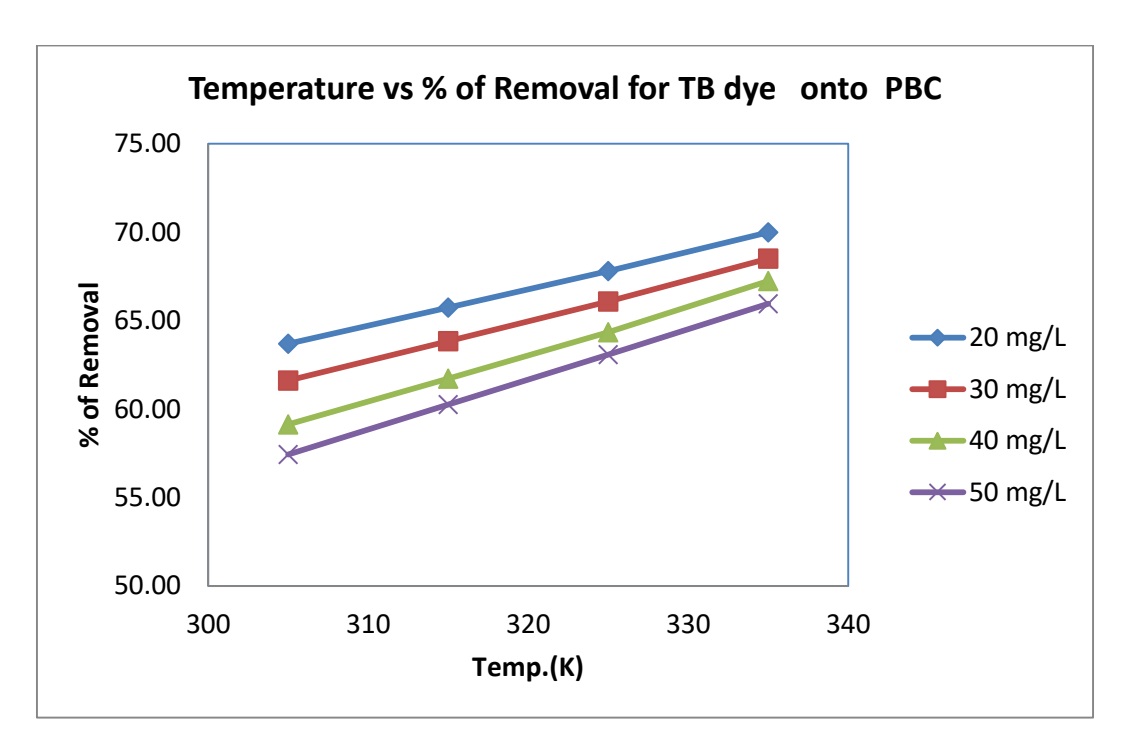


Figure 5.103

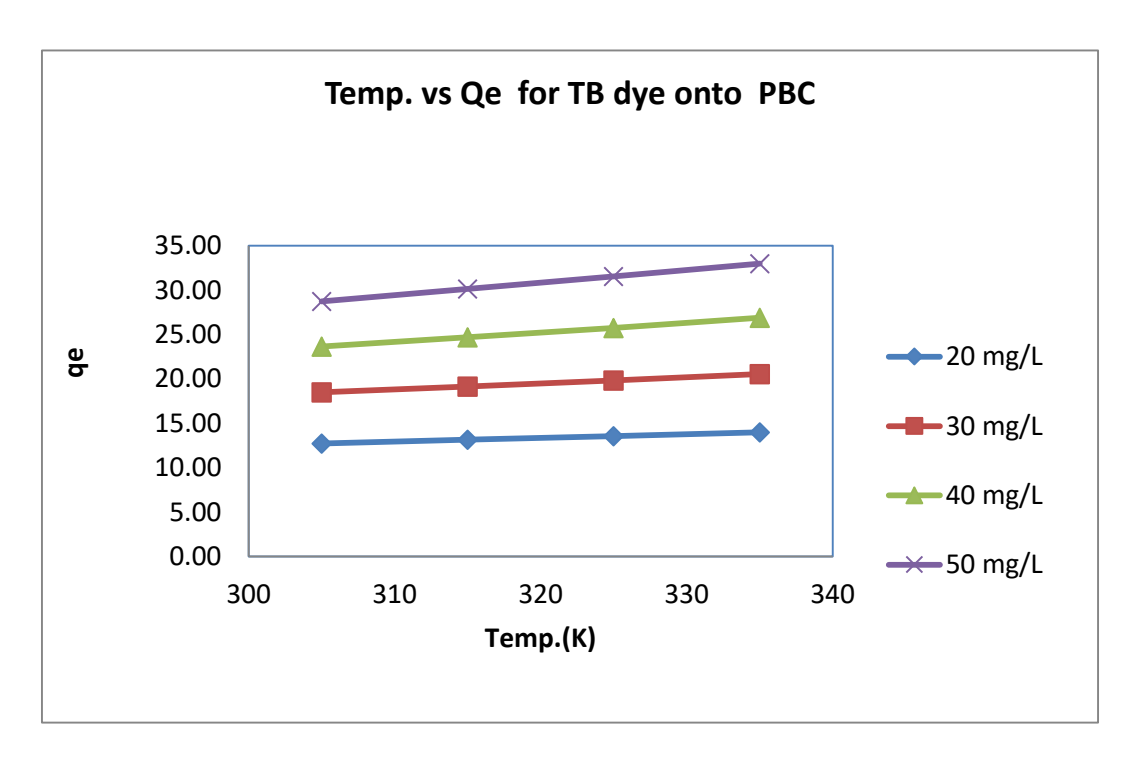


Figure 5.104

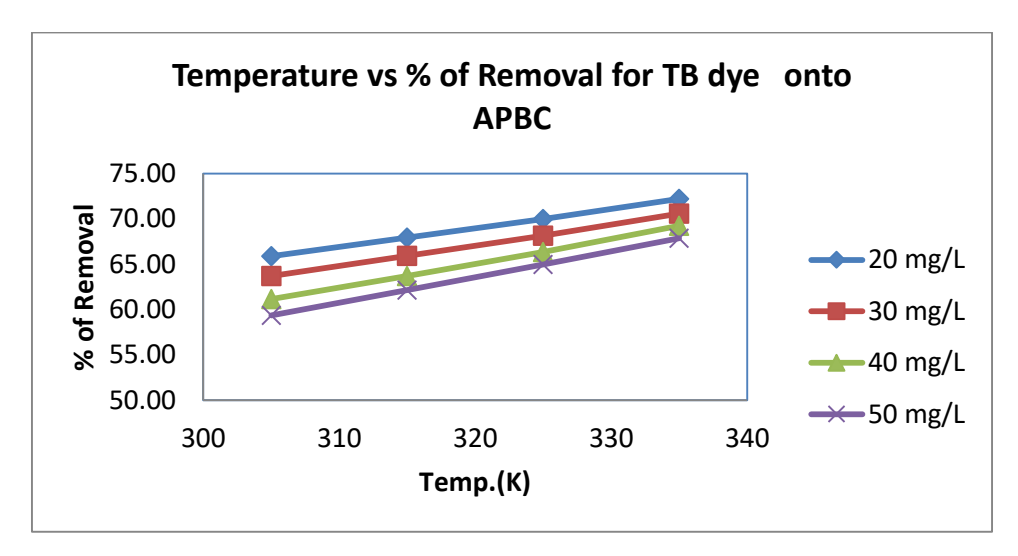


Figure 5.105

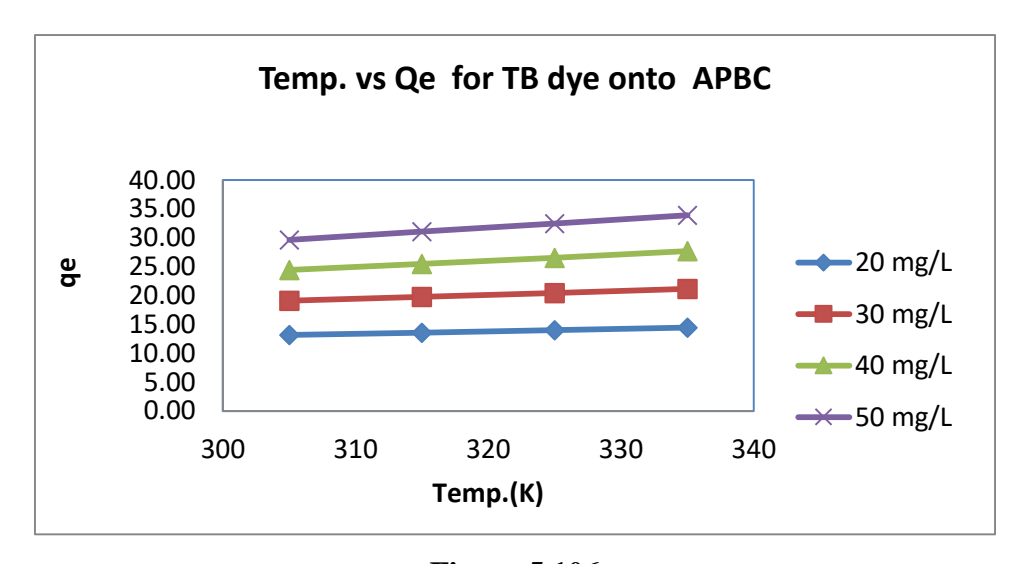


Figure 5.106

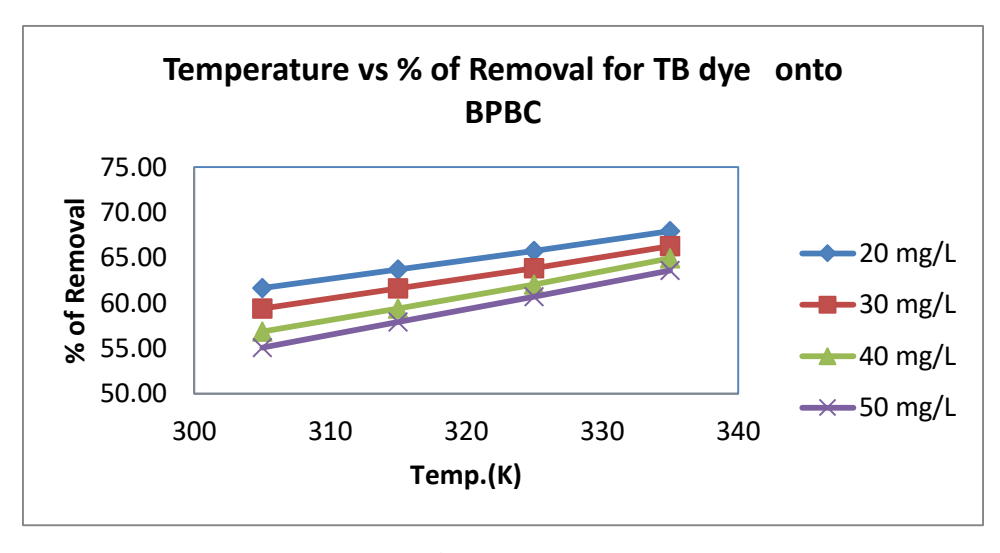


Figure 5.107

5.3.6 Isotherm studies

For solid–liquid adsorption system, adsorption isotherm is important model in the description of adsorption behavior. Adsorption isotherm relates the distribution of adsorbate molecules between the solid phase and the liquid phase at equilibrium state at a particular temperature (Abechiet.al., 2011). Identifying the most appropriate adsorption isotherm model would be helpful to understand the adsorption behavior. In this present study, Langmuir, Freundlich, Temkin and Dubinin Radushkevich isotherm were employed to investigate the adsorption behavior. Adsorption isotherm was studied at four different temperatures viz. 305, 315, 325 and 335K.

5.3.6.1 Langmuir isotherm

Langmuir isotherm plots were drawn between C_e/q_e and C_e which are shown in figures 5.108 to 5.110. The regression coefficient (R^2) values were ranged from 0.9840 to 0.9990 for the four studied temperatures viz.305, 315, 325 and 335Kwhich confirmed the best fitting of the equilibrium data with Temkin isotherms. The value of monolayer adsorption capacity (Q_0) and energy of adsorption (b) determined from this Langmuir isotherm are summarized in table 5.49.

The monolayer adsorption capacity Q0 values (mg/g) for adsorption of TB dye onto PBC APBC and BPBC were ranged from 21.739 to 23.810, 22.222 to 23.810 and 21.739 to 23.810 respectively. The adsorption capacity increased with the increase of temperature.

The values of Langmuir constant 'b' (L/mg) the adsorption energy for adsorption of TB dye onto PBC, APBC and BPBC were ranged from 0.126 to 0.165, 0.152 to 0.242 and 0.141 to 0.219 respectively. These values indicate that the apparent energy of

sorption is less and ruled out the possibility of strong interaction between the solute and adsorption site.

The order of monolayer adsorption capacity of the three adsorbents namely PBC, APBC and BPBC are in following order for the adsorption of TB dye for all the at studied temperatures.

Table - 5.49 Langmuir isotherm results for TB dye onto adsorbents [TBdye, pH=2;Dose=40mg/50mL]

Adsorbents	Temperature (K)	Q0 (mg/g)	b (L/mg)	R ²
	305	80.645	0.026	0.996
PBC	315	92.593	0.024	0.9949
PBC	325	108.696	0.022	0.9945
	335	126.582	0.021	0.9978
	305	79.365	0.029	0.9961
APBC	315	90.090	0.028	0.9951
AFBC	325	104.167	0.026	0.9946
	335	119.048	0.025	0.9975
	305	75.188	0.025	0.9958
BPBC	315	86.957	0.023	0.9945
	325	101.010	0.022	0.9936
	335	117.647	0.020	0.9965

The dimensionless separation factor RLvalues calculated for various initial concentrations at different temperatures were lie between 0 and 1 which indicate the favorable adsorption for all the two systems. These RLvalues are presented in table 5.50.

Table-5.50 Dimensionless separation factor (R_L)

A daawhamta	Temperature (K)					
Adsorbents	305	315	325	335		
PBC	0.500	0.483	0.466	0.442		
APBC	0.573	0.553	0.531	0.504		
BPBC	0.521	0.507	0.490	0.469		

The difference may be due to the following factors such pore volume, pore shape and surface characteristics of the adsorbents. In general Langmuir constant values infer a better performance of prepared adsorbents PBC, APBC & BPBC.

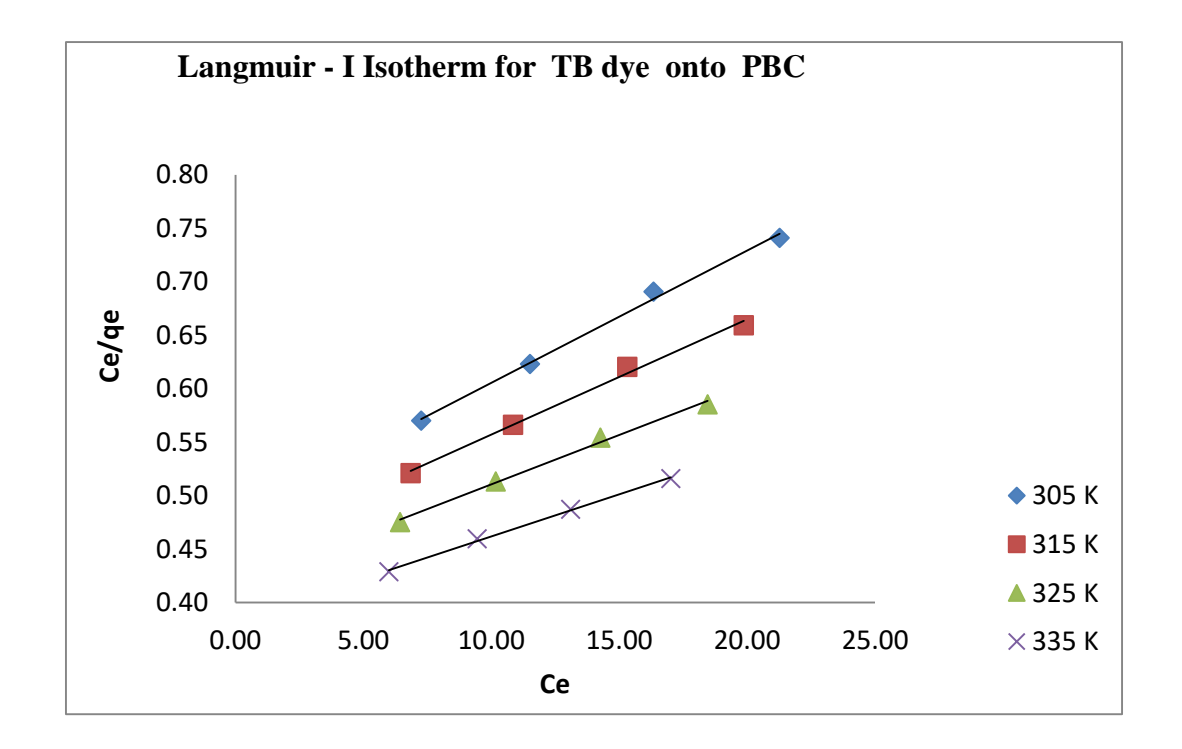


Figure 5.108

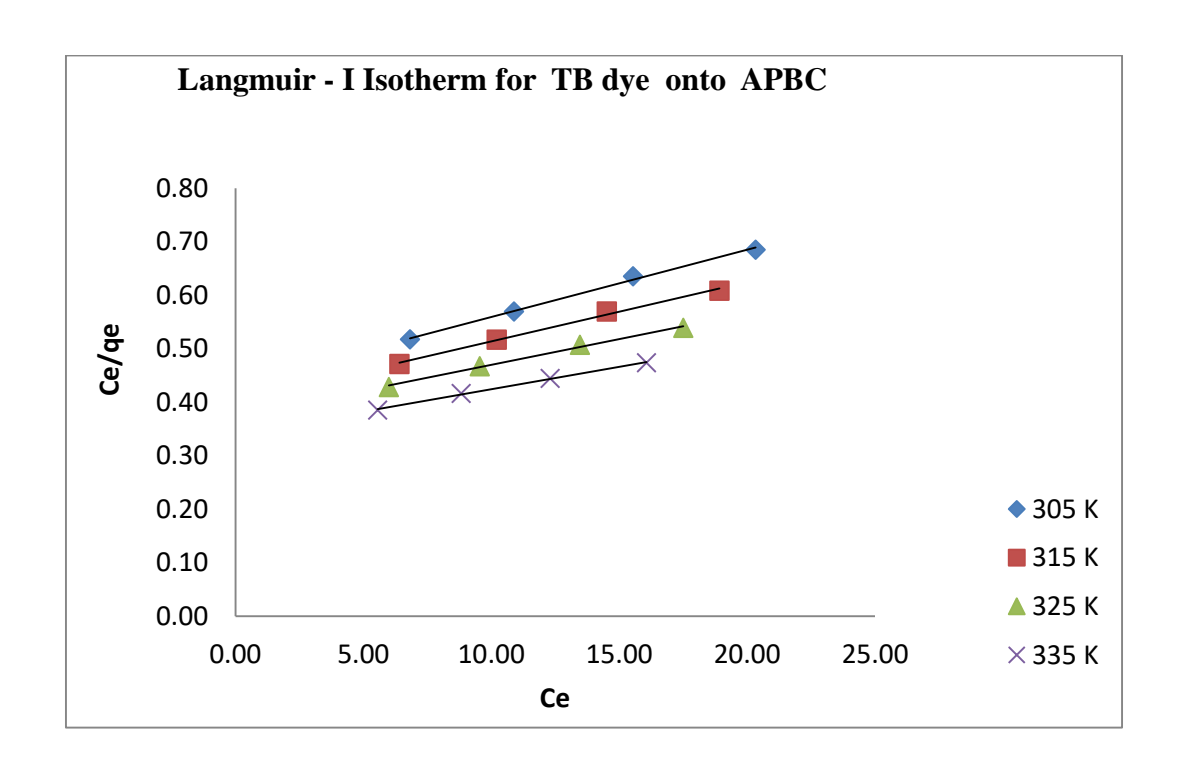


Figure 5.109

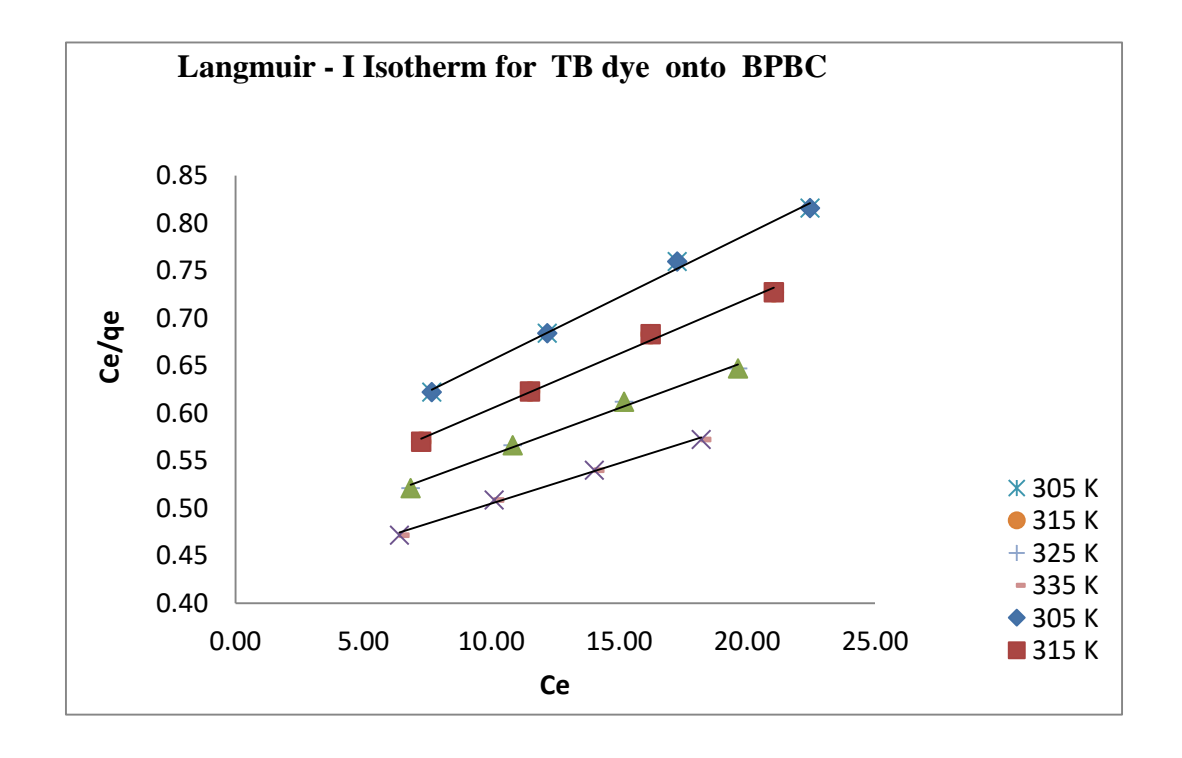


Figure 5.110

5.3.6.2 Freundlich isotherm

Freundlich isotherm plots were drawn between log q_e and log Ce which are shown in figures 5.111 to 5.113. The regression coefficient (R^2) values were ranged from 0.9470 to 0.9940 for the four studied temperatures viz.305, 315, 325 and 335Kwhich revealed the best fitting of the equilibrium data with Temkin isotherms. The value of adsorption capacity (K_f) and intensity of adsorption (n) determined from this Freundlich isotherm are summarized in table 5.51.

Adsorption capacity Kf (mg/g) for TB dye onto PBC, APBC and BPBC were ranged from 3.5975 to 4.4978, 4.2073 to 5.2966 and 3.8994 to 4.8978 respectively. Adsorption capacities of the three adsorbents were in the following order for all the studied temperatures.

It can be understood from the Kf (mg/g) at a particular temperature. These values are given in table 5.52

The adsorption intensity (n) values are ranged from 1.7730 to 2.0367 for all the studied systems. These low values indicate the favorable physical adsorption. Further it is observed that 'n' value increased with the increase of temperature .

 $Table-5.51\ Freundlich\ is other m\ results\ for\ TB\ dye\ onto\ adsorbents$ $[TB\ dye,\ pH=2;Dose=40mg/50mL]$

Adsorbents	Temperature (K)	n	Kf (mg/g)	R ²
	305	1.2137	3.2122	0.9997
PBC	315	1.2489	3.0662	0.9997
PBC	325	1.2877	2.9703	0.9994
	335	1.3270	2.8847	0.9990
	305	1.2395	3.6350	0.9997
APBC	315	1.2740	3.4483	0.9997
AFBC	325	1.3122	3.3212	0.9994
	335	1.3506	3.2092	0.9990
	305	1.2249	2.9923	0.9998
ВРВС	315	1.2607	2.8695	0.9998
врвс	325	1.3006	2.7906	0.9995
	335	1.3414	2.7214	0.9991

Table–5.52 Adsorption capacity Kf (mg/g) values for various adsorbents

Temperature (K)	PBC	APBC	ВРВС
305	3.2122	3.6350	2.9923
315	3.0662	3.4483	2.8695
325	2.9703	3.3212	2.7906
335	2.8847	3.2092	2.7214

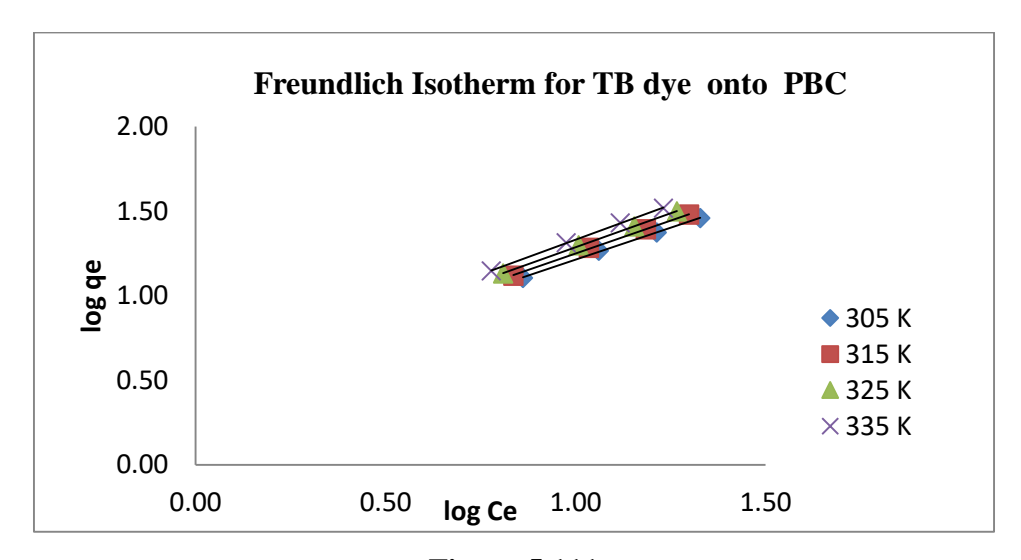


Figure 5.111

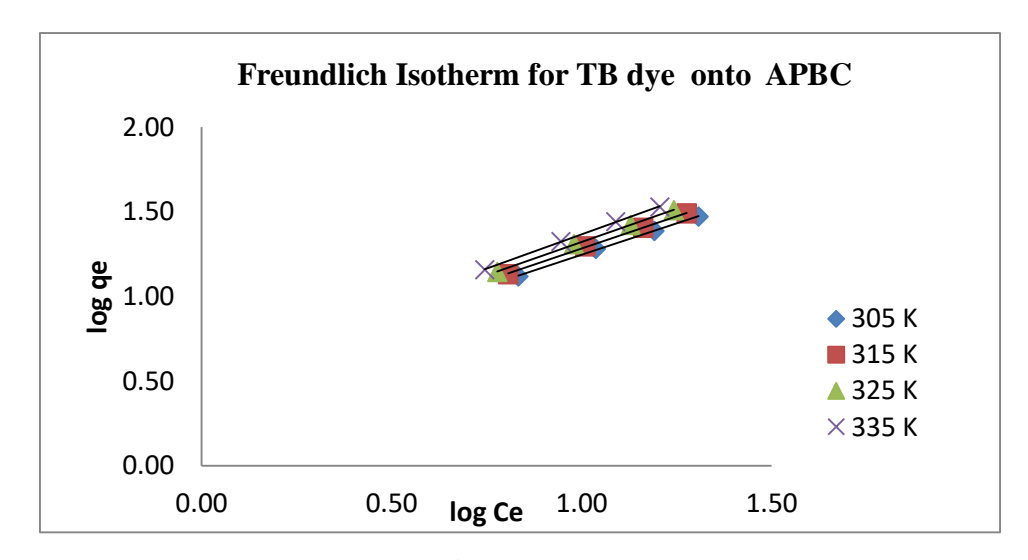


Figure 5.112

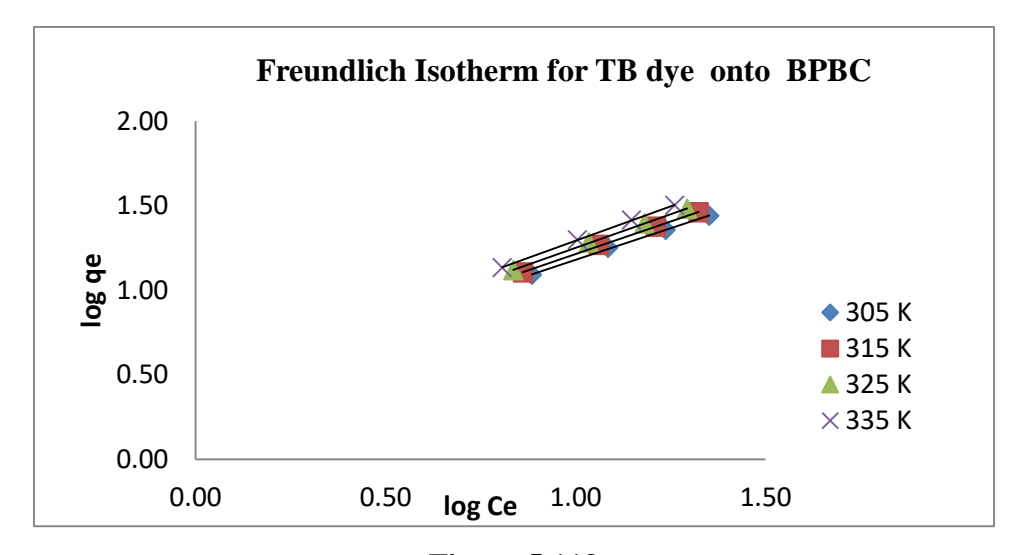


Figure 5.113

5.3.6.3 Temkin isotherm

Temkin plots were drawn between qe and lnCe which were shown in figures 5.114 to 5.116. The regression coefficient (R²) values were ranged from 0.9740 to 0.9990 for the four studied temperatures viz.305, 315, 325 and 335Kwhich revealed the best fitting of the equilibrium data with Temkin isotherms. The Equilibrium binding constant aT values (L/g) and heat of sorption constant bT values determined from Temkin isotherm are summarized in table 5.53.

Equilibrium binding constant aT values (L/g) onto PBC, APBC & BPBC were ranged from 1.051 to 1.474, 1.242 to 1.827 and 1.145 to 1.645 respectively. The heat of sorption constant bT values are ranged from 455.9917 J/mg to 524.8144 J/mg for PBC, 436.5995 to 510.2950 for ABPC and 446.5956 J/mg to 518.2713 J/mg for BPBC for the four studied temperatures viz. 305, 315, 325 and 335 K. These lower values of aT and bT indicate the physisorption nature rather than chemisorption.

Table – 5.53 Tempkin isotherm results for TB dye onto adsorbents [TB dye, pH=2;Dose=40mg/50mL]

Adsorbents	Temperature (K)	bT (J/mg)	a _T (L/g)	\mathbb{R}^2
	305	140.315	0.348	0.9882
PBC	315	155.140	0.334	0.9880
PBC	325	171.537	0.325	0.9895
	335	189.688	0.317	0.9912
	305	139.099	0.382	0.9886
APBC	315	153.440	0.365	0.9883
AFBC	325	169.270	0.353	0.9897
	335	186.712	0.344	0.9914
	305	146.475	0.329	0.9880
BPBC	315	162.202	0.317	0.9878
врвс	325	179.693	0.310	0.9894
	335	199.198	0.305	0.9912

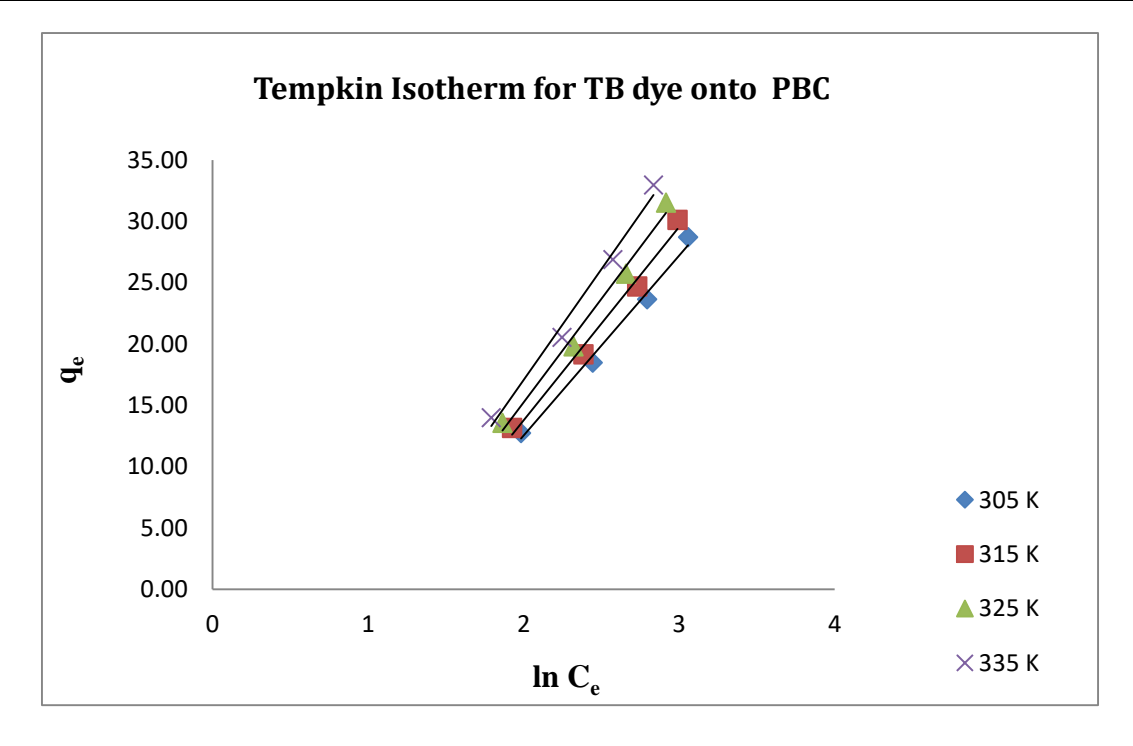


Figure 5.114

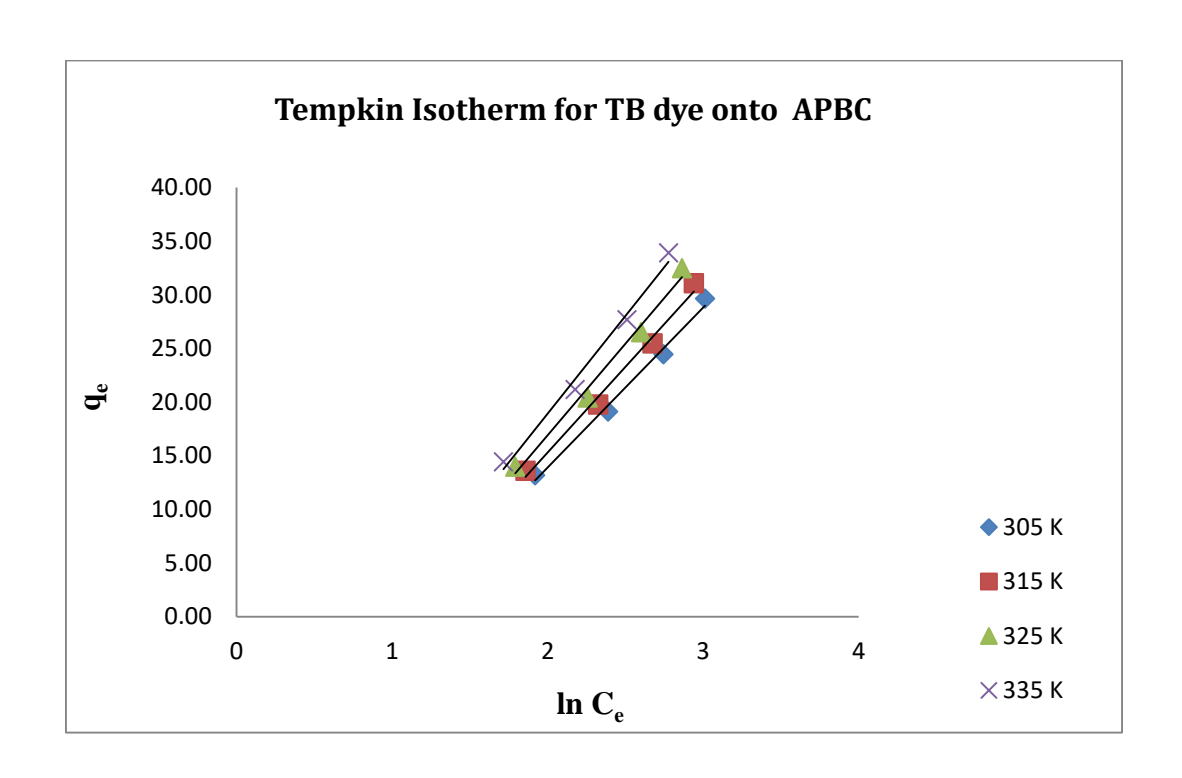


Figure 5.115

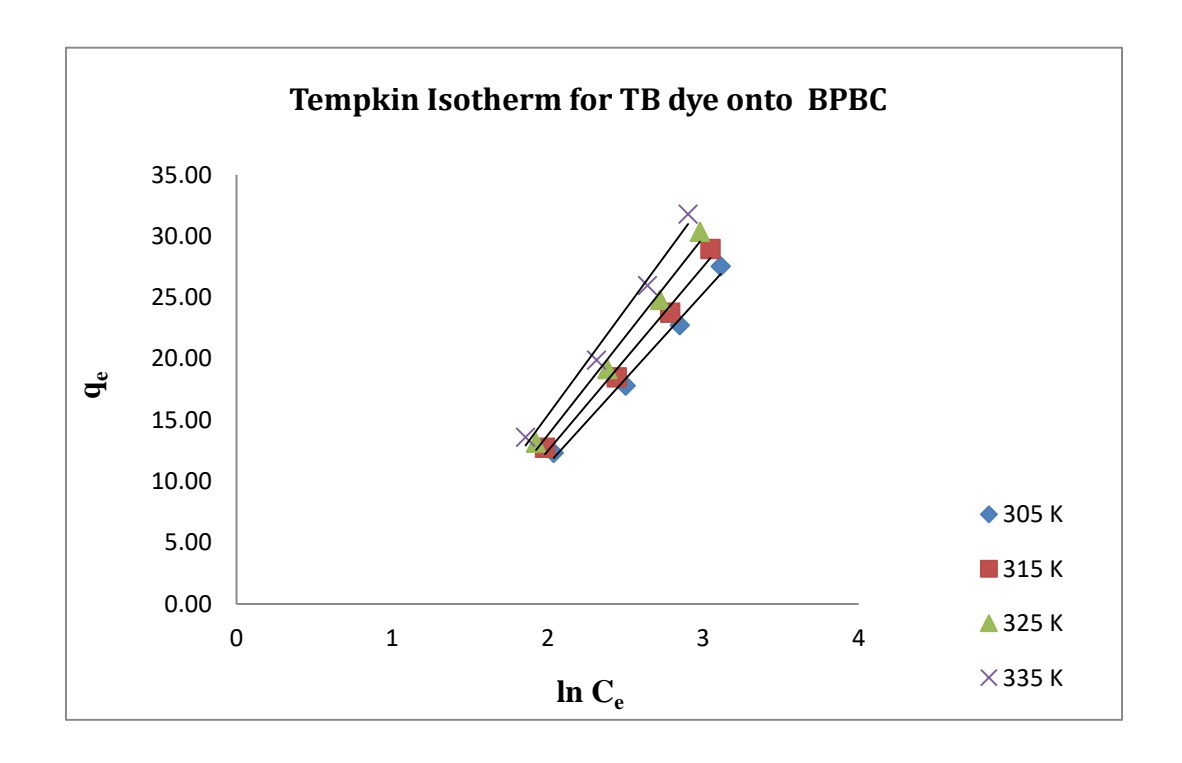


Figure 5.116

5.3.6.4 Dubinin–Radushkevich isotherm

Dubinin–Radushkevich isotherm (DRKplots were drawn between lnqe and $\epsilon 2$ (ϵ : RT ln (1+1/Ce) which were shown in figures 5.117 to 5.119. The regression coefficient (R2) values were ranged from 0.9830 to 0.9870, 0.9720 to 0.9770 and 0.9790 to 0.9830 for the four studied temperatures viz.305, 315, 325 and 335K respectively which revealed the best fitting of the equilibrium data with DRK isotherms. The theoretical saturation capacity q_D values (mg/g) and mean adsorption energy (kJ/mol) values determined are summarized in table 5.54.

The theoretical saturation capacity qD values (mg/g) were ranged from 12.8911 to 14.3467, 13.7600 to 15.2000 and 13.3636 to 14.8280 for PBC, ABPC and BPBC respectively. ABPC found to have a higher saturation adsorption capacity when compared to PBC and BPBC with all the studied temperatures. It is noticed that adsorption capacity increased with an increase in temperature.

The order of theoretical adsorption capacities the adsorbents are in the following order

The values of mean adsorption energy were ranged from 0.6254 kJ/mol to 0.6127 kJ/mol, 0.6176 to 0.6061 and 0.6210 to 0.6089 for PBC, ABPC and BPBC respectively. These values of E are lesser than 8kJ/mol indicate that the adsorption were physisorption (Sivakumar et.al., 2009).

 $Table-5.54\ Dubinin-Radushkevich\ isotherm\ results for\ TB\ dye\ onto\ adsorbents$ $[TB\ dye,\ pH=2;Dose=40mg/50mL]$

Adsorbents	Temperature (K)	Qd (mg/g)	E (J/mol)	В	R ²
	305	29.2357	0.5443	3.3760	0.9456
PBC	315	30.7467	0.5402	3.4264	0.9439
rbc	325	32.3131	0.5364	3.4761	0.9425
	335	34.0444	0.5324	3.5283	0.9437
	305	30.0688	0.5420	3.4041	0.9447
APBC	315	31.5659	0.5382	3.4527	0.9429
AIDC	325	33.1211	0.5345	3.5008	0.9416
	335	34.8886	0.5305	3.5528	0.9428
	305	27.9915	0.5478	3.3325	0.9448
ВРВС	315	29.4853	0.5436	3.3845	0.9428
	325	31.0308	0.5395	3.4356	0.9412
	335	32.7293	0.5354	3.4889	0.9422

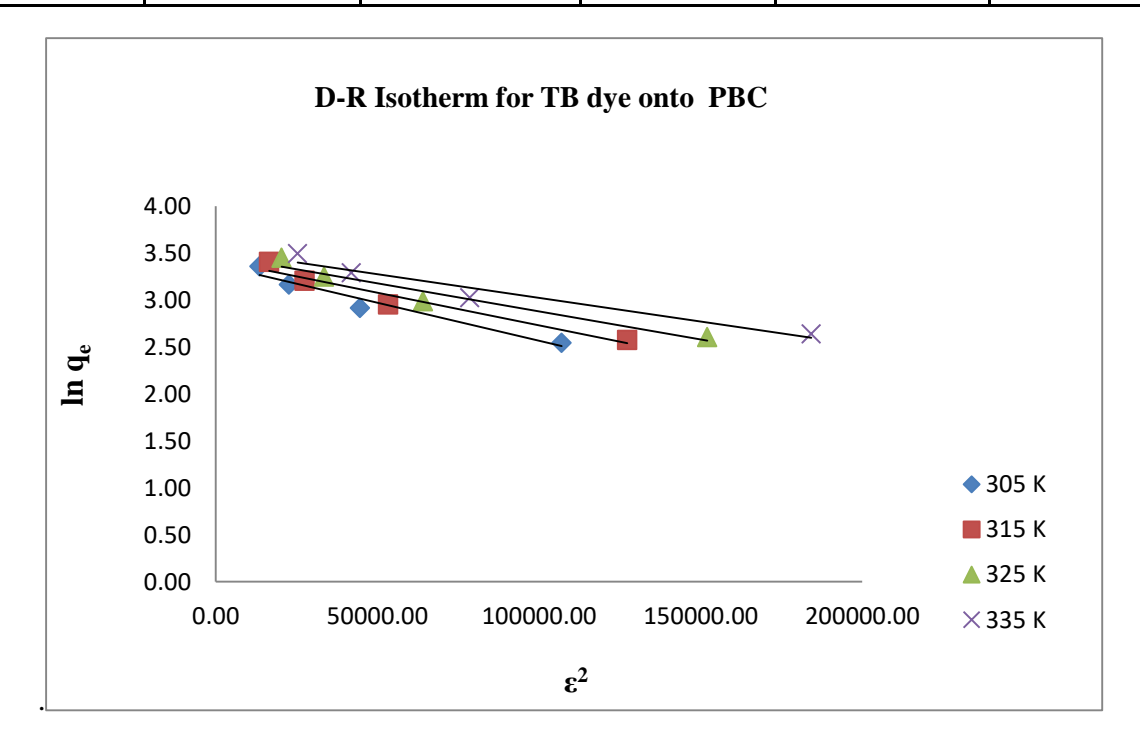


Figure 5.117

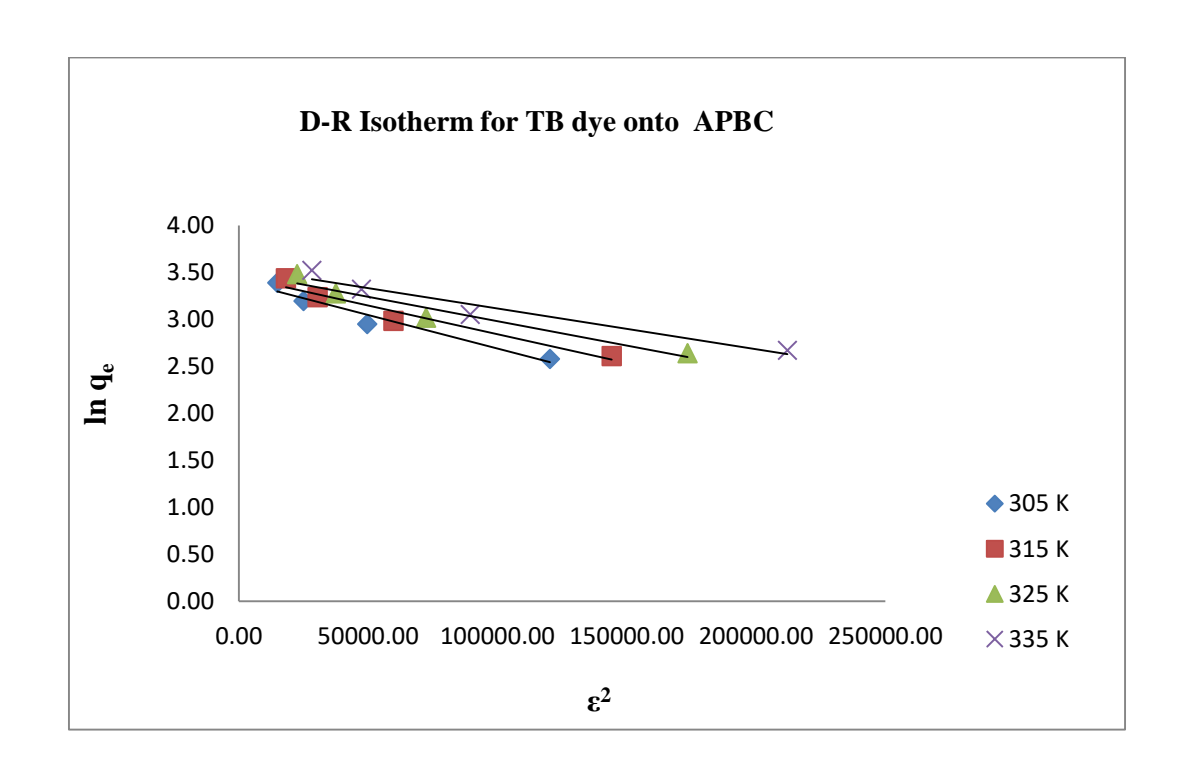


Figure 5.118

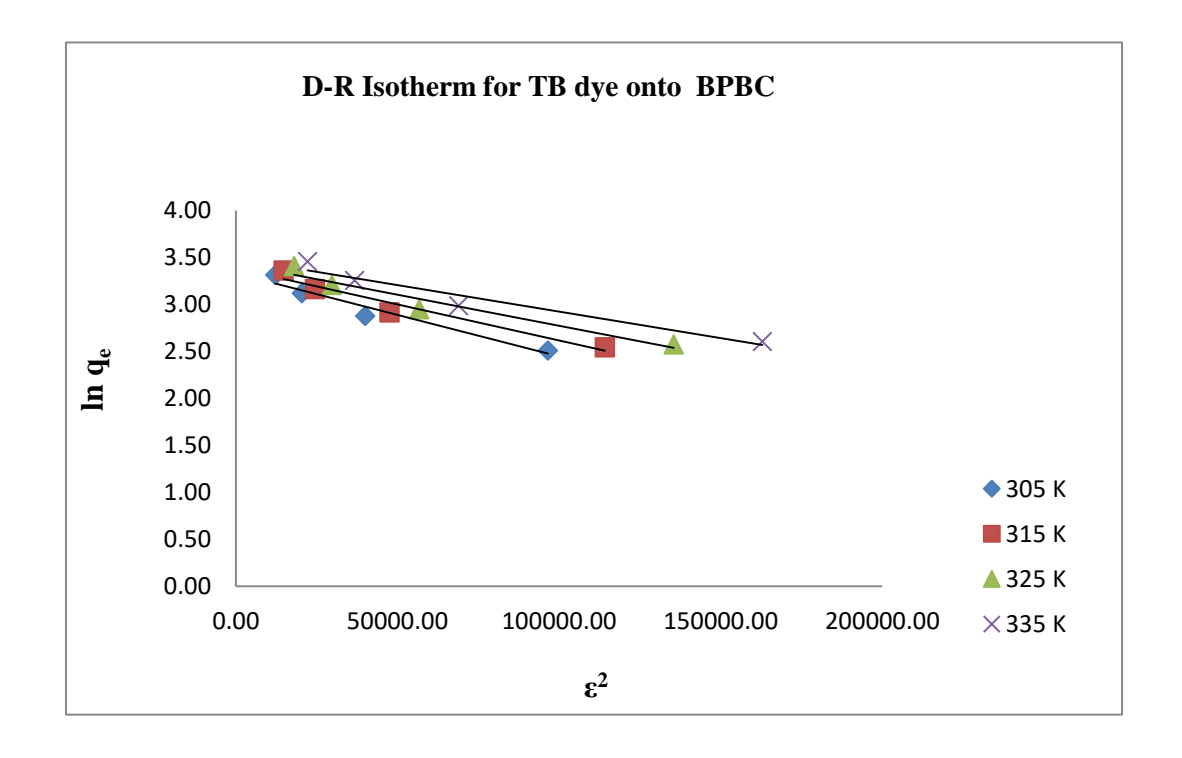


Figure 5.119

5.3.7 Adsorption Kinetics

5.3.7.1 Kinetic study for TB dye adsorption onto PBC, APBC and BPBC

The plots drawn for the Lagergren's pseudo first order kinetic models were shown in figure 5.120 to 5.122. The values of regression coefficient (R2) of the plots for pseudo first order kinetic model for ranged from 0.9340 to 0.9430, 0.9200 to 0.9420 and 0.9100 to 0.9420 for PBC, APBC and BPBC. This indicates that the best fitting of data in pseudo first order kinetic model. The pseudo first order rate constant k1 and the calculated adsorption capacity qe (cal) from pseudo first order kinetic modelwere given in table 5.55, 5.57, &5.59.

The plots drawn for the Ho's pseudo second order kinetic models were shown in figure 5.123 to 5.125. The values of regression coefficient (R2) of the plots for pseudo second order models were ranged from 0.9910 to 0.9940, 0.9910 to 0.9940and 0.9930 to 0.9940. This indicates that the best fitting of data in pseudo second order kinetic model. The regression coefficient values of pseudo second order were greater than the regression coefficient values of pseudo first order models. The pseudo second order rate constant k2 and the calculated adsorption capacity qe (cal) from pseudo second order kinetic model were given in table 5.56, 5.58 & 5.60.

The values of pseudo first order rate constant for PBC, APBC & BPBC k₁ranged from 0.0345 to 0.0392, 0.0345 to 0.0368 and 0.0345 to 0.0368 respectively and pseudo second order rate constant k2 values for PBC, APBC & BPBC ranged from 0.0085 to 0.0210, 0.0076 to 0.0211 and 0.0089 to 0.0211respectively. The pseudo second order initial sorption rate, 'h', increased with an increase of initial concentrations of TB dye at 305K temperature.

The difference between the calculated adsorption capacity qe (cal) obtained from pseudo first order equation and the experimental adsorption capacity qe (exp) were found to be large. Whereas the difference between the calculated adsorption capacity qe (cal) obtained from pseudo second order equation and the experimental adsorption capacity qe (exp) were found to be small. ((table 5.55-5.60).

Best fitting kinetic model is tested with a statistical tool 'Mean of sum of error squares' (MSSE). The MSSE of pseudo first order kinetic model is high when compared to pseudo second order kinetic model (table 5.55, 5.57, 5.59.). The lower MSSE values for pseudo second order kinetic model reflect the suitability of second order kinetic model rather than pseudo first order kinetic model for the adsorption of TB dye onto PBC, APBC & BPBC adsorption system.

Table - 5.55 Pseudo first order Kinetics results for TB dye ontoPBC [pH=2;Dose=40mg/50mL;Contacttime=120min;Temp=305K]

	Pseudo First OrderKinetics						
Concentration (mg/L)	k1×10 ⁻² (min ⁻¹)	qe (cal) (mg/g)	qe (exp) (mg/g)	Δqe	\mathbb{R}^2	MSSE	
20	0.0419	7.3909	12.74	5.347054	0.980		
30	0.0339	13.3229	18.48	5.160062	0.996	4.06	
40	0.0332	10.0485	23.66	13.60753	0.99	4.86	
50	0.0327	17.0020	28.72	11.718	0.994		

Table - 5.56 Pseudo second order Kinetics results for TB dye on to PBC [pH=2;Dose=40mg/50mL;Contacttime=120min;Temp=305K]

	Pseudo Second Order Kinetics					
Concentration (mg/L)	k2×10 ⁻³ (g/mg.min)	qe (cal) (mg/g)	Δqe	h	\mathbb{R}^2	MSSE
20	0.0138	13.35	-0.61313	2.47	0.996	
30	0.0083	19.46	-0.97225	3.13	0.994	0.62
40	0.0063	24.94	-1.28166	3.90	0.994	0.62
50	0.0046	30.49	-1.7678	4.26	O.992	

Table - 5.57 Pseudo first order Kinetics results for TB dye on to APBC [pH=2;Dose=40mg/50mL;Contacttime=120min;Temp=305K]

Concentration (mg/L)	Pseudo First Order Kinetics						
	k1×10 ⁻²	qe (cal) (mg/g)	qe (exp) (mg/g)	Δqe	\mathbb{R}^2	MSSE	
20	0.0417	7.3909	13.18	5.789054	0.981		
30	0.0339	1.3348	19.11	17.77525	0.996	((0	
40	0.0332	10.0693	24.46	14.38668	0.990	6.69	
50	0.0327	17.0451	29.67	12.62488	0.994		

Table - 5.58 Pseudo second order Kinetics results for TB dye onto APBC [pH=2;Dose=40mg/50mL;Contacttime=120min;Temp=305K]

Constant and	Pseudo First Order Kinetics					
Concentration (mg/L)	K2×10⁻² (g/mg.min)	qe (cal) (mg/g)	Δqe	h	\mathbb{R}^2	MSSE
20	0.0140	13.79	-0.6131	2.67	0.996	
30	0.0084	20.08	-0.97032	3.37	0.994	0.62
40	0.0063	25.77	-1.3172	4.21	0.994	0.02
50	0.0046	31.45	-1.77654	4.60	0.993	

Table - 5.59 Pseudo first order Kinetics results for TB dye onto BPBC [pH=2;Dose=40mg/50mL;Contacttime=120min;Temp=305K]

	Pseudo First Order Kinetics						
Concentration (mg/L)	k1×10 ⁻²	qe (cal) (mg/g)	qe (exp) (mg/g)	Δqe	R ²	MSSE	
20	0.0421	7.1978	12.33	5.130196	0.991		
30	0.0341	13.2587	17.81	4.555329	0.996	4.49	
40	0.0334	9.9609	22.73	12.77107	0.998	4.49	
50	0.0329	16.9200	27.54	10.61501	0.993		

Table - 5.60 Pseudo second order Kinetics results for TB dye on to BPBC [pH=2;Dose=40mg/50mL;Contacttime=120min;Temp=305K]

	Pseudo First Order Kinetics						
Concentration (mg/L)	K2×10 ⁻² (g/mg.min)	qe (cal) (mg/g)	Δqe	h	R ²	MSSE	
20	0.0144	12.92	-0.5919	2.40	0.996		
30	0.0082	18.80	-0.98299	2.90	0.993	0.62	
45	0.0062	24.04	-1.30646	3.57	0.993	0.02	
50	0.0045	29.33	-1.79051	3.88	0.992		

.

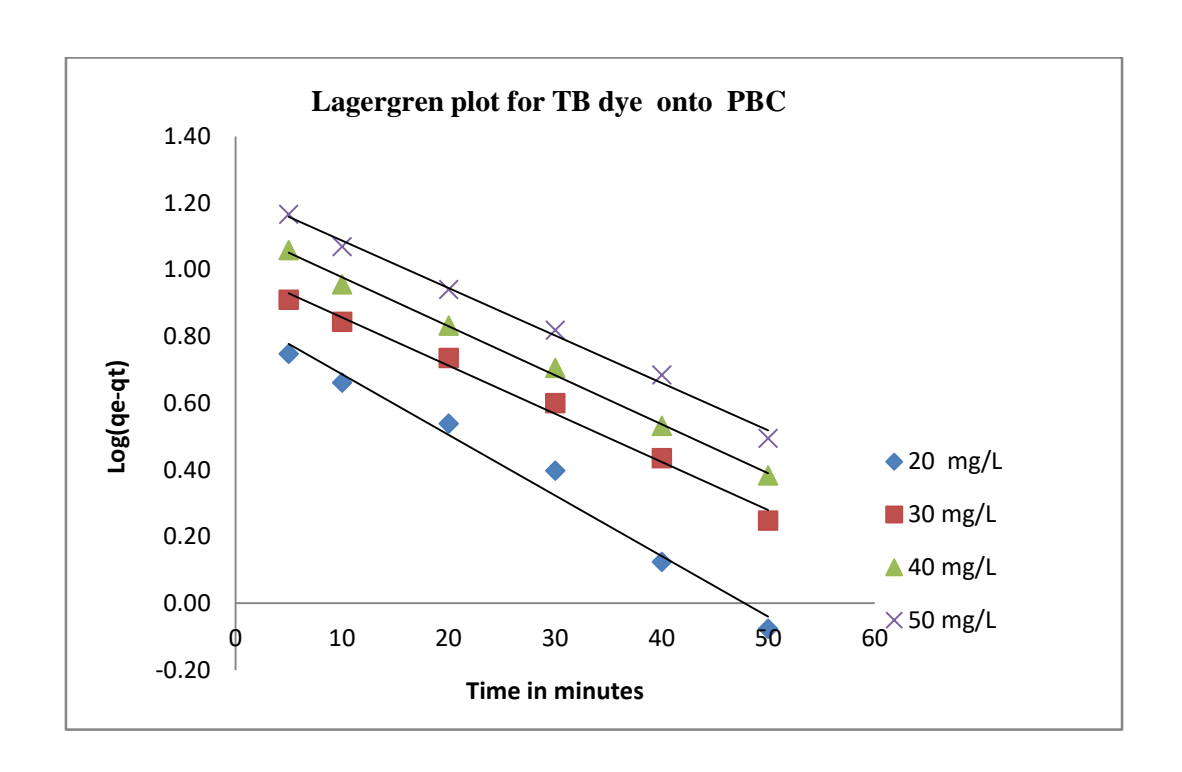


Figure 5.120

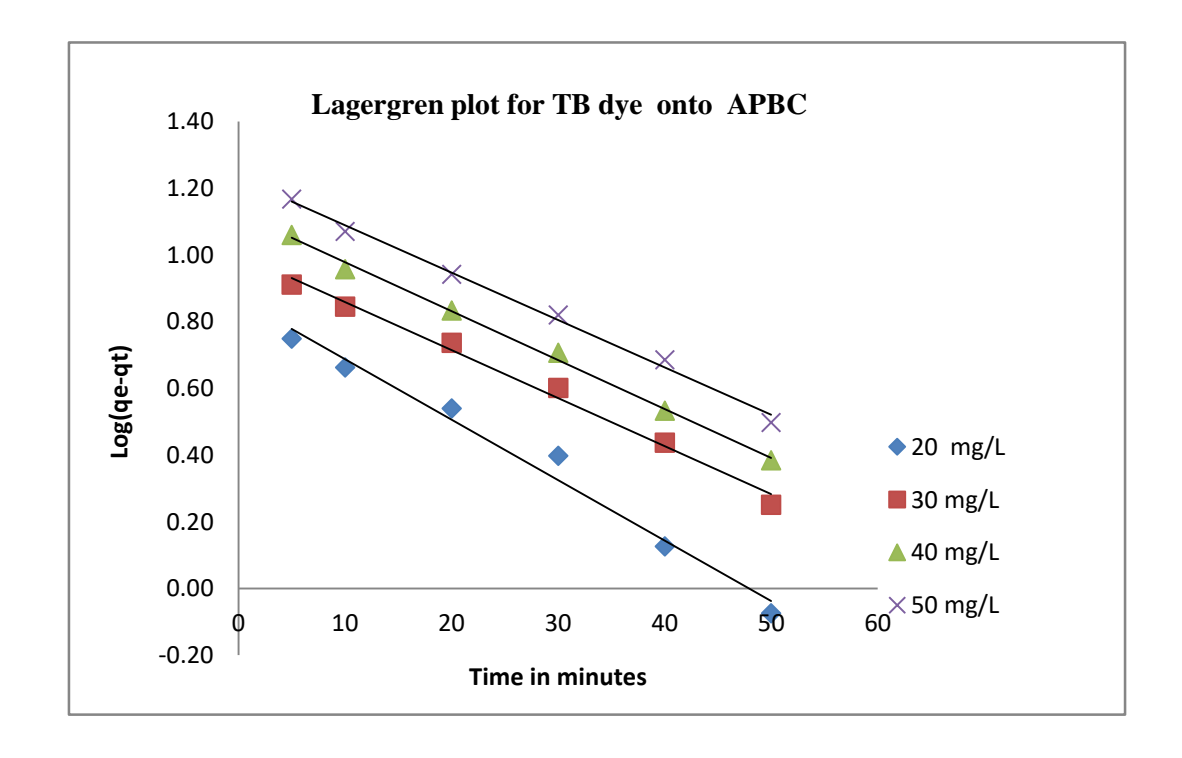


Figure 5.121

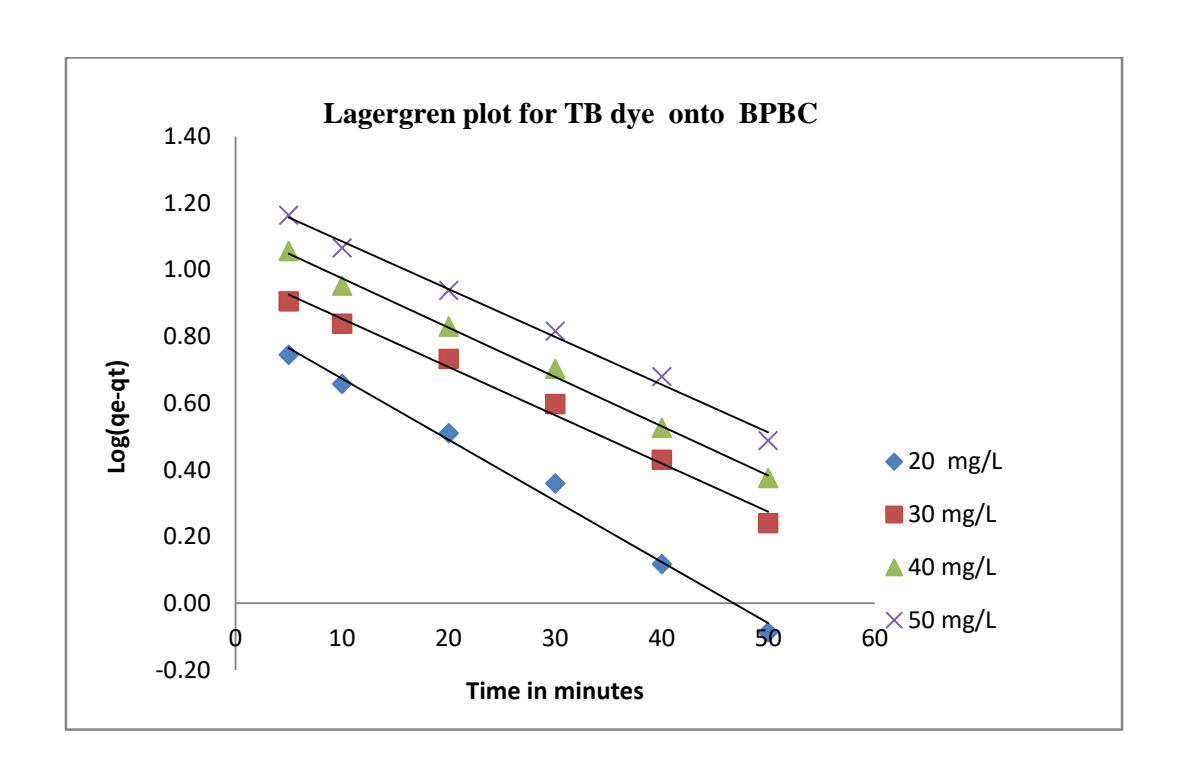


Figure 5.122

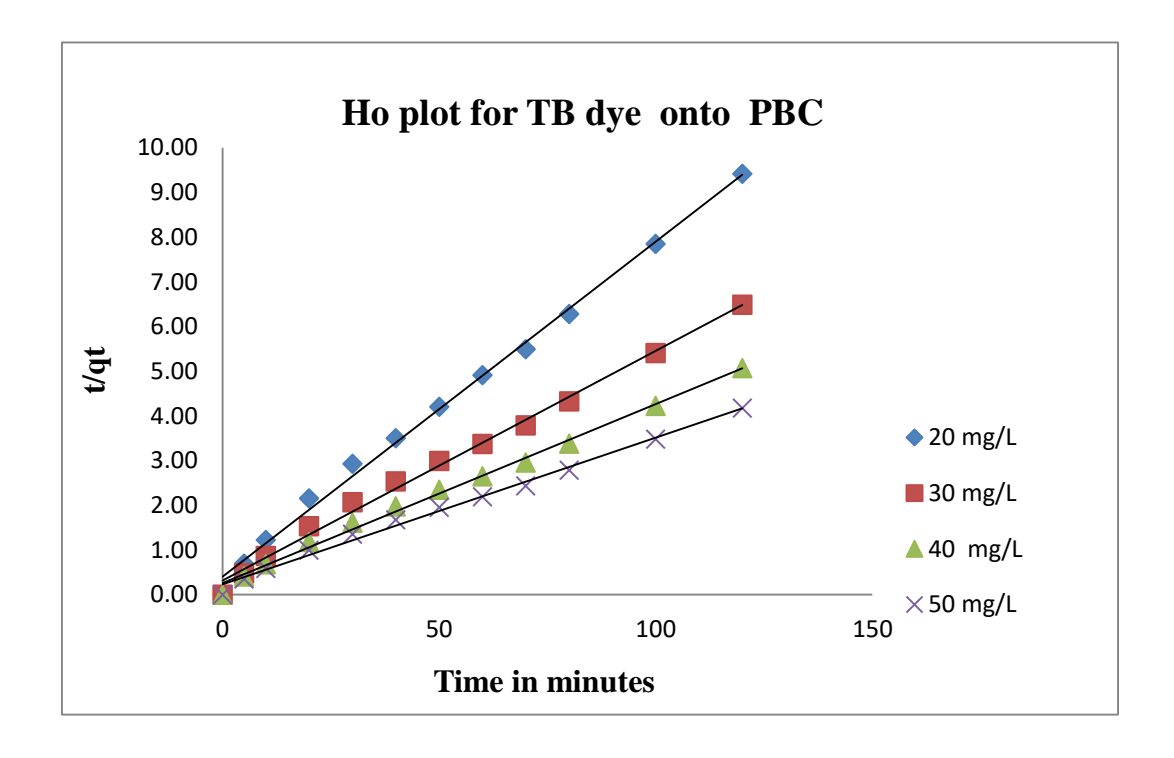


Figure 5.123

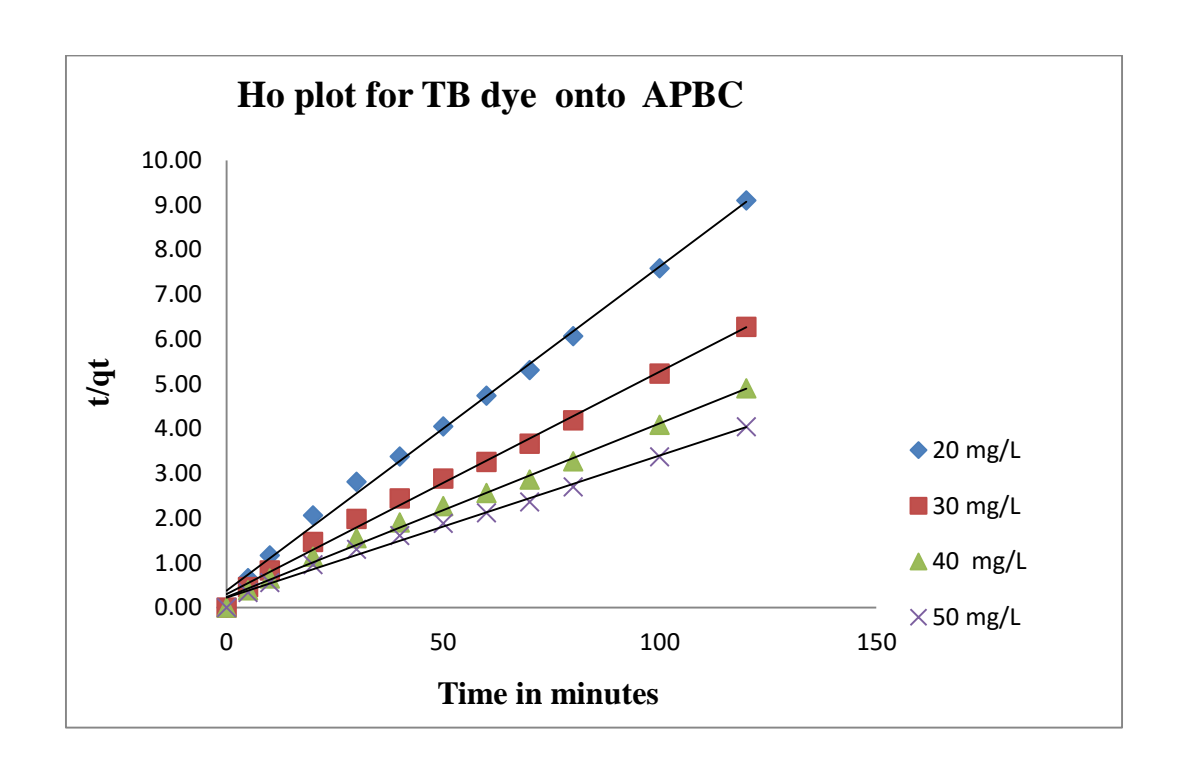


Figure 5.124

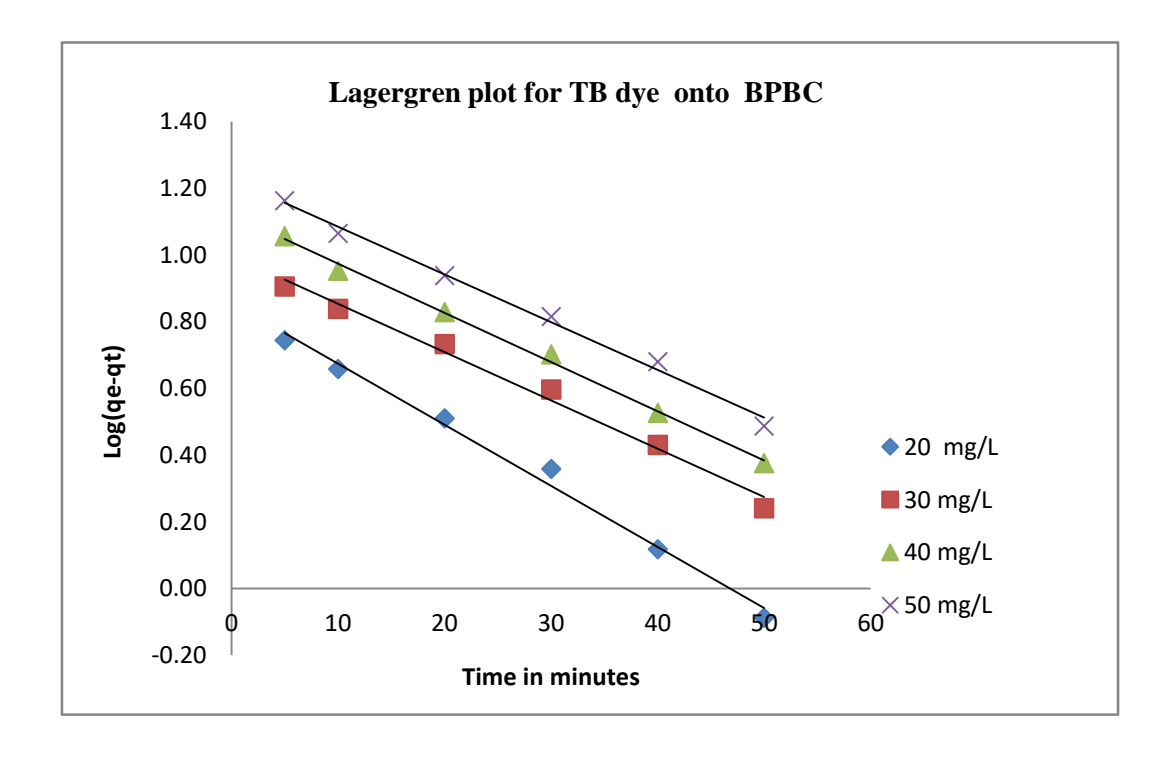


Figure 5.125

5.3.7.2 Intra particle diffusion

The plots for intraparticle diffusion kinetic model was drawn between mass of adsorbate adsorbed per unit mass of adsorbent (qt) versus $t^{0.5}$. It was noticed that the plot consist more than one phases. The initial portion of the plot indicates a boundary layer effect that is film diffusion while the other phases are due to intraparticle diffusion and instantaneous utilization of the most readily available adsorbing sites on the adsorbent surface. Representative Webber-Morris plot is shown in figure (5.126, 5.127, 5.128).

The slopes of the final linear portions of the plots are shown in figure 5.126 to 5.128. The of intra particle diffusion rate constant Kp was determined from the slope of the final linear portion. The values of K_p and R2 values are given in table 5.61.

The Kp values are found to increase with an increase of TB dye concentration that reveals the rate of adsorption governed by the diffusion of adsorbed TB dye within the pores of the adsorbent. Present results were showed that pore diffusion limits the overall rate of TB dye adsorption (Ahmad et.al., 2016, Rambabuet.al., 2020, Yusuff et.al., 2019).

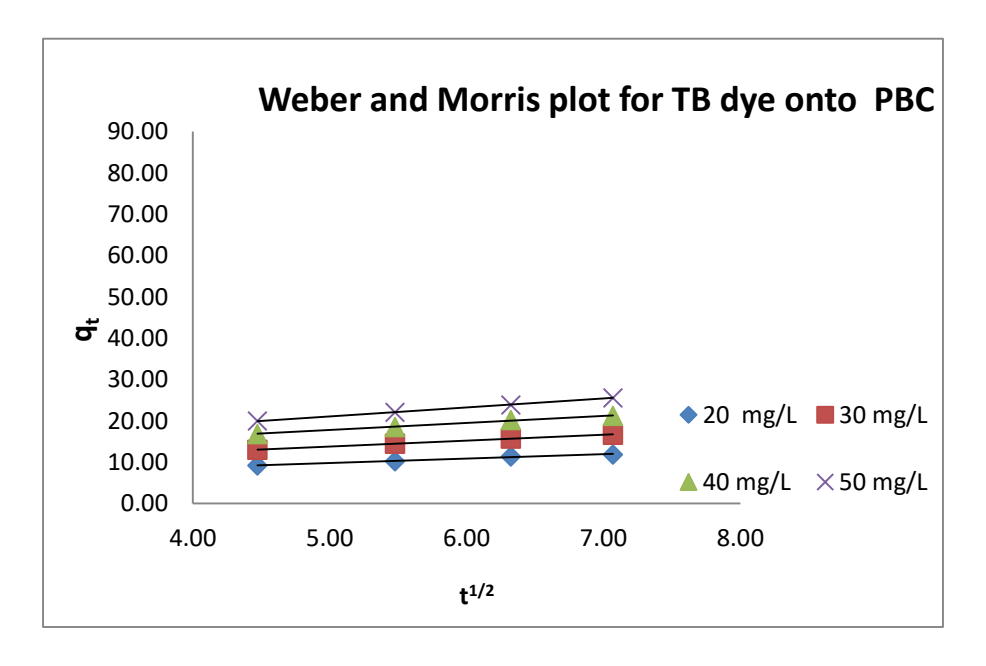


Figure 5.126

Table - 5.61 Intra Particle Diffusion results for adsorption of TB dye onto adsorbents

[pH=2;Dose=40mg/50mL;Contacttime= 120min;Temp=305K]

Ci		kp (mg/g.mi	n)	R ²		
(mg/L)	PBC	APBC	BPBC	PBC	APBC	BPBC
20	1.42	1.42	1.42	0.996	0.996	0.996
30	1.05	1.05	0.96	0.994	0.994	0.993
40	1.72	1.72	1.72	0.994	0.994	0.993
50	2.9310	3.2840	2.5680	0.9920	0.993	0.992

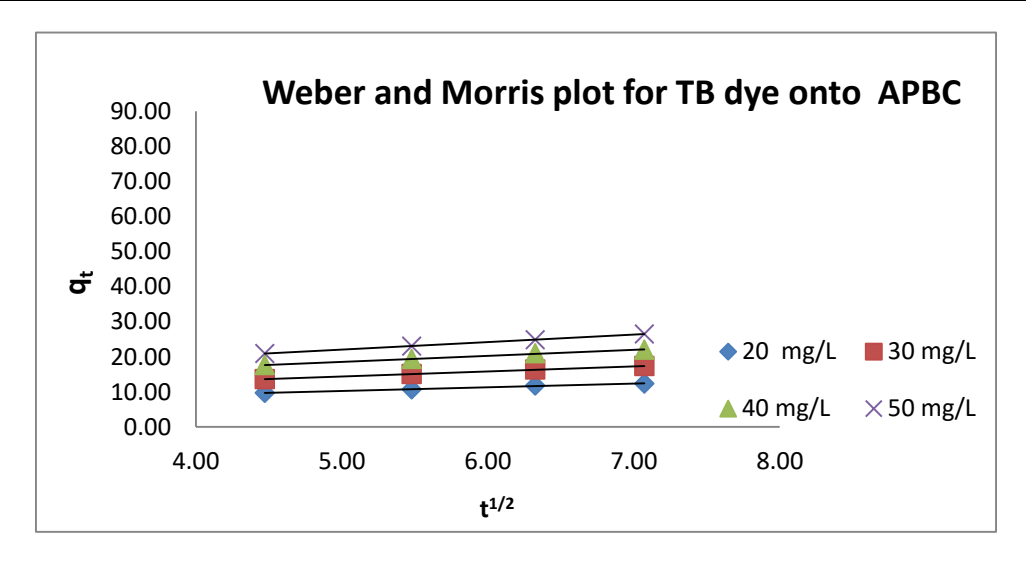


Figure 5.127

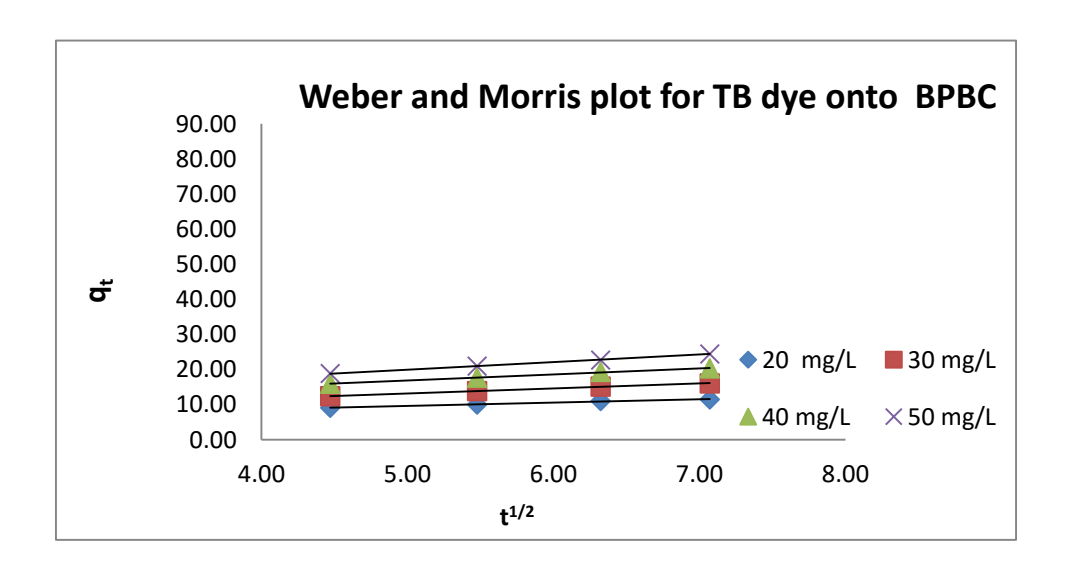


Figure 5.128

5.3.8 Thermodynamic studies

The Van't Hoff plots drawn for the chosen system at four different temperatures are shown in figures 5.129 to 5.131. The thermodynamic parameters calculated are presented in table 5.62.

The negative values of ΔG° (table 5.62) showed that the adsorptions of TB dye onto PBC, APBC & BPBC are highly favorable and spontaneous .

The positive values of ΔH° showed the endothermic nature of adsorption which is supported by the fact that the adsorption capacity of the adsorbent increased with an increase in temperature from 305 to 335K. The magnitudes of ΔH° values were within the range of 5.5022 to 7.5275 (kJ/mol). These values are lesser than 90 kJ which indicates the physisorption and ruled out the possibility of chemisorption (Yao et.al., 2010).

The values of ΔS° of the present studied system ranged from 24.2686 to 29.1200. These positive values of ΔS° showed that the randomness at the solid solution interface. During adsorption some structural changes might have occured at the surface of the adsorbent. The adsorbed water molecules which are displaced by the adsorbate species, might have gained more translational entropy than is lost by the adsorbate molecules, thus allowing the prevalence of randomness in the system (Biswajit Das et.al., 2013).

This ΔS° values found to decrease with an increase of initial concentration of the adsorbates solution. While comparing the ΔS° values with respect to the adsorbents, the ΔS° values for the adsorption onto APBC were found to be high when compared to BPBC and PBC.

The enhancement of adsorption capacity of the adsorbents at higher temperatures was attributed to the enlargement of the size of the pore and the activation of the adsorbent surface (Krishna et.al., 2013).

Table 5.62 Thermodynamic Parameter results for adsorption of TB dye onto adsorbents

[pH=2;Dose =40mg/50mL]

Adsorbents			ΔG° kJ/mol				ΔS° (kJ/mol)
	(mg/L)	305K	315K	325K	335K	kJ/mol	(KJ/IIIOI)
	20	-1.43	-1.20	-0.94	-0.76	10.222	35.9605
PBC	30	-1.67	-1.48	-1.25	-1.09	10.092	36.0703
PBC	40	-1.95	-1.79	-1.58	-1.45	8.7862	32.6557
	50	-2.30	-2.19	-2.03	-1.84	7.3927	28.8404
	20	-1.67	-1.43	-1.15	-0.96	10.437	37.3099
APBC	30	-1.93	-1.72	-1.47	-1.30	10.333	37.5518
APBC	40	-2.23	-2.05	-1.82	-1.67	9.044	34.2395
	50	-2.60	-2.46	-2.29	-2.08	7.7127	30.692
	20	-1.20	-0.96	-0.70	-0.52	10.009	34.4649
DDD C	30	-1.44	-1.23	-0.99	-0.83	9.8695	34.5555
BPBC	40	-1.70	-1.52	-1.32	-1.18	8.5643	31.1517
	50	-2.03	-1.91	-1.75	-1.55	7.1436	27.2965

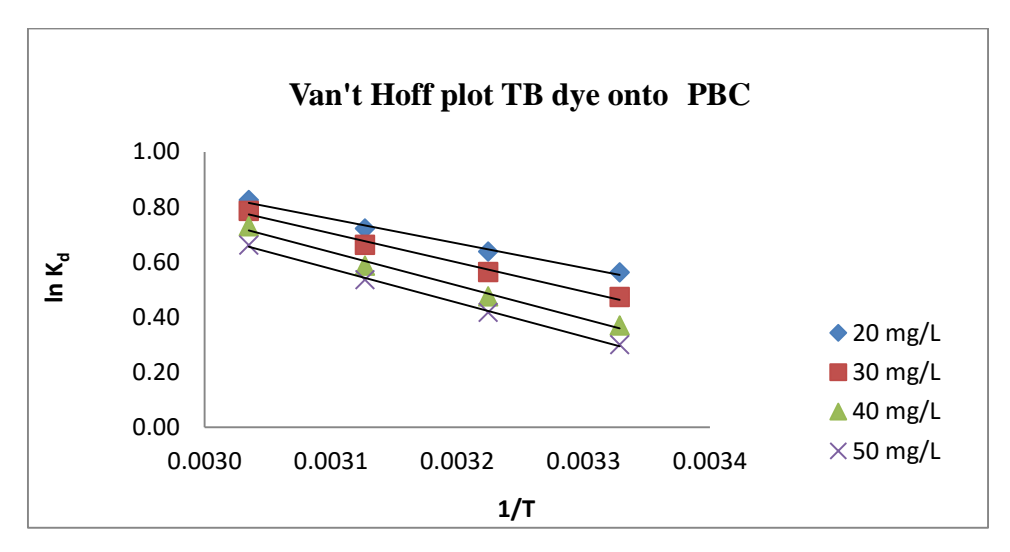


Figure 5.129

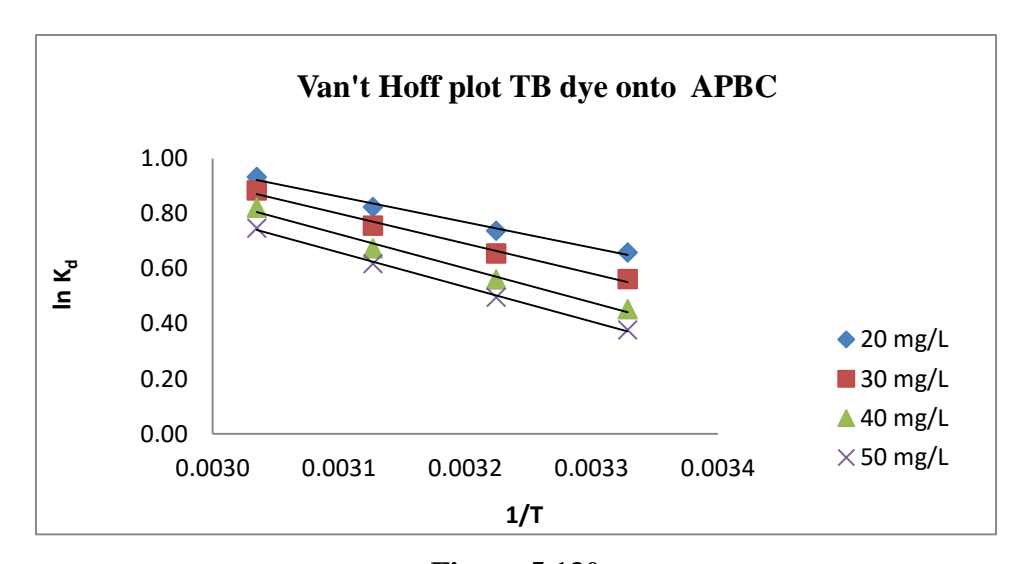


Figure 5.130

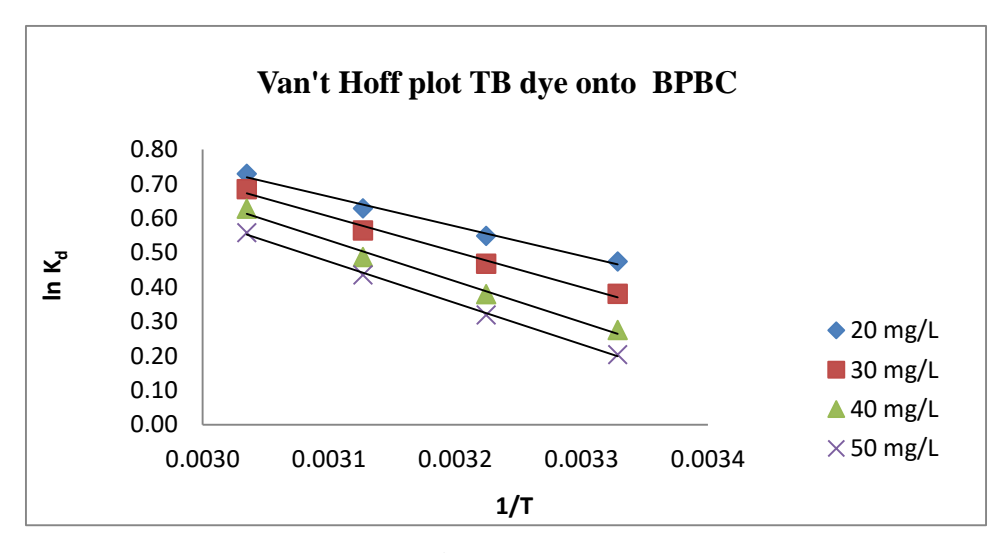


Figure 5.131

5.3.9 Desorption of TB dye

Result of desorption of TB dye from adsorbents loaded with TB dye is presented as column diagram in figure 5.132. The percentage of desorption was more for 0.1N NaOH solution when compared to other desorbing agents water and 0.1N HCl acid. This is due to fact that OH ions replaced the anionic form of TB dye (Bicarbonate) more effectively from the adsorbent through ion exchange process. According to Hemaet.al., 2007 the reversibility of adsorbed ions, supports the physisorption mechanism.

The maximum percentage of desorption is found to be 68 % which suggests that the some TB dye are strongly attached to adsorbent. This strong attachment might be due to chemisorption. Hence it may be concluded that TB dye were bound on the surface of the adsorbent both by physical force and chemical forces. The physical force is normally Vander wall's force. The chemical forces probably due to attachment between TB dye and the functional group present in the surface of the adsorbent.

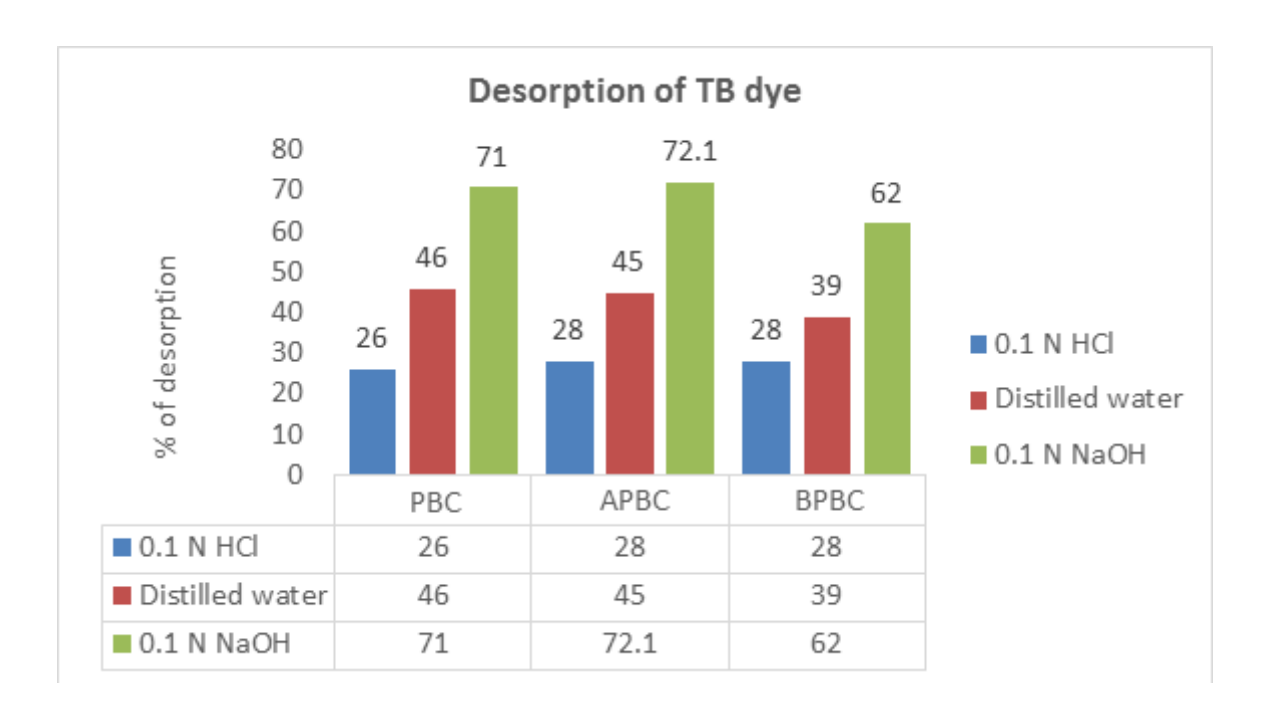


Figure 5.132

5.3.10 Morphological study

Changes in the morphology of adsorbent before and after adsorption were analyzed with FT-IR spectra.

5.3.10. FT-IR Study for the adsorption of Turquoise blue dye

The FT – IR spectrum of PBC, APBC and BPBC loaded with TB dye was shown in figure 5.133 to 5.135.

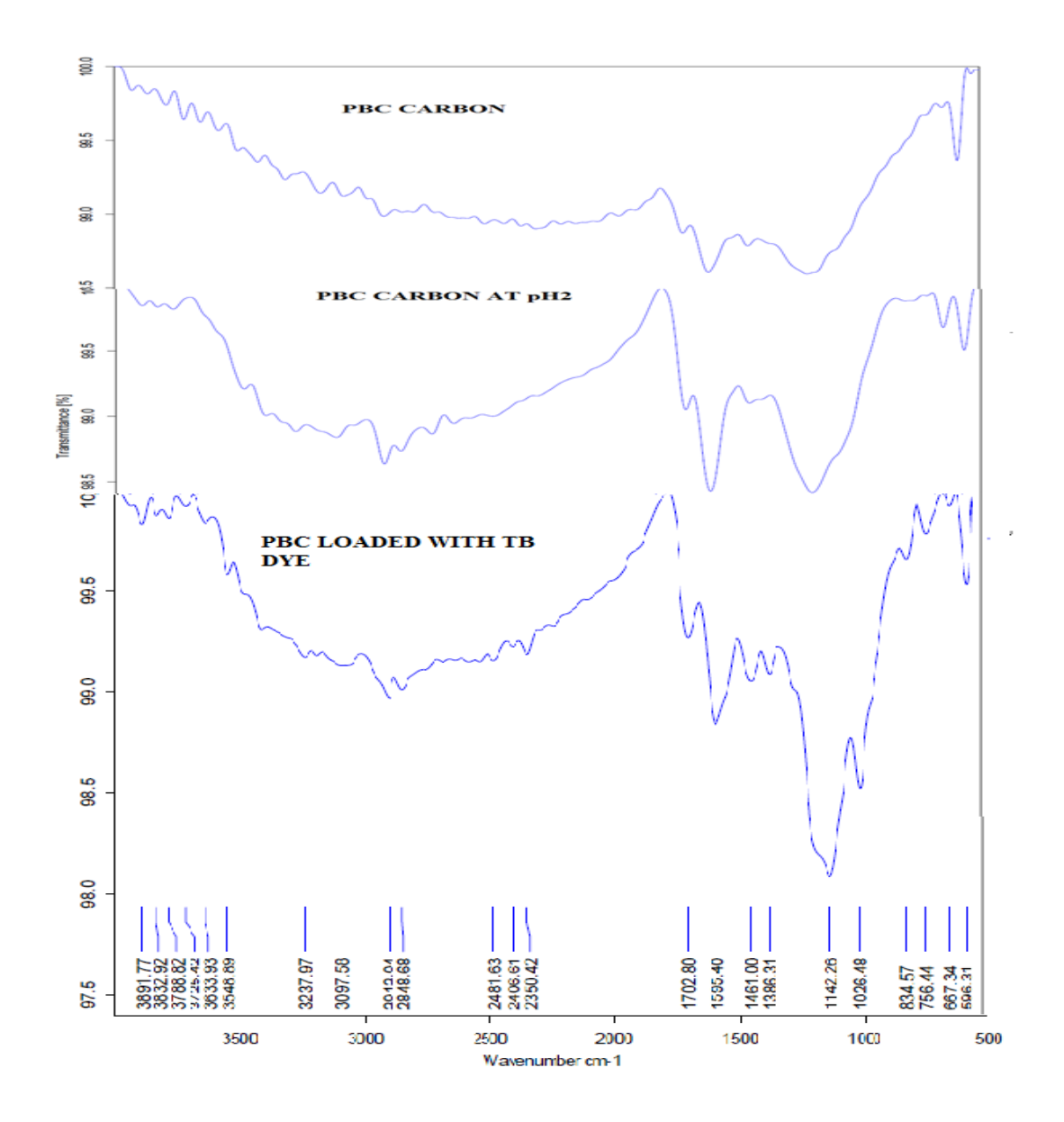


Figure 5.133 FT – IR spectrum of TB dye Loaded with PBC

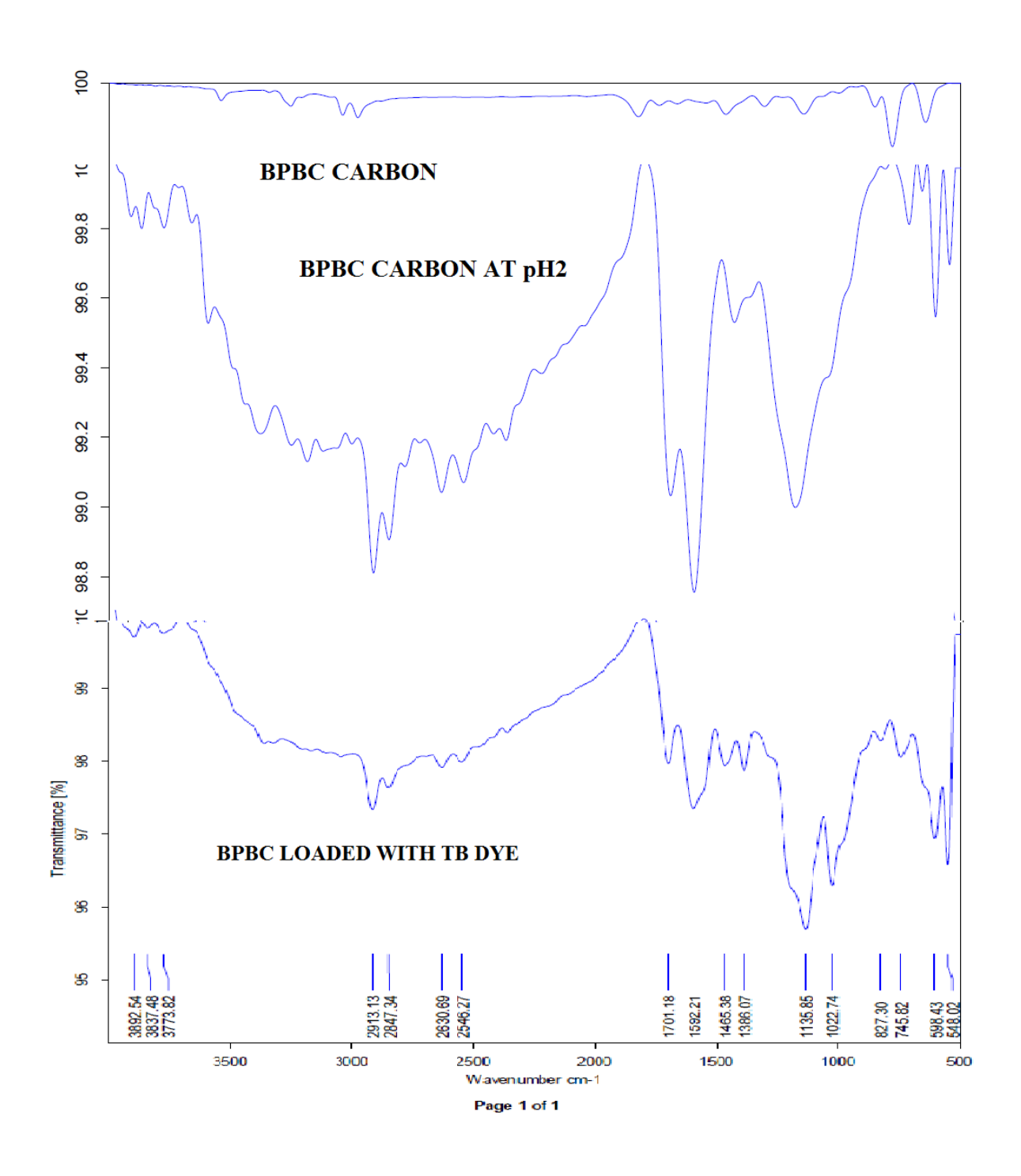


Figure.5.134FT – IR spectrum of TB dye Loaded with APBC

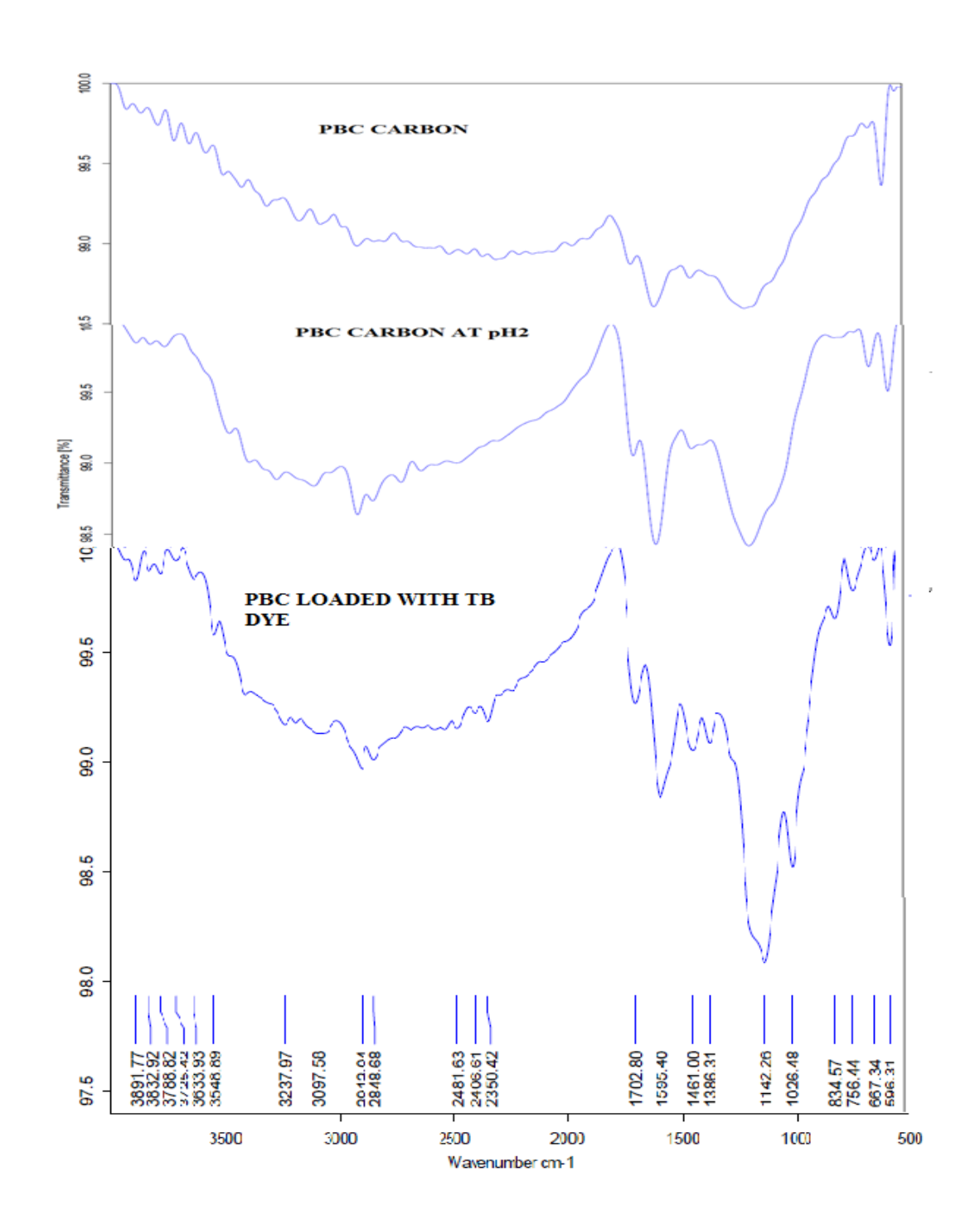


Figure. 5.135FT – IR spectrum of TB dye Loaded with BPBC

Analysis of FTIR peaks of before and after adsorption of TB dye onto PBC, APBC and BPBC infer that intensities of the some peaks were changed, some peaks were diminished and few new peaks were formed. This results leads to conclude that possibility of some chemisorption also took place.

Summary and Conclusion

Three types of activated carbons were prepared from the barks of *Pterocarpus Marsupium*. First one was prepared by treating with phosphoric acid followed by heating in a Microwave oven and it was designated as *Pterocarpus Marsupium activated carbon* (PBC). Second one was prepared by treating 25% of HCL followed by heating in a micro oven and it was designated as Acid 25% *Pterocarpus Marsupium* bark carbon (APBC). Third one was prepared by treating 25% of KOH followed by heating in a micro oven and it was designated as Base 25% *Pterocarpus Marsupium* bark carbon (BPBC) were investigated with the cationic dye Methylene blue dye (MB dye), an anionic dye Turquoise blue (TB dye) and heavy metal ions Cr (VI) from aqueous solution.

A detailed investigation on the adsorption of chosen adsorbates with respect to equilibrium, kinetic and thermodynamic aspects was carried out under batch mode method.

The prepared adsorbents PBC, APBC and BPBC were characterized using standard methods. These three adsorbents were showed that more or less similar FTIR spectra, indicating that method of heating had not much influenced the existence of functional groups.

Other physio chemical properties such as Zero point charge (pH_{zpc}), bulk density, Surface area, moisture content, fixed carbon content, matter soluble in water , matter soluble in acid, ash content and percentage of yield were determined. Values of these

properties revealed that APBC was more effective adsorbent than PBC and BPBC. Significance of each of these properties was discussed well.

The different parameters related to the adsorption study such as effect of solution pH, adsorbent dose and contact time, initial concentration of adsorbate and temperature were determined to establish the adsorption behavior of adsorbents PBC, APBC and BPBC for the chosen three adsorbates.

Optimum pH selected for the adsorption of Methylene Blue dye was 7. For the adsorption of Turquoise blue and Cr (VI) ion, the optimum pH was 2. Reasons behind the selection of optimum pH were discussed based on pH_{zpc} of the adsorbents, electrostatic interaction, and speciation of the adsorbate in the pH of the solution.

Study of the effect of dosage of the adsorbents on the adsorption showed the increase in the percentage removal of adsorbates with an increase in the dosage of adsorbent which observation was due to the increase in surface area and number of adsorption sites. Dose responsible for the percentage of removal between 60 and 80 was selected for the chosen initial concentration of each adsorbate.

Rate of adsorption was known from the study on the effect of contact time. This study inferred that extent of adsorption is rapid in the initial stages and became slow in later stages till the attainment of equilibrium. Time needed to attain equilibrium was 70 to 120 minutes for MB dye, TB dye and 80 to 140 minutes for metal ions adsorption. Equilibrium was attained little bit earlier in the case of APBC when compared to PBC and BPBC.

Equilibrium concentration (C_e) and the quantity adsorbed at equilibrium (q_e) for different initial concentration of the solution studied at a constant temperature is helped

to determine the isotherm parameters. Effect of initial concentration was studied at temperatures 305, 315, 325 and 335K. The quantity of adsorbate adsorbed per unit mass was found to increase with the increase of initial concentrations of adsorbate solutions. But the percentages of removals of adsorbates from aqueous solution at equilibrium decreased when the initial concentrations of adsorbate solutions were increased. This fact is discussed with proper explanation. The increase of temperature increased the percentage of removal of adsorbates. It is evident that an increase in the surface activity of the adsorbent at higher temperatures supported the endothermic process.

Popular isotherm plots such as Freundlich, Langmuir, Temkin and Dubinin Radushkevich were drawn. Regression coefficient (R²) values of the plots indicated that the experimental data fit well into isotherm models which reflected the reliability of the values of the isotherm constants determined. The applicability of Freundlich isotherm inferred that the chosen adsorptions onto APBC, BPBC and PBC were complex in nature. Adsorption capacities (mg/g) calculated from each isotherm found to increase with the increase of temperature. This fact supported the endothermicity of adsorption process. Freundlich and Langmuir adsorption capacities of other adsorbents for the chosen adsorbates were presented for the comparison sake. The adsorption intensity constant 'n' values determined from the Freundlich isotherm ranged from 1 and 10 indicated the favourable adsorption. The dimensionless separation factor R_L values determined from the Langmuir isotherm were in between 0 and 1 which indicated the favourable adsorption of dyes and metal ions onto PBC, APBC and BPBC. Equilibrium binding constant 'a_T' values (L/g) and the heat of sorption, (b_T) values (J/mg) obtained from Temkin isotherms found to be low. These low values suggested the physisorption mechanism. Mean free energy 'E' values were found to be lesser than 8 kJ/mol. This fact also supported the physisorption mechanism. Adsorption capacities determined from the isotherms for APBC were found to be greater than the adsorption capacities determined for BPBC and PBC.

Adsorption kinetics was studied by using linear forms of the pseudo-first-order (Lagergren equation), pseudo second order (Ho equation) and intraparticle diffusion (Weber Morris equation) kinetic models.

Pseudo-first-order rate constant k_1 and pseudo-second-order rate constant k_2 were determined for different initial concentrations. Predicted quantities of adsorption q_e (pr) were determined using pseudo first-order and pseudo second-order rate equations. Deviation of the q_e (pr) values from the quantity of adsorption determined experimentally ' q_e (exp)' for both pseudo first and pseudo second order models for different initial concentrations were evaluated with a statistical tool "Mean of Sum of Squared Error" (MSSE). Lower MSSE value means lower deviation. The kinetic model which has the low deviation is suitable model to describe the kinetic aspects. The results indicated that all the chosen adsorptions carried out on PBC, APBC and BPBC followed pseudo second order kinetics.

The intraparticle diffusion rate constants (k_p mg/g/min0.5) were obtained from the Weber Morris plots (plot of ' q_t ' versus ' $t^{0.5}$ ') had multi linear portions, which informed more number of steps involved in the sorption process. The increase of ' k_p ' values with a rise in initial concentration showed that pore diffusion was the rate controlling step in each adsorption process studied.

The experimental results obtained from the effect of temperature carried out for different initial concentrations were used to determine the thermodynamic parameters such as enthalpy ΔH° (kJ/mol) and entropy, ΔS° (J/K/mol) and change in free energy ΔG° (kJ/mol) associated with the adsorption process.

The negative values of ΔG° indicated the feasibility of the adsorption process. The positive values of ΔS° showed the prevalence randomness at the solid - solution interface. The positive values of ΔH° indicated that the adsorptions were endothermic. Magnitudes of enthalpy changes were below 40 kJ mol⁻¹ for PBC, APBC and BPBC adsorbents. These low values suggested the physisorption mechanism.

Desorption studies were conducted to understand the mechanism of adsorption as well as to know the re - usability property of adsorbent in addition to recover the adsorbates. The results expressed that 0.1 N NaOH was the best desorbing agent for MB dye, TB dye and Cr (VI) ions. This result was in agreement with the pH dependent results obtained earlier study and suggested that the dye and metal ions were adsorbed onto the PBC, APBC and BPBC through physisorption.

FTIR spectra of adsorbents laden with the adsorbates (Dyes and metal ions) were compared with the FTIR spectra of raw adsorbents. No appreciable changes were observed in the peak positions before and after adsorption except slight shift of the band position and reductions in the intensities. This study supported that majority of adsorptions took place via physical forces and very few via chemical forces.

EDAX pattern of Cr (VI) ions showed that were fitted into the crystalline structure of the carbon. Peaks of certain Cr (VI) ions are very small which infers the surface adsorption through Vander Walls force.

The SEM photographs clearly indicates that maximum number of pores present on the external surface of the adsorbents PBC, APBC and BPBC which are countable for the adsorption of metal/dye onto the adsorbents.

Among the three adsorbents, PBC, APBC and BPBC the metal/dye removal efficiency of the adsorbent APBC was higher than PBC and BPBC. This is be owing to greater surface area of APBC adsorbent.

On the basis of the above investigations, it can be concluded that the adsorbents PBC, APBC and BPBC prepared from bark of *Pterocarpus Marsupium* carbon have high potential to remove heavy metal ions and dyes. Performance of APBC was found to be better than BPBC and PBC. Hence microwave heating can be adopted instead of muffle furnace heating while preparing the adsorbent. The values of equilibrium parameters, isotherm constants, and thermodynamic parameters obtained can be used to design water treatment plants for the studied adsorbate - adsorbent system.

REFERENCE

- Abdullah, A.Z., Salamatinia, B.and Kamaruddin, A.H., Application of response surface methodology for the optimization of NaOH treatment on oil palm frond towards improvement in the sorption of heavy metals, Desalination, Vol. 244, 2009, 227–238.
- Abechi, E.S., Gimba, C.E., Uzairu, A., Kagbu, J.A Archives of Applied Science Research, 3 (1), (2011), 154-164.
- Abegunde et al., 2020 Abegunde S.M., Idowu K.S., Sulaimon A.O. Plant-mediated iron nanoparticles and their applications as adsorbents for water treatment—a review J. Chem. Rev., 2 (2) (2020), pp. 103-113
- Adeyemo et al., 2017 Adeyemo A.A., Adeoye I.O., Bello O.S. Adsorption of dyes using different types of clay: A review Appl. Water Sci., 7 (2) (2017), pp. 543-568
- Ahmad, M.A., N.S. Afandi, K.A. Adegoke, O.S. Bello, Desalination Water Treat. 57 (2016)
- Ahmaruzzaman M. Adsorption of phenolic compounds on low-cost adsorbents: A review Adv. Colloid Interface Sci., 143 (1–2) (2008), pp. 48-67
- Almansa, C., Molina-Sabio, M., Rodriguez-Reinoso, F., 2004. Adsorption of methane into ZnCl₂-activated carbon derived discs. Micropor Mesopor Mat., 76, 185-191.
- Alventosa-deLara, E., Barredo-Damas, S., Alcaina-Miranda, M.I. and Iborra-Clar, Ultrafiltration technology with a ceramic membrane for reactive dye removal: optimization of membrane performance, J. Hazard. Mater, Vol.209 –210, 2012, 492–500.
- Arivoli, S., Hema, M., Karuppaiah, M. and Saravanan, S., Adsorption of Chromium Ion by Acid Activated Low Cost Carbon-Kinetic, Mechanistic, Thermodynamic and Equilibrium Studies, E-Journal of Chemistry, Vol. 5, No.4, 2008, 820-831.
- Artioli.Y., Reference Module in Earth Systems and Environmental Sciences Encyclopedia of Ecology 2008, Pages 60-65
- Askalany A.A., Salem M., Ismael I.M., Ali A.H.H., Morsy M.G., Saha B.B.An overview on adsorption pairs for cooling Renew. Sust. Energ. Rev., 19 (2013), pp. 565-572

- Aygun, A., Yenisoy-Karakas, S. and Duman, I. (2003). Production of granular activated carbon from fruit stones and nutshells and evaluation of their physical, chemical and adsorption properties, Micropor Mesopor Mater 66:189–195 2015.
- Babel S., Kurniawan T.A. Low-cost adsorbents for heavy metals uptake from contaminated water: A review J. Hazard. Mater., 97 (1–3) (2003), pp. 219-243
- Baker, F.S., Miller, C.E., Repic A.J. and Tolles, E.D., Activated Carbon. Kirk-Othmer Encyclopedia of Chemical Technology, Vol. 4, 1992, 1015-1037.
- Banat, I.M., Nigam, P., Singh, D., Marchant, R., 1996. 'Microbial decolorization of textile-dye-containing effluents: a review', Bioresource Technology. 58, 217-227.
- Bansal, R.P. and Goyal, M., Activated Carbon Adsorption. 6000 Broken Sound Parkway NW, Suite 300 Boca Raton, FL, USA 33487–2742: CRC Press, Taylor & Francis, 2005.
- Belchinskaya L.I., Kh odosova N.A., Strelnikova O.Yu., Petukhova G.A., Ciganda L. Regulation of sorption processes on natural nanoporous aluminosilicates. I. Acidic and basic modifications Prot. Met. Phys. Chem. Surf., 51 (5) (2015), pp. 779-786
- Bernard, E., Jimoh, A and Odigure, J.O., Research Journal of Chemical Sciences Vol. 3(8), 2013, 3-9
- Bertazzo and Rezwan, 2010 Bertazzo S., Rezwan K. Control of alpha-alumina surface charge with carboxylic acids Langmuir, 26 (5) (2010), pp. 3364-3371
- Bertazzo S., Zambuzzi W.F., da Silva H.A., Ferreira C.V., Bertran C.A. Bioactivation of alumina by surface modification: A possibility for improving the applicability of alumina in bone and oral repair Clin. Oral. Implants Res., 20 (3) (2009), pp. 288-293
- Bilal M., Shah J.A., Ashfaq T., Gardazi S.M.H., Tahir A.A., Pervez A., Mahmood Q. Waste biomass adsorbents for copper removal from industrial wastewater—a review J. Hazard. Mater., 2 (63) (2013), pp. 322-333
- Bioresour. Technol., 2003,87, 221-230.
- Biswajit Das., Naba Kumar Mondal., Palas Roy. and Soumya Chattoraj., Application of Response Surface Methodology for Hexavalent Chromium Adsorption onto

- Alluvial Soil of Indian Origin, *International Journal of Environmental Pollution and Solutions*, 2, 72-87 (2013)
- Boehm, 2002 Boehm H.P. Surface oxides on carbon and their analysis: A critical assessment Carbon, 40 (2002), pp. 145-149
- Caturla, F., Molina-Sabio, M., Rodriguez-Reinoso, F., 1991. Preparation of activated carbon by chemical activation with ZnCl₂- Carbon. 9, 999-1007.
- Chen J.P., Yiacoumi S., Blaydes T.G. Equilibrium and kinetic studies of copper adsorption by activated carbon Sep. Technol., 6 (2) (1996), pp. 133-146
- Choi, H.J., Removal of Pb (II) from aqueous solution using hybrid adsorbent of sericite and spent coffee grounds, Appl. Chem.Eng., 29(5),571-580 (2018).
- Chou M.I.M. Fly ash Encyclopedia of Sustainability Science and Technology, Springer, New York (2012), pp. 3820-3843
- Crawford and Quinn, 2017Crawford C.B., Quinn B.The interactions of microplastics and chemical pollutantsMicroplastic Pollut. (2017), pp. 131-157
- Czernik, S., Review of Fast Pyrolysis of Biomass. Presentation, National Renewable Energy Laboratory, Golden 2002.
- Dana, 2017Dana E. Adsorption of heavy metals on functionalised-mesoporous silica: A review Microporous Mesoporous Mater, 247 (2017), pp. 145-157
- Danje, S., Fast Pyrolysis of Corn Residues for Energy Production.M.Sc. Thesis, StellenboschUniversity, Department of Chemical Engineering, South Africa, 2011.
- DaSilva E.B., Zabkova M., Araújo J.D., Cateto C.A., Barreiro M.F., Belgacem M.N., R odrigues A.E. An integrated process to produce vanillin and lignin-based polyurethanes from Kraft lignin Chem. Eng. Res. Des., 87 (9) (2009), pp. 1276-1292
- Demirbas E., Kobya M., Senturk E. and Ozkan T., Adsorption kinetics for the removal of chromium (VI) from aqueous solutions on the activated carbons prepared from agricultural wastes, *Water SA* 30(4), 533 -539 (2004)
- Desphande, S.D., 2001. Ecofriendly dyeing of synthetic fiber. Indian Journal of Fiber & Textile Research. 26, 136-142

- El-Nady, FE. and Atta, MM., Toxicity and bioaccumulation of heavy metals to some marine biota from the Egyptain coastal waters. J. Environ. Sci. Health. Vol.31 (7), 1996, 1529-1545
- Esther Forgacs, Tibor Cserhati & Gyula Oros 2004. Removal of synthetic dyes from wastewaters: a review. Environment International. 30, 953-971.
- Ezeokonkwo M.A., Ofor O.F., Ani J.U. Preparation and evaluation of adsorbents from coal and Irvingia gabonensis seed shell for the removal of Cd (II) and Pb (II) ions from aqueous solutions Front. Chem., 5 (2018), p. 13
- Foo, K.Y., Hameed, B.H., Preparation of activated carbon bymicrowave heating of lang sat (LansiumDomesticum) empty fruitbench waste. Bioresour. Technol. 116, 2012, 522–525
- Fu, Y., & Viraraghavan, T., 2001. Fungal decolorization of dye wastewaters: a review. Bioresource Technology. 79, 251-262
- Gao, Y., Yue, Q., Gao, B., Sun, Y., Wang, W., Li, Q., Wang, Y., 2013. Comparisons of porous, surface chemistry and adsorption properties of carbon derived from enteromorpha prolifera activated by H4P2o7 and KOH. Chem. Eng. J. 232, 582– 590.
- García-Monta no, J., Xavier Domènech, X., García-Hortal, J.A., Torrades, F.and Peral, J., The testing of several biological and chemical coupled treatments for Cibacron Red FN-R azo dye removal, J. Hazard. Mater, Vol.154, 2008, 484–490.
- Garg V.K., Gupta R, Yadav A. and Kumar K., Dye removal from aqueous solution by adsorption on treated sawdust, *Bioresource Technology*, **89**, 121 124 (**2003**)
- Garrido, J., Linares Solano, A., Martin, J.M., Molina, M., Rodriguez-Reinoso F., Torregrosa, R., 1987. Use of N₂ vs. CO₂ in the characterization of activated carbons. Langmuir. 3, 76-81.
- Gayathri R., Gopinath K.P., Kumar P.S., Suganya S. Adsorption capability of surface-modified jujube seeds for Cd(II), Cu(II) and Ni(II) ions removal: Mechanism, equilibrium, kinetic and thermodynamic analysis Desalin. Water Treat., 140 (2019), pp. 268-282
- Gonzalez, J.C., Sepulveda-Escribano, A., Molina-Sabio, M., Rodriguez-Reinoso, F., Production, properties and applications of activated carbon, in Characterization of Porous Solids. Vol. IV, Eds.

- Gottipati Ramakrishna and Mishra Susmita., Res. J. Chem. Sci., 2012, 2(2), 40-48.
- Guo, J. and Lua, A.C., Adsorption of sulphur dioxide onto activated carbon prepared from oil-palm shells with and without pre-impregnation. Separation and Purification Technology, Vol. 30, 2003, 265-273
- Gupta, G.S., Prasad, G., Singh, V.H., 1990. Removal of chrome dye from aqueous solutions by mixed adsorbents: fly ash and coal. Water Research. 24, 45-50
- Haimour, N.M., Emeish, S., 2006. Utilization of date stones for production of activated carbon using phosphoric acid. Waste management. 26, 651-660.
- Hayati, B., Mahmoodi, N.M., 2012. Modification of activated carbon by the alkalinetreatment to remove the dyes from wastewater: mechanism, isotherm and kinetic.Desalination Water Treat. 47 (1–3), 322–333.
- Hema, M. and Arivoli, S., Int. J. Phys. Sci., 2007, 2 (1), 010-017.
- High-Risk Pollutants in Wastewater, Elsevier (2020), pp. 169-207.
- Horsfall, M Jnr. and Spiff, A. I., Effects of temperature on the sorption of pb²⁺ and cd²⁺ from aqueous solution by caladium bicolor (wild cocoyam) biomass. Electronic Journal of Biotechnology, Vol 8, No 2, Aug 2005
- HosseiniKoupaie, E., AlaviMoghaddam, M.R. and Hashemi, S.H., Post-treatment of anaerobically degraded azo dye Acid Red 18 using aerobic moving bed biofilm process: enhanced removal of aromatic amines, J. Hazard. Mater, Vol. 195, 2011, 147–154
- Hu and Ke, 2020 Hu H., Ke X. Physicochemical technologies for HRPs and risk control
- Huang et al., 2019 Huang B., Liu G., Wang P., Zhao X., Xu H.Effect of nitric acid modification on characteristics and adsorption properties of lignite Processes, 7 (2019), p. 167
- Huang C.P., Wu M.H. The removal of chromium(IV) from dilute aqueous solution by activated carbon Water Res., 11 (1977), pp. 673-679
- Igwe, J.C. and Abia, A.A., Maize Cob and Husk as Adsorbents for removal of Cd, Pb and Zn ions from wastewater. The physical Sci.Vol.2, 2003, 83-94.
- Ip A.W.M., Barford J.P., McKay G. Reactive black dye adsorption/desorption onto different adsorbents: Effect of salt, surface chemistry, pore size and surface area J. Colloid Interface Sci., 337 (1) (2009), pp. 32-38

- Ispas C., Sokolov I., Andreescu S. Enzyme-functionalised mesoporous silica for bioanalytical applications Anal. Bioanal. Chem., 393 (2) (2009), pp. 543-554
- Jagtoyen, M., Derbyshire, F., 1998. Activated carbons from yellow poplar and white oak by H₃PO₄ activation. Carbon. 36, 1085-1097.
- Johnson, P. D., Watsonm, M.A., Brown, J., Jeffcoat, I. A., 2002. Peanut hull pellets as a single use sorbent for the capture of Cu(II) from wastewater. Waste Management. 22, 471-480
- Juang, R.S., Wu, F.C. and Tseng, R.L., Characterization and use of activated carbons prepared from bagasses for liquid-phase adsorption, Colloid Surf. A: Physicochem. Eng. Aspects Vol. 201, 2002, 191–199
- Juang. Et al 1997 Juang, R.S., Wu, F.C., Tseng, R.L., 1997. The ability of activated clay for the adsorption of dyes from aqueous solutions. Environmental Technology. 18, 525-531.
- Kaveeshwar A.R., Kumar P.S., Revellame E.D., Gang D.D., Zappi M.E., Subramanian R Adsorption properties and mechanism of barium (II) and strontium (II) removal from fracking wastewater using pecan shell based activated carbon J. Clean. Prod., 193 (2018), pp. 1-13
- Khadka Deba Bahadur and Mishra Paramatma, Adsorptive Removal of Cr (VI) from Aqueous Solution by Sugarcane Biomass, *Res. J. Chem. Sci*, 4(5), 32-40 (2014).
- Khalili, N.R., Campbell, M., Sandi, G. and Golas, J., Production of micro and mesoporous activated carbon from paper mill sludge I. Effect of zinc chloride activation Carbon, 2000
- Kim, J.N., Sohn, M.H., Kim, D.S., Sohn, S.M. and Kwon ,Y.S., Production of Granular Activated Carbon from waste walnut shell and its adsorption characteristics for Cu²⁺ ion. J.Hazard. Mater, Vol. 85, 2001, 301-15.
- Kirk-Othmer, Encyclopedia of Chemical Technology, John Wiley and Sons Inc., 2003.
- Kong M., Huang L., Li L., Zhang Z., Zheng S., Kuang Wang M.Effect of oxalyc and citric acids on three clay minerals after incubation Appl. Clay Sci., 99 (2014), pp. 207-214.
- Körbahti et al., 2011 Körbahti, B.K., Artut, K., Geçgel, C. and Özer, A., Electrochemical decolorization of textile dyes and removal of metal ions from textile dye and metal ion binary mixtures, Chem. Eng. J. Vol. 173, 2011, 677–688.

- Krishna D. and Padma Sreeb R., Removal of Chromium from Aqueous Solution by Custard Apple (*Annona Squamosa*) Peel Powder as Adsorbent, *Int. J. Appl. Sci. Eng.*, 11, 2, 171-194 (2013)
- Krishna B.S., Murty D.S.R., Prakash B.J. Surfactant-modified clay as an adsorbent for chromate Appl. Clay Sci., 20 (1–2) (2001), pp. 65-71
- Kulkarni Sunil J., Patil Suhas V., Tapre Ravi W. and Goswami Ajaygiri K., Adsorption of Chromium from Wastewater on Different Adsorbents, *Int. J. Res. Chem. Environ*, 3(1), 231-236 (2013)
- Kyzas, G.Z., Bomis, G., Kosheleva, R.I., Efthimiadou, E.K., Favvas, E.P., Kostoglou, M., Mitropoulos, A.C., 2019. Nanobubbles effect on heavy metal ions adsorption by activated carbon. Chem. Eng. J. 356, 91–97
- L.wu,w. wan, Z. Shang, X.Gao, N.Kobayashi, G.Luo, and Z.Li,Surface modification of Phosphoric acid activated carbon by using nonthermal plasma for enhancement of Cu (II) adsorption from aqueous solution, sep. purify technology., 197, 156-169. (2018).
- Laine, J., Lunes J.L.S., 1992. Effect of the preparation method on pore size distribution of activated carbon from coconut shell. Carbon. 30, 601-604
- Li, Q. Z., Chai, L.Y. & Zhao, J. 2009 Lead adsorption from modified spent grain. Transactions of Nonferrous Metal Society of China 19, 1371-1376.
- Lillo-Rodenas, M., Lozano-Castello, D., Cazorla-Amoros, D. and Linares-Solono, A., Preparation of Activated Carbons from Spanish Anthracite: II Activation by NaOH. Carbon, Vol.39, 2001, 751-759
- Lin S.H., Juang R.S.Adsorption of phenol and its derivatives from water using synthetic resins and low-cost natural adsorbents: A review J. Environ. Manage., 90 (3) (2009), pp. 1336-1349
- Liu, M., Xiao, C., 2018. Research progress on modification of activated carbon. In: E3S Web of Conferences 38:02005 EDP Sciences
- Lozano-Castello, D., Lillo-Rodenas, M.A., Cazorla-Amoros, D. and Linares- Solono A, Preparation of Activated Carbons from Spanish Anthracite: I Activation by KOH.Carbon, Vol.39,2001, 741-749
- Lu G.Q. Preparation and evaluation of adsorbents from waste carbonaceous materials for SOx and NOx removal Environ. Prog., 15 (1) (1996), pp. 12-18

- Makó et al., 2006 Makó É., Senkár Z., Kristóf J., Vágvölgyi V. Surface modification of mechanochemically activated kaolinites by selective leaching J. Colloid Interf. Sci., 294 (2) (2006), pp. 362-370
- Malik, P.K., Use of activated carbons prepared from sawdust and rice-husk for adsorption of acid dyes: a case study of acid yellow 36, Dyes Pigments, Vol. 56, 2003, 239–249.
- Manory, R.R., 1990. Some principles for understanding surface modification of metals
- Minobe S., Watanabe T., Sato T., Tosa T., Chibata I. Preparation of adsorbents for pyrogen adsorption J. Chromatogr. A, 248 (3) (1982), pp. 401-408
- Mittal, A.K., Gupta, S.K., 1996. Biosorption of cationic dyes by dead macro fungus Fomitopsis carnea: Batch studies. Water Science Technology. 34, 81-87.
- Mohamed Ahmedna, Wayne, E., Marshall, Abdo, A., Husseiny, Ramu, M., Rao and IpekGoktepe, The use of nutshell carbons in drinking water filters for removal of trace metals, Water Research, 2004
- Mohamed, M.M., Acid dye removal: comparison of surfactant modified mesoporous FSM with activated carbon derived from rice husk, J. Colloid Interface Sci., Vol.272, 2004, 28–34
- Mokhtar, A., Nargess, Y.L., Niyaz, M.M. and Nooshin, S.T., Equilibrium and kinetics studies for the adsorption of direct and acid dyes from aqueous solution by soy meal hull, J. Hazard. Mater, Vol, 135, 2006, 171–179
- Molina, S.M., Rodríguez, R.F., Caturla, F., Sellés, M.J., 1995. Porosity ingranular carbons activated with phosphoric acid. Carbon. 33,1105-1113.
- Mwaikambo, L.Y., Ansell, M.P., 1999. Die. Angew. Chem. Int. Ed. 272, 108–124
- Namasivayam, C. and Kavitha, D., Removal of Congo Red from water by adsorption onto activated carbon prepared from coir pith, an agricultural solid waste. Dyes and Pigments, 54, 2002, 47–58.
- Namasivayam, C., Prabha, D. and Kumutha, M., Removal of direct red and acid brilliant blue by adsorption onto banana pith, Bioresource Technology., Vol. 64, 1998, 77–79.

- Njikam, E.& Schiewer,S.2012 Optimization and kinetic modeling of cadmium desorption from citrus peels:a process for biosorbent regeneration. *Journal of Hazardous Materials* 213-214 (1), 242 248.
- Nowicki, P., Pietrzak, R. and Wachowska, H., Siberian anthracite as a precursor material for microporous activated carbons. Fuel, Vol.87, 2008, 2037-2040
- Ofudje, E.A., Akiode, O.K., Oladipo, G.O., Adedapo, A.E., Adebayo, L.O., Awotula, A.O.,2015. Application of raw and alkaline-modified coconut shaft as a biosorbent for Pb2+ removal. BioResources 10 (2), 3462–3480.
- Ogunlaja et al 2013 Ogunlaja, A., Olomo, O.O., Olukanni, D.O., 2013. Aerobic bacterial degaders in effluent from Itoku textile industry. Abeokuta. 12, 6954-6958.
- Olasehinde and Abegunde, 2020b Olasehinde E.F., Abegunde S.M. Preparation and characterisation of a new adsorbent from raphia taedigera seed Res. Eng. Struct. Mater., 6 (2) (2020), pp. 167-182
- Olasehinde E.F., Abegunde S.M. Adsorption of methylene blue onto acid modified raphia taedigera seed activated carbon Adv. J. Chem. A, 3 (5) (2020), pp. 663-679
- Panday and Nair 1974 Pandey, S.N.; Nair, P. (1974). Effect of Phosphoric Acid Treatment on Physical and Chemical Properties of Cotton Fiber1. Textile Research Journal, 44(12), 927–933.
- Park, S.J., Jang, Y.S., 2002. Pore structure and surface properties of chemically modified activated carbons for adsorption mechanism and rate of Cr (VI). J. Colloid Interface Sci. 249 (2), 458–463
- Piatak N.M., Parsons M.B., Seal II R.R. Characteristics and environmental aspects of slag: A review Appl. Geochem., 57 (2015), pp. 236-266
- Pinthong, P., Co-pyrolysis of Rice Husk, Polyethylene and Polypropylene Mixtures: A Kinetic Study, M.Sc., Thesis, KasetsartUniversity, Chemical Engineering, 2009.
- Plaza M.G., Pevida C., Martín C.F., Fermoso J., Pis J., Rubiera F. Developing almond shell-derived activated carbons as CO2 adsorbents Sep. Purif. Technol., 71 (1) (2010), pp. 102-106
- Pollard, S.J.T., Fowler, G.D., Sollars, C.J. and Perry, R., Low cost adsorbents for waste and wastewater treatment: a review, Sci. Total Environ, Vol. 116, 1992, 31–52.

- Raghuvanshi, S.P., Singh, R.and Kaushik, C.P., 43.Kinetics study of methylene blue dye boiadsorption on bagasse, Appl. Ecol. Environ. Res., Vol. 2, 2005, 35
- Rambabu, K., Bharath, G., Banat, F., Show, P.L., 2020. Environmental Research 187,. https://doi.org/10.1016/j.envres.2020.109694 109694.
- Rashed M.N. Adsorption technique for the removal of organic pollutants from water and wastewater Organic Pollutants-Monitoring, Risk and Treatment (2013), pp. 167-194
- Rehman et al., 2019 Rehman A., Park M., Park S.J. Current progress on the surface chemical modification of carbonaceous materials Coatings, 9 (103) (2019), pp. 1-22
- Rehman, A., Park, M., Park, S.J., 2019. Current progress on the surface chemical modification of carbonaceous materials. Coatings 9 (103), 1–22.
- Renmin Gong., Yingzhi Sun., Jian Chen., Huijun Liu. and Chao Yang., Dyes and Pigments., 2005, 67, 179-195.
- Rezaei F., Webley P. Structured adsorbents in gas separation processes Sep. Purif. Technol., 70 (3) (2010), pp. 243-256
- Rich, G. and Cherry, K., Hazardous Waste Treatment Technologies, Pudvan Publishers, New York,1987
- Rio S., Le Coq L., Faur C., Lecomte D., Le Cloirec P. Preparation of adsorbents from sewage sludge by steam activation for industrial emission treatment Process Saf. Environ., 84 (4) (2006), pp. 258-264
- Robinson, T., McMullan, G., Marchant, R., Nigam, P., 2001. Remediation of dyes in textile effluent: a critical review on current technologies with a proposed alternative. Bioresource Technology. 77, 247-255.
- Rodriguez Reinoso and Linares Solano 1989 b Rodriguez-Reinoso F., Garrido, J., Martin-Martinez, J.M., Molina-Sabio, M., Torregrosa, R., 1989. The combined use of different approaches in the characterization of microporous carbons. Carbon. 27, 23-32.
- Rostami et al., 2018 Rostami E., Norouzbeigi R., Kelishami A.R.Thermal and chemical modification of bentonite for adsorption of an anionic dye Adv. Environ. Technol., 1 (2018), pp. 1-12

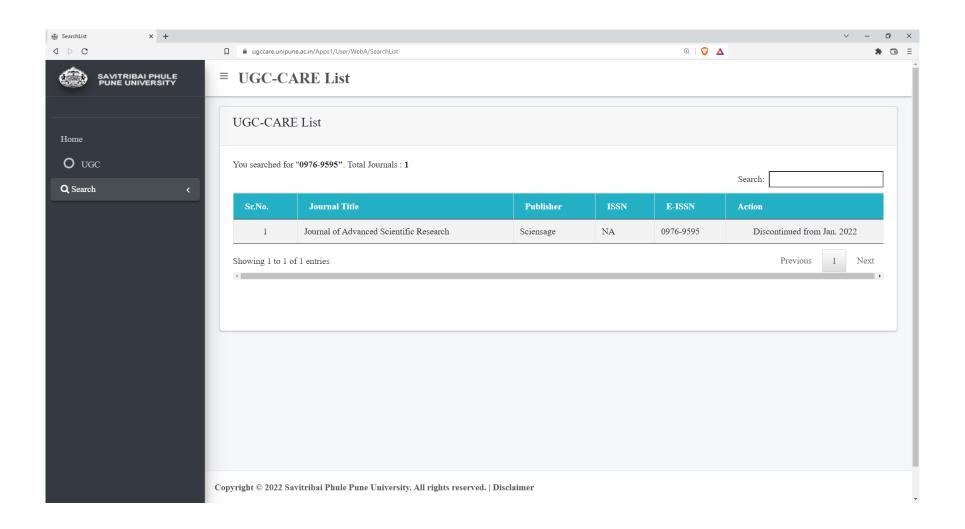
- Rozada, F., Calvo, L.F., Garcia, A.I., Martin-Villacorta, J. and Otero, M.,
- Saadiyah Ahmed Dhahir, Enaas Abdul Hussein, Noor Faraj, 2013. Adsorption of malachite green dye from aqueous solution onto iraqiraw al-hussainiyat deposit. European Chemical Bulletin. 2, 866-872.
- San Miguel, G, Fowler, GD, Sollars, CJ: A study of the characteristics of activated carbons produced by stream and carbon dioxide activation of waste tyre rubber. vol. 41, pp. 1009-1016. Carbon (2003).
- Sankaranarayanan, N., Madhyashtha, M. N., 1985. Current pollution researches in India. Trivdey R K and Goel P K (Eds.), Environmental Publications, Karad, India. 2 Sharma M., Singh J., Hazra S., Basu S. Adsorption of heavy metal ions by mesoporous ZnO and TiO2@ZnO monoliths: Adsorption and kinetic studies Microchem. J., 145 (2019), pp. 105-112.
- Sapna Kochher, Sandeep Kumar,2012. Screening for potential textile dye decolorizing bacteria. International Journal for Science and Emerging Technologies with Latest Trends. 2, 36-48.
- Schwarz et al., 1995 Schwarz J.A., Contescu C., Contescu A. Methods for preparation of catalytic materials
- Segun Michael Abegunde *, Kayode Solomon Idowu, Olorunsola Morayo Adejuwon, Tinuade Adeyemi-Adejolu, A review on the influence of chemical modification on the performance of adsorbents, Resources, Environment and Sustainability 1 (2020) 100001
- Selvaraj K., Manonmani S. and Pattabhi S., Removal of hexavalent chromium using distillery sludge, *Bio resource Technology*, 89(2), 207–211 (2003)
- Selvi K., Pattabhi S. and Kadirvelu K., Removal of Cr (VI) from aqueous solution by adsorption onto activated carbon, *Bioresource Technology*, 80, 87 89 (2001)
- Senturk et al., 2009 Senturk H.B., Ozdes D., Gundogdu A., Duran C., Soylak M. Removal of phenol from aqueous solutions by adsorption onto organomodified Tirebolu bentonite: Equilibrium, kinetic and thermodynamic study J. Hazard. Mater., 172 (1) (2009), pp. 353-36
- Sharma, S.G., Moreton, D., Vincent, B., 2003. Adsorption isotherm and atomic force microscopy studies of the interactions between polymers and surfactants on steel surfaces in hydrocarbon media. J. Colloid Interf. Sci. 263 (2), 343–349.

- Shen Y., Zhao P., Shao Q. Porous silica and carbon derived materials from rice husk pyrolysis char Microporous Mesoporous Mater., 188 (2014), pp. 46-76
- Shim et al., 2001Shim J.W., Park S.J., Ryu S.K. Effect of modification with HNO3 and naoh on metal adsorption by pitch-based activated carbon fibers Carbon, 39 (11) (2001), pp. 1635-1642
- Sinha, S., Jhalani, A., Ravi, M. R. and Ray, A., Modelling of Pyrolysis in Wood: A Review.Indian Institution of Technology, Department of Mechanical Engineering, New Delhi, 2004
- Siperko and Thomas, 1989 Siperko L.M., Thomas R.R.Chemical and physical modification of fluoropolymer surfaces for adhesion enhancement: A review J. Adhes Sci. Technol., 3 (1) (1989), pp. 157-173
- Sivakumar P. and Palanisamy P.N., Adsorption studies of basic red 29 by a nonconventional activated carbon prepared from *Euphorbia Antiquorum L*, Int. *J. ChemTech* Res., 1(3), 502-510 (2009)
- Smisek, M. and Cerny, S., Activate Carbon Manufacture, Properties and Applications. Elsevier Pub., Comp., New York, 1970
- Solomon Sabiro Shale, Removal of Fluoride Ions From Water Using Rice Husk Based Activated Carbon, Ph.D., Thesis, Addis AbabaUniversity, Addis Ababa, Ethiopia, 4 January 2016
- Solum, M.S. R.J. Pugmire; M. Jagtoyen; F. Derbyshire (1995). Evolution of carbon structure in chemically activated wood., 33(9), 1247–1254.
- Srinivasakannan, C. and MohamadZailani Abu Bakar, Production of activated carbon from rubber wood sawdust, Vol. 27, Issue 1, 2004, 89-96
- Srinivasakannan; Mohamad Zailani Abu Bakar (2004). Production of activated carbon from rubber wood sawdust., 27(1), 89–96
- Suk Soon Choi, Tae Ryeong Choi, Hee Jeong Choi surface modification of Phosphoric acid- activated Carbon in spent Coffee Grounds to Enhance Cu(II) Adsorption from Aqueous Solutions Appl.Chem.Eng, Vol. 32, No 5, October 2021, 589-598.
- Sun S., Zhu J., Zheng Z., Li J., Gan M. Biosynthesis of β-cyclodextrin modifiedschwertmannite and the application in heavy metals adsorption Powder Technol., 342 (2019), pp. 181-192

- Supriya Singh., Tripathi Alka, Srivastava S. K. and Ram Prakash, Removal of Hexavalent Chromium by Using *Mangifera Indica* Bark (Biosorption), *Int. J. Res. Chem. Environ*, 3(4), 61-67 (2013)
- Tamon and Okazaki, 1996 Tamon H., Okazaki M. Influence of acidic surface oxides of activated carbon on gas adsorption characteristics Carbon, 34 (1996), pp. 741-746
- Tan, I.A.W., Ahmad, A.L. and Hameed, B.H., Preparation of activated carbon from coconut husk: optimization study on removal of 2, 4, 6-trichlorophenol using response surface methodology, J. Hazard. Mater, Vol. 153, 2008, 709–717
- Tarleton S., Wakeman R. Solid/Liquid Separation: Equipment Selection and Process Design Elsevier (2006)
- Temuujina J., Jadambaab T.S., Burmaaa G., Erdenechimegb Sh, Amarsanaab J., MacK enzie K.J.D. Characterisation of acid activated montmorillonite clay from Tuulant (Mongolia) Ceram. Int., 30 (2004), pp. 251-255
- Teng, H., Ho, J.A. and Hsu, Y.F., Preparation of activated carbons from bituminuous coals with CO₂ activation influence of coal oxidation, Carbon, Vol.35, 1997, 275–283.
- Terrazas C.G.D., Ibarra R.J., Ortiz-Méndez U., Torres-Martínez L.M. Iron leaching of a mexican clay of industrial interest by oxalic acid Adv. Technol. Mat. Mat. Process., 7 (2) (2005), pp. 161-166
- Terrazas, C.G.D., Ibarra, R.J., Ortiz-Méndez, U., Torres-Martínez, L.M., 2005. Iron leaching of a mexican clay of industrial interest by oxalic acid. Adv. Technol.Mat. Mat. Process. 7 (2), 161–166
- Thakur et al., 2014 Thakur V.K., Vennerberg D., Kessler M.R.Green aqueous surface modification of polypropylene for novel polymer nanocompositesACS Appl. Mater. Inter. (12) (2014), pp. 9349-9356
- Thakur L.S., Semil P. Removal of arsenic in aqueous solution by low-cost adsorbent: A short review Int. J. Chemtech. Res., 5 (3) (2013), pp. 1299-1308
- Tseng, R.L., Wu, F.C. and Juang, R.S., Liquid-phase adsorption of dyes and phenols using pinewood-based activated carbons, Vol. 41, 2003, 487–495
- Tseng, R.L., Wu, F.C. and Juang, R.S., Liquid-phase adsorption of dyes and phenols using pinewood-based activated carbons, Vol. 41, 2003, 487–495.

- Vadivelan, V. and Vasanthkumar, K., Equilibrium, Kinetics, Mechanism and Process Design for the Sorption of Methylene Blue onto Rice Husk, J. Colloid Interf. Sci., Vol. 286, 2005, 91.
- Valix, M., Cheung, W.H. and McKay, G., Preparation of activated carbon using low temperature carbonisation and physical activation of high ash raw bagasse for acid dye adsorption, Chemosphere, Vol. 56, 2004, 493–501.
- Venkatraman B.R., Hema K., Nandhakumar V., Arivoli S., Adsorption Thermodynamics of Malachite Green Dye onto Acid Activated Low cost Carbon J.Chem.Pharm. Res.,3(2),637-649 (2011).
- Vieira et al., 2010 Vieira M.G.A., Neto A.A., Gimenes M.L., Da Silva M.G.C. Removal of nickel on bofe bentonite calcined clay in porous bed J. Hazard. Mater., 176 (1–3) (2010), pp. 109-118
- Vijayakumar, G., Tamilarasan, R. and Dharmendirakumar, M., Adsorption, Kinetic Equilibrium and Thermodynamic studies on the removal of basic dye Rhodamine-B from aqueous solution by the use of natural adsorbent perlite, J. Mater. Environ. Sci., Vol.3 (1), 2012, 157-170.
- Vlasova, M., Dominiguez-Patino, G., Kakazey, N., Dominiguez-Patino, M., Juarez-Romero, D., Mendez, Y.Enriquez., 2003. Structural-phase transformations in bentonite after acid treatment. Sci. Sinter 35, 155 166.
- Wigmans, T., Carbon and Coal Gasification. (Edited by Figueriedo, J. L. and Moulijn, J. A.,), MartinusNijhoff Pub., Lancaster, 1985, 559-601.
- Wu F.C., Tseng R.L. High adsorption capacity NaOH-activated carbon for dye removal from aqueous solution J. Hazard. Mater., 152 (3) (2008), pp. 1256-1267
- Wu X., Gao P., Zhang X., Jin G., Xu Y., Wu Y. Synthesis of clay/carbon adsorbent through hydrothermal carbonisation of cellulose on palygorskite Appl. Clay Sci., 95 (2014), pp. 60-66
- Yadav A., Garg V.K. Industrial wastes and sludges management by vermicomposting
- Yagmur .E, Ozmak. M, Aktas .Z, A novel method for production of activated carbon from waste tea by chemical activation with microwave energy, Fuel, Vol.87, No.15-16, 2008, 3278-3285.
- Yao Z, Qi J, Wang L, "Journal of hazardous materials, 2010,174, pg 137-143.

- Yuh-shan Ho, R., Malarvizhi, Sulochana N., Equilibrium Isotherm studies of Methylene Blue Adsorption onto Activated carbon Prepared from Delonix Regia Pods. Journal of Environmental Protection Science, 3, 111-116. (2009).
- Yusuff, A.S., 2019. Arab Journal of Basic and Applied Sciences 26, 89–102.
- Zhang, G., Yi, L. and Deng, H. and Sun, P., Dyes adsorption using a synthetic carboxymethyl cellulose-acrylic acid adsorbent, J. Environ. Sci., Vol. 26, 2014, 1203–1211
- Zhao, X.T., Zeng, T., Li, X.Y., Hu, Z.J., Gao, H.W., Xie, Z., Modeling and mechanism of the adsorption of copper ion ontonatural bamboo sawdust. Carbohydr.Polym. 89, 2012, 185–192.
- Zheng, C., Ling, Z., Xiaobai, Z., Zhimin, F., An, L., 2013. Treatment technologies for organic wastewater. Water Treat. 11, 250–286
- Zhuang, H., Y.Zhong, and L.Yang, Adsorption equilibrium and kinetics studies of divalent manganese from phosphoric acid solution by using cationic exchange resin, Chinese J. Chem. Eng., 28, 2758 2770 (2020).





Journal of Advanced Scientific Research

ISSN
0976-9595
Research Article

Available online through http://www.sciensage.info

ADSORPTION OF TURQUOISE BLUE DYE FROM AQUEOUS SOLUTION ONTO ACID ACTIVATED CARBON PREPARED FROM *PTEROCARPUS MARSUPIUM* BARKS

S. Surya¹, V. Nandhakumar*¹, N. Balasubramaniam², K.Murugaiah¹

¹PG & Research Department of Chemistry, A.V.V.M. Sri Pushpam College
(Affiliated to Bharathidasan University), Poondi, Thanjavur (Dt), Tamil Nadu, India.

²Department of Chemistry, SRM Institute of Science and Technology, Ramapuram, Chennai, TamilNadu, India

*Corresponding author: drvnchem@gmail.com

ABSTRACT

Adsorption interaction of Turquoise Blue dye from aqueous solution onto acid and base surface modified activated carbons prepared from *Pterocarpus Marsupium* barks using microwave and phosphoric acid were investigated. Batch method adsorptions were carried out. Influences of the parameters such as agitation time, initial dye concentrations and temperature on adsorption were studied. Equilibrium data were fitted with Langmuir, Freundlich, Tempkin and Dubinin-Raduskevich isotherms. Best describing isotherms were ordered based on R² values.

Keywords: Adsorption, Phosphoric acid activated Pterocarpus Marsupium Barks Carbon, Isotherms, Turquoise Blue dye.

1. INTRODUCTION

Dyes are problematic to environment due to their high water solubility and low biodegradability. They interfere with the transmission of sunlight into stream, thereby reducing the photosynthesis activity [1]. The carcinogenic species are settled at the surroundings through the degradation of azo groups. Frequent discharges of dye and allied chemicals from dye industries cause considerable variation in the wastewater characteristics like pH, BOD, COD [2]. Turquoise Blue, a well-known anionic reactive dye, is widely used in textile industries. The resulting textile wastewater is coloured deep blue and affects water quality [3-5]. The molecular formula of the dye is C₃₂H₁₄CuN₈Na₂O₆S₂. The adsorption process provides an attractive alternative for the treatment of dye-contaminated waters, especially if the sorbent is inexpensive [6] Some numerous cheap and indigenous materials have been identified as successful adsorbents which remove these pollutants. Activated carbon is the most widely used adsorbent for dye removal due to its high porosity and surface area [6].

Recently, microwave energy has been widely used in several fields of applications on both research and industrial processes [7]. In particular, microwave heating arises from the direct interaction of matter with electromagnetic energy which increases the interest for materials processing as it offers a number of potential advantages over conventional heating [8].

The main objectives of the present investigations are reparation of carbon from *Pterocarpus Marsupium* barks through microwave irradiation approach. To optimize various experimental parameters to get an efficient carbon as an adsorbent and To study the adsorbing behaviour of the prepared carbon with *Turquoise Blue dye*.

Table 1: Data Processing Tools

S. No.		Parameters	Formulae		
	Mass balance	% of Removal	$(C_i - C_t) \times V / C_i$		
1.	relationships	Quantity adsorbed at equilibrium, q _e	$(C_i - C_e) \times V/W$		
	Telationships	Quantity adsorbed at the time t , q_t	$(C_i - C_t) \times V / W$		
		Langmuir Separation factor	$C_e/Q_e = 1/Q_0b + C_e/Q_0R_L = 1/(1+bC_0)$		
		Freundlich	$\log Q_e = \log K_f + 1/n \log C_e$		
2	Isotherms	Tempkin	$q_e = RT/b_T \ln a_T + RT/b_T \ln C_e$		
Э.	isotherms	Dubinin $-$ Raduskevich,	$\ln { m q_e} = \ln { m q_D}$ - ${ m B} { m \epsilon}^2$		
		Polanyi potential	$\varepsilon = RT \ln (1 + 1/C_e)$		
		Mean free energy of adsorption	$E = 1/(2B)^{\frac{1}{2}}$		

2. EXPERIMENTAL PROCEDURE

2.1. Material And Methods

Small pieces of dried barks of *Pterocarpus Marsupium* were powdered in a pulveriser. 25g of this powder was mixed with 100 mL of phosphoric acid solution of desired concentration (25, 50 and 75 %) and kept at room temperature for 24 hours. The slurry was placed to microwave heating (450, 600 and 850 watts and 10, 13 and 15 minutes) for simultaneous carbonization and activation. Thus carbonized samples were washed with cold distilled water 0.5 M HCl, hot distilled water successively and finally washed with cold distilled water until the pH of the washings reach 7. The carbon was filtered and dried at 425 K.

Totally 27 variety of activated carbons have been prepared under various preparation conditions. The carbon which removed maximum dye from the aqueous solution was selected for further adsorption study and named as PBC (*Pterocarpus Marsupium* barks carbon).

10g of the prepared carbons were mixed with 25% solutions of modifying agent (HCl and KOH) and placed in a microwave oven for 10 minutes. Then the carbon was again washed with hot distilled water and cold distilled water successively. Surface modified with 25% HCl acid solution was named as Acid treated *Pterocarpus Marsupium* Bark Carbon (APBC) and Surface modified with 25% KOH solution was named as Base treated *Pterocarpus Marsupium* Bark (BPBC).

2.2. Adsoption Studies

Adsorption of TB dye onto BPBC was studied with the varying parameters of solution pH, initial concentration of dye solution, contact time and temperature by batch mode approach. Pre-determined dose of the adsorbent and 50 mL and pre-determined concentration of the dye solution were poured into 250mL iodine flask. Then the content of the flask was agitated using rotary shaker with 180 rpm for pre- determined duration. Then the aliquot was centrifuged. Concentration of the centrifugate was measured after proper dilution using Systronics Double Beam UV-visible spectrophotometer: 2202 on the wave length of 680 nm.

3. RESULTS AND DISCUSSION

3.1. Effect of Contact time and Concentration on adsorption

The effect of contact time on the percentage removal was studied by taking 50 mg of the adsorbent and 20 mg/L, 30 mg/L, 40 mg/L and 50 mg/L solutions as initial concentrations. The adsorption process was

characterized by a rapid uptake of the adsorbate at the initial stages [9-12]. The rate of percentage removal was found to decrease after 10 minutes increases and become constant after attaining equilibrium stage in all the cases.

The percentage removal was found to decrease from 63.69 to 57.44, 65.90 to 59.34 and 61.64 to 55.07 as the initial concentration of TB dye increased from 20 mg/L, 30 mg/L, 40 mg/L to 50 mg/L respectively. It is clear that the removal of dyes depends on the concentration of the dye solution for all the studied systems were given in table 2 and shown in Figs. 1-9.

On comparing the adsorption capacities of the studied carbons, carbon modified with acid had more adsorption capacity than the other two carbons.

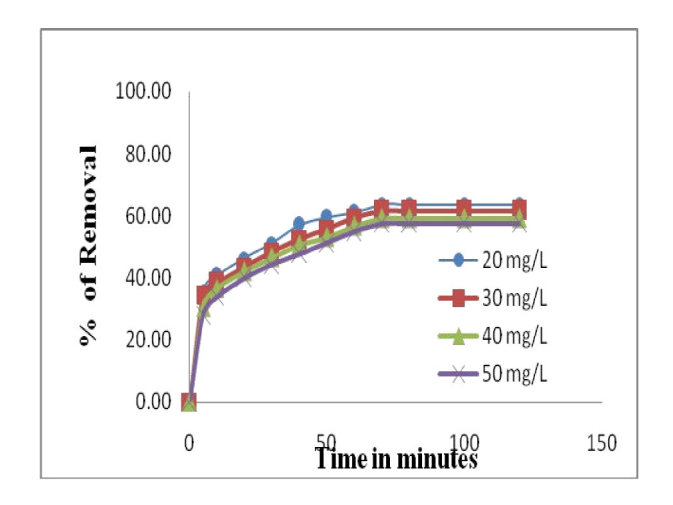


Fig. 1: Effect of contact time TB dye onto PBC

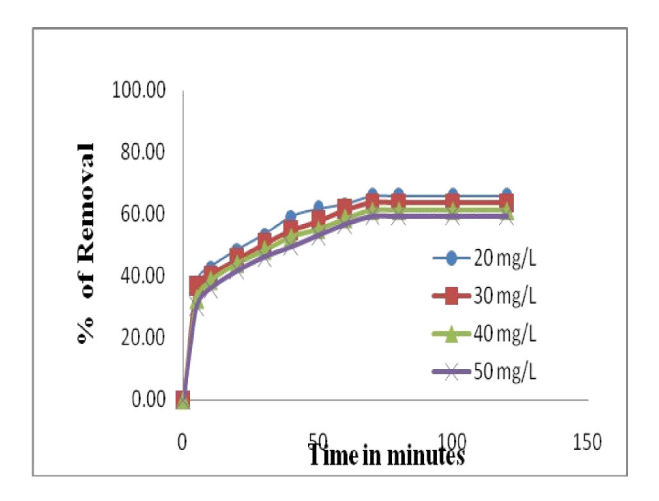
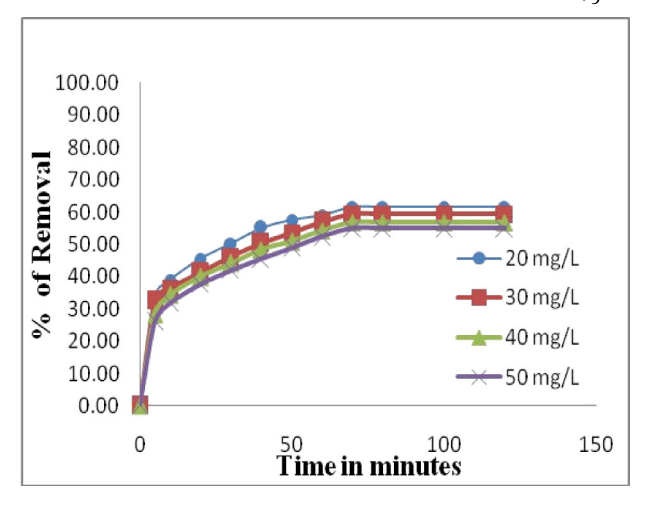


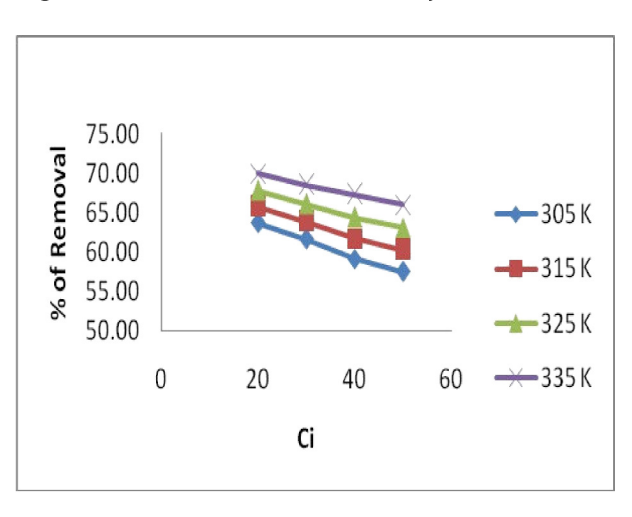
Fig. 2: Effect of contact time TB dye onto APBC



75.00 70.00 % of Removal 65.00 -305 K 60.00 315 K -325 K 55.00 -335 K 50.00 0 20 60 40 Ci

Fig. 3: Effect of contact time TB dye onto BPBC

Fig. 6: C_ivs. % of Removal for TB dye onto APBC



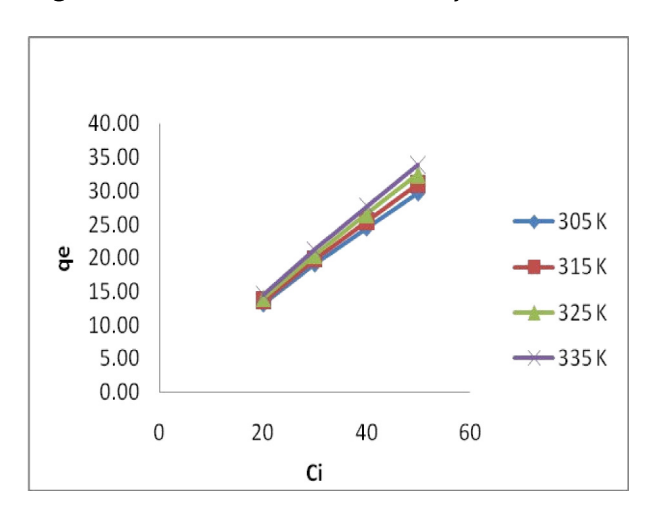
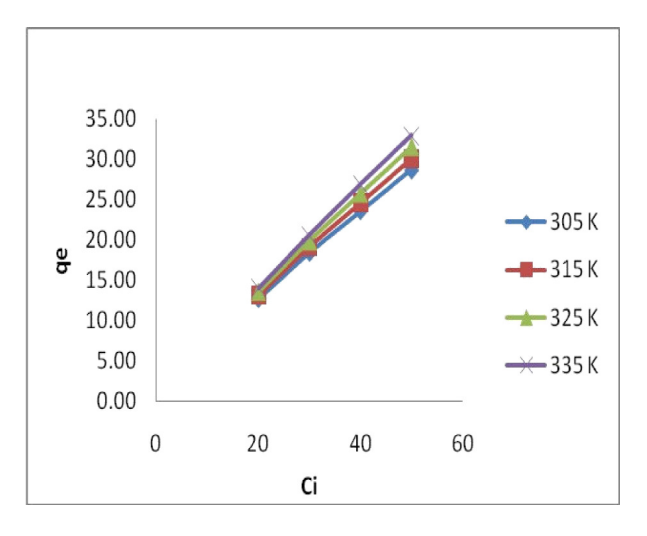


Fig. 4: Civs. % of Removal for TB dye onto PBC

Fig. 7: C_ivs. qe for TB dye onto APBC



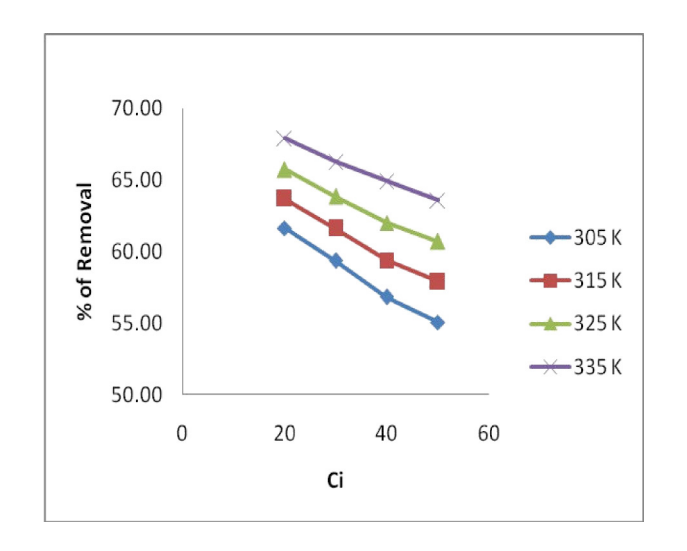


Fig. 5: Ci vs. qe for TB dye onto PBC

Fig. 8: C_ivs. % of Removal for TB dye onto BPBC

Table 2: Results for C_ivs % Removal and C_ivs qe

C	Т	PI	3C	AF	PBC	BP	BC
$\mathbf{C}_{\mathbf{i}}$	Temp	% R	qe	% R	qe	% R	qe
	305	63.69	12.74	65.90	13.18	61.64	12.33
20	315	65.74	13.15	67.95	13.59	63.69	12.74
20	325	67.79	13.56	70.00	14.00	65.74	13.15
	335	69.99	14.00	72.20	14.44	67.94	13.59
	305	61.61	18.48	63.70	19.11	59.38	17.81
30 -	315	63.84	19.15	65.93	19.78	61.61	18.48
	325	66.08	19.82	68.17	20.45	63.85	19.15
	335	68.51	20.55	70.60	21.18	66.28	19.88
	305	59.14	23.66	61.14	24.46	56.83	22.73
40	315	61.72	24.69	63.72	25.49	59.41	23.76
40	325	64.34	25.74	66.34	26.54	62.03	24.83
	335	67.24	26.90	69.24	27.70	64.93	25.97
	305	57.44	28.72	59.34	29.67	55.07	27.54
-	315	60.26	30.13	62.16	31.08	57.89	28.9
50	325	63.08	31.54	64.98	32.49	60.71	30.36
-	335	65.96	32.98	67.86	33.93	63.59	31.80

pH = 2; Dose = 50 mg/50 mL

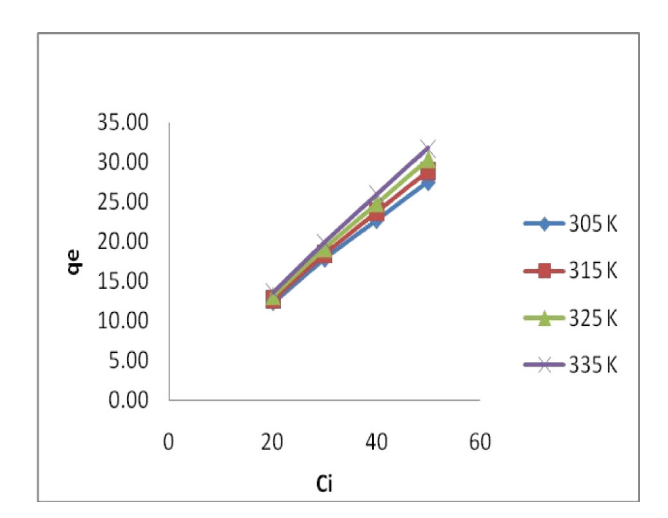


Fig. 9: C_ivs. qe for TB dye onto BPBC

3.2. Isotherm Studies

The equilibrium data obtained from the experiments were processed with different isotherm models such as Langmuir, Freundlich, Tempkin and Dubinin-Radushkevich. It is an important step for finding a suitable model in order to design Environmental treatment plant [13-18]. Inference obtained from each isotherm was discussed in detail one by one.

3.2.1. Langmuir Isotherm

The Langmuir isotherm represents the equilibrium distribution of dye molecules between the solid and

liquid phases [19]. The regression coefficient (R^2) values ranged from 0.9936 to 0.9978 for the three studied temperatures viz. 305, 315, 325 and 335 K. These results show the best fitting of the equilibrium data with Langmuir isotherm (How-proof). The mono layer adsorption capacity Q_m values (mg/g) for adsorption of TB dye onto three prepared carbons with TB dye system ranged from 75.18 to 126.58 mg/g. The adsorption capacity increased with the increase of temperature [20]. On comparing the Langmuir monolayer adsorption capacities of the studied carbons, carbon modified with acid had higher value than the other two carbons. The value of R_L in all cases lies between 0 and 1, indicating that the adsorption process was favourable.

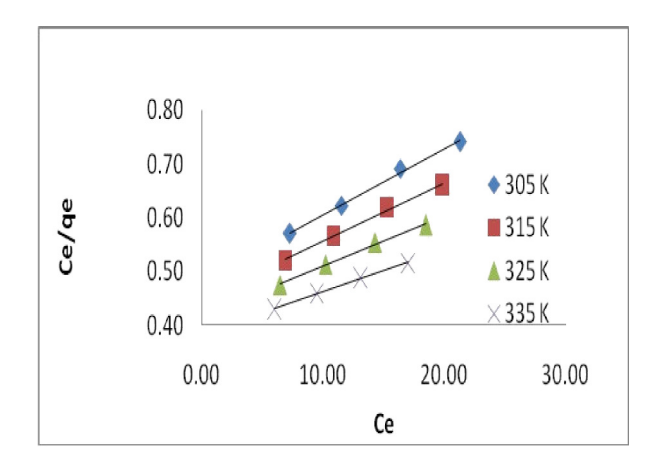
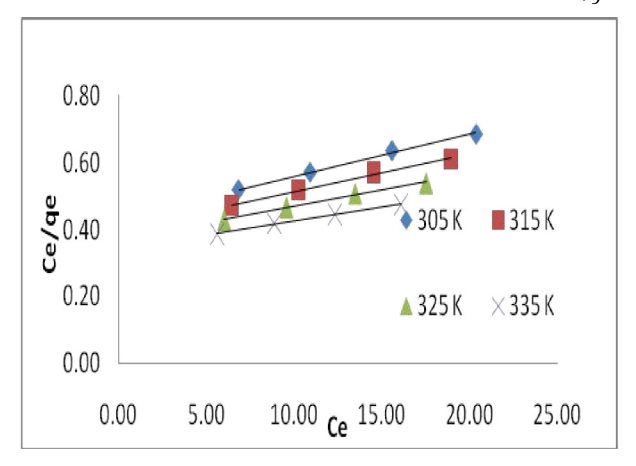


Fig. 10: Langmuir Isotherm for TB dye onto PBC



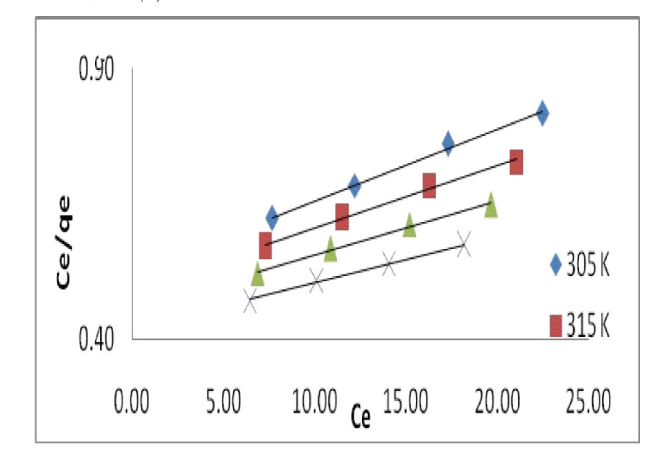


Fig. 11: Langmuir Isotherm for TB dye onto APBC

Fig. 12: Langmuir Isotherm for TB dye onto BPBC

Table 3: Langmuir isotherm results for the adsorption of Cr (VI) ions onto PBC, APBC and BPBC

				,	. ,			
Adsorbent	Temperature	\mathbf{Q}_{m}	b]	R_L		\mathbb{R}^2
Adsorbent	(K)	(mg/g)	(L/mg)	20 mg/L	30 mg/L	40 mg/L	50 mg/L	IX
	305	079.36	0.029	0.632	0.534	0.462	0.420	0.9961
PBC	315	090.09	0.028	0.644	0.547	0.475	0.437	0.9951
TBC	325	104.16	0.026	0.660	0.564	0.492	0.296	0.9946
	335	119.04	0.025	0.669	0.574	0.503	0.447	0.9975
	305	080.64	0.026	0.660	0.564	0.492	0.454	0.996
APBC	315	092.59	0.024	0.675	0.581	0.509	0.476	0.9949
AI BC	325	108.69	0.022	0.694	0.602	0.531	0.296	0.9945
	335	126.58	0.021	0.708	0.617	0.548	0.492	0.9978
BPBC	305	075.18	0.025	0.662	0.567	0.495	0.459	0.9958
	315	086.95	0.023	0.680	0.586	0.515	0.479	0.9945
DI DC	325	101.01	0.022	0.697	0.605	0.535	0.296	0.9936
	335	117.64	0.020	0.711	0.622	0.552	0.497	0.9965

[pH = 2; Dose = 50 mg/50 mL]

3.2.2. Freundlich Isotherm

The Freundlich adsorption capacity constant K_f (mg/g) values ranged from 2.7214 to 3.6350 mg/g. The magnitude of n reveals the favorability of the adsorption. The values of 0 < 1/n < 1 represent favourable adsorption conditions [21].

On comparing the K_i values of the studied carbons, carbon modified with acid had higher value than the other two carbons

3.2.3. Tempkin Isotherm

Equilibrium binding constant a_T values (L/g) ranged from 0.305 to 0.382 and the heat of sorption constant b_T values ranged from 139.099 J/mg to 199.198 J/mg for the three studied temperatures viz. 305, 315 and 325 K. The lower values of a_T and b_T with respect to adsorption of TB dye adsorption indicate physisorption rather than chemisorption [22-26].

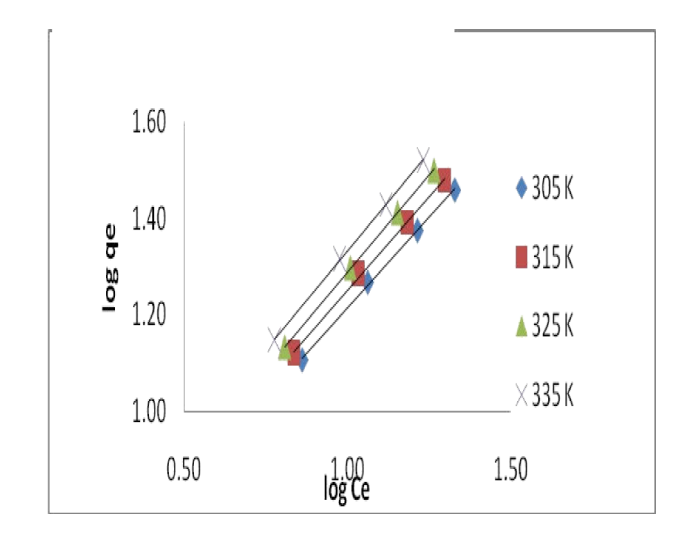


Fig. 13: Freundlich Isotherm for TB dye onto PBC

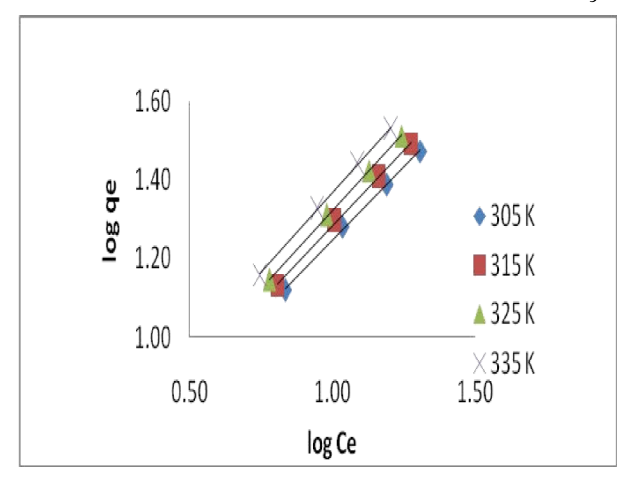


Fig. 14: Freundlich Isotherm for TB dye onto APBC

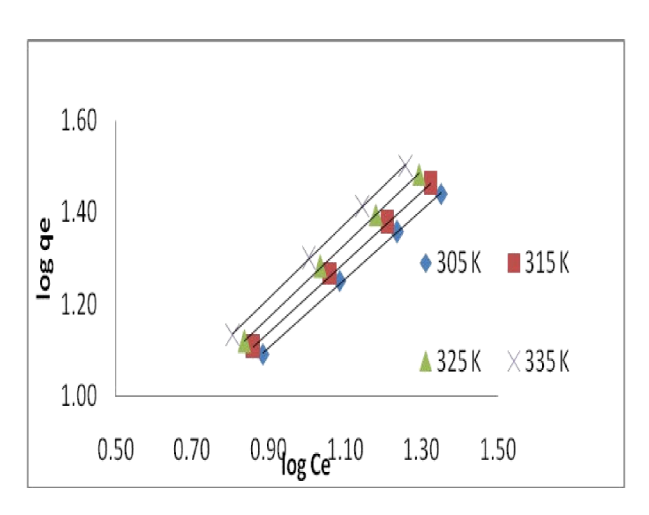


Fig. 15: Freundlich Isotherm for TB dye onto BPBC

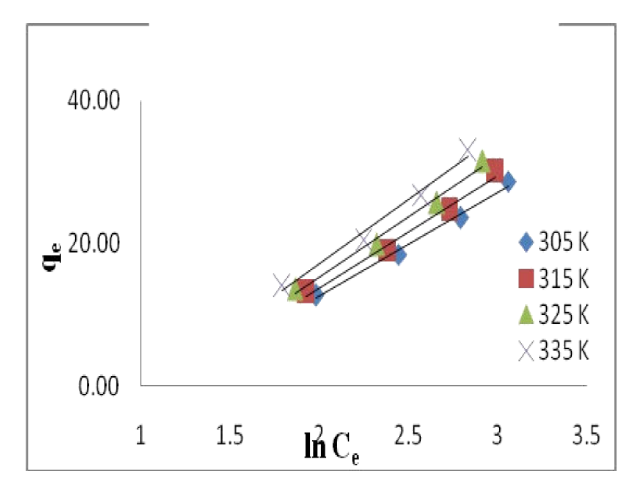


Fig. 16: Tempkin Isotherm for TB dye onto PBC

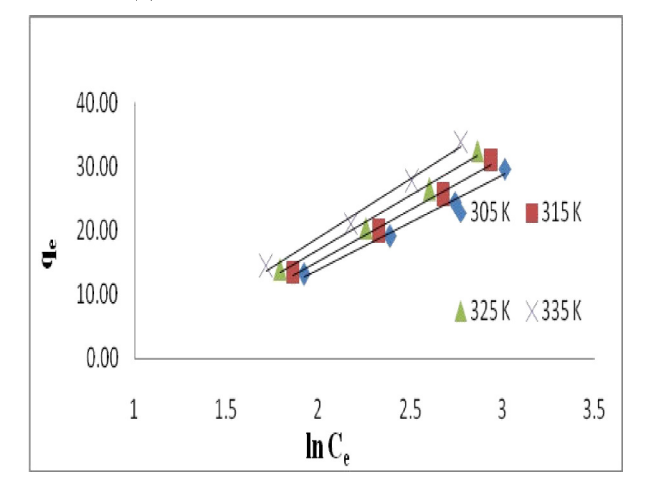


Fig. 17: Tempkin Isotherm for TB dye onto APBC

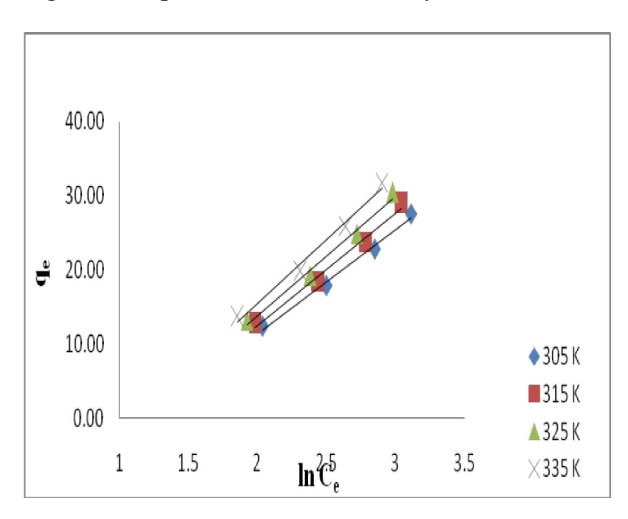


Fig. 18: Tempkin Isotherm for TB dye onto BPBC

4.3.4 D-R isotherm

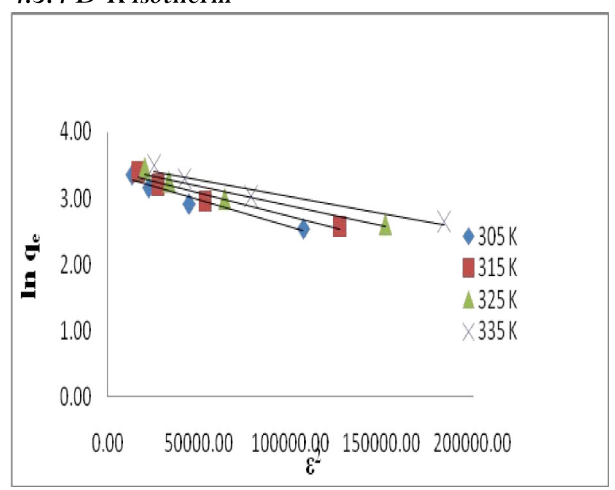


Fig. 19: D-R Isotherm for TB dye onto PBC

Table 4: Freundlich isotherm results for the adsorption of TB dye onto PBC, APBC and BPBC

Adsorbent	Temperature (K)	n	$k_f(mg/g)$	\mathbb{R}^2
	305	1.2137	3.2122	0.9997
PBC	315	1.2489	3.0662	0.9997
PDC	325	1.2877	2.9703	0.9994
	335	1.3270	2.8847	0.9990
	305	1.2395	3.6350	0.9997
APBC	315	1.2740	3.4483	0.9997
AFBC	325	1.3122	3.3212	0.9994
	335	1.3506	3.2092	0.9990
	305	1.2249	2.9923	0.9998
BPBC	315	1.2607	2.8695	0.9998
DFBC	325	1.3006	2.7906	0.9995
	335	1.3414	2.7214	0.9991

TB dye, pH = 2; Dose = 50 mg/50 mL]

Table 5: Tempkin isotherm results for the adsorption of TB dye onto PBC, APBC and BPBC

Adsorbent	Temperature (K)	aT L/g	b _T J/mg	\mathbb{R}^2
	305	0.348	140.315	0.9882
PBC	315	0.334	155.140	0.9880
PBC	325	0.325	171.537	0.9895
	335	0.317	189.688	0.9912
	305	0.382	139.099	0.9886
APBC	315	0.365	153.440	0.9883
ArbC	325	0.353	169.270	0.9897
	335	0.344	186.712	0.9914
	305	0.329	146.475	0.9880
ВРВС	315	0.317	162.202	0.9878
	325	0.310	179.693	0.9894
	335	0.305	199.198	0.9912

TB dye, pH = 2; Dose = 50 mg/50 mL]

Table 6: D-R isotherm results for the adsorption of TB dye onto PBC, APBC and BPBC

Adsorbent	Temperature (K)	$q_{\scriptscriptstyle D}$	E kJ	\mathbf{R}^2
	305	29.2357	0.5443	0.9456
PBC	315	30.7467	0.5402	0.9439
PBC	325	32.3131	0.5364	0.9425
	335	34.0444	0.5324	0.9437
	305	30.0688	0.5420	0.9447
ADDC	315	31.5659	0.5382	0.9429
APBC	325	33.1211	0.5345	0.9416
	335	34.8886	0.5305	0.9428
	305	27.9915	0.5478	0.9448
ВРВС	315	29.4853	0.5436	0.9428
	325	31.0308	0.5395	0.9412
	335	32.7293	0.5354	0.9422

TB dye, pH = 2; Dose = 50 mg/50 mL]

'E' is a parameter used in predicting the type of adsorption. An E value less than 8 kJ/mol is an indication of physisorption [27].The mono layer adsorption capacity $q_{\rm D}$ values (mg/g) are ranged from 27.9915 to 34.8886 mg/g for all the studied temperatures. Further it is noticed that adsorption capacity increased with the increase of temperature. The very low values of E infer the physisorption interaction.

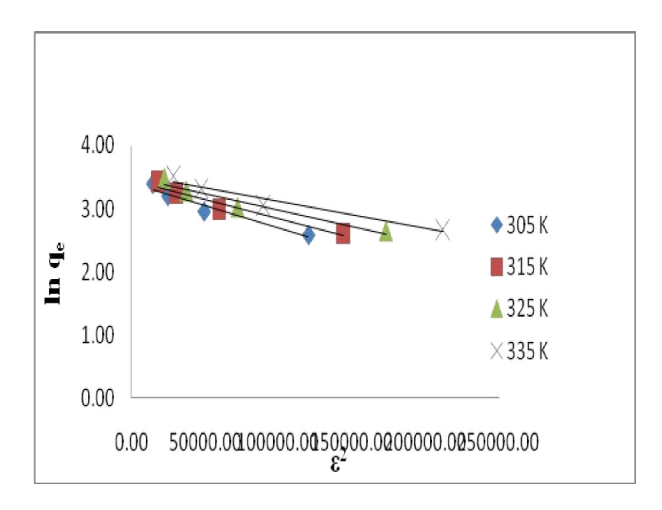


Fig. 20: D-R Isotherm for TB dye onto APBC

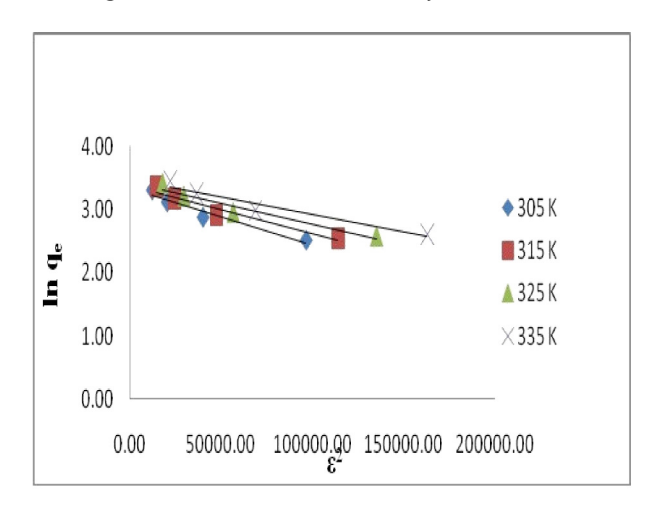


Fig. 21: D-R Isotherm for TB dye onto BPBC

4. CONCLUSION

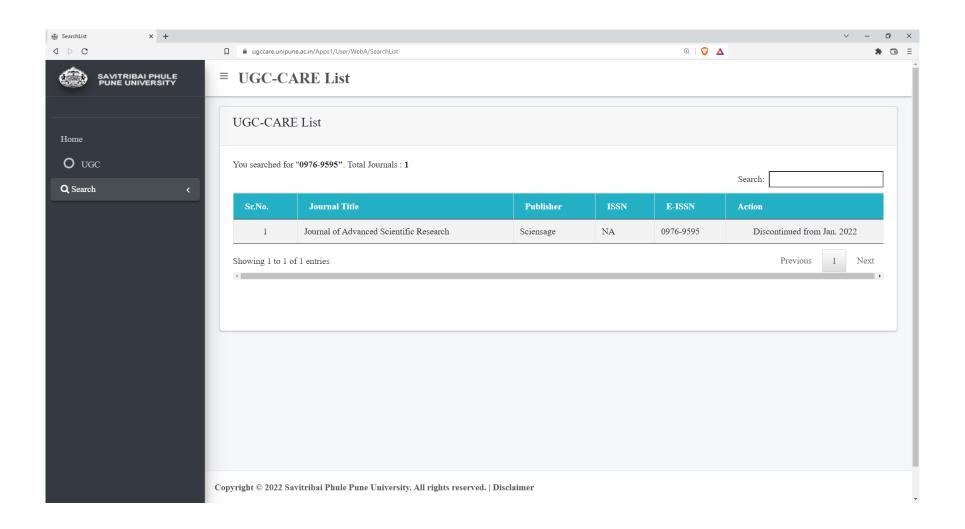
The equilibrium parameter R_L values obtained in Langmuir isotherm study were in between 0 and 1 showing the favourable adsorption process. The values of n were found to be greater than one indicating a favourable adsorption. The Mean free energy B value obtained from Dubinin Radush Kevich isotherm was

ranged from 0.020 to 0.029. These values indicated that the adsorption was physisorption in nature. Order of equilibrium isotherms according to increasing R^2 value was found as Freundlich > Langmuir > Tempkin > Dubinin-Radushkevich. Values of those parameters revealed the possibility of multi-layer, physisorption and heterogeneous pore distribution.

5. REFERENCES

- Balcioglu A, Arslan I, et al. J. Environ Technology., 1977; 18:1053-1059.
- 2. Zaharia Carmen, Suteu Daniela, et al. *Environmental* and Analytical update, 2012; **(2)**:953-978.
- 3. Schimmel D, Fagnani KC, Oliveira dos Santos JB. *J. Chem. Eng.*, 2010; **27(2)**.
- 4. Ta Wee Seow, Chi Kim Lim. Int J of Apllied Engineering Research, 2016; 11(4):2675-2679.
- 5. Alau KK, Gimba CE, et al. Archives of Applied Science Research, 2010; **2(5)**:456-461.
- 6. Allen SJ, Koumanova B, et al. *J. Univ. Chem. Technol. Metal.*, 2005; **40**:175-192.
- 7. Yagmur E, Ozmak M, Aktas Z, et al. Fuel, 2008; 87:3278-3285.
- 8. Williams H, Parkes G, et al. *Carbon*, 2008; **46(8)**:1169-1172.
- 9. Lagergren S, Sven K, Vetenskapsakademiens H. 1898; 24:1-39.
- 10. Kavitha D, Namasivayam C, et al. *Dyes and Pigments*, 2007; **74**:237 248.
- 11. Weber WJ, Morris JC, et al. *J.Sanit.Eng.Div.*, ASCE 1963; 89:31 -59.
- 12. Sureshkumar MV, Namasivayam C, et al. *Physicochem.Eng.Aspects*, 2008; **317**:277-283.
- 13. Sivakumar P, Palanisamy PN, et al. *International Journal of Chem Tech Research*, 2009; **1(3)**:502-510.
- 14. Hardiljeet K, Booparai, MeeraJoseph, Denis Carroll MO, et al. *Journal of Hazardous Materials.*, 2010;
- 15. Namasivayam C, Sangeetha D, et al. *Journal of Hazardous Materials*, 2006; **135**:449-452.
- Zukiswa Mbolekwa, Chris Buckley, et al. pollution Research Group – University of Kwazulu- Natal Durban 2006;
- 17. Namasivayam C, Muniasamy N, Gayathri K, Rani M, et al. *Bioresource Technology*, 1996; **57**:37-43.
- 18. Ismadji S, Bhatia SK, et al. *J.Chem.Eng.*, 2000; **78**:892-901.
- 19. Fethi Kooli, Liu Yan, Rawan, Al-Faze, et al. *Arabian Journal of Chemistry*, 2015; **(8)**:333-342.

- 20. Palanisamy PN, Sivakumar P. *Indian Journal of Chemical Technology*, 2011; **(20)**:245-251.
- 21. Cerofolini GF, Jaroniec M, et al. *Colloid Polym.Sci.* 1978; **256**:471-477.
- 22. Hameed BH, Din et al. *J. Hazard. Material.*, **141(3)**:819-825.
- 23. Renmin Gong, Yingzhi Sun, Jian chen. *Dyes and Pigments*, 2007; **67**:179-195.
- 24. Amarasinghe BMWPK, Williams RA, et al. *Journal of Chemical Eng.*, 2007; **132(1-3)**:299-309.
- 25. Cay S, Uyanik A, Ozasik A, et al. Sep.Purif. Technol. 2004; **38(3)**:273-280.
- 26. Namasivyam C, Yamuna RT, et al. *Environ Pollut.*, 1995; **89(1)**:1-7.
- 27. Fozio Batool, JamshedAkbar et al. *Bioorganic Chemistry and Applications*, 2018; 1-11.





Journal of Advanced Scientific Research

ISSN
0976-9595
Research Article

Available online through http://www.sciensage.info

ADSORPTION DYNAMICS OF METHYLENE BLUE DYE ONTO SURFACE MODIFIED ACTIVATED CARBON PREPARED FROM *PTEROCARPUS MARSUPIUM* BARKS

S. Surya, V. Nandhakumar*, S.K.Thiyagarajan, G.Vishnuvarthanaraj

PG & Research Department of Chemistry, A.V.V.M. Sri Pushpam College (Affiliated to Bharathidasan University),
Poondi, Thanjavur (Dt), Tamil Nadu, India
*Corresponding author: drvnchem@gmail.com

ABSTRACT

Pterocarpus Marsupium barks have been utilised to prepare activated carbon with the aid of orthogonal array experimental techniques with the parameters inclusive of microwave radiation energy, radiation time, concentration of H₃PO₄ acid and impregnation time. Radiation energy 850W, radiation time 15 min, 50% of H₃PO₄acid, impregnation time 24 hours were found to be the optimum conditions. Thus prepared carbon was designated as PBC (Pterocarpus Marsupium Bark Carbon). Surface of the PBC was modified with Hydrochloric acid solution and also separately with Potassium hydroxide solution. Influences of initial dye concentration on adsorption kinetics were studied. Kinetic models such as Pseudo first order, Pseudo second order and Intra Particle diffusion had been used to describe the mechanism of this adsorption process.

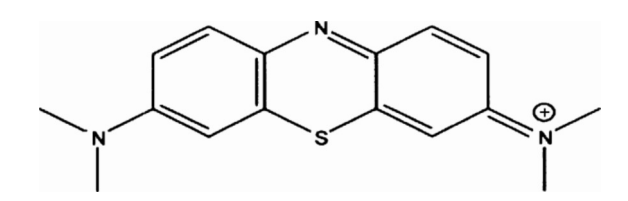
Keywords:

1. INTRODUCTION

Discharged wastewater through a few industries causes tremendous environmental problems. Natural water in our bodies such as ponds, lakes, rivers and their watershed would be subjected to critical environmental issue, if untreated effluent is discharged into them as such. Researchers have investigated the use of activated charcoal as an adsorbent for the elimination of dyes from the effluent water let out from big as well as tiny printing and dyeing units [1]. Adsorption method is mostly used as an effective approach for isolating organic and inorganic pollutants from water and waste water which involves carbon adsorption [2]. Activated carbon is the popular adsorbent for the elimination of many natural contaminants. The use of activated carbon for the adsorption method, however, activated carbon is expensive when produced from coal and hence limits its application. Therefore, less expensive activated carbon has to be produced from waste substances. Numerous investigations were stated the production of activated carbons from agricultural wastes [3]. A number of studies have been carried out using activated carbon prepared from agricultural wastes for the removal of dyes from aqueous solution [4, 5].

Many researchers used Methylene blue dye as a model adsorbate for adsorption of organic substance because

of its known strong adsorbing ability on to activated carbon [6].



Structure of MB

In this study, a try has been made to know the adsorption dynamics of surface modified activated carbons prepared from the barks of *Pterocarpus Marsupium*. The *Pterocarpus Marsupium* tree produces brown woody barks.

Recently, microwave energy has been broadly utilized in the research field and business methods [7]. The microwave irradiation approach has come as an advantageous heating method in place of traditional muffle furnace heating techniques [8-10].

- Interior heating
- Choice of heating
- Extensive heating rates
- Good manage of heating method
- Small gadget size

- Reduced wastage production
- No direct touch among heating supply and heating substances.

2. MATERIAL AND METHODS

2.1. Preparation of Adsorbents

Small pieces of well dried barks were powdered in a pulveriser. 25 g of the powdered barks was mixed with 100mL of phosphoric acid solution of desired concentration (25, 50 and 75 %). To ensure the access of the H₃PO₄acid into the *Pterocarpus Marsupium* Barks, the slurry was kept at room temperature for 24 hours. Then the slurry was subjected to microwave heating under different conditions (450, 600 and 850 watts and 10, 13 and 15 minutes) for simultaneous carbonization and activation. Thus obtained carbonized samples were washed with distilled water at room temperature followed by 0.5 M HCl acid, hot distilled water and cold distilled water until the pH of the washings reach 7. Then the carbon was filtered and dried at 425 K.

 ${
m H_3PO_4}$ acid generates more interspaces between carbon layers which gives more surface area and micro porosity to that carbon. ${
m H_3PO_4}$ acid activation causes swelling in the molecular structure of cellulose through electrolytic action, which leads to the breaking of lateral bonds in the cellulose molecules resulting in increased inter and intra voids.

Totally 27 number of activated carbons were prepared by varying preparation parameters. The carbon which is responsible for maximum percentage removal was chosen for further study and the chosen carbon was designated as PBC (*Pterocarpus Marsupium* Barks Carbon). 10 g of the PBCwas mixed with 25% solutions of HCl and also with KOH separately in two containers. They were heated in a microwave oven for 10 minutes. Then the carbons were again washed with hot distilled water and cold distilled water successively. HCl acid treated carbon was and designated as acid treated (Acid modified *Pterocarpus Marsupium* Barks Carbon) APBC and KOH treated carbon was designated as Base modified *Pterocarpus Marsupium* Barks Carbon BPBC.

2.2. Preparation of stock Solution

Analar grade Methylene blue dye belongs to Merck Company was used without in additional purification. 1000 mg/L dye stock solution was prepared using double distilled water. The experimental solutions were prepared from the stock solution by appropriate dilution.

2.3. Characterization of prepared carbons

Particle size (μ m), Surface area (m^2/g), Pore volume (cm^3/g), Pore size or Pore width (nm), Bulk density (g/mL), Fixed Carbon (%), Moisture content (%) and pHzpc have been determined.

2.4. Adsorption experiments

The effect of parameters studied includes initial concentration of dye solution, adsorbent dose and contact time by batch mode approach due to its simplicity. Pre-determined dose of the adsorbent was taken in 250mL iodine flask having lid and 50mL and pre-determined concentration of the dye solution was poured into the flask. Then the content flask was agitated using rotary shaker (Orbit Company) with 180 rpm for a pre-determined duration. Then the aliquot was centrifuged. Concentration of the centrifugate was measured after necessary dilution using Systronics Double Beam UV-visible spectrophotometer: 2202 on the wave length of 680nm.

The kinetics experiments were carried out for the contact times 5, 10, 20, 40, 60, 80, 100, 120 and 140 minutes with an operating solution pH of 7.

2.5. Data processing tools

2.5.1. Pseudo First order kinetics

Legergren equation is [11,12] was used for analysing pseudo first order kinetics. Legergren equation islog $(q_c-q_t)=\log q_c - k_1/2.303 \times t$

Where q_e and q_i are the amounts of dye adsorbed (mg/g) at equilibrium and at time t (min), respectively and k_1 is the rate constant for this adsorption dynamics (l/min).

2.5.2. Pseudo Second order kinetics

Ho equation is [13]

$$t/q_t = 1/k_2.q_e^2 + 1/q_e t$$

The initial adsorption rate, h (mg/(g min)), as t \rightarrow 0 can be defined as

$$h = k_2 q_e^2$$

The initial adsorption rate (h), the equilibrium adsorption capacity (q_e), and the second-order constants k_2 (g/ (mg min)) can be determined experimentally from the slope and intercept of plot of t/ q_e versus t.

2.5.3. Intra particle diffusion

Weber-Morrris equation is [14]

$$q_t = k_p t^{1/2} + C$$

Where k_p is the intra-particle diffusion rate constant, a plot of q_t versus $t^{1/2}$ should be a straight line with a slope

 \boldsymbol{k}_p which is the rate constant for intra particle diffusion and intercept \boldsymbol{C} is the thickness of the boundary film.

2.5.4. Test for kinetics models

The Mean of sumoferrorsquaresisas follows;

MSSE (%) = $\sqrt{\sum[(q_e)_{exp} - (q_e)_{cal}]^2} / N$

Where N is the number of data points, $(q_e)_{exp}$ is the experimental q_e , $(q_e)_{cal}$ is the calculated q_e^{-12} .

3. RESULTS AND DISCUSSION

3.1. Optimization of adsorbent preparation parameters

The prepared 27 carbons prepared under orthogonal array of experiments were subjected to remove MB dye from aqueous solution with 20 mg of the adsorbent, 50 mL of MB dye solution of concentration of 100 mg/Land 1 hour agitation time. Percentage of removal increased with the increase of radiation time, radiation power and concentration of H_3PO_4 solution. Based on results, 50% H_3PO_4 solutions, radiation power 850 watts, radiation time 15 minutes and impregnation time 24 hours were chosen as optimum conditions.

3.2. Effect of contact time for different initial concentrations

The percentages of removal of MB from aqueous solution with respect to different contact times and with different initial concentrations were shown in Fig. 1-3.

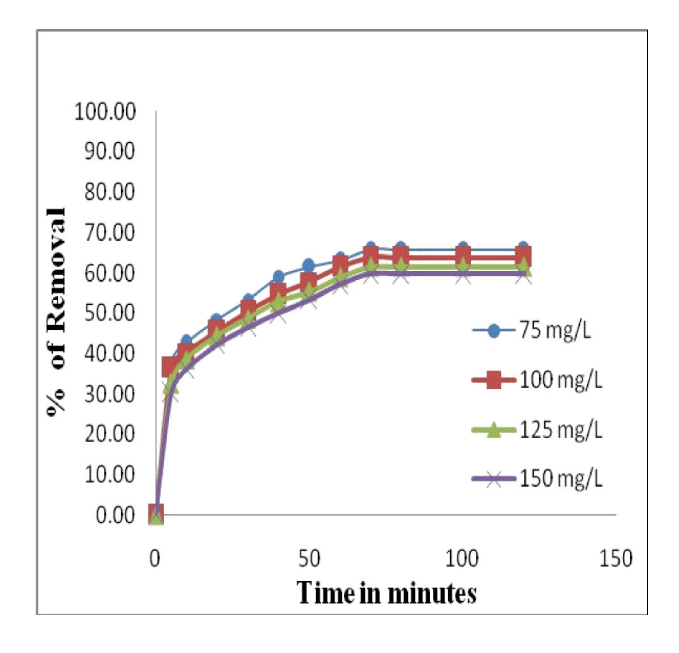


Fig. 1: Effect of contact time MB dye onto PBC

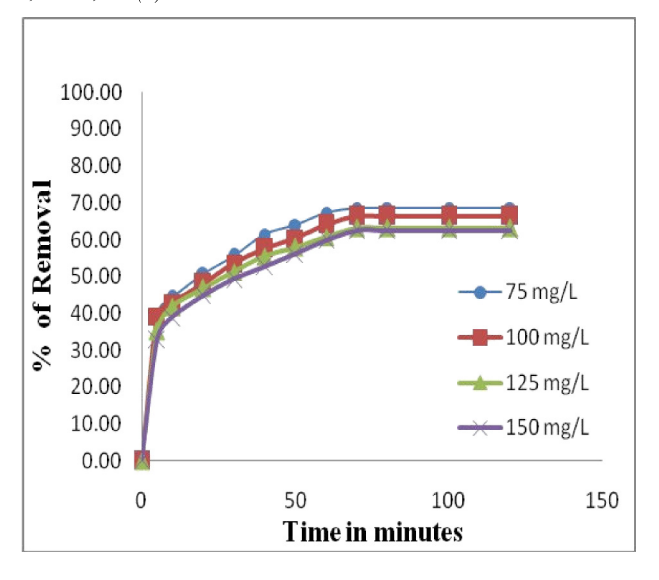


Fig. 2: Effect of contact time MB dye onto APBC

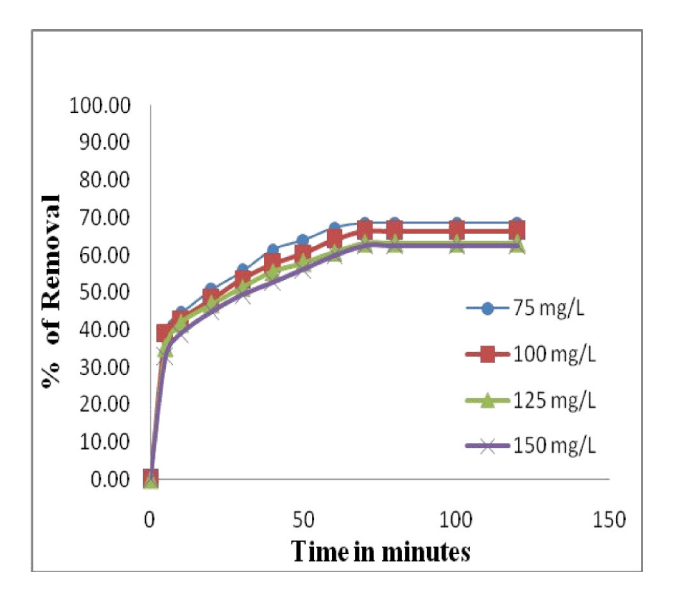


Fig. 3: Effect of contact time MB dye onto BPBC

The rapid uptake of the adsorbates in the initial stages is noticed as revealed by the curves. The percentage of removal increased with the increase in contact time and decreased with the increase of initial concentration of the dye. However the amount of dye adsorbed on the adsorbent increased with the increase of initial concentration of the dye solution as depicted in the Fig. 1-3. The time to attain equilibrium was found to increase when the initial concentration of the dye was increased were given in the table 1. The percentage of removal as well as the quantity adsorbed at equilibrium was found to be high for BPBC when compared to other carbons.

Table 1: Results for C_ivs % Removal and C_ivs qe

C:	Т	PBC		APBO	C	BPBC	2
Ci	Temp	% Removal	qe	% Removal	qe	% Removal	qe
	305	65.74	49.31	64.50	48.38	68.51	51.38
	315	66.29	49.72	65.05	48.79	69.06	51.79
75	325	66.83	50.13	65.59	49.20	69.60	52.20
	335	67.42	50.57	66.18	49.64	70.19	52.64
	305	63.84	63.84	62.40	62.40	66.42	66.42
100	315	64.51	64.51	63.07	63.07	67.09	67.09
100	325	65.18	65.18	63.74	63.74	67.76	67.76
	335	65.91	65.91	64.47	64.47	68.49	68.49
	305	61.45	76.81	60.40	75.50	63.21	79.01
125	315	62.19	77.74	61.14	76.43	63.95	79.94
125	325	62.95	78.69	61.90	77.38	64.71	80.89
	335	63.80	79.75	62.75	78.44	65.56	81.95
	305	59.81	89.72	57.10	85.65	62.56	93.84
150	315	60.08	90.13	57.37	86.06	62.83	94.25
150	325	60.36	90.54	57.65	86.47	63.11	94.66
	335	60.65	90.98	57.94	86.91	63.40	95.10

3.3. Kinetic models

The adsorption kinetics shows the evolution of the adsorption capacity through time and it is necessary to identify the types of adsorption mechanism in a given system. Plots of different kinetic models applied were given in the Figs. 4-12 and the kinetic parameters calculated were given in the Tables 2-4.

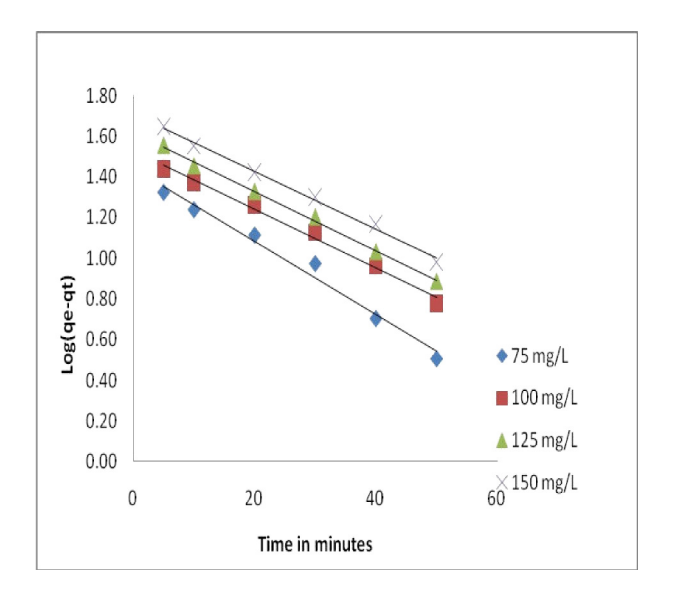


Fig. 4: Lagergren plot for MB dye onto PBC

Between the pseudo first order and pseudo second order, second order kinetic model seems to best describe the above adsorption system as it has R^2 values very close to unity. Moreover, difference between q_e (cal) and q_e (exp) values of pseudo second order is small when compared to pseudo first order kinetic model. Statistically it is tested with the tool mean sum of error squares (MSSE). The Δq_e and MSSE values were given in the Tables 2 & 3, from which it was concluded second order kinetic model was more appropriate rather than first order kinetic model.

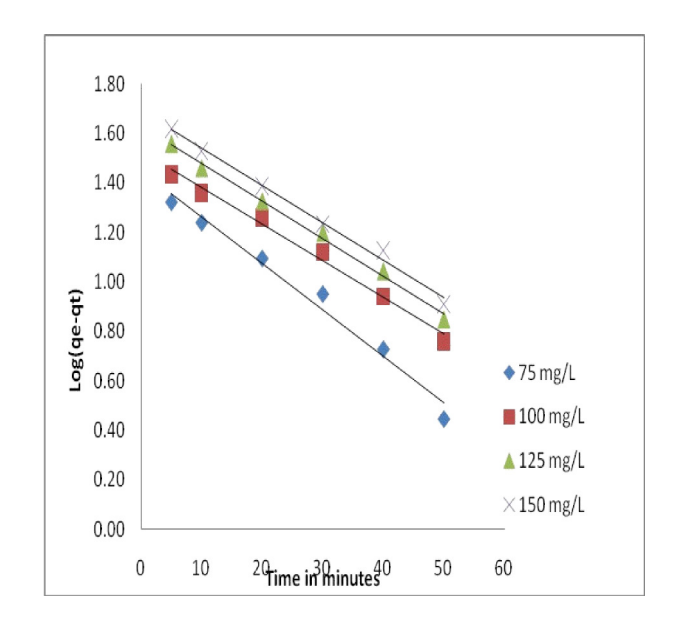


Fig. 5: Lagergren plot for MB dye onto APBC

Table 2: Pseudo first order Kinetic parameters for the removal of MB dye onto adsorbents

Adsorbents	Concentration mg/L	K ₁ min ⁻¹	q _e (Cal) mg/g	q _e (Exp) mg/g	\mathbb{R}^2	MSSE	
	75	0.0415	27.80	49.31	0.9819		
PBC	100	0.0336	41.84	63.84	0.997	17.19	
FBC	125	0.0327	51.25	76.81	0.9944	17.19	
	150	0.0332	33.78	89.72	0.9911		
	75	2.7360	28.18	48.38	0.9794		
APBC	100	0.0350	42.67	62.40	0.9945	16.19	
AFBC	125	0.0348	48.98	75.50	0.9931		
	150	0.0341	33.77	85.65	0.9885		
ВРВС	75	0.0408		51.38	0.9851		
	100	0.0359	41.05	66.42	0.9945	10 (7	
	125	0.0327	51.25	79.01	0.9944	18.67	
	150	0.0336	33.63	93.84	0.9943		

Table 3: Pseudo second order Kinetic parameters for the removal of MB dye onto adsorbents

Adsorbents	Concentration mg/L	$k_2 \times 10^{-4}$ g/mg.min	q _e (Cal) mg/g	Н	\mathbb{R}^2	MSSE
PBC	75	0.0037	51.5464	9.86	0.9962	
	100	0.0025	67.1141	11.21	0.9945	1.95
PBC	125	0.0020	80.6452	13.21	0.9934	1.95
	150	0.0015	95.2381	13.97	0.9934	
	75	0.0038	50.7614	9.77	0.9964	
APBC	100	0.0025	65.7895	10.95	0.9944	1.80
ArbC	125	0.0020	79.3651	12.72	0.9944	1.60
	150	0.0018	90.0901	14.31	0.9947	
ВРВС	75	0.0037	53.7634	10.57	0.9963	
	100	0.0026	69.4444	12.56	0.996	1.85
	125	0.0023	82.6446	15.43	0.9942	1.05
	150	0.0016	99.0099	15.60	0.9942	

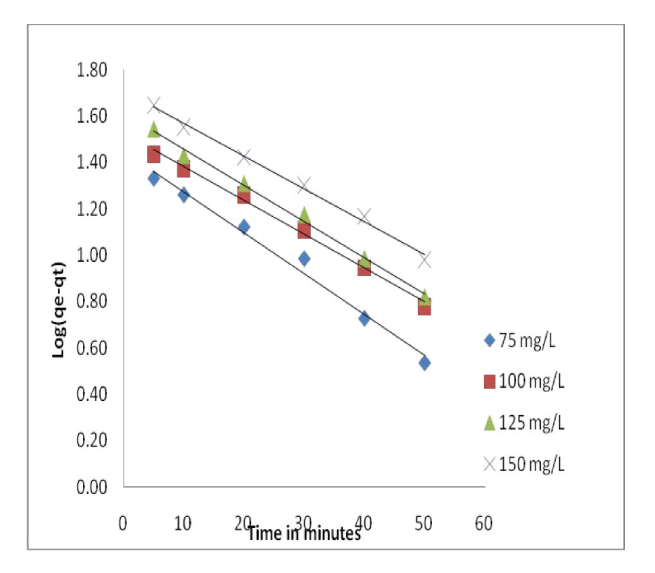


Fig. 6: Lagergren plot for MB dye onto BPBC

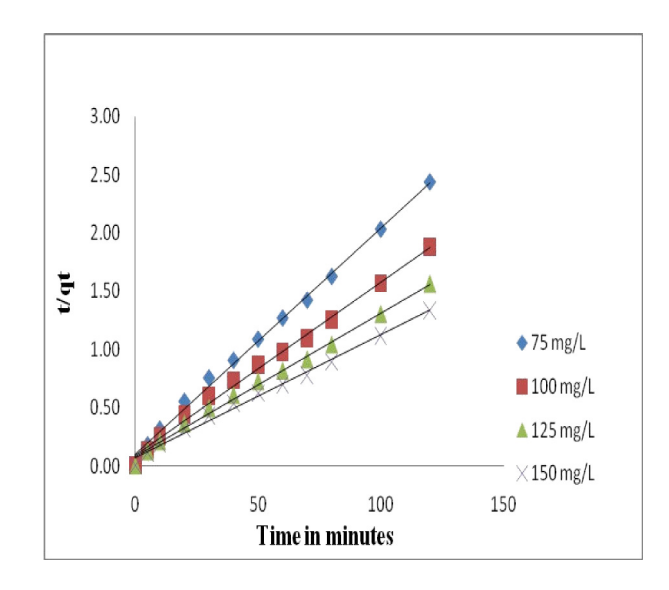


Fig. 7: Ho plot for MB dye onto PBC

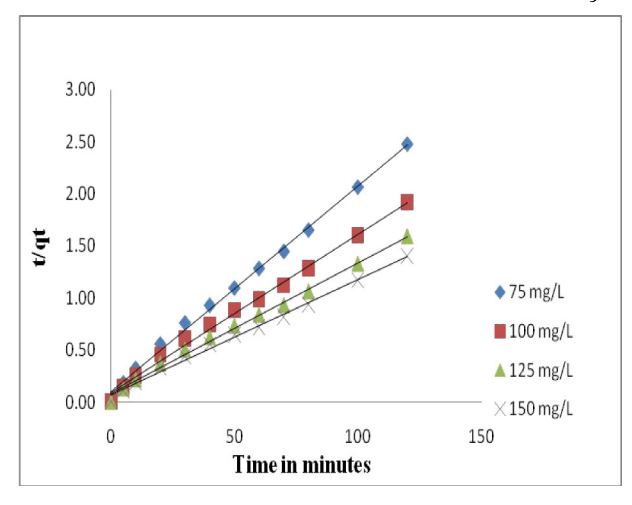


Fig. 8: Ho plot for MB dye onto APBC

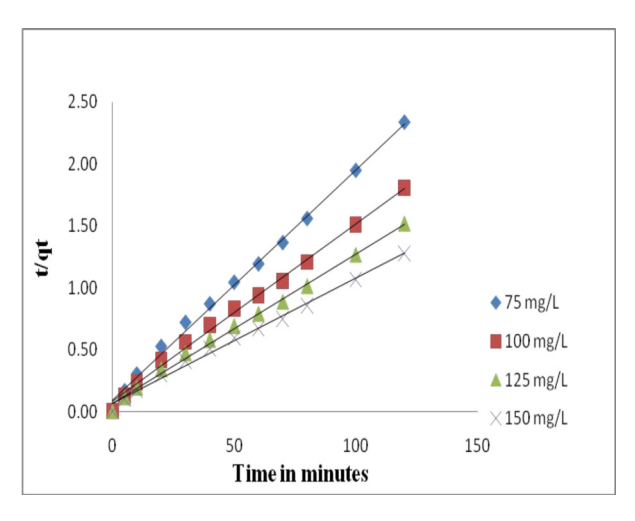


Fig. 9: Ho plot for MB dye onto BPBC

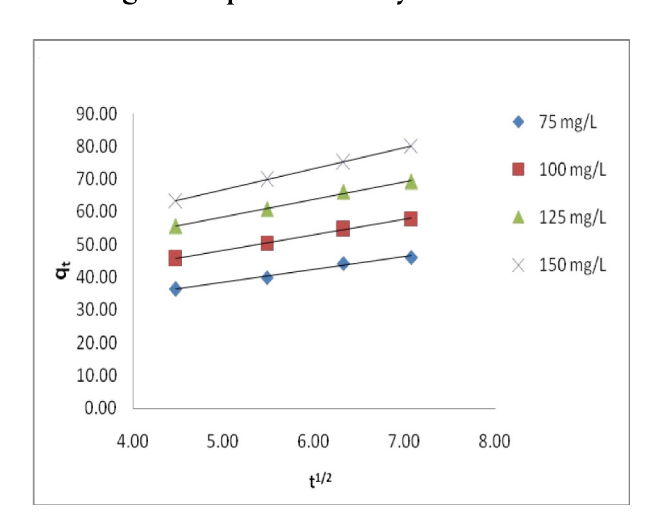


Fig. 10: Weber and Morris plot for MB dye onto PBC

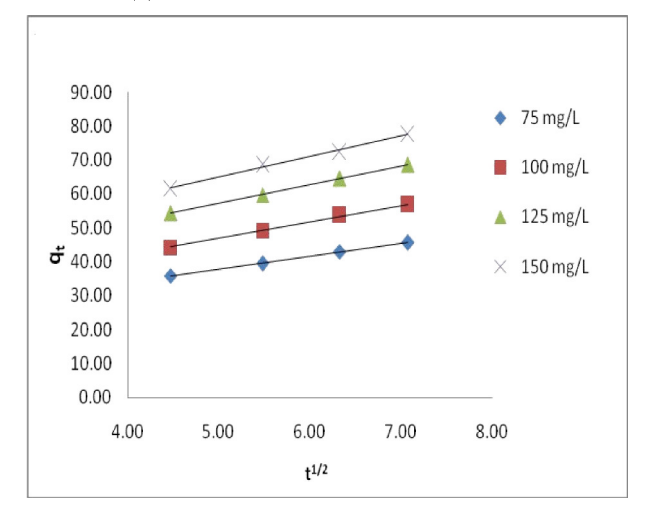


Fig. 11: Weber and Morris plot for MB dye onto APBC

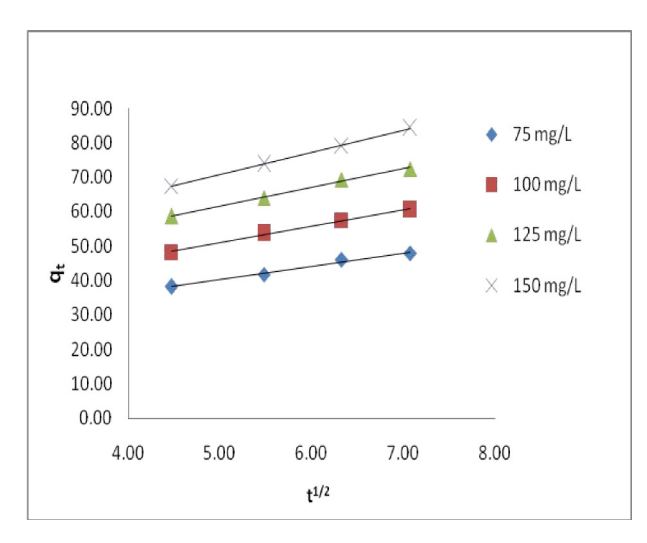


Fig. 12: Weber and Morris plot for MB dye onto BPBC

Table 4: Intra Particle diffusion parameters for the removal of MB dye onto adsorbents

Adsorbents	Concentration mg/L	k _p (mg/ g.min)	\mathbb{R}^2
	75	3.93	0.9872
PBC	100	4.73	0.9992
TBC	125	5.37	0.9957
	150	6.44	0.9996
	75	3.77	0.9983
APBC	100	4.87	0.9975
AFBC	125	5.45	0.9999
	150	6.07	0.9921
	75	3.92	0.9882
BPBC	100	4.73	0.9947
DLDC	125	5.41	0.9952
	150	6.44	0.9996

Figs.10-12 show the final liner portions of plots drawn between mass of dye adsorbed per unit mass of adsorbent (q_t) versus $t^{1/2}.$ These linear plots are attributed to the pore diffusion which is the accessible sites of adsorption. This is attributed to the instantaneous utilization of the most readily available adsorbing sites on the adsorbent surface. The values of $k_{\rm p}$ obtained from the slopes of straight lines are listed in Table 4.

4. CONCLUSION

Microwave assisted H₃PO₄ activated carbons (PBC, APBC and BPBC) were prepared from Pterocarpus Marsupium barks found to have good capacity of adsorption. Experimental data indicated that PBC, APBC and BPBC were effective in removing MB dye from aqueous solution. Equilibrium adsorption was achieved in about 70 minutes for the dosage of 20 mg/50 mL of solution at room temperature of 305 K for the initial concentration of dye solutions ranging from 75 to 150 mg/L. Kinetic studies revealed that the process of adsorption follows pseudo second order kinetics. Adsorption studies inferred that KOH surface modified carbon was more effective than other adsorbents for the adsorption of MB dye. Order of best fitting kinetic model according to increasing R² value and MSSE was found as Second Order>First Order.

	Avera	age R²	MS	SSE
Carbons	First	Second	First	Second
	Order	Order	Order	Order
PBC	0.9911	0.9944	17.19	1.95
APBC	0.9889	0.9950	16.19	1.80
BPBC	0.9921	0.9952	18.67	1.85

Conflict of interest

None declared

5. REFERENCES

- Moreno-Castilla C, et al. Carbon, 2004; 42(1):83-94.
- 2. Abechi ES, Gimba CE, Zairu AU, Kagbu JA. et al. *Arch. Appl. Sci. Res*, 2011; **3 (1)**:154-164.
- 3. Yuh-Shan Ho, Malarvizhi R, Sulochana R. et al. *Journal of Environmental Protection Science*, 2009; 3:111-116.
- 4. Yagmur E, Ozmak M, Aktas Z, et al. Fuel, 2008; 87:3278-3285.
- 5. Bykov YV, Rybakov KI, Semenov VE, et al. *J. Phys*, 2001; **34(2)**:55-75.
- 6. Foo Keng Yuen, Hameed BH, et al. Advances in Colloid and Interface Science, 2009, 149(1):19-27.
- 7. Makeswari M, Santhi TV, et al. *Journal of chemistry*, 2013; **20**(13):1-12.
- 8. Venkatraman BR, Hema K, Nandhakumar V, Arivoli S, et al. *J. Chem. Pharm. Res*, 2011; **3(2)**:637-649.
- 9. Chao-Yin Kuo. *J. Hazard. Mater*, 2008; **152(3)**:949-954.
- 10. Chiang PC, Chang EE, Wu JS, et al. *Water Sci. Tech*, 1997; **35**:279-285.
- 11. Lagergren S, Svenska BK, Vetenskapsakad. *Handl*, 1898; **24(2):**1-39.
- 12. Ramesh K, Rajappa A, Roopa V, Nandhakumar V, et al. Int. J. Res. Chem. Pharma. Sci. 2014; 1(1):28-36.
- 13. McKay G, Ho YS, et al. *Processe Biochem*. 1999; **34(5)**:451-465.
- 14. Weber Jr, MoMBis JC, et al. *J. Sanit. Eng. Div*, 1963; ASCE. **89 (SA2)**:31-59.